12

Report No. R-1493

HELICOPTER NOISE REDUCTION

DESIGN TRADE-OFF STUDY

Michael A. Bowes

January 1977

Final Report

Prepared for

DEPARTMENT OF TRANSPORTATION
Federal Aviation Administration
Operations Section A
Washington, D. C. 20591

DISCLAIMER NOTICE

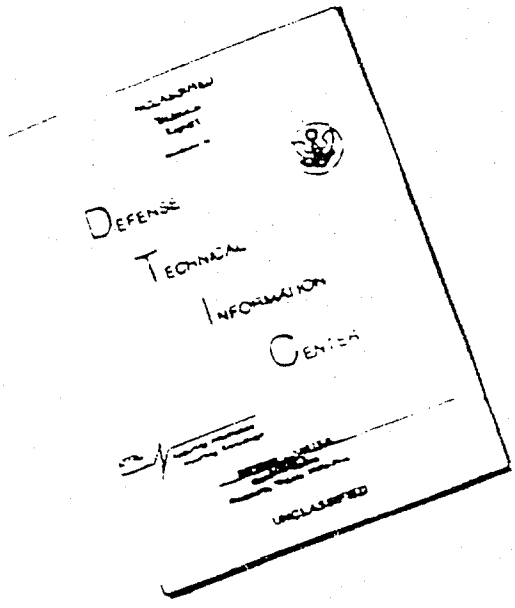

THIS DOCUMENT IS BEST QUALITY AVAILABLE. THE COPY FURNISHED TO DTIC CONTAINED A SIGNIFICANT NUMBER OF PAGES WHICH DO NOT REPRODUCE LEGIBLY.

DISCLAIMER NOTICE

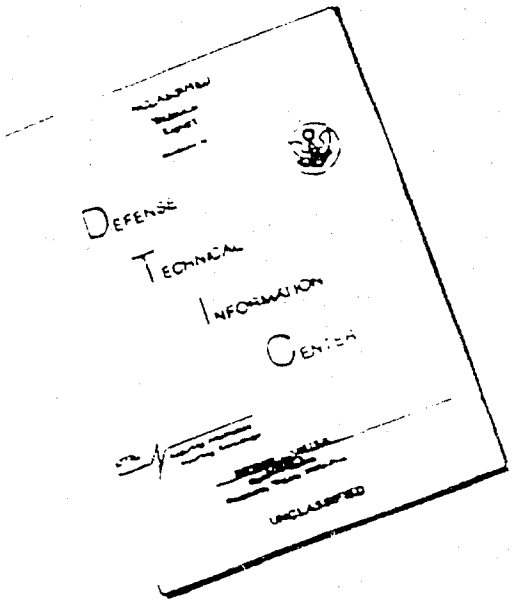

THIS DOCUMENT IS BEST QUALITY AVAILABLE. THE COPY FURNISHED TO DTIC CONTAINED A SIGNIFICANT NUMBER OF PAGES WHICH DO NOT REPRODUCE LEGIBLY.

Technical Report Documentation Page

1. Report No.	2. Government Accession No.	3. Recipient's Catalog No.
(18) FAA-AEQ-77-4 (19)		(12) 252 p.

4. Title and Subtitle
(6) HELICOPTER NOISE REDUCTION DESIGN TRADE-OFF STUDY

5. Report Date
(11) January 1977

6. Performing Organization Code

7. Author(s)
(10) Michael A. Bowes

8. Performing Organization Report No.
(14) R-1473

9. Performing Organization Name and Address
Kaman Aerospace Corporation
Bloomfield, Connecticut 06002

10. Work Unit No. (TRAIS)

11. Contract or Grant No.
(15) DOT-FA76WA-3791

12. Sponsoring Agency Name and Address
U.S. Department of Transportation
Federal Aviation Administration
Operations Section A
Washington, D.C. 20591

13. Type of Report and Period Covered
(9) Final rept.
March 1976 - January 1977

14. Sponsoring Agency Code
ALG-331

15. Supplementary Notes

16. Abstract

A study was performed to determine the noise reduction benefits and economic costs associated with applying state-of-the-art noise reduction methods to future design civil helicopters. As part of this study, a survey of the make-up of the civil fleet was performed, and this fleet make-up was projected to the 1980 time frame. Analytical methods were developed and/or adopted for calculating helicopter component noise, and these methods were incorporated into a unified total vehicle noise calculation model. Analytical methods were also developed for calculating the effects of noise reduction methodology on helicopter design, performance and cost. The analytical methods were used to calculate baseline noise and cost characteristics of several existing civil helicopters. These methods were also used to calculate changes in noise, design, performance and cost due to the incorporation of engine and main rotor noise reduction methods. All noise reduction techniques were evaluated in the context of an established mission performance criterion which included consideration of hover ceiling, forward flight range/speed/payload and rotor stall margin.

40,136

17. Key Words		18. Distribution Statement
Helicopter Noise	Rotor Noise	Document is available to the public through the National Technical Information Service, Springfield, Virginia 22151
Noise Reduction Cost	Engine Noise	
Helicopter Design	Transmission Noise	

19. Security Classif. (of this report)	20. Security Classif. (of this page)	21. No. of Pages	22. Price
Unclassified	Unclassified	~~236~~ 252	

Form DOT F 1700.7 (8-72) Reproduction of completed page authorized

PREFACE

The technical program described within this report was performed by Kaman Aerospace Corporation, Bloomfield, Connecticut, with subcontracting assistance provided by Bolt Beranek and Newman, Inc., Cambridge, Massachusetts. Kaman Aerospace Corporation personnel participating in this effort included Mr. M. A. Bowes, Mr. N. Giansante, Mr. W. Smyth, Mr. A. Plaks and Mr. R. E. Collins. Bolt Beranek and Newman personnel involved were Mr. R. White and Mr. K. Aravamudan. The contract monitor for this effort was Mr. L. Bedore. The contributions of all of these individuals are gratefully acknowledged.

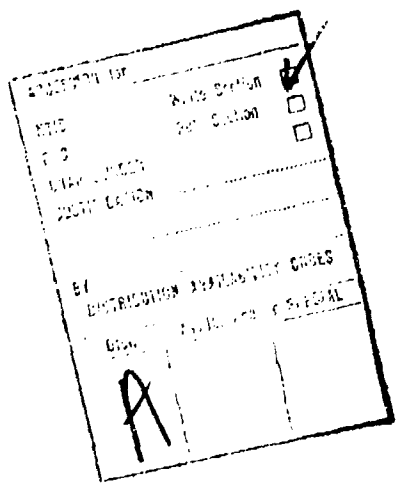

SUMMARY

A study was performed to determine the noise reduction benefits and economic costs associated with applying state of the art noise reduction methods to future design civil helicopters. As part of this study, a survey of the make-up of the civil fleet was performed, and this fleet make-up was projected to the 1980 time frame. Analytical methods were developed and/or adopted for calculating helicopter component noise, and these methods were incorporated into a unified total vehicle noise calculation model. Analytical methods were also developed for calculating the effects of noise reduction methodology on helicopter design, performance and cost. The analytical methods were used to calculate baseline noise and cost characteristics of several existing civil helicopters. These methods were also used to calculate changes in noise, design, performance and cost due to the incorporation of engine and main rotor noise reduction methods. All noise reduction techniques were evaluated in the context of an established mission performance criterion which included consideration of hover ceiling, forward flight range/speed/payload and rotor stall margin.

The existing domestic civil helicopter fleet consists of more than 4000 vehicles with thirty-three different types. Included in this fleet are helicopters ranging in size from the 1600 pound gross weight Hughes 269 to the 42,000 pound gross weight Sikorsky S-64. Powerplants used include single reciprocating (piston) and shaft turbine engines, as well as twin turboshaft installations. While the majority of vehicles now in use are of domestic manufacture, a significant number are foreign made. Civil helicopter annual usage rates range from 360 hours per a/c year, for those vehicles in private use, to over 1200 hours per a/c year for scheduled passenger carriers.

Projection of the domestic civil helicopter fleet to the 1980 time frame indicates that fleet size will increase to over 6000 vehicles. The majority of this growth will be due to continued production of existing vehicle types. However, several new vehicle types, now in the prototype or initial production stage, will be introduced in small but significant numbers by 1980. These new types are all twin turbine powered, and their gross weights and overall design characteristics are well within the ranges of existing vehicle types.

Analytical methods have been developed for: calculating helicopter noise; estimating changes in vehicle design and performance characteristics due to the application of noise reduction methods; and, calculating helicopter life cycle costs. The noise calculation method considers the rotor system, engine and transmission contributions separately then adds these contributions to determine total vehicle noise spectra. Total vehicle noise is calculated in terms of a time history of 1/3 octave band sound pressure level spectra relative to a given observer location

and steady forward flight condition. These spectra are converted to overall sound pressure level, A-weighted sound pressure level, perceived noise level and tone corrected perceived noise level time histories, and are further analyzed to determine effective perceived noise level. Comparison of calculated component (rotor system, engine and transmission) noise levels with available test data indicates good correlation.

Changes in vehicle design and performance characteristics due to noise reduction methodology are calculated with an iterative analytical model which includes the following elements:

- Vehicle airframe weights
- Engine weight and performance
- Vehicle hover performance
- Vehicle forward flight performance
- Fuel load requirements
- Rotor stall margin

This method is used to adjust vehicle airframe, engine and fuel weights, and installed power to compensate for changes in vehicle design, associated with reducing vehicle noise. These characteristics are adjusted based on established hover and forward flight mission performance requirements.

Helicopter life cycle cost is calculated in terms of initial investment cost, indirect operating cost and direct operating cost elements. The cost calculation method uses historically based trends relating the various cost elements to pertinent vehicle design and performance characteristics. Costs are calculated in absolute (1976) dollar terms, and provisions are included for calculating percentage changes in elemental and life cycle costs due to incorporation of noise reduction methodology.

Calculations of baseline noise, cost and performance were made for several existing civil helicopters felt to be representative of the civil helicopter fleet. Total vehicle noise was calculated, in terms of 1/3 octave band sound pressure levels, OASPL, dBA, PNdB, PNLT and EPNL for simulated steady level flight conditions. Component (rotor system, engine and transmission) noise was also calculated, in similar terms, and used to establish the relative significance of each component source with respect to their contributions to total vehicle EPNL. In all cases, the main rotor and engines were found to contribute most.

A survey of state of the art helicopter noise reduction methods was performed and specific methods were chosen for further analytical evaluation. Those methods chosen included techniques applicable to the main rotor and engines only, since these sources were found to be most significant. Main rotor noise reduction methods selected were increased rotor radius, blade chord and blade number and reduced rotor tip speed. The use of exhaust duct treatment was selected for reducing engine noise.

The effects of turbine engine exhaust duct treatment were determined for three differing civil helicopter models, ranging in size from 2500 lb G.W. to 19,500 lb G.W. A range of duct treatments was considered for each study vehicle, with silencer system weights up to approximately 3% of base vehicle gross weight. Trends of silencer weight with vehicle EPNL reduction were calculated, and these trends were similar for the three study vehicles. Maximum vehicle noise reductions achieved with exhaust duct treatment were approximately 3 EPNL, for all vehicles considered.

The impact of engine exhaust duct treatment on vehicle design and performance was calculated, based on the established mission performance requirements. Changes in vehicle gross weight, airframe weight, engine weight, installed power and fuel load induced by exhaust treatment weight and engine performance degradation were determined. Achievement of a 2.5 EPNdB vehicle noise reduction through exhaust duct treatment was shown to result in a 2.8% to 3.4% gross weight growth, a 1.8% to 2.1% airframe weight growth, engine growth of 2.2% to 2.7% in weight and 4.3% to 5.2% in installed power and required fuel load growth of 1.5% to 1.7%.

The impact of engine exhaust duct treatment on life cycle cost was also calculated. Both direct and induced cost changes were considered. A 2% to 3% life cycle cost increase was shown for a vehicle noise reduction of 2.5 EPNL.

A similar study was performed considering the effects of main rotor noise reduction methodology. Increasing rotor radius, blade chord and blade number were evaluated, both individually and in concert with reduced rotor tip speed. Allowable tip speed reduction was predicated on the established rotor stall margin criterion. Rotor radius increases up to 25% were considered. Blade chord was increased up to 50%, and blade number up to twice the number of blades on the baseline rotor. The three study vehicles used for the engine noise reduction evaluation were also used to evaluate main rotor noise reduction methods.

Net noise reduction obtainable with each rotor noise reduction method was calculated, considering rotor design and performance induced growth in vehicle gross weight and rotor thrust. In all cases, the net noise reduction was shown to be small. Induced vehicle design, performance and cost changes, however, were shown to be substantial. On the basis of this unfavorable cost to benefit ratio, it was concluded that the rotor noise reduction methods evaluated were not cost effective means for reducing helicopter noise.

TABLE OF CONTENTS

TABLE OF CONTENTS (Continued)

TABLE OF CONTENTS (Continued)

LIST OF FIGURES

LIST OF FIGURES (Continued)

LIST OF FIGURES (Continued)

LIST OF FIGURES (Continued)

LIST OF FIGURES (Continued)

LIST OF TABLES

LIST OF TABLES (Continued)

INTRODUCTION

The increasing use of commercial helicopters in the community has sharply increased the public's awareness of and reaction to the helicopter's characteristic noise signature. This type of vehicle, which was only a short time ago relegated to use almost exclusively in the military sector, is now finding application in a wide variety of civil missions, many of which require operation over heavily populated areas. The helicopter's economic viability is being proven through the performance of such diverse roles as scheduled passenger carrier, corporate/executive transporter and aerial crane, supporting the construction industry. Additionally, it is being used as a public servant for police work and as an aerial ambulance. It is the increasing use of the helicopter in these roles, coupled with the need to protect the public's quality of life, which has brought about the necessity for a helicopter noise certification rule.

The establishment of a noise certification rule for new design civil helicopters must consider the desires and needs of both the community and the helicopter operator. While the promulgation of a rule restricting helicopter noise to totally unobtrusive levels would be desirable to the community, such a rule could very well severely reduce the helicopter's economic viability and/or limit its utility. Consequently, definition of a reasonable specification requires knowledge of both the communities' subjective acceptance of helicopter noise, and the technological and economic aspects of helicopter noise reduction. The present program deals with the second of these problems, namely, definition of the technological and economic aspects of helicopter noise reduction.

The objective of the present program is to determine both the degree of helicopter noise reduction obtainable in future design helicopters using existing helicopter noise reduction technology, and the cost of applying this technology. In order to satisfy this objective, the following questions must be answered:

(1) What are the sources of helicopter noise and what are the relative contributions of each source to the total helicopter vehicle noise?

(2) What methods exist for reducing the various helicopter noise sources, and how much reduction in total vehicle noise can be achieved with these methods?

(3) What direct and indirect changes in vehicle design and performance are induced as a result of application of these methods?

(4) What changes in vehicle cost result from the induced changes in vehicle design and performance?

A great deal of work in the area of helicopter noise reduction has been performed[1], and this work has led to partial answers to several of the preceding questions. The information available from these studies is not, however, sufficient to completely answer all of the pertinent questions. The function of the present study is to provide these necessary answers, using the available data as a technical base.

SOURCES OF HELICOPTER NOISE

The noise signature of a helicopter is composed of contributions from a number of vehicle components. The main rotor, or rotors, which provide the lift and thrust forces for the vehicle, generate sound by virtue of the inherent aerodynamic forces on the blades. These forces give rise to both periodic and random noise components which appear in the vehicle acoustic spectrum over the entire audible range, generally dominating the signature in the low to mid frequency region.

The noise contribution of the powerplant varies depending upon the type of engine installed. For reciprocating engine powered vehicles, the major powerplant noise source is the pulsating exhaust stream, which radiates noise at frequencies equal to the engine firing frequency and its harmonics. Reciprocating engines also radiate noise due to vibrating structural elements and intake airflow. Noise generation in turboshaft engines results from a number of causes. Both intake and exhaust flows generate noise aerodynamically, due to free turbulence and interaction of turbulence with solid boundaries. Within the engine itself, turbulence associated with the unsteady combustion process results in noise radiation through the exhaust stream, and excitation and reradiation from the engine case. The rotating elements of the engine (compressor and turbine fans) generate noise in a manner similar to that of the helicopter rotors. Engine fan noise is modified, however, by the presence of stators and the fact that these fans are enclosed in a duct.

In a typical helicopter, power from the engine or engines is transmitted to the rotors through a geared transmission system. Noise is generated within this system through the meshing of gear teeth. Forces generated during gear meshing excite shaft vibration which is transmitted structurally to the transmission case through shaft support bearings. Vibration of the case results in noise radiation from both the case itself and attached airframe structure. The gearbox component of vehicle noise consists of multiple pure tones at frequencies equal to gear tooth clash rates and their harmonics.

The relative significance of the various helicopter noise sources depends upon the particular vehicle configuration, its flight condition, the

---

[1] Magliozzi, B., et al, "A Comprehensive Review of Helicopter Noise Literature", DOT/FAA Report No. FAA-RD-75-79, June 1975.

relative orientation of vehicle and observer and the method which is used to evaluate the noise signature. Considering equal weighting of frequency content and moderate observer to source separation, the rotor of a turboshaft powered helicopter generally dominates the overall sound pressure level, with the engine contribution second in importance and the gearbox contributing least. If a reciprocating engine is installed, its contribution may exceed that of the rotor system. This hierarchy is generally valid for conventional helicopters which do not incorporate noise reduction measures.

Vehicle flight condition and vehicle/observer orientation may have a significant effect on relative source importance. All helicopter noise components are highly directional, and directionality as well as source efficiency is influenced by vehicle forward speed. During hovering flight, helicopter rotors exhibit directionality only out of their plane of rotation. However, since all existing helicopters utilize more than one rotor, either in tandem or as a main and tail rotor combination, the total noise contribution of the rotor system will vary about the azimuth. Variation with elevation angle will also occur because of the rotors inherent out of plane directionality. Consequently, depending upon helicopter/observer angular orientation, any of the vehicle noise components may dominate the overall sound pressure level. For the forward flight case, additional complexity is introduced by the fact that the rotors will exhibit both in-plane and out-of-plane directionality.

In general, the contributions of the various helicopter noise sources cannot be quantified using test data because of masking effects. Consequently, analytical methods must be used to define the constituent parts of the vehicle spectrum. Noise spectra for each component source can be calculated with reasonable accuracy using existing aralytical techniques. These component spectra may then be added, resulting in the total vehicle spectrum. In this way the individual source contributions are quantified and their relative significance for any specific vehicle flight condition and observer orientation are determined. This approach has been taken in the present program.

HELICOPTER NOISE REDUCTION

A large body of information has been developed relative to helicopter noise reduction[1]. Methods exist for the reduction of each component noise source and in many cases, these methods have been shown to be effective through direct experimental evaluation. In most cases, however, these methods have been evaluated on an individual component basis only and, consequently, little information exists as to the degree of total vehicle noise reduction which can be achieved through the application of these methods.

This lack of information is due to two factors. First, the expense of deriving this information by experimental means is prohibitive, and the resulting data is difficult to interpret, because in many cases individual noise reduction methods cannot be applied in an isolated manner due to vehicle safety and/or flight performance requirements. Secondly, while this information can be obtained using analytical means, this approach requires the use of a unified helicopter vehicle noise calculation method which, until the present program, has not been available.

An additional factor must be taken into account before a valid assessment of the actual vehicle noise reduction obtainable with these methods can be determined. While significant noise reduction may be theoretically obtainable with a given component noise reduction method, secondary changes in this or some other vehicle component may be required in order to apply the method. These induced changes can, of themselves, cause noise level changes which may either add to or subtract from the theoretically obtainable noise reduction. Determination of the net vehicle noise reduction associated with any component noise reduction method requires consideration of all of these significant induced changes.

To illustrate the significance of this factor, consider the net effect of a change in the helicopter rotor system, for example, the addition of a rotor blade to a multibladed rotor, which would be expected to reduce the rotor noise[1]. Addition of this blade will add incrementally to the rotor system weight, and will also cause an increase in vehicle structural weight. This change may also modify vehicle hover performance and the combined weight and performance change could necessitate a change in installed power, and consequently, engine weight. These changes may also induce changes in power required to cruise and fuel consumption rate during cruise, necessitating a change in fuel load to maintain constant cruise range/speed capability. Given these changes in weight, the rotor thrust requirement at any flight condition could be different with the added blade, and the net noise level change associated with the change in blade number must include the effect of this change in thrust.

Previous efforts to quantify the effects of helicopter noise reduction methods have not generally considered the above induced vehicle changes. In the present program, however, these factors have been considered and accounted for.

INFLUENCE OF NOISE REDUCTION ON HELICOPTER DESIGN

As mentioned in the previous section, induced changes in vehicle design due to the application of component noise reduction methods must be considered before valid estimates of the net effects of these methods can be made. In order to be meaningful, these induced changes in design must be considered in the context of fixed vehicle mission performance criteria. This approach permits the direct comparison of the noise and cost characteristics of existing and reduced noise helicopter vehicles having equal mission capability.

Present generation helicopters have been designed to specific performance requirements, usually specified in terms of both a hover and a forward flight capability. Hover capability is normally stated in terms of ability to sustain a given payload, out of ground effect (OGE) under given conditions of altitude and temperature. Forward flight performance capability may be specified either in terms of the ability to carry a given payload a prescribed distance at a given speed, or in terms of the ability to carry a given payload for a prescribed period of time. These performance requirements define vehicle mission capability, and within this mission capability, vehicle parameters are normally selected on the basis of maximizing the ratio of payload weight to gross vehicle weight, since this tends to minimize vehicle cost.

Future helicopters will undoubtedly be designed in much the same way, using similar performance requirements and design goals. The inclusion of a specific noise limiting regulation will not change the design process itself. Rather, the requirement to limit vehicle noise to a specified value will be treated as an additional performance criterion, impacting vehicle design in much the same way as hover/payload and speed/range/payload performance requirements. Within the present program the influence of noise reduction on helicopter design has been determined in exactly this manner.

INFLUENCE OF NOISE REDUCTION ON VEHICLE COST

While helicopter noise reduction represents a benefit to the community, the induced changes in vehicle design and performance represent, at least potentially, an added cost to the civil helicopter operator. Given the nature and magnitude of these changes in design and performance the associated cost changes may be calculated and directly related to the respective noise reductions. This is a most meaningful relationship since it enables the direct evaluation of the economic cost associated with a given degree of noise reduction. Comparison of these relationships also permits evaluation of the relative cost of the various alternate noise reduction methods.

Within the present program changes in economic cost have been calculated on the bases of total vehicle life cycle cost and its constituent cost elements. Total life cycle cost is the total dollar cost of owning and operating a helicopter vehicle for a specified number of yearly operating hours, for the total expected useful vehicle life. Cost elements which make up the total life cycle cost are the initial acquisition cost, the indirect operating cost and the direct operating cost. Each of these cost elements can be related to one or more of the vehicle design parameters using historically based trending relationships. These relationships have been used in the present program to calculate baseline dollar costs of several existing helicopter vehicles, as well as percentage changes in cost associated with reduced noise configurations of these baseline vehicles.

NOISE REDUCTION CRITERIA

In order for the study results to be meaningful, the degree of obtainable noise reduction must be stated in terms which can be related to community acceptance, which is a subjective quantity. While a significant amount of work has been performed to develop a criteria for evaluating community response to helicopter noise, no universally acceptable criteria exists.[1] Of those criteria which have been suggested for use, however, the effective perceived noise level (EPNL) unit has the widest acceptance. EPNL is presently used as part of FAR Part 36 for the certification of fixed wing subsonic jet transports.[2] In the present program, EPNL is used as the primary noise reduction criteria, although A-weighted sound pressure level (dBA) and overall sound pressure level (OASPL) data are also presented.

The observed noise of a helicopter is a function of both helicopter flight condition and relative observer location. The observed change in noise level due to the application of component noise reduction methods will also, in general, be a function of these variables. This is true because, as pointed out previously, the significance of the various component noise sources is dependent on observer orientation and vehicle flight condition. Variation may also occur because, in many cases, the changes in component noise levels themselves are influenced by these factors. For practical purposes, however, present program efforts have been limited to consideration of only one flight condition and three observer locations.

---

[2] Sperry, W. C., "Aircraft Noise Evaluation", DOT/FAA Report No. FAA-NO-68-34, September 1968.

The flight condition used in the present program is steady level flight at maximum vehicle gross weight and best range cruise speed, at a 300 foot altitude. Observer locations used are five feet above ground level directly below the flight path and 500 feet to either side.

PROGRAM SCOPE

This program was performed in four tasks. The first of these tasks involved determination of the make-up of the existing civil helicopter fleet and projection of this fleet make-up to the 1980 time frame. This survey effort resulted in definition of the numbers and types of helicopters in use as of 1 January 1976, and expected to be in use by 1 January 1980. Also established were the design and performance characteristics of these vehicles. Fleet make-up was categorized with respect to generalized use (mission) categories, and yearly usage rates were determined for each use category.

The analytical methods used to calculate vehicle noise, changes in vehicle design and performance characteristics and cost were developed in the second program task. For the most part, existing analytical techniques for the calculation of helicopter component noise were used. These included separate computer based models for calculating rotor noise, piston engine noise and turbine engine noise. The model for calculating transmission noise was derived during this task of the present program. These individual component models were joined with existing rotor performance and EPNL/dBA/OASPL calculation models to form the required unified total vehicle noise calculation method.

A computer based method for calculating induced changes in vehicle design characteristics was also derived as part of this task. This method consists of a parametric helicopter component weights model which is coupled to simplified hover and forward flight performance calculation models. This task also included the development of an historically based parametric life cycle cost model. These models were used to calculate the baseline noise, performance and cost characteristics for several representative baseline helicopter vehicles selected from the fleet survey data. These calculated baseline characteristics were compared to available test data to validate the analytical methods.

The third task of the program involved a survey of potential helicopter component noise reduction methods and selection of suitable methods for evaluation. Suitability of the various methods was assessed with regard to relative component source significance, which was established through evaluation of the baseline vehicle noise calculations. Consideration of the general applicability of these methods to the various helicopter types was also considered in this selection process, and noise reduction methods thought suitable for only one of these types were not selected for evaluation.

Changes in noise level, vehicle design and cost due to the selected noise reduction methods were calculated in the fourth program task. These efforts were limited to evaluation of main rotor and turbine engine noise reduction methods since it was determined that these component noise sources contributed most to the total vehicle effective perceived noise level, for the large majority of existing and near term new design helicopter vehicles.

REPORT FORMAT

The format of this report reflects the task breakdown of the program. Separate sections dealing with each program task are included. General conclusions are given in the final section.

FLEET SURVEY

A survey was performed to determine the make-up of the domestic civil helicopter fleet in terms of:

(1) Helicopter types (models) in service.

(2) Design characteristics of each helicopter type.

(3) Number of each type in service.

(4) Fleet breakdown by use category.

(5) Average annual usage rate for each use category.

This information was needed to serve as baseline data for the noise reduction trade-off portion of the study. Specifically, fleet make-up by helicopter type and number were used, along with vehicle design characteristics, as a reference for selecting suitable representative vehicle configurations for further study. The vehicle design characteristics were also used to calculate baseline vehicle and component noise levels and performance characteristics. The average annual utilization rate data were used as a reference for selecting the utilization rates evaluated in the life cycle cost analyses.

All of the fleet survey data were derived from information available in the open literature. Fleet make-up by type was derived from information contained in Reference 3, and verified through comparison with similar data given in Reference 4. Design characteristics of each helicopter type were obtained from a number of sources, including References 5, 6,

---

[3] "Directory of Helicopter Operators in the United States, Canada and Puerto Rico", Aerospace Industries Association of America, Inc., November 1975.

[4] "Model Inventory Summary, July 1975", Helicopter Association of America, July 1975.

[5] "Aviation Week and Space Technology - Aerospace Forecast and Inventory", Vol. 104, No. 11, March 15, 1976.

[6] "The World's Current Helicopters - 1976", Interavia, January 1976, pp 68-71.

7, 8, and 9. In cases where required data were not available for a given civil helicopter type, data given for the pertinent military version were used. Where more than one derivative version of a given general helicopter type was found to be in use, the characteristics of the most common version were used.

The following general categories of use were established.

(1) Personal.

(2) Corporate and executive.

(3) Government.

(4) Commercial utility.

(5) Heavy lift.

(6) Scheduled carrier.

The information of Reference 3 was used to generate a breakdown of the domestic civil helicopter fleet according to these categories. In cases where a specific vehicle was indicated as being used in more than one of the established use categories, it was placed in that category which represented its most probable primary use. In this manner, each specific vehicle was ascribed to only one use category, with the sum of the vehicles in all categories of use equal to the total number of helicopters in service.

Average annual utilization rates for each of the established use categories were derived using information given in References 4, 10, and 11. Because of the lack of definitive information regarding civil helicopter utilization the data derived from these sources should be

---

[7] "1969 Encyclopedia of Vertical Lift Craft", Vertical World, Volume 3, No. 11, November 1968.

[8] "Business Helicopters 75", Flight International, 30 October 1975.

[9] "Janes All the World's Aircraft".

[10] "Helicopters Meet New Challenges", Aviation Week and Space Technology, Volume 103, No. 13, September 29, 1975.

[11] Cayce, B. V., "Census of U. S. Civil Aircraft - Calendar Year 1974", Federal Aviation Administration, DOT, December 31, 1974.

considered only as a rough estimate. Precise information of this type was not needed to perform any of the subsequent analyses and therefore no attempt was made to improve the accuracy of these estimates.

1976 CIVIL HELICOPTER FLEET

As of 1 January 1976 the domestic civil helicopter fleet comprised 4112 vehicles including 33 different types of both domestic and foreign manufacture. The make-up and use category breakdown of this fleet are given in Table 1. By far the largest number of helicopters fall into the commercial utility use category which represents 60% of the total fleet. The second largest category is corporate and executive, which includes approximately 18% of the fleet, and this is followed closely by the number in civil government service, which exceeds 15% of the total. The personal use category includes approximatley 5%, while helicopters used for heavy lift and scheduled carrier operations include, respectively, less than 1% and .2% of the total fleet.

With respect to manufacturers, the Bell Helicopter Company has the largest number of helicopters in civil uses. Bell Helicopters constitute almost 60% of the civil helicopter fleet, including six different types (models). Vehicles manufactured by Hughes Helicopters constitute over 17% of the total fleet, with three types presently in service. Sikorsky Aircraft manufactured helicopters contribute approximately 5% to the total. Ten different types of Sikorsky helicopters are presently in use. The only foreign helicopter manufacturer contributing significantly to the domestic civil helicopter fleet is Aerospatiale of France, whose five different models constitute slightly less than 4% of the total. Enstrom Helicopters and Hiller Helicopters each constitute approximately 5% of the total. The remaining four manufacturers account for less than 5% of the total civil helicopter fleet.

Pertinent design characteristics of each of the civil helicopter types identified in Table 1 are given in Table 2. These data include maximum gross vehicle weight and detail characteristics of the engine, main rotor and tail rotor subsystems. Engine data given in Table 2 consists of number, type (reciprocating or turbine), model and manufacturer, and rated shaft horsepower. Rotor system (main and tail) data include rotor type, number of blades, rotor diameter, blade chord and airfoil section, and rotor speed (rpm).

Average annual utilization rates for each of the use categories of Table 1 are presented in Table 3. These range from a high of over 1200 hours/aircraft/year in the scheduled carrier category, to a low of 359 hours/aircraft/year for helicopters in private use.

TABLE 1. CIVIL HELICOPTER FLEET BREAKDOWN

Vehicle		Fleet Breakdown (No. of Vehicles)						
Manuf.	Model	Personal Use	Corp & Exec	Govt	Comm Utility	Heavy Lift	Sch. Carrier	Total Model
Bell	47	43	94	264	880	-	-	1281
	204	-	-	9	10	-	-	19
	205	-	7	11	84	-	-	102
	206	24	245	109	599	-	-	977
	212	-	6	2	30	17	-	55
	214	-	-	-	3	-	-	3
Hugnes	269	38	28	2	2	-	-	70
	300	34	76	140	176	-	-	426
	500	17	63	16	132	-	-	228
Aerosp. (France)	Alou II	-	-	-	33	-	-	33
	Alou III	-	6	-	41	-	-	47
	Lama	1	-	-	22	-	-	23
	Gazz.	1	23	1	25	-	-	50
	Dauph.	-	2	-	1	-	-	3
Sikorsky	S-51	2	-	-	2	-	-	4
	S-52	-	-	-	2	-	-	2
	S-55	-	11	2	54	-	-	67
	S-56	-	-	-	-	1	-	1
	S-58	-	12	10	40	-	-	62
	S-61	-	3	-	6	-	7	16
	S-62	-	10	-	7	-	-	17
	S-64	-	-	-	-	8	-	8
	S-55T	-	-	-	9	-	-	9
	S-58T	-	3	-	10	-	-	13
Enstrom	F-28	24	86	7	87	-	-	204
	280	-	2	-	2	-	-	4
Fairchild	FH-1100	4	13	10	55	-	-	82
Hiller	12	8	29	47	118	-	-	202
	SL	-	-	-	3	-	-	3
Boeing	H-21	-	-	-	-	6	-	6
	V-107	-	-	-	-	7	-	7
Boelkow	BO-105	-	14	2	7	-	-	23
Brantly	B-2	17	19	-	29	-	-	65

TABLE 2. SUMMARY OF CIVIL HELICOPTER VEHICLE PARAMETERS

Vehicle Desc.			Engine Desc.		Main Rotor Parameters								Tail Rotor Parameters				
Manuf.	Model	GW (lb)	Type & No.	Model	SHP	Type	N_b	Dia (ft)	Chord (ft)	Airfoil	Ω (rpm)	Type	N_b	Dia (ft)	Chord (ft)	Airfoil	Ω (rpm)
Bell	47	2950	R/1	LYC-VO435	260	Tet.	2	37.1	.92	0012	355	Tet.	2	5.8	.41	N/A	1810
	204	8500	T/1	LYC-T53-L-11	1100	Tet.	2	48.0	1.75	0012	324	Tet.	2	8.5	.70	0015	1454
	205	9500	T/1	LYC-T53-13B	1400	Tet.	2	48.0	1.75	0012	324	Tet.	2	8.5	.70	0015	1618
	206	3000	T/1	AL-250-C18	317	Tet.	2	33.3	1.08	11% Thick Droop Snoot	394	Tet.	2	5.2	.427	0021	2570
	212	11200	T/2	PW-PT6T-3	1800	Tet.	2	48.2	2.36	0012/0009 Tapered Tip	324	Tet.	2	8.5	.96	0018/0015	1653
	214	13000	T/1	LYC-LTC-4B-8D	2930	Tet.	2	50.0	2.75	Double Swept Tip	324	Tet.	2	9.7	1.0	N/A	N/A
Hughes	269	1600	R/1	LYC-HIO-360-B1A	180	Art.	3	25.2	.56	0015	483	Tet.	2	3.8	.29	0015	4138
	300	1900	R/1	LYC-HIO-360-A1A	180	Art.	3	25.3	.56	0015	483	Tet.	2	3.8	.29	0015	4138
	500	2550	T/1	AL-250-C18	317	Art.	4	26.3	.56	0015	470	Tet.	2	4.25	.394	0014	3309
Aerosp. (France)	Alou II	3650	T/1	TM-AST-IIA	530	N/A	3	33.5	N/A	N/A	N/A	N/A	2	5.9	N/A	N/A	N/A
	Alou III	4850	T/1	TM-ART-IIID	670	N/A	3	36.2	N/A	N/A	N/A	N/A	3	6.3	N/A	N/A	N/A
	Lama	4850	T/1	TM-ART-IIIB	662	N/A	3	36.2	N/A	N/A	N/A	N/A	3	6.3	N/A	N/A	N/A
	Gazz.	4000	T/1	TM-AST-IIIA	592	Rigid	3	34.5	.98	0012	378	Rigid	3	2.3	N/A	N/A	5774
	Dauph.	6170	T/1	TM-AST-18	1020	Rigid	4	37.7	1.15	0012	349	Rigid	3	5.9	N/A	N/A	N/A
Sikorsky	S-51	4985	R/1	PW-R985-B4	450	Art.	3	N/A	N/A	N/A	N/A	N/A	3	6.4	N/A	N/A	1651
	S-52	2700	R/1	FR-0-425-1	245	Art.	3	33	N/A	N/A	N/A	N/A	2	5.5	N/A	N/A	N/A
	S-55	7100	R/1	WR-R-1300	800	Art.	3	53	1.366	0012	212	Tet.	2	8.75	1.3/.55	0016.5/0012	1481
	S-55	30342	R/2	PW-R-2800-54	4200	Art.	5	72	1.792	0012	185	S-Art	4	16.0	1.126	0012	840
	S-58	10513	R/1	WR-R-1820-84	1425	Art.	4	56	1.366	0012	221	S-Art	4	9.3	.612	0012	1358
	S-61	19000	T/2	GE-T58-140-2	3000	Art.	5	62	1.52	0012	203	S-Art	5	10.3	.612	0012	1243
	S-62	7900	T/1	GE-CT-58-110-1	1250	Art.	3	53	1.366	0012	212	Tet.	2	8.75	1.08/.46	0016.5/0012	1483
	S-64	42000	T/2	PW-JFTD-12A-1	8100	Art.	6	72	1.972	0010.91	185	S-Art	4	16.0	1.284	0012	837
	S-65T	7200	T/1	GAR-TEE-331-3W	800	Art.	3	53	1.366	0012	212	Tet.	2	8.75	1.3/.55	0016.5/0012	1481
	S-68T	13700	T/2	PW-PT6T6	1800	Art.	4	58	1.366	0012	221	S-Art	4	9.3	.604	0012	1358
Enstrom	F-28	2150	R/1	LYC-HIO-360-C1A	205	Art.	3	32	.79	0013.5	330	Tet.	2	4.7	.28	0015	2365
	280	2150	R/1	LYC-HIO-360-C1A	205	Art.	3	32	.79	0013.5	330	Tet.	2	4.7	.28	0015	2365
Fairchild	FH-1100	2750	R/1	AL-250-C18	317	Tet.	2	35.4	.85	63$_2$015	369	Tet.	2	6.0	.28/.65	0012	2182
Hiller	12	2300	R/1	LYC-VO-540-C2A	323	Tet.	2	35.4	1.16/.87	0015	370	Tet.	2	5.5	.24	N/A	2230
	SL	3500	R/1	LYC-TIVO-540-A2A	315	Tet.	2	35.4	1.16/.87	0015	370	Tet.	2	5.5	.24	N/A	2230
Boeing	H-21	12500	R/1	CW-R1820-103	1425	Tand. Art	3	44	1.5	0012	258	-	-	-	-	-	-
	V-107	19000	T/2	GE-CT58-110	2400	"	3	50	1.5	0012 Mod	264	-	-	-	-	-	-
Boelkow	BO-105	5070	T/2	AL-250-C20	800	Rigid	4	32.2	.88	23012	424.5	Tet.	2	6.2	.57	N/A	2228
Brantly	B-2	1670	R/1	LYC-VO-360	162	Rigid	3	23.7	.74/.67	0029/0012	470	Tet.	2	4.25	N/A	N/A	2900

TABLE 3. CIVIL HELICOPTER UTILIZATION RATES

Category	Utilization Rate - Hrs/Ac/Yr
Scheduled Carrier	1233
Commercial Utility	465
Heavy Lift	871
Corporate/Executive	627
Government	632
Private	359

1980 CIVIL HELICOPTER FLEET

Projections of the domestic civil helicopter fleet to the 1 January 1980 time frame have been made using manufacturers production estimates contained in References 10, 12, 13 and 14, as well as the general historical trending data of References 3 and 11. These projections consider additions to the existing fleet due to continued production of many helicopter types already in service, plus the introduction of several new types. No consideration was given to reductions in the number of any existing type both because of the difficulty of estimating attrition and/or replacement rates and because of the characteristically unpredictable nature of civil helicopter useful life. In any case, it is felt that such losses would be relatively insignificant over the short span of time covered by the projection.

Table 4 lists the types and use category breakdowns for those helicopter types which are expected to show a significant increase in number by 1 January 1980. Vehicle types not shown in Table 4 are not expected to show changes, either in total number or use category breakdown, relative to their 1976 values, which are given in Table 1. The fleet use category breakdowns of Table 4 have been established simply by maintaining constant ratios of the number of each helicopter type in each category to the total number of that type.

The data of Table 4 include additions due to the introduction of three new helicopter types, the Sikorsky S-76, Bell 222 and Augusta A-109. While several other new vehicle types may be introduced into the civil helicopter fleet by 1 January 1980, it is felt that these will not be introduced in any substantial numbers. Design characteristics of the S-76, Bell 222 and A-109 are given in Table 5.

Based on the projections of Table 4 the domestic civil helicopter fleet will grow from the present (1 January 1976) 4112 vehicles to a 1 January 1980 total of 6042 vehicles. This projection agrees very well with the historical trend of civil helicopter fleet growth given in Reference 3 and presented in Figure 1.

---

[12] "General Optimism Among American Manufacturers", Interavia, January 1976, pp 39-43.

[13] "European Helicopter Manufacturers - Pushing New Products and New Technologies", Interavia, January 1976, pp 27-31.

[14] "The 1976 Helicopter Association of America Meeting", Interavia, March 1976, pp 206-210.

TABLE 4. ESTIMATED CIVIL HELICOPTER FLEET BREAKDOWN, PROJECTED FOR 1 JANUARY 1980*

Vehicle		Fleet Breakdown (No. of Vehicles)						
Manuf.	Model	Personal Use	Corp & Exec	Govt	Comm Utility	Heavy Lift	Sch. Carrier	Total Model
Bell	205	-	13	21	158	-	-	192
	206	35	364	162	890	-	-	1451
	212	-	24	8	192	-	-	224
	222	-	40	-	40	-	-	80
Hughes	300	456	125	232	291	-	-	704
	500	43	160	40	335	-	-	578
Aerospat.	Alou III	-	6	-	44	-	-	50
	Lama	3	-	-	60	-	-	63
	Gazelle	2	54	2	58	-	-	116
Enstrom	F-28	33	117	10	118	-	-	278
	280	-	127	-	127	-	-	254
Sikorsky	S-76	-	2	-	8	-	-	10
Augusta	A-109	-	10	-	30	-	-	40

* Vehicles not shown will not change substantially from 1976 breakdown.

TABLE 5. PARAMETERS OF NEW CIVIL HELICOPTERS EXPECTED IN SERVICE BY 1 JANUARY 1980

Vehicle Desc.			Engine Desc.		Main Rotor Parameters								Tail Rotor Parameters				
Manuf.	Model	GW (lb)	Type & No.	Model	SHP	Type	N_b	Dia (ft)	Chord (ft)	Air-foil	Ω (rpm)	Type	N_b	Dia (ft)	Chord (ft)	Air-foil	Ω (rpm)
Bell	222	6700	T/2	LYC-LTS-101-650C	1200	Tet.	2	40	3.1	N/A	N/A	Tet.	2	N/A	N/A	N/A	N/A
Sikorsky	S-76	9700	T/2	AL-250C30	1400	Art.	4	44	(1.0)	(0012)	300	(Art)	4	8.0	(.25)	(0012)	(1670)
Augusta	A-109	5400	T/2	AL-250C20B	840	(Art)	4	36	N/A	N/A	N/A	(Tet)	2	N/A	N/A	N/A	N/A

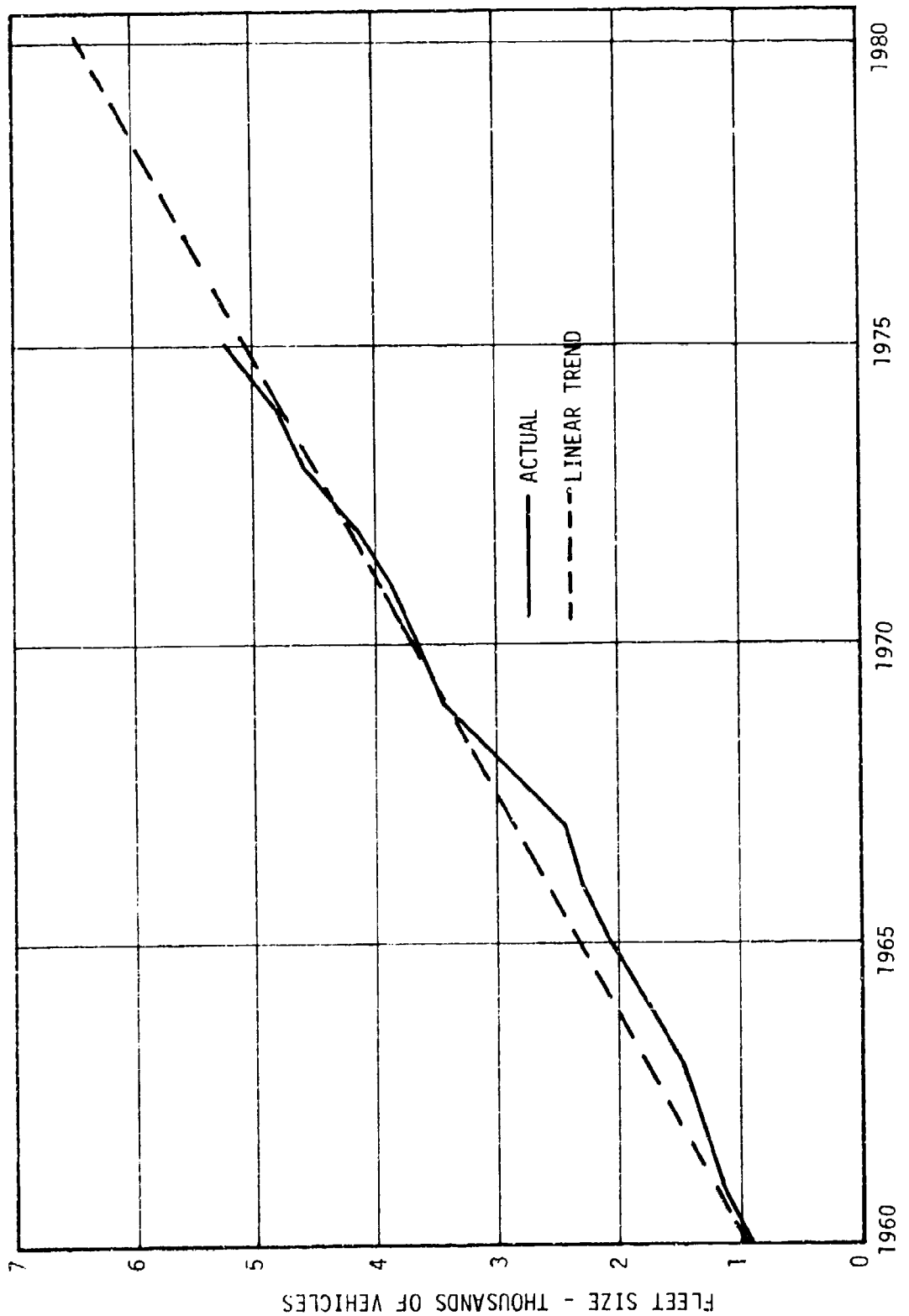

Figure 1. Historical Trend of Domestic Civil Helicopter Fleet Size

As stated previously, no change in relative usage category breakdown is anticipated over the short span of the projection. It is further assumed that annual utilization rates will similarly not change, and that the 1976 utilization rates of Table 3 will be equally applicable for the 1 January 1980 time frame.

SELECTION OF REPRESENTATIVE VEHICLE TYPES FOR BASELINE ANALYSIS

As indicated in Tables 2 and 5 the domestic civil helicopter fleet consists of many diverse types of vehicles. Because of practical limitations in the scope of the present effort it was not considered feasible to consider each of these types on an individual basis, in the subsequent noise trade-off analyses. Consequently, the data of Tables 2 and 5 were reviewed, in conjunction with the fleet breakdown data of Tables 1 and 4, and a small number of representative vehicle types were selected for further study. The specific vehicles chosen were:

- Bell Helicopter models 47, 205 and 206
- Hughes Helicopters models 300 and 500
- Sikorsky Aircraft models S-61 and S-64

Considerations involved in making this selection included the relative similarity of selected vehicle design characteristics to those of other vehicle types, the relative number of vehicles of a given type in service and the probable impact of the noise of a given vehicle on the community. Specifically, the Bell Model 47 and 206 were chosen primarily because these two vehicle types constitute over half the domestic civil helicopter fleet. Furthermore, these two types are very similar in design to several other vehicle types, such as the Fairchild FH-1100 and the Hiller Models 12 and SL.

The Bell Model 205 was chosen primarily because it is representative of a medium gross weight transport helicopter with a high tip speed, two bladed main rotor. This type of rotor design has a tendency to lead to high rotor noise levels, and because of this fact the probable impact of the noise of this vehicle on the community was judged to be higher than would be expected based only on the number in service. The Hughes 300 and 500 were selected because they represent the light single engine, multi-bladed rotor class of helicopter. These two vehicles are similar in design to many of the other helicopter types of Tables 2 and 5, such as the Enstrom F-28 and 280, the Aerospatiale Alouette II and III, Lama and Gazelle and the Brantly B-2.

Selection of the Sikorsky S-61 was predicated on the fact that it is the only civil helicopter presently used in regular scheduled passenger service. Because of its use in this area the probable impact of its noise on the community was judged to be very much higher than the number

in service would indicate. The Sikorsky S-64 was chosen because it is the largest civil helicopter presently in service, and will undoubtedly remain so well beyond the 1980 time frame.

The set of helicopter types selected for study adequately represent the general make-up of the existing and projected civil helicopter fleet. Vehicle gross weights included range from 1900 pounds to 42000 pounds. Both reciprocating and turbine (single and twin) engine powered types have been included, with installed powers ranging from 180 horsepower to over 8000 horsepower. Furthermore, all of the established usage categories are represented by one or more of the selected helicopter types.

ANALYTICAL METHODS

The analytical methods developed and/or adapted for use in the present program fall into three general categories. These are:

(1) Noise calculation.

(2) Vehicle design and performance calculation.

(3) Cost calculation.

With respect to noise, analytical models have either been derived or adapted from existing methods, which enable calculation of the rotor system, engine (turbine and reciprocating) and transmission noise components. These component models have been incorporated in a unified vehicle noise calculation method which has the capability of generating 1/3 octave sound pressure level spectra, as a function of time, at any observer location, for any steady state translational flight condition*. These calculated 1/3 octave spectra are automatically converted to effective perceived noise level (EPNL) and instantaneous A-weighted sound pressure level (dBA), overall sound pressure level (OASPL), perceived noise level (PNdB) and tone corrected perceived noise level (PNLT) units. All noise level calculation methods have been computerized in FORTRAN language for use on the IBM 360 system.

A separate analytical method has been developed to enable the calculation of changes in helicopter design and performance characteristics which result from the application of noise reduction to the various noise producing vehicle components. This method considers this problem in the context of a predesign study, wherein perturbations in one or more of the basic vehicle design parameters are evaluated in terms of their effects on the remaining design parameters. Performance characteristics which are included are out-of-ground effect hover ceiling, forward flight range/speed capability and rotor stall margin. Design parameters considered include vehicle gross weight, payload, airframe component weight, engine weight, fuel load, installed power, cruise speed and engine fuel consumption. The method is used by first establishing a baseline vehicle configuration and specifying a mission performance requirement. Next the design parameter or parameters to be changed are defined and their values assigned. Given these new design parameters, the remaining design parameters are adjusted so that the prescribed performance can be attained. The solution is obtained in an iterative fashion considering the interrelationships of the various design and performance parameters.

* The existing method will not accurately predict hovering flight noise because of inherent limitations in the rotor airloads calculation method which has been used. This deficiency can, however, be overcome by using a more involved airloads calculation method which considers variable rotor inflow.

The vehicle design and performance calculation method has been computerized in the basic language for use on the Hewlett Packard interactive (Time Sharing) computer system.

The cost calculation method used in the present program has been developed from historical helicopter cost data, which relate the three elements of life cycle cost to the various vehicle design parameters. This model considers initial investment cost to be related to vehicle airframe weight and installed engine weight, and indirect operating cost related to vehicle total empty weight. Direct operating cost is assumed to be a function of both empty weight and installed engine power. The cost calculation method permits calculation of both absolute vehicle dollar costs and percentage changes in costs relative to an established baseline helicopter design. Life cycle costs are calculated as a function of both annual usage rate and total useful life. As for the design and performance calculation method, the cost calculation method has been computerized for use on the Hewlett Packard computer.

The analytical methods used in the present program are described in more detail in the following sections of this report. These descriptions are intended only to define in basic terms what the analyses do, how they do it, and what are the nature and extent of any underlying assumptions and approximations. Mathematical derivations have not been included, since, in most cases this information is contained in other sources which are referenced. The general technical bases of all analytical methods are, however, briefly discussed.

HELICOPTER NOISE CALCULATION

A unified, computer oriented helicopter vehicle noise calculation method was developed for use in the present program. This method consists of individual analytical models for each of the vehicle component noise sources including the rotor system, main transmission and engine(s). These individual models are coupled through a control routine which maintains consistency between the individual component noise calculations, and combines the calculated component noise levels to form the total vehicle noise spectra. The total vehicle noise spectra are then analyzed to determine vehicle EPNL, dBA and OASPL characteristics. A schematic diagram illustrating the helicopter noise calculation method is shown in Figure 2.

The rotor system noise calculation method requires detailed information regarding the airload distributions of the various rotors which comprise the system. These data are obtained through the use of rotor performance calculation methods. The main, or lifting, rotor airload distribution is generated with a vehicle trim program (IF trim). Input information consists of detailed vehicle (fuselage and rotor) design characteristics and definition of the desired flight condition. The trim program solves the force and moment equilibrium equations for this desired flight condition and calculates the resulting main rotor airload distribution.

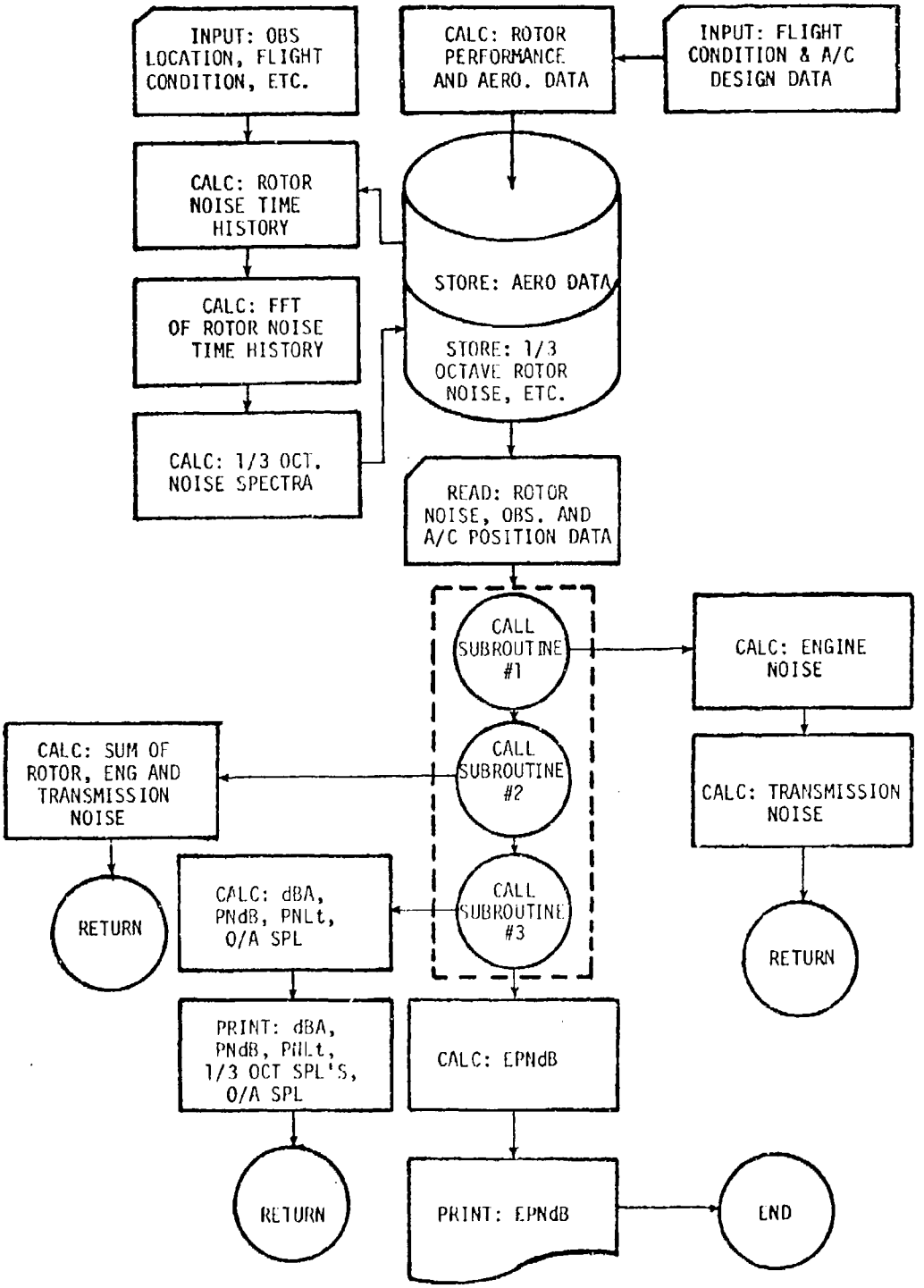

Figure 2. Helicopter Noise Calculation Method

Also calculated are the integrated rotor forces, rotor power required, tail rotor thrust required and the spatial attitudes of the rotor and fuselage. Calculated rotor airload data are permanently stored within the computer, along with other pertinent trim program output data, and this data set is assigned a storage location identifying title.

A similar procedure is used to obtain the auxiliary (tail) rotor airload distribution data needed for the rotor system noise calculation. In this case, however, an isolated rotor performance calculation method is used since vehicle trim is not required. Input data for this program include details of the auxiliary rotor design and aerodynamic characteristics and definition of the desired thrust and flight condition. Rotor thrust used is that calculated by the main rotor trim program. The isolated rotor performance program calculates rotor airload distribution and power required as well as rotor spatial attitude. Program output information required for the rotor system noise calculation is permanently stored within the computer along with a storage location identifying title.

The rotor system component of total vehicle noise is calculated using an analytical method developed by the Research and Applied Sciences in Aeronautics Division of Systems Research Laboratories, Inc. This method, which was developed under the direction of Eustis Directorate, U. S. Army Air Mobility Research and Development Laboratory, is fully described in Reference 15.

Input information required to apply this method include airload distributions, aerodynamic characteristics, geometry and spatial attitudes of each rotor in the system, vehicle geometry, spatial attitude, initial location, and flight condition, and observer location. Given this information, rotor system noise at the observer location is calculated in terms of a sound pressure time history, with instantaneous sound pressures calculated for any specified time increment and total flight time.

Within the present program the rotor system noise calculation method is used in the following manner. First the characteristics of the vehicle under study are defined in terms of the identifying titles for vehicle/main rotor and tail rotor data sets previously stored in the computer. Also defined are the observer location, initial vehicle location, total flight time and time increment of the desired sound pressure time history. Given this input information, the program retrieves the stored rotor airload data, performs the necessary calculations and generates a rotor system sound pressure time history. This time history is then converted to a set of constant bandwidth sound pressure level spectra, using a Fast Fourier Transform routine. These spectra are digitally

[15] Johnson, H. K. and W. M. Katz, "Investigation of the Vortex Noise Produced by a Helicopter Rotor", USAAMRDL TR 72-2, February 1972.

filtered, using a 1/3 octave filter representation, and thereby converted to a set of 1/3 octave bandwidth sound pressure level spectra. Each of these 1/3 octave spectra corresponds to an instantaneous vehicle location. This set of spectra, along with the instantaneous vehicle locations corresponding to each individual spectrum and the observer location, are permanently stored within the computer.

Separate analytical models have been developed for the calculation of reciprocating and shaft turbine engine noise components. These engine noise calculation methods generate 1/3 octave sound power levels in terms of the total engine spectrum and the spectra of the various constituent engine noise sources. Two constituent noise sources, the engine casing and exhaust, are included in the reciprocating engine noise model. The shaft turbine engine noise model is considerably more complex in that it considers four constituent noise sources. These are forward and aft radiated compressor noise, combustion noise and jet noise.

Both engine noise calculation methods require as input definition of engine design characteristics and operating conditions. Given these inputs, the reciprocating engine model calculates the constituent noise source sound power level spectra and sums these to produce the total engine sound power level spectrum, which is then identified and permanently stored within the computer. The shaft turbine model similarly calculates the constituent noise source sound power level spectra, but in this case these spectra are not summed but are identified and stored separately. Retention of the constituent source spectra is required so that directivity corrections which are different for each constituent source can be applied at a later stage in the total vehicle noise calculation program. These corrections are not applied at this stage so that the same basic engine noise data can be used for any vehicle/observer orientation. This is not required for the reciprocating engine noise, since its constituent sources are assumed to be non-directional.

Helicopter transmission noise is calculated using a simplified analytical method derived from a more involved analytical technique, described in References 16 and 17, developed under Eustis Directorate, U. S. Army Air

---

[16] Berman, A. and N. Giansante, "CHIANTI - Computer Programs for Parametric Variations in Dynamic Substructure Analysis", Kaman Aerospace Corporation, 47th Sound and Vibration Symposium, 19-21 October 1976.

[17] Berman, A, "System Identification of a Complex Structure", Kaman Aerospace Corporation, AIAA Paper 75-809, May 1975.

Mobility Research and Development Laboratory sponsorship.[18] The calculation method used generates a 1/3 octave sound power level spectrum for the main transmission, considering each gear mesh as a noise source. Enclosure of the main transmission within the helicopter fuselage is also considered, with source sound power levels reduced by an amount consistent with the nature and extent of transmission shielding, if any. As for the previously discussed noise source spectra, the calculated transmission sound power level spectrum is stored within the computer and identified for later retrieval.

The total helicopter vehicle noise characteristics are calculated by retrieving the previously stored component noise source spectra and combining them in a manner appropriate to the particular vehicle flight condition and observer orientation under study. A control routine is used to perform this operation. Input information required by the control routine consists only of the identifying titles for each of the component noise source data sets which are to be combined. Given this information, the rotor system noise data set is first retrieved. This data set consists of a matrix of 1/3 octave sound pressure level spectra. Also included in this data set are the fixed observer location coordinates and the instantaneous vehicle location coordinates which correspond to each rotor system noise spectrum.

The vehicle and observer location coordinates are used to determine vehicle/observer slant ranges and angular orientations pertinent to each available rotor system noise spectrum. The slant range data derived in this manner are then used to calculate a set of 1/3 octave band attenuation curves which reflect the transmission loss between the vehicle and observer. Included in this calculation are losses due to spherical spreading, atmospheric attenuation and turbulence induced scattering. These attenuation data are needed to convert the calculated engine and transmission sound power levels to sound pressure at the observer locations. They are not needed for conversion of the rotor system component noise, since rotor system noise is calculated directly in terms of sound pressure level at the observer. The vehicle/observer angular orientation data are used to generate 1/3 octave band directivity corrections for each constituent turbine engine noise source.

Next, the engine and main transmission sound power level spectra are retrieved. These are converted into 1/3 octave band sound pressure level spectra, at the observer location, using the previously derived attenuation data and, where applicable, turbine engine source directivity corrections. The engine and transmission sound pressure level spectra

---

[18] Bowes, M. A., "Helicopter Transmission Vibration and Noise Reduction Program", USAAMRDL TR (To be published), 1977, Contract No. DAAJ02-74-C-0039.

derived in this manner are coherent with the previously available rotor system spectra, and each represents the contribution of that component noise source to the total vehicle noise at a given instant in time. These component contributions are then summed, on the basis of power*, at each instant of time for which component noise spectra are available. This results in a set of total vehicle noise spectra, each of which corresponds to the noise received at the observer location at some point in time during a simulated vehicle flight.

The 1/3 octave band sound pressure level spectra generated in the above manner are further analyzed in terms of selected subjective noise rating criteria. Each instantaneous spectrum is evaluated with regard to overall sound pressure level, A-weighted sound pressure level, perceived noise level and tone corrected perceived noise level. The instantaneous tone corrected perceived noise levels are further analyzed, and the effective perceived noise level corresponding to the total subjective impact of the simulated flight is calculated.

The total helicopter vehicle noise calculation method developed in the present program provides the means for analytically determining the effects of physical changes in the individual component noise sources within the context of the total vehicle. The validity of these calculated effects will, of course, be directly related to the accuracy of the noise levels calculated with the individual component noise source models. The technical basis for each of these models is discussed in the following paragraphs. Included in these discussions are comparisons of analytically predicted and measured component noise levels.

ROTOR SYSTEM NOISE CALCULATION

The analytical method used to calculate the rotor system component of helicopter noise is fully discussed in Reference 15. This method equates the helicopter rotor to a set of elemental acoustic dipole sources, which are distributed over the span of each rotor blade. Each elemental source causes a time variant incremental change in local atmospheric pressure, which propagates from the source location at the speed of sound. The combination of incremental pressures due to all of the elemental sources represents the total time variant incremental pressure due to the rotor, and this fluctuating pressure is perceived as rotor noise.

Fundamentally, the elemental acoustic dipole noise sources are due to the aerodynamic forces induced by the rotor blade. At any instant in time, the incremental pressure due to one elemental noise source is given by:

* The sum of two noise sources of equal sound pressure is three decibels higher than either individual source.

$$P = \frac{1}{4\pi C(1 - M_R)^2} \left\{ \frac{1}{R^2} \left[F \cdot V \cdot \cos\theta + \frac{F_R \cdot C \cdot (1 - M^2)}{(1 - M_R)} \right] \right.$$

$$\left. - \frac{1}{R} \left[\dot{F}_R + \frac{F_R \dot{M}_R}{(1 - M_R)} \right] \right\} \qquad (1)$$

where: P = incremental pressure at observer location

C = speed of sound

M_R = component of source Mach No. in direction of observer

R = distance from source to observer

F = magnitude of aerodynamic force

V = magnitude of source velocity

θ = angle between aerodynamic force and source velocity

M = source Mach number

$\dot{F}_R$ = time rate of change of the component of aerodynamic force in the direction of the observer

$\dot{M}_R$ = time rate of change of the component of source Mach No. in the direction of the observer

Those terms in Equation (1) which are multiplied by the factor $1/R^2$ are referred to as near field terms, and their contribution to the incremental pressure (P) decreases rapidly with increasing source/observer separation. Neglecting these terms leaves an expression for far field radiation which is:

$$P_F \approx \frac{-1}{4\pi C(1 - M_R)^2 R} \left[\dot{F}_R + \frac{F_R \cdot \dot{M}_R}{(1 - M_R)} \right] \qquad (2)$$

where: P_F = incremental pressure at significant distance from the source

In Equation (2), P_F is the sound pressure produced by one elemental rotor noise source, at an observer location a distance R from the source. Analysis of Equation (2) reveals the significance of the source variables on the resulting sound pressure.

Neglecting the constants ($4\pi C$) and the observed source separation (R) only four source variables effect the magnitude of induced sound pressure. These are the magnitude and time rate of change of the components of aerodynamic force and source Mach No. in the direction of the observer. Generally, increases in any of these variables will increase the resulting sound pressure. More specifically, the following conclusions can be drawn from Equation (2):

- Both steady and time variant aerodynamic forces may generate sound.
- Steady aerodynamic forces will generate sound only if they are in motion, and only if either the direction or magnitude of that motion varies with time, relative to the point where the sound is observed.
- Non-steady aerodynamic forces may generate sound even if they are not in motion.
- In order for an aerodynamic force to radiate sound to a given observer this force must have either a non-zero component in the direction of the observer, or a non-zero time rate of change in magnitude in the observer direction.

As mentioned previously, the rotor system noise calculation method used in the present program considers a number of elemental noise sources distributed over the span of each rotor blade. This method uses Equation (1) to calculate the sound pressure due to each of these elemental sources. The combination of these elemental contributions takes into account the retarded time effects associated with the fact that the individual sources are spatially distributed over an extended area equal to the rotor disk area. Because of this fact, the distances between the various elemental sources and the observer location are different, and the time required for the incremental pressures to propagate from these sources to the observer location are not equal. Therefore, incremental pressures generated at the element sources at the same instant in time reach the observer at differing times. The present analysis accounts for this effect by determining appropriate source locations for a given unique observer time, and using values for the required aerodynamic force and Mach No. variables of Equation (1) specific to these source locations.

The problem of retarded time effects is further compounded in the present analytical method, because this method accounts for multiple source to observer transmission paths due to ground reflection. This adds considerable complexity to the problem, since with this consideration, the same elemental source will contribute two incremental pressures to the instantaneously observed total sound pressure, and these will have been generated at two differing (retarded) times and from two different spatial coordinates. Nonetheless, the problem is tractable, given the appropriate geometrical data, and is handled by the present analytical method.

The use of Equation (1) and Equation (2) to calculate rotor sound pressure requires knowledge of rotor induced aerodynamic forces and blade motions. The present analysis assumes aerodynamic forces of two basic types. The first type includes all forces developed by the blade section in the generation of rotor lift and drag. These distributed lift and drag forces may be either steady or periodically variant at a rate proportional to the rotor rotation rate, and they are responsible for the discrete frequency components which appear in the rotor noise spectrum.

The second type of aerodynamic force considered in the present analytical method is the force induced on the blade section due to the shedding of vortices. These vortices are shed at a rate which is related to local blade section geometry and flow conditions, and which is not related to the rotor rotation rate. The forces induced by vortex shedding are, therefore, periodic with regard to local conditions which are different at each blade spanwise station, and which also vary with time as the blade travels about the azimuth. Because of the variation in force periodicity with time and spanwise location, the vortex shedding induced forces do not contribute discrete frequency components to the rotor noise spectrum, but are responsible for the broad band content of rotor noise generally referred to as vortex noise.

The present analysis calculates the required aerodynamic forces, as well as blade motions, based on data generated using separate rotor performance calculation methods. The rotor performance calculation methods used are discussed in the following section of this report. These methods calculate the spanwise and azimuthal distributions of rotor blade angle of attack, blade resultant velocity and induced inflow, as well as all required information pertaining to vehicle and rotor motions and attitudes. This information is used, in conjunction with known blade airfoil characteristics, to calculate the rotor rotation rate related lift and drag force distributions, and the components of rotor noise due to these forces. The vortex shedding induced aerodynamic force distributions are established, using the same input information, based on an empirically derived equation which relates the vortex shedding induced force at any blade station to the local angle of attack and Mach number. The equation used is:

$$F_V = 2(1 - M)(1 + (\alpha/4)^2) \qquad (3)$$

where: F_V = vortex shedding induced aerodynamic force

M = local Mach No.

α = local angle of attack

This equation is valid for local Mach numbers less than one, and local angles of attack below the stall angle.

The preceding discussion of the rotor system noise calculation method is intended only to briefly summarize the analytical basis for this method. As stated previously, a more thorough description of this method is contained in Reference 15. Additional information pertaining to this method is given in References 19 and 20, which also present comparisons of calculated rotor system noise levels with measured data. Selection of this method for use in the present program was predicated on the following features, which are not available in other existing rotor noise calculation techniques:

(1) Representation of broad band rotor noise as due to vortex shedding induced aerodynamic force components, which removes the requirement to calculate higher harmonic periodic lift and drag force distributions.

(2) The capability of simultaneously considering the noise contributions of more than one rotor in a multiple rotor system, which inherently includes the effects of acoustic interactions between main and tail or tandem rotors.

(3) Consideration of ground reflection effects.

Within the present program, the rotor system noise calculation method was applied in the following manner. Ten spanwise distributed elemental noise sources were defined for each blade, for each rotor studied. Aerodynamic

[19] Johnson, H. K., "Development of a Technique for Realistic Prediction and Electronic Synthesis of Helicopter Rotor Noise", USAAMRDL TR 73-8, March 1973.

[20] Johnson, H. K., "Development of an Improved Design Tool for Predicting and Simulating Helicopter Rotor Noise", USAAMRDL TR 74-37, June 1974.

characteristics, in terms of local angle of attack, resultant velocity and inflow angle, were calculated for each elemental source (blade station) for twelve azimuth angles. Based on these input data, rotor noise was calculated in terms of a finite duration sound pressure time history for several time intervals within a total simulated flight duration. Pressure time histories of .1 second duration were determined at time intervals of one second. Within each time history, instantaneous sound pressures were calculated at increments of .00039 seconds, resulting in 256 instantaneous sound pressures for each time history. The discontinuous, but highly detailed, sound pressure time histories developed in this manner were assumed to be representative of the instantaneous sound pressure at each one second time interval. These time histories were Fourier analyzed, using a Fast Fourier Technique, to establish 10 Hz constant bandwidth frequency spectra for each interval. Sufficient incremental data was available to construct spectra covering the frequency range of 10 Hz to 1KHz. These constant bandwidth spectra were converted to 1/3 octave band spectra using a digital representation of the 1/3 octave filter characteristic. Rotor noise spectra covering the range of 1/3 octave band center frequencies of 50 Hz to 1KHz, were derived in this manner, at one second intervals, for a simulated flight duration of, typically, 30 seconds. This resulted in 30 1/3 octave band rotor noise spectra per simulated flight.

Generation and processing of the analytically calculated rotor noise data in the preceding manner imposes definite limitations on the resulting rotor noise spectra. First, and most importantly, only sufficient time history data is generated to produce 1/3 octave spectra up to 1KHz, while in actuality the rotor will generate noise over the entire audible frequency range. This limitation was imposed in order to maintain a reasonable machine computation time and its validity is predicated on the assumption that vehicle noise sources other than the rotor system will dominate above 1KHz. While this assumption cannot be verified through available test data, analytical calculations made in the present program do tend to support its validity. These efforts are discussed in a subsequent section of this report.

The second limitation in these data relates to the fact that spectra are generated discontinuously, at discrete points in time. Using these spectra it is not really possible to determine the value of peak noise levels occurring during the simulated flight, nor the time when the peak occurs. This limitation, however, is felt to be of minor importance both because of the relatively short, one second, time interval used and because the generated data are to be used for comparative purposes only, to evaluate changes in noise level caused by changes in vehicle component design. As for the limitation on frequency range, this limitation was imposed in order to minimize machine computation time.

CORRELATION OF ROTOR SYSTEM NOISE CALCULATIONS

Extensive measured helicopter noise levels are available, in References 21 and 22. These measurements were made using standard and modified versions of the Hughes/Army model OH-6A and Sikorsky/Navy model SH-3A helicopters. These vehicles are military versions of the Hughes Model 500 and Sikorsky Model S-61 civil helicopters, which are among the vehicles under study in the present program. For this reason, the data of References 21 and 22 were used to determine the degree of correlation obtained with the rotor system noise calculation method. To provide comparative analytical data, calculations of the rotor system noise components for these two vehicles were made, for vehicle configurations, flight conditions and observer (measurement) locations as nearly as possible identical to those tested*.

Figure 3 shows the comparisons of calculated rotor noise with the measured S-61 vehicle noise levels taken from Table 9 of Reference 22. Both measured and calculated data refer to steady level flight at 200 feet altitude and 120 knots airspeed. Vehicle gross weight is 15576 pounds. Figure 3A relates to an observer directly below the aircraft flight path, while Figures 3B and 3C are for an observer 500 feet to the port and starboard sides, respectively. The tail rotor of the S-61 is on the port side of the aircraft.

The measured and calculated S-61 noise spectra presented in Figure 3 show reasonable agreement over most of the frequency range where rotor system noise can be expected to be dominant in the vehicle spectrum. Above 500 Hz, other vehicle noise sources, primarily the engine(s), contribute significantly, and this is believed to be the reason why the measured spectra of Figure 3 tend to exceed the calculated spectra in this frequency range. Furthermore, the trends of noise level with frequency shown in Figure 3 tend to validate the assumption, discussed previously, that the contribution of rotor system noise can be neglected above 1KHz. Lack of good correlation in the low frequency range, below 100 Hz, which is indicated in Figures 3A and 3B, is not readily explainable, but this is not considered to be a significant problem within the

* Insufficient data is given in References 21 and 22 to establish actual vehicle trim conditions flown. Noise calculations were made on the basis of a normal trim condition, with a nominal a/c center of gravity.

[21] Henderson, H. R., R. J. Pegg and D. A. Hilton, "Results of the Noise Measurement Program on a Standard and Modified OH-6A Helicopter", NASA TN D-7216, September 1973.

[22] Pegg, R. J., H. R. Henderson and D. A. Hilton, "Results of the Flight Noise Measurement Program Using a Standard and Modified SH-3A Helicopter", NASA TN D-7330, December 1973.

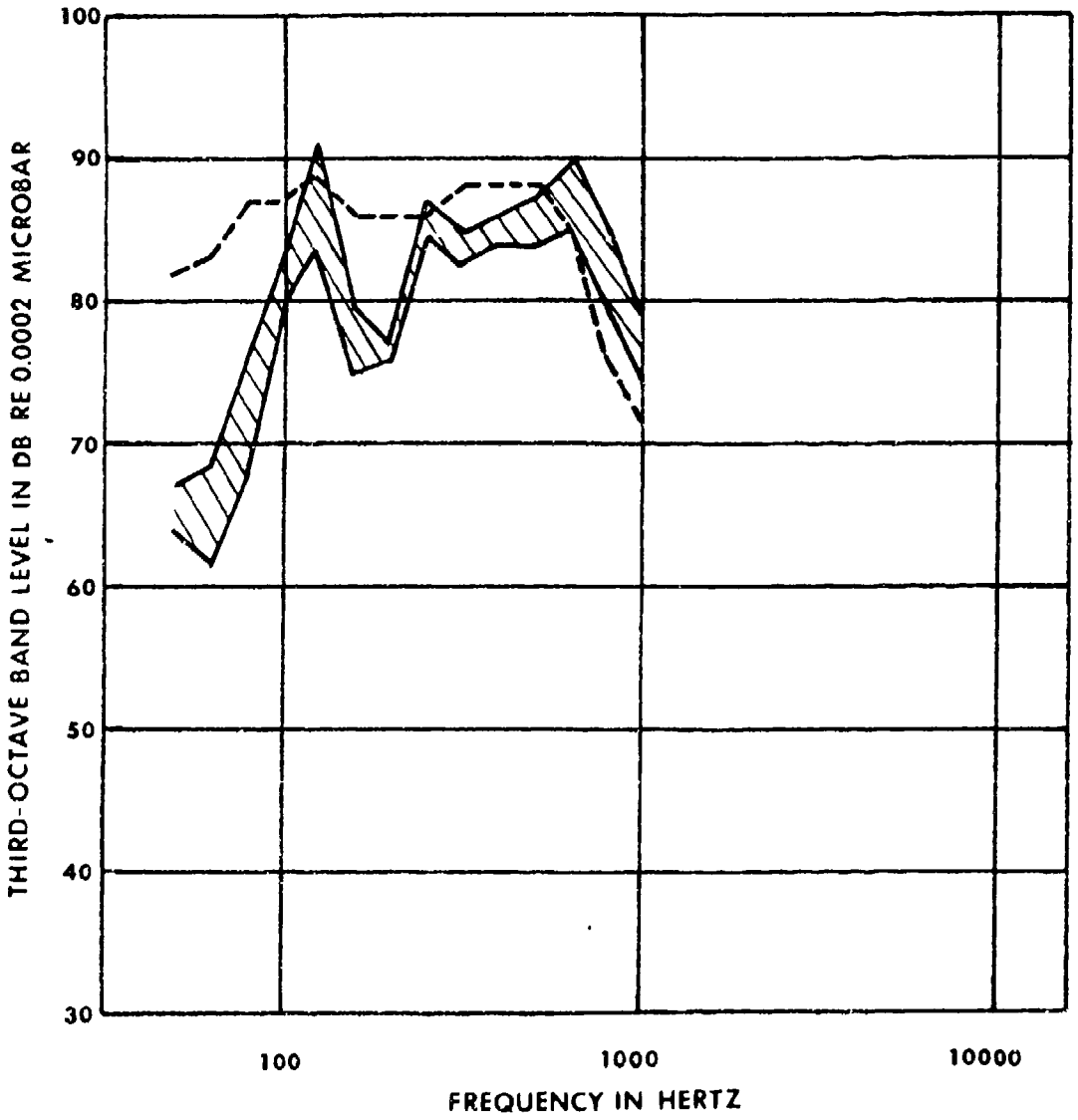

A. Fly-Over, 200 Ft Altitude

Figure 3. Comparison of Measured and Calculated SH-3A (S-61) Rotor Noise, 120 Kts S.L. Flight

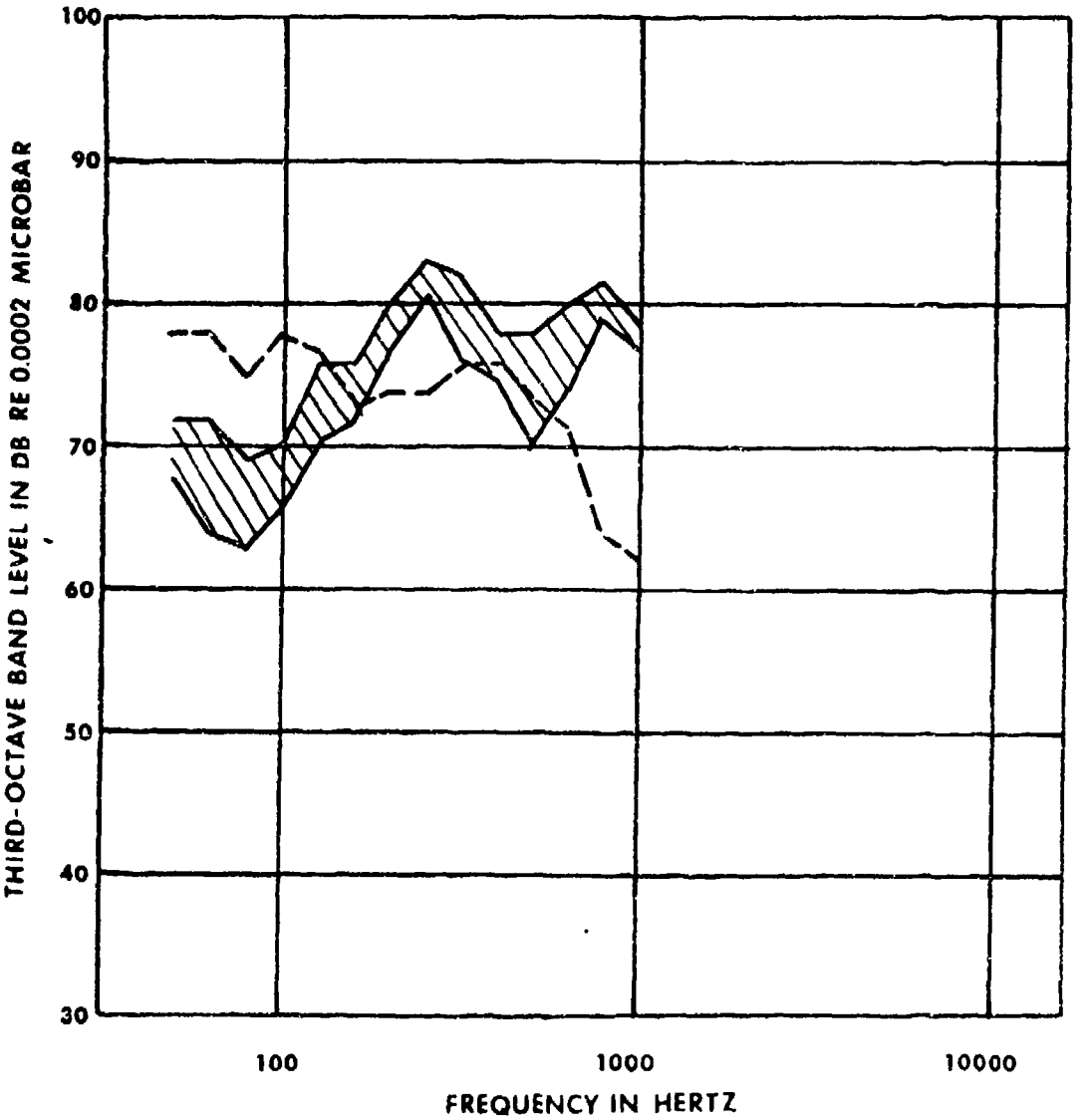

B. Fly-By, 200 Ft Altitude,
500 Ft to Port Side

Figure 3. Comparison of Measured and Calculated SH-3A (S-61) Rotor Noise, 120 Kts S.L. Flight - Continued

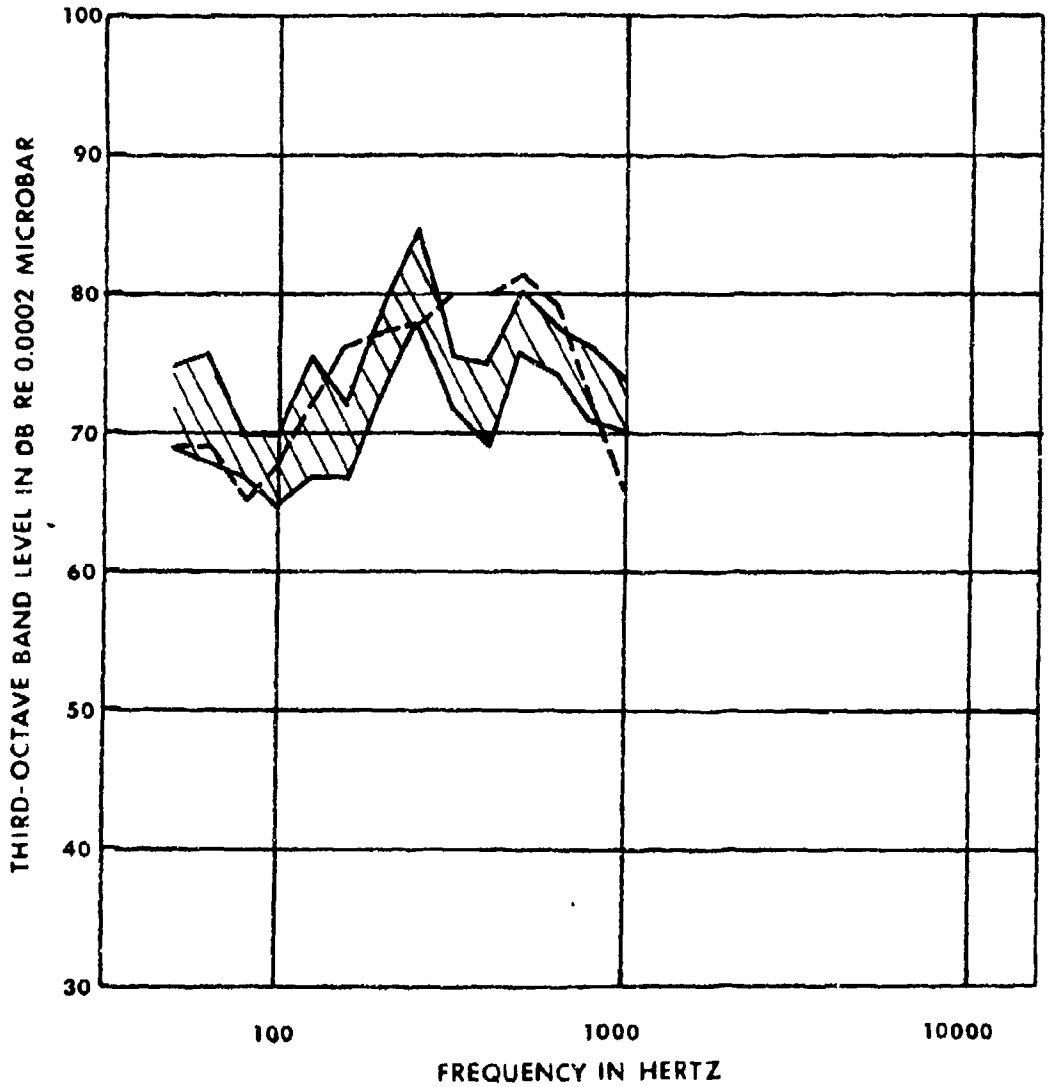

C. Fly-By, 200 Ft Altitude,
500 Ft to Starboard Side

Figure 3. Comparison of Measured and Calculated SH-3A (S-61) Rotor Noise, 120 Kts S.L. Flight - Concluded

present program, since noise in this frequency range does not materially contribute to any of the subjective noise criteria used in the present study.

Comparisons of measured and calculated H-500 noise spectra are shown in Figure 4. These data relate to a steady level flight condition of 100 knots airspeed at 100 foot altitude, with a vehicle gross weight of 2407 pounds. Figure 4A refers to an observer (measurement) location directly below the aircraft flight path, while Figures 4B and 4C are for observer locations 500 feet to the port and starboard sides, respectively. The H-500 tail rotor is also located on the port side of the aircraft.

The degree of correlation in the fly-over spectra of Figure 4A is similar to that shown previously for the S-61. Correlation of fly-by noise spectra, shown in Figures 4B and 4C is, however, substantially worse than that shown previously. This lack of good correlation is believed to be due to an inherent limitation in the analytical noise calculation method, which does not permit valid noise estimation for observer locations which are very nearly exactly in-plane of the rotor.

While some disagreement exists with regard to the exact characteristics of rotor noise directionality, the existence of a well defined minimum near the rotor plane is universally accepted. This minimum can be very sharp with large changes in noise for small changes in observer orientation about the rotor plane. The present analysis method treats this directionality characteristic in an exact manner, as do most, if not all other analytical rotor noise calculation methods. In reality, however, the theoretical directionality of the rotor is obscured somewhat due to acoustic refraction. Rotor noise directionality is also somewhat difficult to interpret from measured data, because the orientation of the rotor disk is not absolutely fixed in flight, but experiences perturbations due to gust loading and small control input changes. These factors make correlation of measured and analytically calculated noise difficult to obtain, for measurement points which are close to the plane of the rotor. The observer locations shown in Figures 4B and 4C are less than 12 degrees from the rotor disk, and this is believed to be the reason why poor correlation is shown in these figures.

This is not felt to be a serious problem within the context of the present program, since the sideline observation points which are used are approximately 30 degrees from the rotor plane.

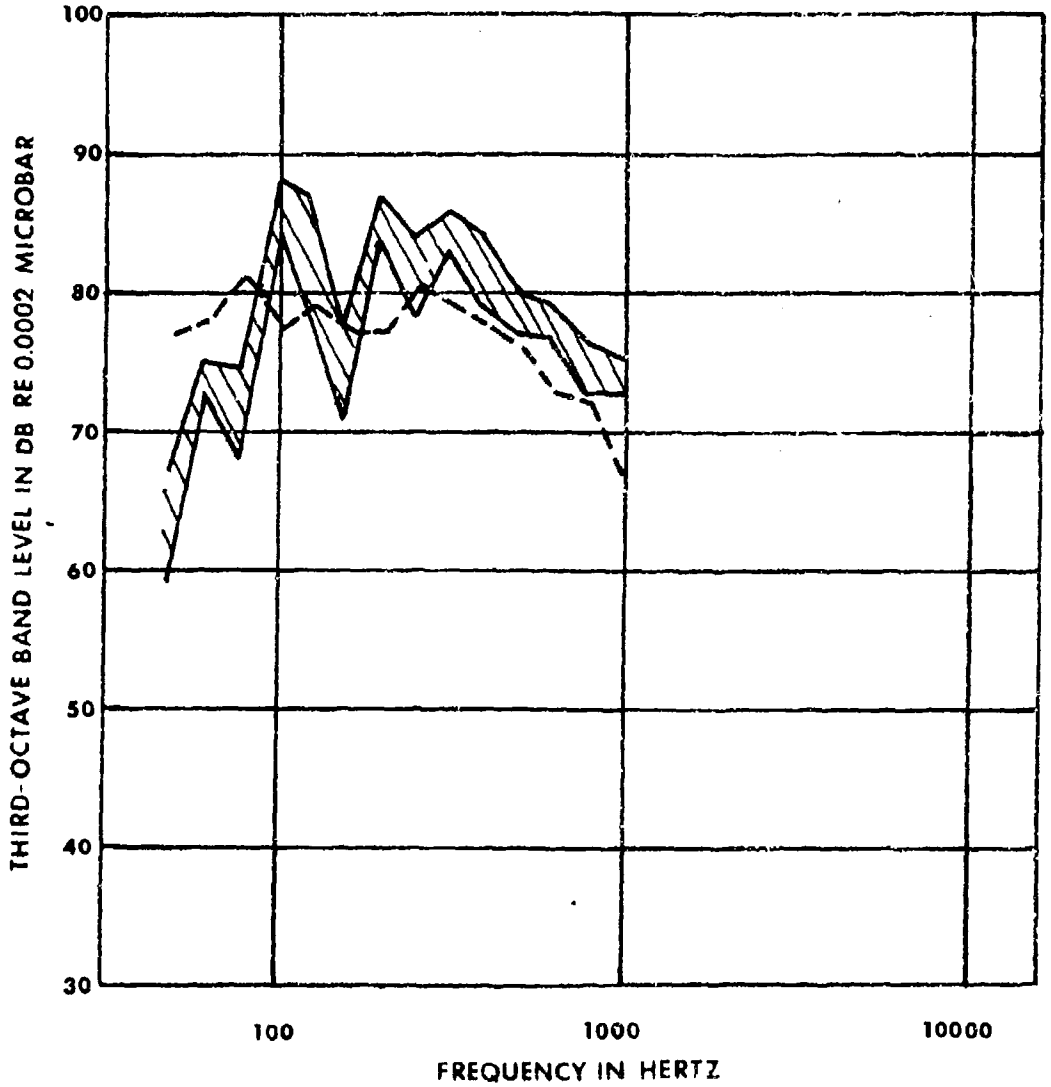

A. Fly-Over, 100 Ft Altitude

Figure 4. Comparison of Measured and Calculated OH-6 (H-500) Rotor Noise, 120 Kts S.L. Flight

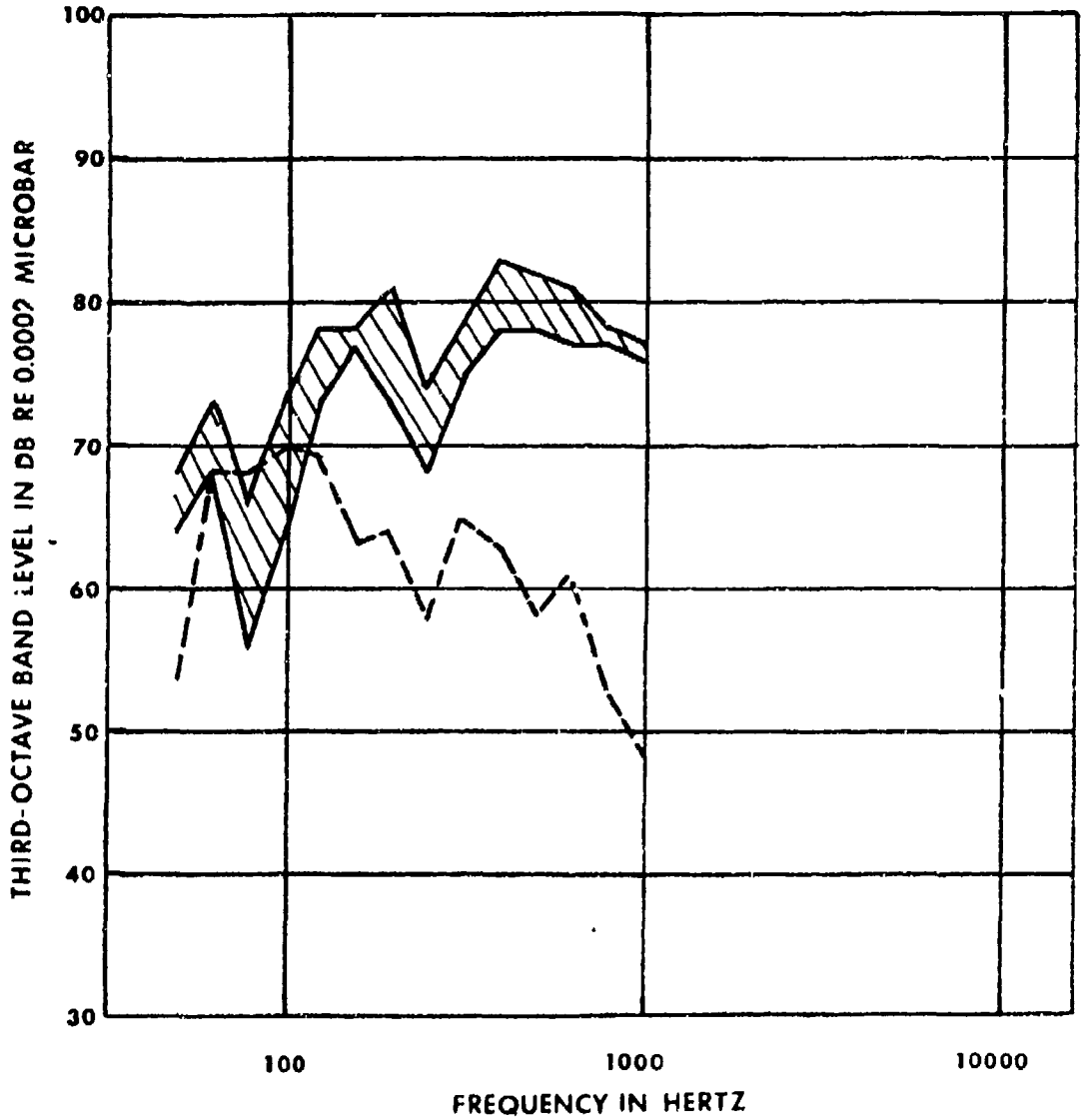

B. Fly-By, 100 Ft Altitude,
500 Ft to Port Side

Figure 4. Comparison of Measured and Calculated OH-6 (H-500) Rotor Noise, 120 Kts S.L. Flight - Continued

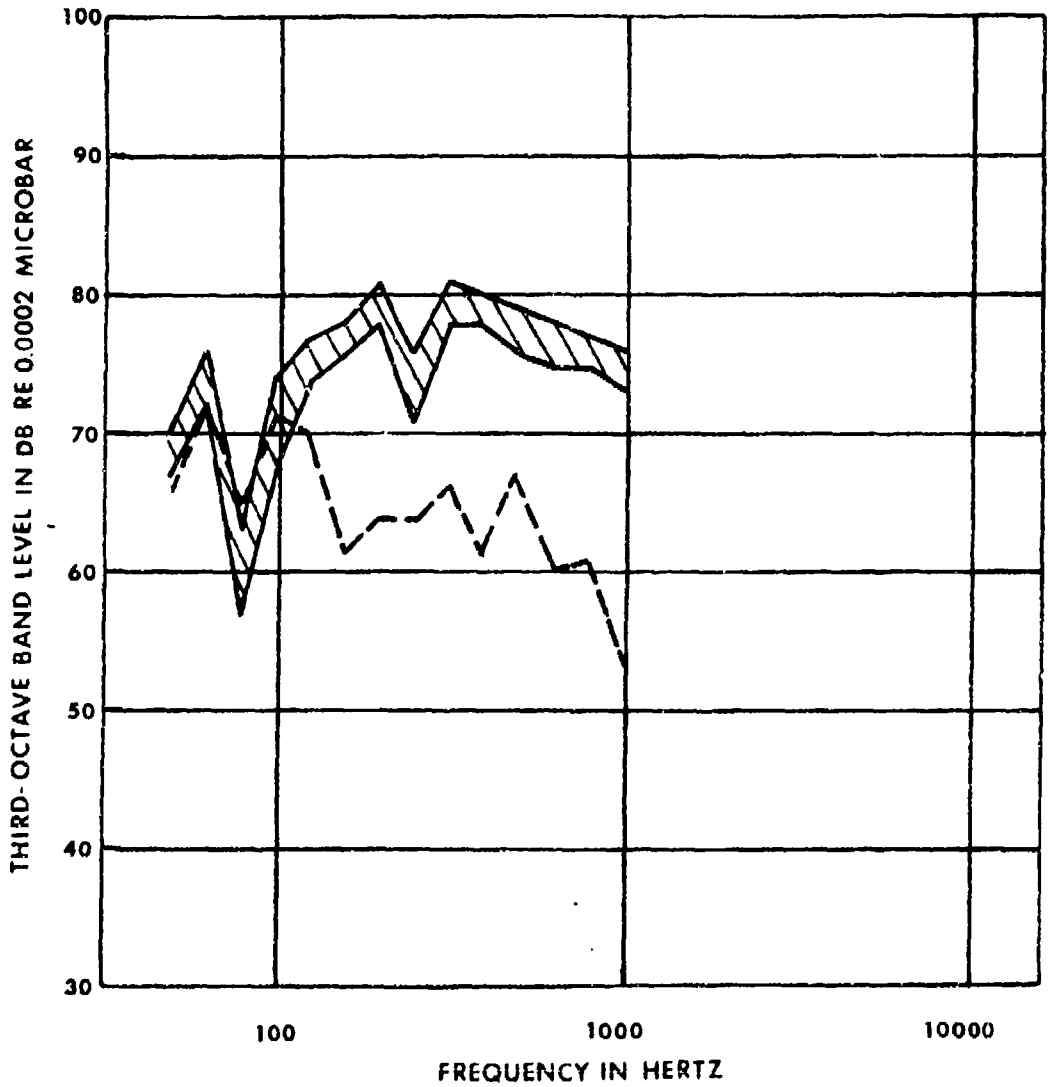

C. Fly-By, 100 Ft Altitude,
500 Ft to Starboard Side

Figure 4. Comparison of Measured and Calculated OH-6 (H-500) Rotor Noise, 120 Kts S.L. Flight - Concluded

ROTOR PERFORMANCE AND AIRLOAD CALCULATION

The rotor aerodynamic data required for the rotor system noise calculation method were generated using analysis techniques developed from the fundamental work of Reference 23. The specific methods used in the present program were adapted from existing techniques, which have been in use at Kaman Aerospace Corporation for a number of years. While several distinct computerized methods have been used, these methods all have the same technical foundations, which will be reviewed in general terms only. A more thorough review of these methods is presented in Reference 24.

The rotor system noise calculation method discussed in the previous section requires, as input data, spanwise and azimuthal distributions of rotor blade local angle of attack, resultant velocity and inflow angle, for each rotor in the system. Also required as inputs are the blade motions, in terms of the azimuthal distributions of blade flapping angle and flapping velocity, and the rotor spatial orientation. In the present program these data are generated in two steps, the first dealing with the main (lifting) rotor and fuselage combination, the second dealing with the auxiliary (tail) rotor.

Main rotor aerodynamic data are calculated using a vehicle trim analysis, which establishes force and moment equilibrium between the main rotor and fuselage. This analysis considers the tail rotor only to the extent that the tail rotor thrust required to balance main rotor torque (and any fuselage induced lateral forces) is calculated. The forces and moments considered are shown in Figure 5.

Input data required for the vehicle trim analysis includes all fuselage and main rotor geometric, aerodynamic, mass, and inertial characteristics. Given these data, forces and moments due to the fuselage are balanced by rotor induced forces and moments based on a prescribed steady flight condition. First, the rotor is placed in flapping and feathering equilibrium for an initially estimated blade collective pitch setting. Only rigid body flapping is considered, and for the present program, a uniform inflow distribution is assumed. Once rotor equilibrium is established, rotor airloads are calculated and integrated to determine the net forces and moments generated by the rotor.

The forces and moments generated by the fuselage are calculated based on the given flight condition, fuselage characteristics and an assumed

[23] Gessow, A. and A. D. Crim, "A Method for Studying the Transient Blade-Flapping Behavior of Lifting Rotors at Extreme Operating Conditions", NACA TN 3366, January 1955.

[24] Lemnios, A. Z. and N. Giansante, "The Dynamic Behavior of Rotor Entry Vehicle Configurations. Volume I - Equation of Motion", NASA CR-73390, February 1969.

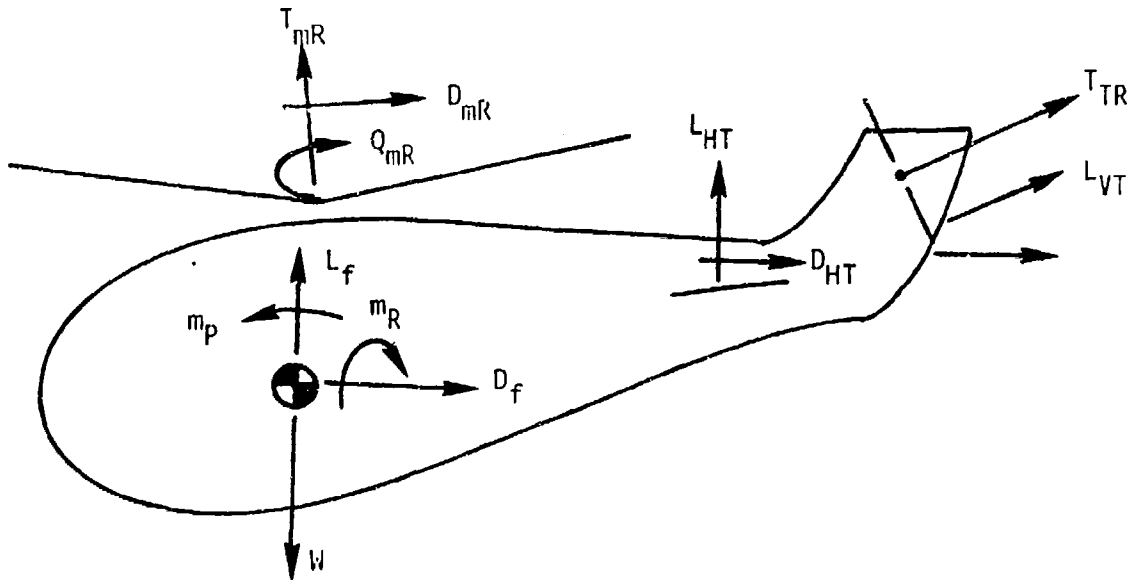

where: T_{mR} = main rotor thrust

D_{mR} = main rotor drag

Q_{mR} = main rotor torque

L_f = fuselage lift

D_f = fuselage drag

W = vehicle weight

L_{HT} = horizontal tail lift

D_{HT} = horizontal tail drag

L_{VT} = vertical tail lift

D_{VT} = vertical tail drag

T_{TR} = tail rotor thrust

m_P = fuselage pitch moment

m_R = fuselage roll moment

Figure 5. Helicopter Trim Forces and Moments

initial value of fuselage attitude. The net forces and moments due to the fuselage are then compared to the forces and moments generated by the rotor. Based on this comparison, rotor control inputs and fuselage attitude are changed from their initial values until rotor and fuselage forces and moments are put in equilibrium. The rotor aerodynamic distributions required for the rotor system noise analysis are calculated based on this trimmed flight condition and stored for later retrieval by the rotor noise program.

The main rotor/vehicle trim analysis also calculates main rotor torque and power required, as well as tail rotor thrust required. The former data is used to perform engine and transmission noise analyses, while tail rotor thrust required is used to calculate tail rotor performance and airload distributions. These required tail rotor aerodynamic characteristics are generated using an analytical method which is similar to that used to obtain main rotor/vehicle trim. In this case, however, tail rotor generated thrust is made equal to required tail rotor thrust for an assumed zero rotor angle of attack, and the data needed for the rotor noise analysis is calculated based on this equilibrium rotor configuration.

The rotor performance and airloads calculation methods used in the present program provide a reasonably precise estimate of rotor angle of attack, resultant velocity and inflow angle distributions. The degree to which these calculations reflect the real life situation is, however, somewhat limited by the basic assumptions of the analysis. Since only rigid body blade motions are assumed, the higher harmonic motions and airloads are not calculated. This is not considered a serious drawback, however, because the rotor noise analysis calculates high frequency rotor noise as due to vortex shedding effects, and not higher harmonic airloads. The assumption of uniform rotor inflow, on the other hand, may be a major shortcoming, particularly with regard to the calculation of tail rotor aerodynamics. The assumption of uniform inflow is predicated on undisturbed flow conditions, both ahead of and behind the rotor. For the tail rotor the presence of the tail fin disturbs the flow through the rotor and, more importantly, tail rotor flow is affected by the main rotor wake and, usually, the engine exhaust. These factors tend to bring into question the assumption of uniform tail rotor inflow, and may cause errors in noise levels calculated using aerodynamic characteristics based on this assumption. Unfortunately, however, the actual conditions of tail rotor flow are not well understood and analytical methods for modeling these conditions are beyond the present state of the art. Furthermore, the assumption of uniform rotor inflow for high speed forward flight conditions is a universally accepted approximation whose limitations, if not quantitatively known, are at least qualitatively understood.

ENGINE NOISE CALCULATION

The existing civil helicopter fleet includes both reciprocating (gasoline/piston) and shaft turbine engine powered vehicles. Separate analytical methods were developed for calculating the noise produced by these two types of engines.

Shaft Turbine Engine

Shaft turbine engines have three principal noise sources:

- Combustion noise
- Compressor noise
- Exhaust jet noise

Methods for predicting sound power levels from these three noise sources, as well as directivity corrections, are presented in this section.

Compressor Noise Prediction

Compressor noise is radiated both forward and rearward from the engine. Its noise spectrum consists of discrete frequency components at the compressor blade passage frequency, and its harmonics, along with broad band noise. Since these two sound generating mechanisms are independent of each other, they are predicted separately.

The method used herein for predicting compressor noise is based upon work originally performed by Smith and House[25] and later modified by Grande, et al[26]. This method provides independent equations for harmonic and broad band noise and includes rotor-stator separation and compressibility. The equations for maximum linear sound pressure levels at a distance of 100 ft for a single stage compressor are as follows:

$$(SPL)_{\text{Discrete Tone}} = 85 + 50 \log [U_r/1000] + 10 \log [\dot{m}(c/s)^2] + \Delta F \quad (4)$$

[25] Smith, M.J.T. and M. E. House, "Internally Generated Noise From Gas Turbine Engines: Measurement and Prediction", Journal of Engineering for Power, Trans. of ASME (April 1967), pp 177-190.

[26] Grande, E., D. Brown, L. Sutherland, and R. Tedrick, "Small Turbine Engine Noise Prediction, Volume II, Noise Prediction Methods", Tech. Report AFAPL-TR-73-79, Volume II December 1973

$$(SPL)_{Broad\ band} = 75 + 50 \log (U_r/1000) + 10 \log [\dot{m}(c/s)_{mean}]$$

$$+ \alpha_{mid} + 10 \log [U_a/U_r] + \Delta F \qquad (5)$$

where: U_r = relative blade tip speed (ft/sec)

U_a = axial flow velocity (ft/sec)

s/c = rotor-stator separation at tips, in upstream blade chords

α_{mid} = mean incidence deviation (in deg) from the blade lift curve peak

ΔF = flow correction factor (discussed in the next paragraph)

To develop the complete spectrum, the discrete frequency components are assumed to decay as 20 log n, where n is the harmonic number[27]; a representative spectrum shape is assumed for the broad band noise.

The flow correction factor given by Smith and House seems to be inaccurate. This is attributed to the assumption that a direct relationship exists between the axial velocity of the flow and the absolute velocity of the blade tip. Grande, et al[26], derived a new set of factors which are based on the local relative velocity rather than that of tip relative velocity. Therefore, the forward and rearward noise is obtained by integrating over the blade sweeping area. The factors are as follows.

$$\Delta F = 10 \log \eta_t \qquad \text{for forward propagation}$$

$$= 10 \log (2 - \eta_t) \qquad \text{for rearward propagation,} \qquad (6)$$

where:

$$\eta_t = 1 - \frac{2}{3c_1} \frac{[(c_1 r_t^2 + c_2)^{3/2} - (c_1 r_h^2 + c_2)^{3/2}]}{(r_t^2 - r_h^2)} \quad \text{for } M_t < 1$$

$$= \left(\frac{r_s^2 - r_h^2}{r_t^2 - r_h^2}\right) \left[1 - \frac{2}{3c_1} \frac{[(c_1 r_s^2 + c_2)^{3/2} - (c_1 r_h^2 + c_2)^{3/2}]}{(r_s^2 - r_h^2)}\right] \text{for } M_t > 1$$

[27] Goldstein, M. E., "Aeroacoustics", NASA SP-346, November 1974.

where: M_t = tip Mach number

r_h = hub radius

r_t = tip radius

r_s = radius at which tip velocity is sonic

$$c_1 = \frac{1}{c_0^2}\left(\frac{2\pi N}{60}\right)^2$$

$$c_2 = M_{ax}^2$$

M_{ax} = axial flow Mach number

c_0 = local speed of sound

N = rpm of compressor

Further, it was observed that for forward propagating discrete tones[26], the predictions were well correlated with measured data when the constant in Equation (4) is changed from 85 to 80. For a multistage compressor, the factors ΔF are multiplied by the stage number. The resulting equations used in the prediction scheme are as follows.

$$(SPL)_{\substack{\text{Discrete tones}\\ \text{forward}}} = 80 + 50 \log (U_r/1000) + 10 \log [\dot{m}(c/s)^2] + (\Delta F_f)N_s \quad (7)$$

$$(SPL)_{\substack{\text{Discrete tones}\\ \text{forward}}} = 85 + 50 \log (U_r/1000) + 10 \log [\dot{m}(c/s)^2] + [\Delta F_f + \Delta F_r - 1/2(N_T - N_s)] \quad (8)$$

$$(SPL)_{\substack{\text{White noise}\\ \text{forward}}} = 75 + 50 \log (U_r/1000) + 10 \log [\dot{m}(c/s)_{mean}] + \alpha_{mid} + 10 \log [U_a/U_r] + \sum_{i=1}^{N_s} (\Delta F_r)_i \quad (9)$$

$$(SPL)_{\substack{\text{White noise}\\ \text{rearward}}} = 75 + 50 \log (U_r/1000) + 10 \log [\dot{m}(c/s)_{mean}] + \alpha_{mid} + 10 \log [U_a/U_r] + [\Delta F_r - 1/2(N_T - N_s)] \quad (10)$$

where: N_T = total number of stages

N_s = stage number

ΔF_f, ΔF_r are forward and rearward factors from Equation (6)

The power levels of the compressor are calculated by assuming simple spherical spreading. It should be noted that the predicted power levels are higher because the directivity effects are not included in the calculation of power levels.

Combustion Noise

Huff, Clark and Dorsch[28] recommended a procedure for the prediction of low frequency core engine noise. The scheme predicts the overall noise power and the frequency at which it peaks. The spectrum is then predicted by fitting the peak level with an averaged spectrum.

Evidence indicates that the low frequency core noise due to combustion and internal flow is dependent on combustor type and design. However, these parameters are difficult to extract from the farfield noise data. Hence, the choice of prediction scheme was based on the simplicity of equations and the fact that the required parameters were readily available.

Motsinger[29] gave a formula for predicting the overall sound power level:

$$OAPWL = 56.5 + 10 \log \dot{m}_a \left[(T_4 - T_3) \frac{P_3}{P_0} \frac{T_0}{T_3}\right]^2 \qquad (11)$$

The frequency (neglecting the Doppler shift factor) corresponding to the peak of the spectrum is given by:

$$f_p = 740 \sqrt{\frac{1}{\dot{m}_a} \frac{P_3}{P_a} \frac{\sqrt{T_R}}{T_4}} \qquad (12)$$

[28] Huff, R. G., B. J. Clark and R. G. Dorsch, "Interim Prediction Method for Low Frequency Core Engine Noise", NASA TMX-71627, November 1974.

[29] Motsinger, R. E. and J. J. Emmerling, "Review of Theory and Methods for Combustion Noise Prediction", AIAA Paper 75-541, 2nd Aeroacoustics Conference, Hampton, VA, March 1975.

where: $\dot{m}_a$ = total mass flow through the combustor (lb/sec)

P_3 = total pressure at combustor inlet (lb/ft^2)

T_3 = total temperature at combustor inlet (°R)

T_4 = total temperature at combustor exit (°R)

P_R = reference pressure (lb/ft^2)

T_R = reference temperature (consistent with T_3, T_4)

T_0 = atmospheric temperature

Figure 6 shows the normalized spectrum shape as a function of dimensionless frequency f/f_p.

Jet Noise

The engine noise prediction program is being used to predict noise levels of typical engines used on civil helicopters, where the exhaust jet velocities are typically low subsonic. At these velocities, it is very unlikely that the noise produced by the jet will be a dominant source. However, a jet noise prediction scheme has been included for completeness.

The peak overall pressure level along a side line parallel to the jet axis at 200 ft is given by[30]:

$$OASPL_j = 10 \log F(u) + 10 \log (\rho^2 A) \qquad (13)$$

where: ρ = weight density of fully expanded jet (lb/ft^3)

A = effective nozzle area, ft^2

r = sideline distance, ft

The value of 10 log F(u) for a given jet velocity is obtained directly from Figure 7.

[30]Anonymous, "Jet Noise Prediction", SAE AIR 876, October 1965.

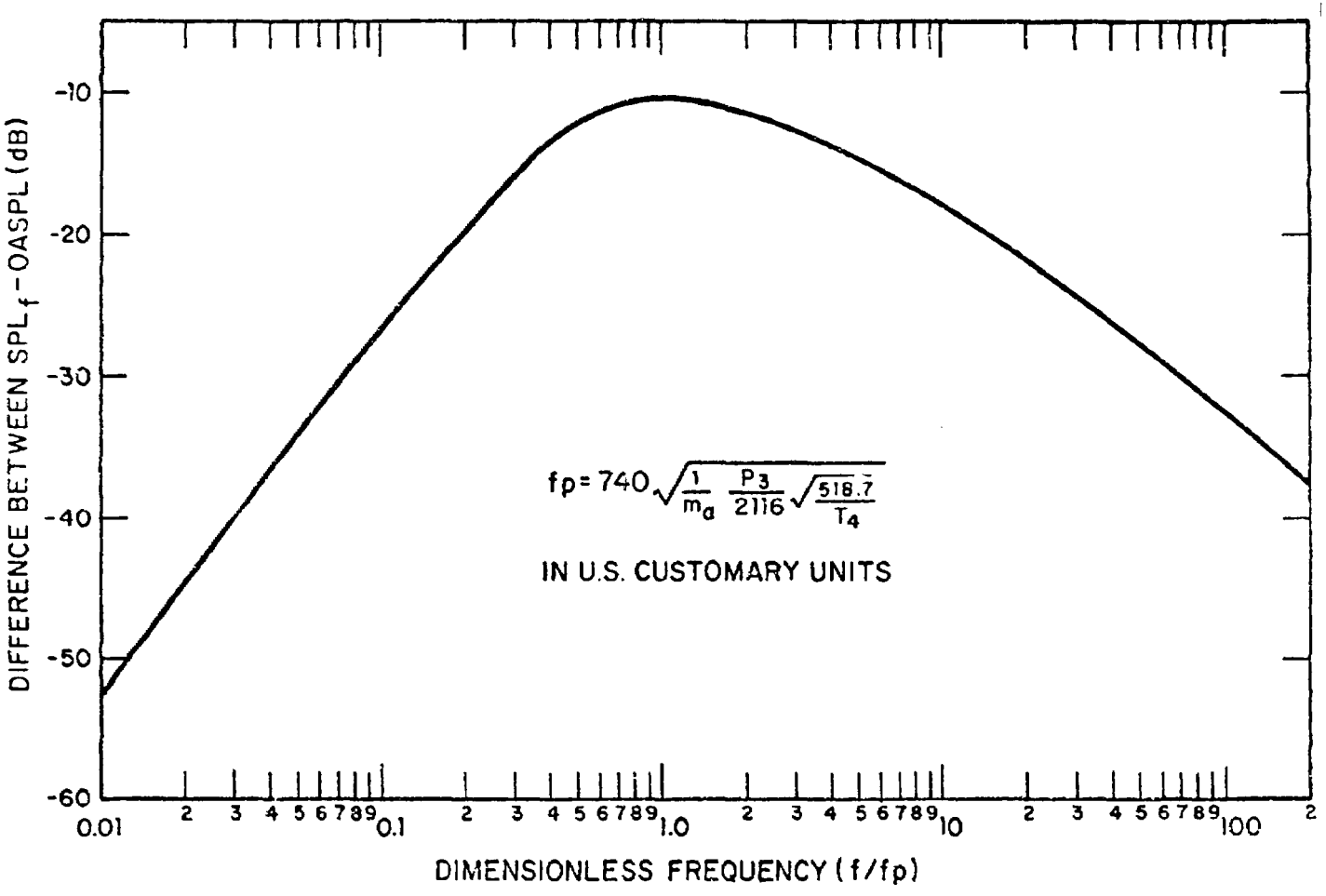

Figure 6. Spectrum Shape for Core Engine Noise

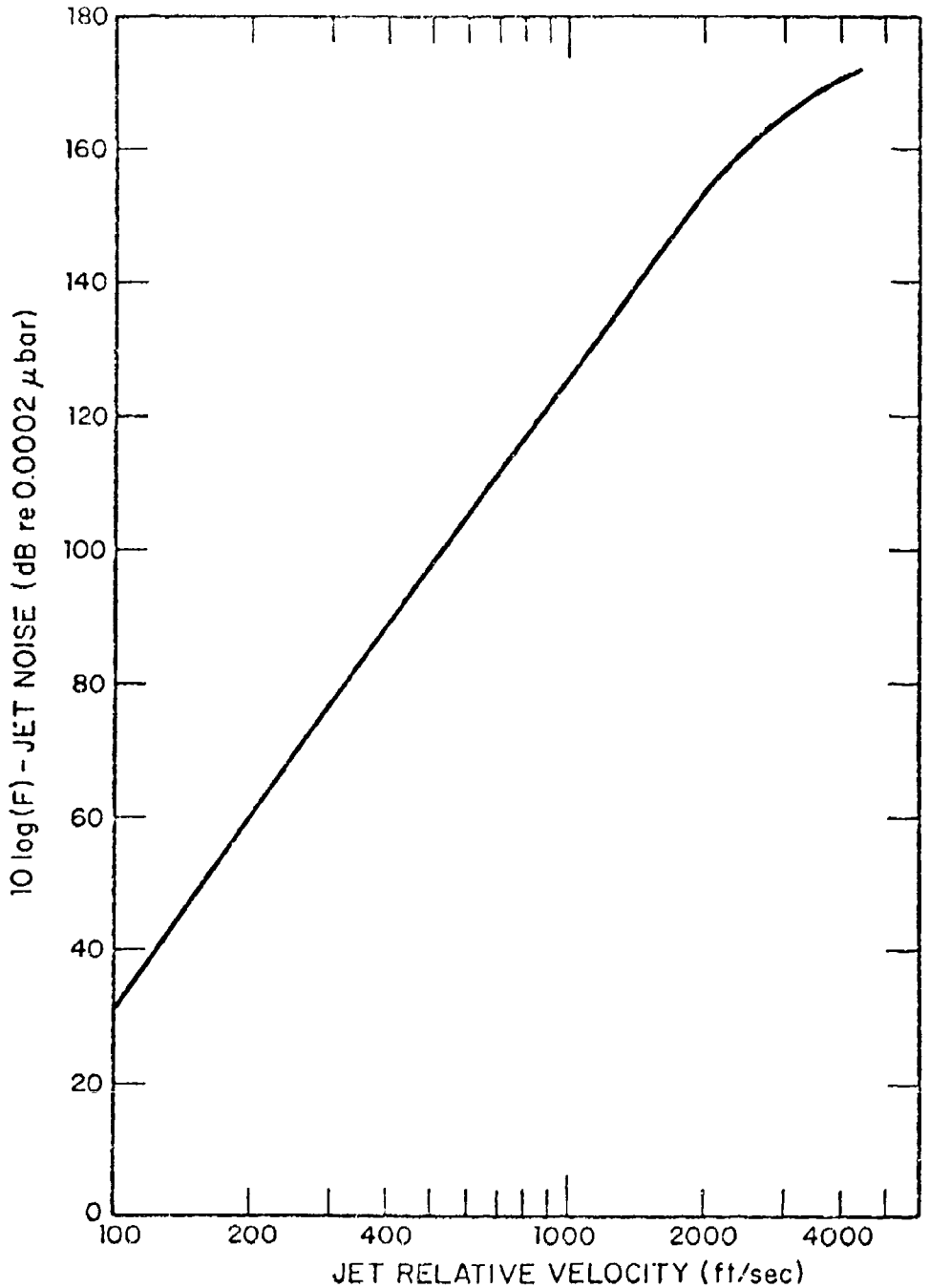

Figure 7. Normalized Jet Noise Vs Jet Relative Velocity

The Strouhal number is calculated by using the effective diameter of a jet exhaust stream, given by:

$$D_e = 1.13 \sqrt{A} \tag{14}$$

and the Strouhal number is given by:

$$S_j = \frac{f_j D_E}{U_E} \tag{15}$$

The corresponding attenuation F_j is obtained by using Figure 8. Hence, the octave band sound pressure level is given by:

$$SPL_{jet}\ (j) = OASPL - F_j \tag{16}$$

Directivity Corrections

The various noise sources involved in the evaluation of total engine noise are directional, the effects of which can not be overlooked. Since the inlet as well as exhaust characteristics of engines are by no means standardized, the evaluation of directivity functions is rather complicated. The procedure adopted here is the one recommended by NASA[31]. Figures 9 and 10 give the directivity of forward and rearward propagating compressor noise sources. Figure 11 gives the directivity of the low frequency core engine noise coming out of the exhaust duct, and Figure 12 gives the directivity of the subsonic jet noise. Subtraction of these directivity functions from the calculated power levels of the various sources yields the sound pressure levels at unit distance from the source.

Reciprocating Engines

Reciprocating engine noise has three components: intake noise, casing noise, and exhaust noise. Acoustic measurements have been made on numerous diesel and gasoline engines in order to quantify noise levels for each of these noise components. Such measurements are reported in References 32, 33 and 34. The results of these measurements indicate the following trends.

[31]Heidmann, "Interim Prediction Method for Fan and Compressor Source Noise", NASA TMX-71763, December 1974.

[32]Ungar, E. E., "A Guide for Predicting the Aural Detectability of Aircraft", AFFDL-TR-71-22, July 1971.

[33]Ungar, E. E. and F. R. Kern, "Exhaust, Casing, and Intake Noise of Continental IO-520D Aircraft Engine", BBN Report No. 2520A, June 1973.

[34]Priede, T., "Diesel Engine Noise Conference", SAE Report SP-397, Aug. 1975.

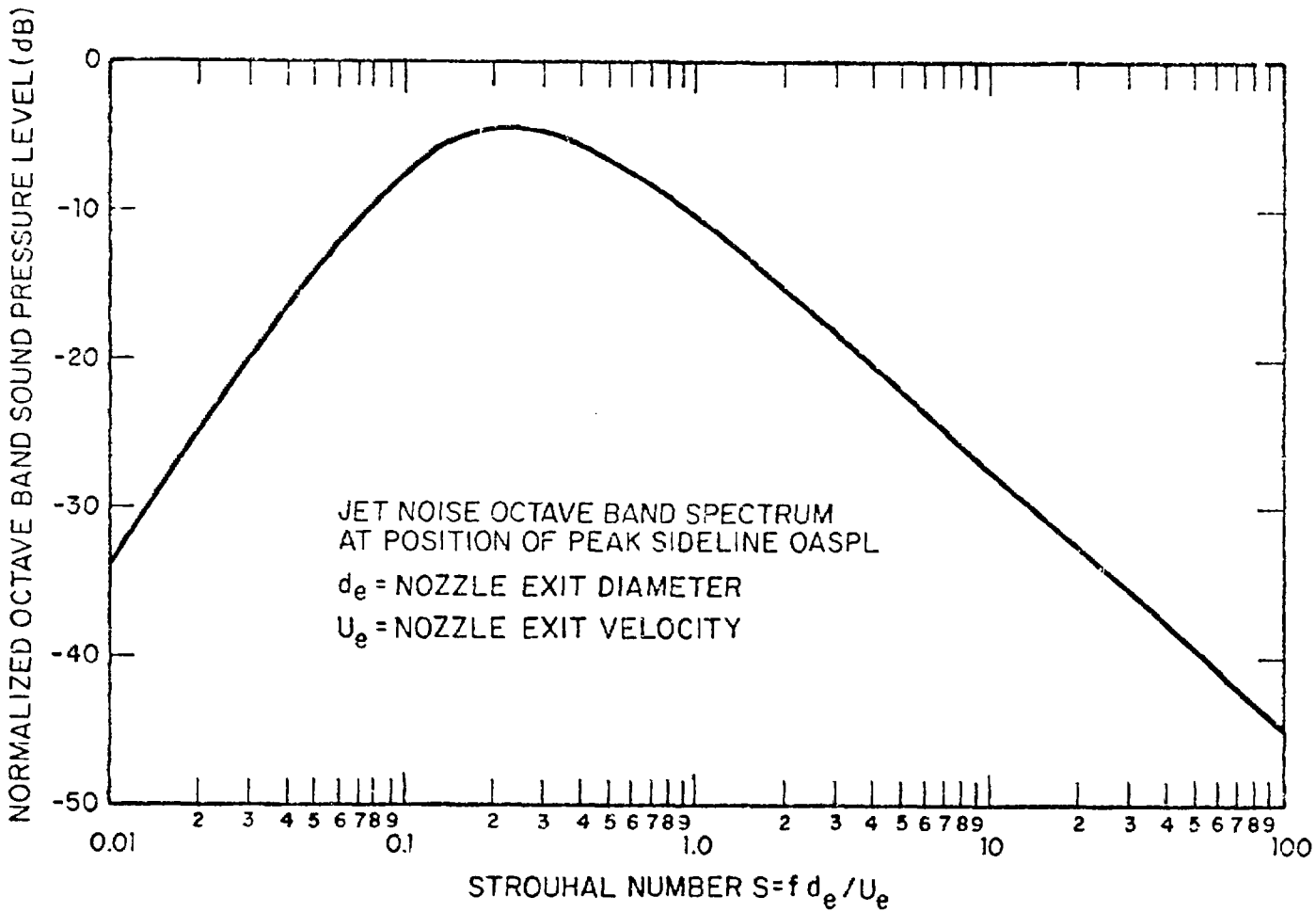

Figure 8. Octave Band Sound Pressure Level at Peak Sideline Position

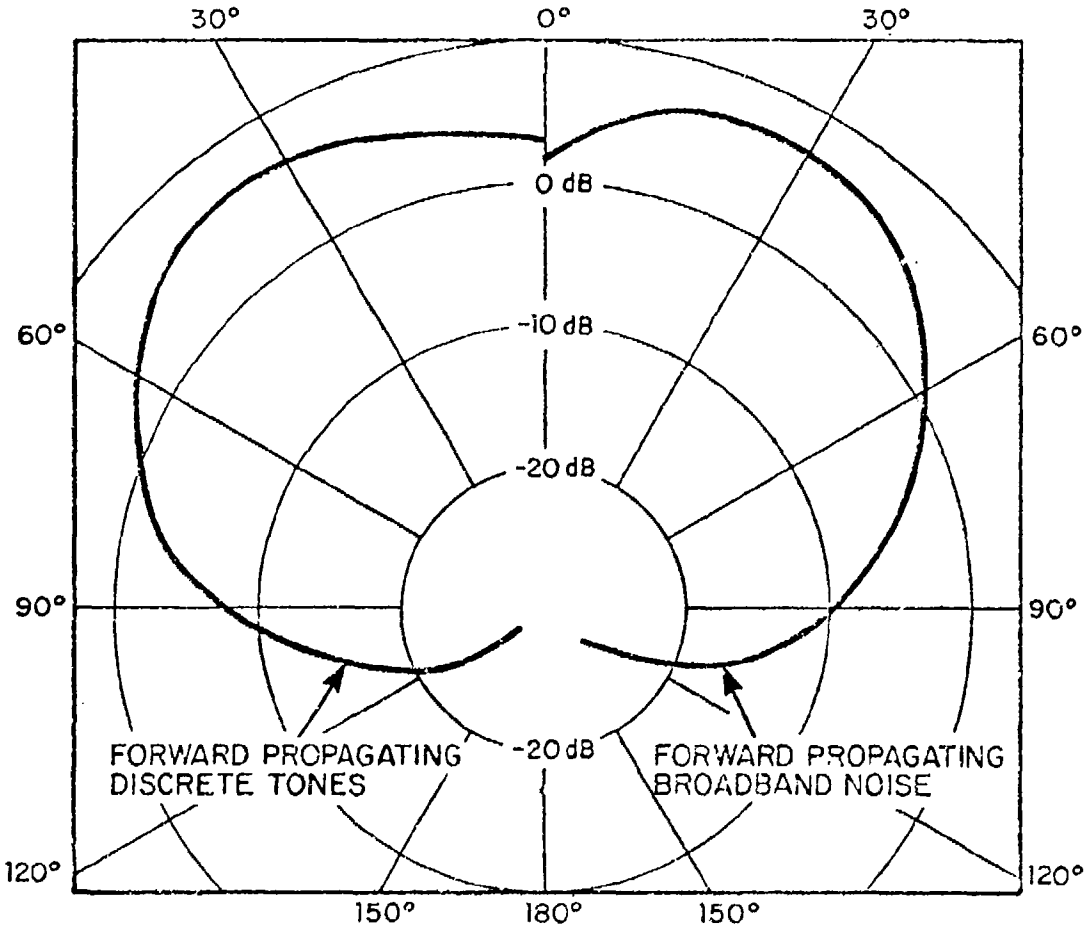

Figure 9. Directivity of Forward Propagating Compressor Noise Sources

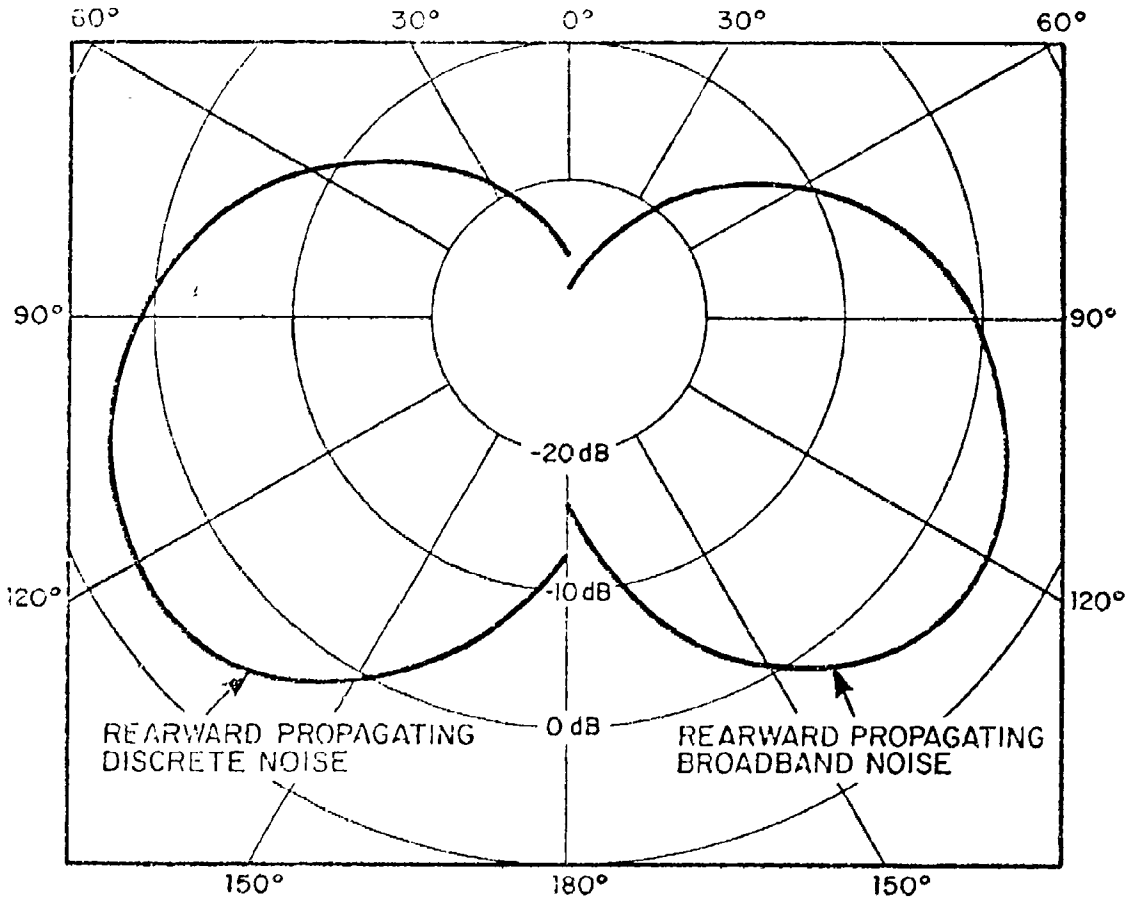

Figure 10. Directivity of Rearward Propagating Compressor Noise Sources

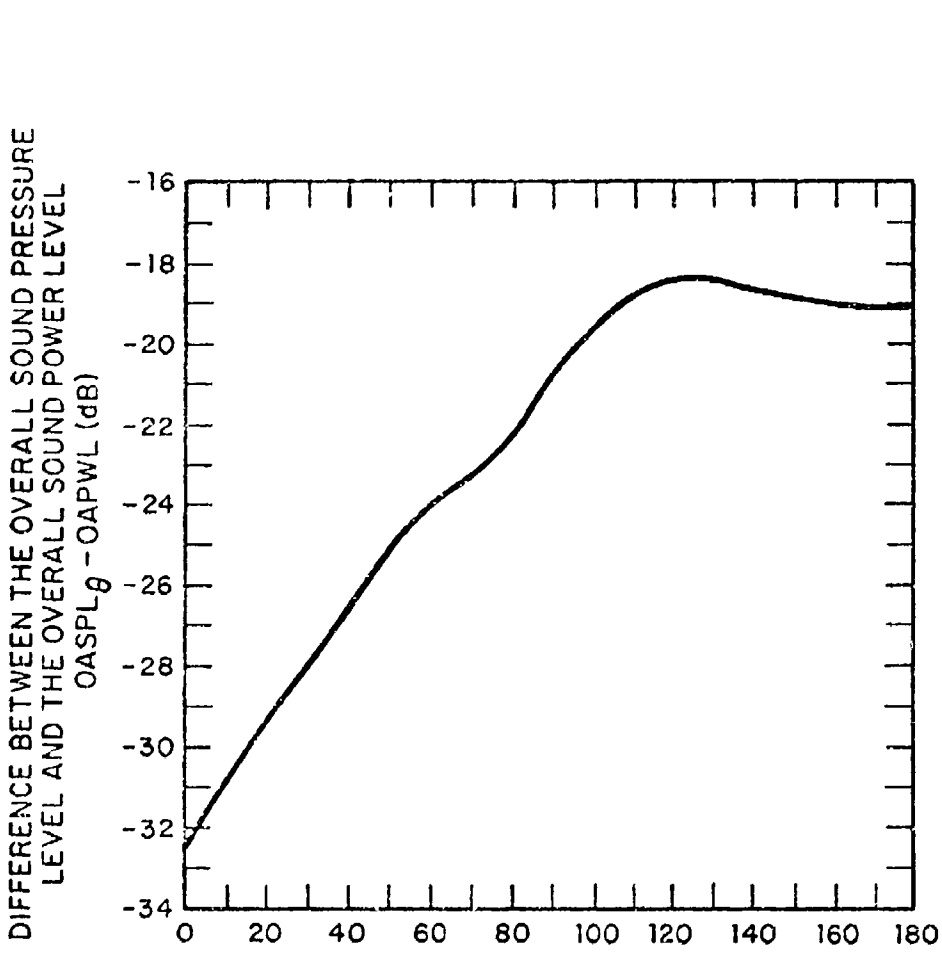

Figure 11. Directivity of Low Frequency Core Engine Noise

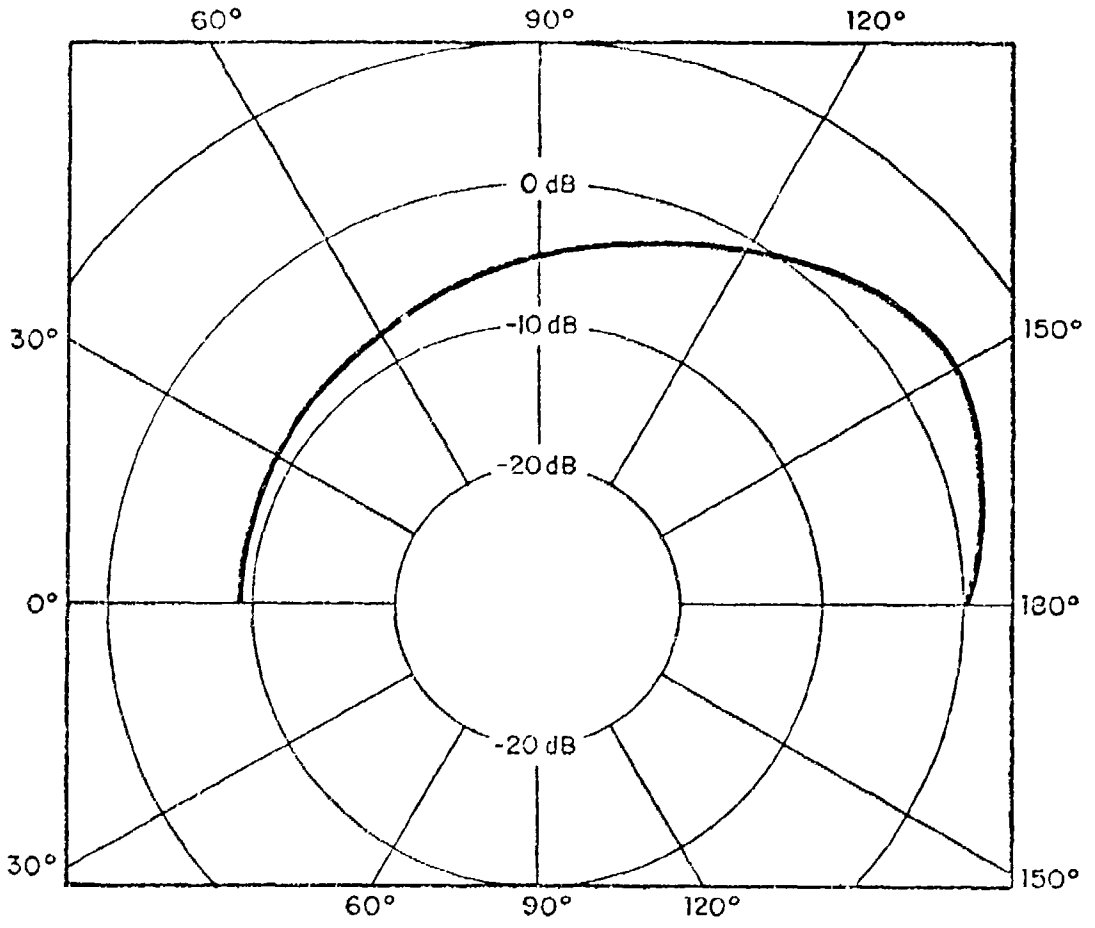

Figure 12. Directivity of Jet Noise

- Generally, noise levels for an unmuffled exhaust are higher than those for casing noise, which in turn are higher than those for unmuffled intake noise.

- Intake noise is often inseparable from casing noise; in this report, intake noise is neglected since its sound power levels are usually at least 10 dB below those for casing noise.

- For all three noise components, measurements show that acoustic intensity is directly proportional to engine output horsepower, which can, therefore, be used to normalize measured noise data.

- Engine noise signatures contain discrete frequency tones at the firing frequency and at several harmonics and subharmonics of this frequency; also, noise levels are maximum at the firing frequency, which can be used to normalize frequency.

- Even when the above normalization procedures are adopted, sound power spectra typically show 10-dB to 20-dB scatter between different engines.

- Noise levels for diesel engines are generally higher than those for gasoline engines which are used for all piston engine driven helicopters; however, diesel engine noise has received much greater attention than gasoline engine noise.

The empirical equation that relates engine sound power level to engine horsepower and frequency is:

L_W = sound power level (dB re 10^{-12} watts)

$$= 10 \text{ Log}_{10} (hp) + A + B \text{ Log}_{10}(f/f_o) \quad (17)$$

where: hp = output horsepower of engine

f = frequency (Hz)

(A,B) = empirical constants

f_o = engine firing frequency (Hz)

$$= SN/(30n) \quad (18)$$

where: S = engine speed (rpm)

N = number of cylinders

n = 2 or 4 = number of cycles

Equation (17) is used herein for prediction of one-third octave band sound power levels for exhaust and casing noise. The quantities A and B are different for exhaust and casing noise, and they vary with nondimensional frequency (f/f_o) bands.

Casing Noise

Priede[34] measured casing noise levels for six automotive gasoline engines in the 90-hp to 130-hp range. One-third octave band sound pressure levels at 1.0 meter from the sides of these engines are listed in Table 6 for the frequency range of 100 to 10,000 Hz. Also listed in Table 6 are the engine characteristics.

The distance from the microphone to the center of the engine is assumed to be R = 1.25 m. The following equation is then used to convert sound pressure levels in Table 6 to sound power levels.

$$L_W = \text{one-third octave band sound power level (dB re } 10^{-12} \text{ watts})$$

$$= SPL + 10 \text{ Log}_{10} (4\pi R^2)$$

$$= SPL + 13 \text{ dB}$$

SPL = one-third octave band sound pressure level (dB re $2.92 \cdot 10^{-9}$ psi) listed in Table 6 (19)

These sound power levels are then normalized by engine horsepower using the equation:

$$L_W - 10 \text{ Log}_{10} \text{ hp} = SPL + 13 \text{ dB} - 10 \text{ Log}_{10} \text{ hp} \quad (20)$$

Calculated values of the normalized sound power levels are listed in Table 7 for the six engines. Here the frequency (f) is shown normalized by the firing frequency (f_o). Actually, the one-third octave bands in Table 6 were shifted so that the band containing the firing frequency falls in the normalized band $f/f_o = 1.0$ in Table 7. This table also lists the normalized sound power levels for a 140 hp Continental Aircraft Engine[33]. Figure 13 shows an envelope of the sound power levels listed in Table 7, and an average spectrum which rises at 6 dB/oct for $f/f_o < 1.0$ is constant at 82 dB for $1.0 < f < 2.5$, and rolls off at 12 dB/oct for $f/f_o \geq 25$. At the firing frequency $f = f_o$, an average value of 87 dB is selected as the pure tone level. This average spectrum has been used to reflect normalized casing noise. Values of A and B for Equation (17) are:

TABLE 6. ONE-THIRD OCTAVE BAND SPL'S OF CASING NOISE MEASURED 1.0 METER FROM THE SIDES OF SIX 4-CYCLE GASOLINE ENGINES; REFERENCE 10

	Engine Characteristics					
	1	2	3	4	5	6
Type	In-Line	In-Line	In-Line	In-Line	In-Line	V-Form
No. Cyl.	4	4	4	6	4	(6)
Disp. (in^3)	90	90	120	120	150	210
rpm	6000	5000	5500	5500	6000	5000
hp	95	90	103	99	105	130
Freq (Hz)	One-Third Octave Band SPL					
100			82	76	73	
125		85	81	79	70	
163	83	96	88	82	90	75
200	93	78	96	89	98	79
250	86	77	94	96	89	75
315	83	82	94	91	90	80
400	87	79	85	83	94	82
500	92	81	90	86	91	84
630	88	83	98	81	94	86
800	83	86	93	85	91	87
1000	84	92	93	88	91	85
1250	84	85	93	85	92	87
1630	87	92	91	92	94	84
2000	87	87	92	85	96	84
2500	88	83	89	86	95	82
3150	85	83	90	84	96	79
4000	85	81	89	86	95	77
5000	86	79	88	85	92	74
6300	84	79	86	85	91	72
8000	82	78	85	84	88	70
1000	83	76	84	83	84	68
SPL (dBA)	95	95	103	110	105	97.6

TABLE 7. ONE-THIRD OCTAVE BAND SOUND POWER LEVELS OF CASING NOISE FOR SEVEN GASOLINE ENGINES

	Engine Characteristics						
	1	2	3	4	5	6	7
Type	In-Line	In-Line	In-Line	In-Line	In-Line	V-Form	Radial
No. Cyl.	4	4	4	6	4	6	
Disp. (in^3)	90	90	120	120	150	210	
rpm	6000	5000	5500	5500	6000	5000	2150
hp	95	90	103	99	105	130	140
f/f_0	L_W - 10 Log_{10} (hp) - dB re 10^{-12} Watts						
0.40				69			
0.50			75	72	66		
0.63			74	75	63		
0.80	76	78	81	82	83	67	70
1.00	86	89	89	89	91	71	75
1.25	79	71	87	84	82	67	70
1.63	76	70	87	76	83	72	75
2.00	80	75	78	79	87	74	73
2.50	85	72	83	74	84	76	74
3.15	81	74	91	78	87	78	84
4.00	76	76	86	81	84	79	77
5.00	77	79	86	78	84	77	77
6.30	77	85	86	75	85	79	78
8.00	80	78	84	78	87	76	80
10.00	80	85	85	79	89	76	79
12.50	81	80	82	77	38	74	79
16.30	78	76	83	79	89	71	74
20.00	78	76	82	78	88	69	74
25.00	79	74	81	77	85	66	76
31.50	77	72	79	77	84	64	74
40.00	75	72	78	76	81	62	71
50.00	76	71	77		77	60	72
63.00		69					72

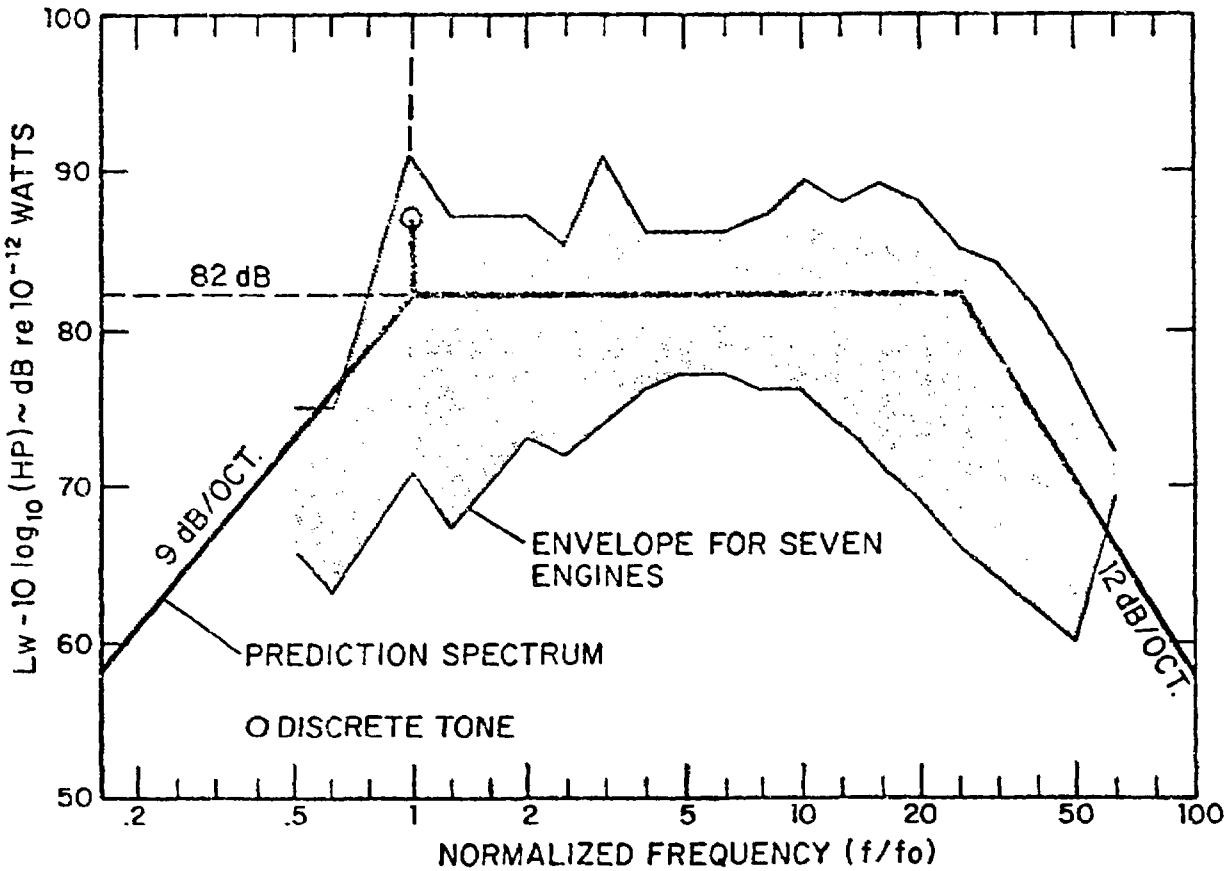

Figure 13. One-Third Octave Band Sound Power Levels of Casing Noise for Gasoline Engines

Frequency	A	B
$f/f_o < 1.0$	82	30
$f/f_o = 1.0$	87	0
$1.0 < f/f_o \leq 25$	82	0
$25 \leq f/f_o$	138	-40

Unmuffled Exhaust Noise

In Reference 32 Ungar presents measured, octave band sound power levels of exhaust noise from nine diesel engines whose operating characteristics span the following ranges:

hp = 160 to 7000 horsepower

S = 240 to 1800 rpm

n = 2 and 4 cycles

f_o = 30 to 480 Hz firing frequency

These data extend over a frequency range of 31.5 to 8000 Hz, and exhibit a typical scatter of 10 to 20 dB. From these data, Ungar developed a "smoothed-out" spectrum that is approximately equal to the mean plus one standard deviation; the resulting spectrum is shown in Figure 14 in the alternate form of one-third octave band sound power levels.

Spectrum levels in Figure 14 are normalized by horsepower, and frequency is normalized by the firing frequency. These normalizations are consistent with those indicated in Equation (17). The discrete tone levels associated with Ungar's prediction are 5 dB above the "smoothed-out" spectrum.

For purposes of comparison, Figure 14 also shows exhaust sound power levels recommended in Reference 35 for prediction of shipboard noise from diesel and gasoline engines. For each type of engine (diesel, gasoline), the spectrum varies by 6 dB to account for various engine speeds, turbochargers, and in-line or V-form configurations. On the average, the gasoline engines radiate 10 dB less exhaust noise than the diesel engines.

---

[35] Bolt Beranek and Newman, Handbook for Shipboard Airborne Noise Control, USCG-NSES Report.

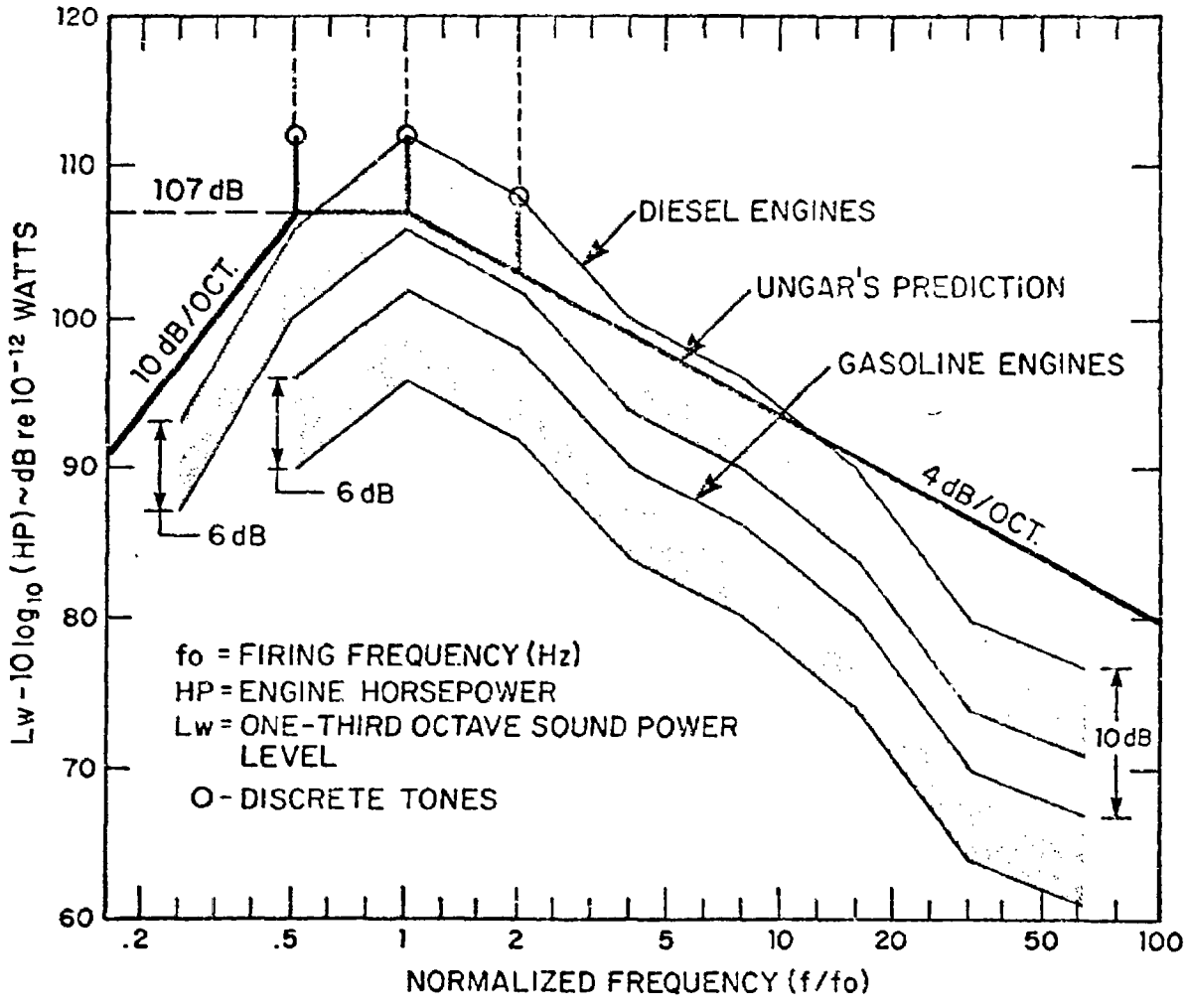

Figure 14. One-Third Octave Band Sound Power Levels for Exhaust Noise From Diesel and Gasoline Engines

Ungar's prediction method is used in the present model to calculate exhaust noise. Numerical values of the quantities A and B as in Equation (17) are:

Frequency	A	B
$f/f_o < 1/2$	117	33.22
$f/f_o = 1/2$	112	0
$1/2 < f/f_o < 1$	107	0
$f/f_o = 1$	112	0
$1 < f/f_o < 2$	107	-13.29
$f/f_o = 2$	108	0
$2 < f/f_o$	107	-13.29

CORRELATION OF ENGINE NOISE CALCULATIONS

The engine noise calculation methods are empirically based and, consequently, correlation with test data is fundamental to their development. Because of this, little correlation work with these methods was performed in the present program, and the efforts which were undertaken were intended only to insure that the methods were being correctly applied. Furthermore, even these limited efforts were hampered by a lack of available helicopter engine noise test data.

Figure 15 shows a comparison of calculated and measured reciprocating engine noise for the Bell Model 47 helicopter engine. These data are presented in terms of sound pressure level vs engine firing frequency harmonic. The test data of Figure 15 were taken from Figure 7 of Reference 36. The degree of correlation indicated in Figure 15 is consistent with the range of scatter expected in measured reciprocating engine noise, and, based on this it is concluded that this noise calculation method is performing properly.

No measured helicopter shaft turbine engine noise data were found which would be suitable for correlating the noise calculation method. Because of this, it was decided to evaluate the validity of this method by comparing measured and calculated total vehicle spectra, and inferring method correlation from the degree of agreement in the frequency range

[36] Parrott, T. L., "An Improved Method for Design of Expansion-Chamber Mufflers With Application to an Operational Helicopter", NASA TN D-7309, October 1973.

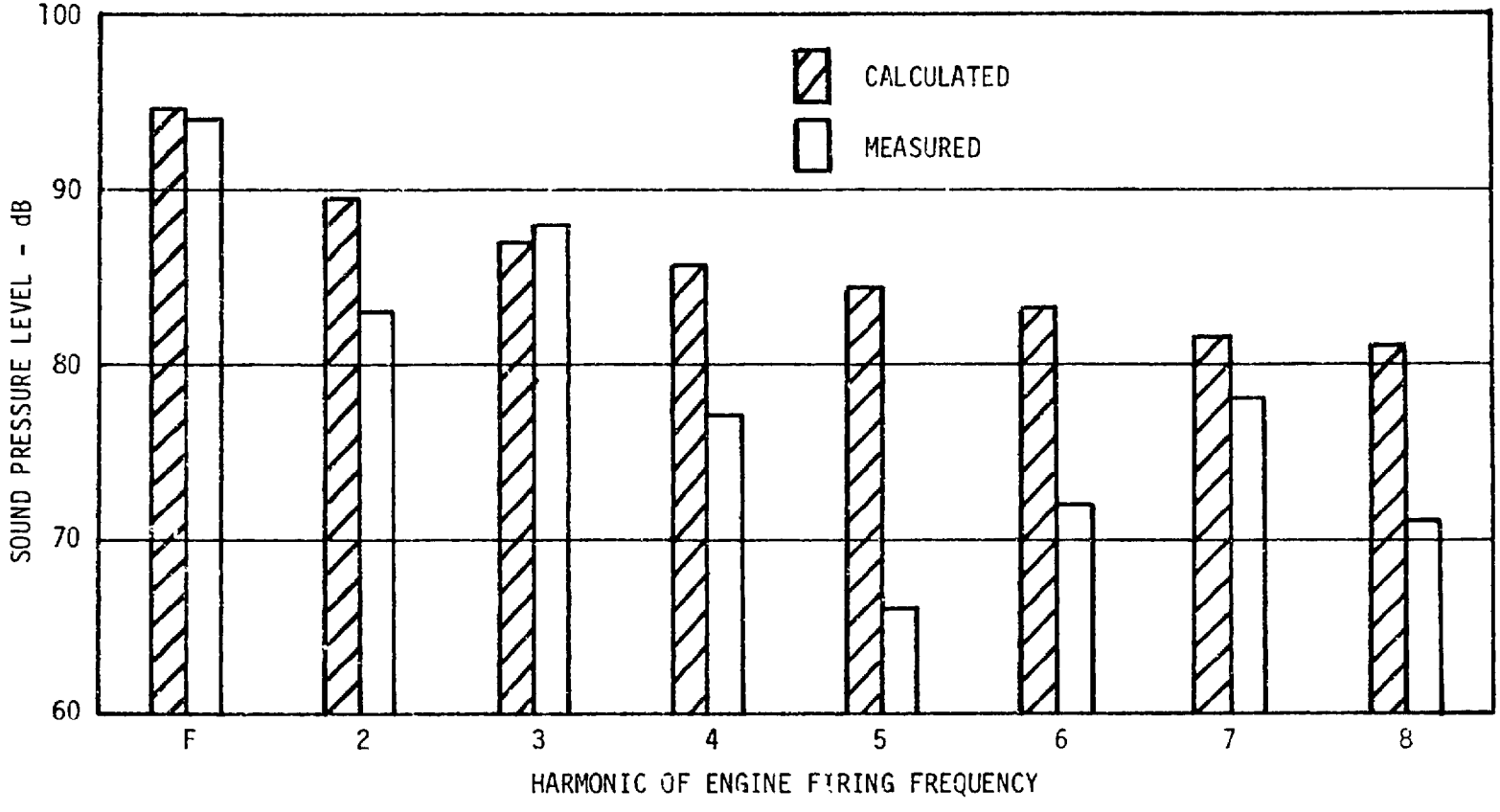

Figure 15. Comparison of Measured and Calculated Bell Model 47 Engine Noise

where engine noise would be expected to dominate the spectrum. Comparisons of calculated and measured total vehicle spectra for the Sikorsky S-61 and Hughes 500 vehicles are given in Figure 16. Measured data have been taken from References 21 and 22.

General agreement between measured and calculated vehicle noise spectra is indicated in Figure 16. The validity of the shaft turbine engine noise calculation method is demonstrated by the correlation of measured and calculated spectra in the frequency range of 1KHz to 10KHz.

TRANSMISSION NOISE CALCULATION

The transmission component of helicopter vehicle noise consists of multiple pure tones (discrete frequencies) associated with the various gear meshes within the main transmission. While the transmission is not generally thought to be a significant contributor to helicopter external noise[1], it has been considered in the present program because the discrete frequency nature of transmission noise makes it a potentially significant contributor to vehicle EPNL. The simplified method used to calculate transmission noise in the present program has been derived from a more complex analytical method, which is discussed in References 16, 17 and 18.

The analytical method of References 16, 17 and 18 considers the helicopter transmission as a complex dynamic system consisting of many mechanical elements. In this method, all gears/gearshafts, shaft support bearings and the transmission case are dynamically modeled individually and these individual elemental models are then coupled to form a system dynamic model. Excitations, in the form of gear mesh deflections, are applied to the resulting system model, and transmission dynamic responses and case radiated noise are calculated directly. Gear mesh deflection excitations are calculated based on unsteady gear tooth bending, which occurs as a result of the transmission of torque across the mesh.

Within the Reference 18 study, a dynamic model of the Kaman/Navy SH-2D helicopter transmission was developed. Testing was performed on this transmission and model calculations of transmission noise were correlated with measured data. The degree of correlation obtained with this model is indicated in Figure 17.

While a high degree of correlation is obtainable with the detailed transmission noise model of Reference 18, the complexity of this model, and the extent and nature of input data required for its use, make direct application of this method to the present program impractical. Consequently, an alternate approach was adopted, and a simplified transmission noise calculation technique was derived, based on parametric trend data, developed from the detailed SH-2D transmission model. The validity of this simplified method is predicated on the assumption that the SH-2D transmission has dynamic response and noise radiation characteristics which are representative of current generation helicopter

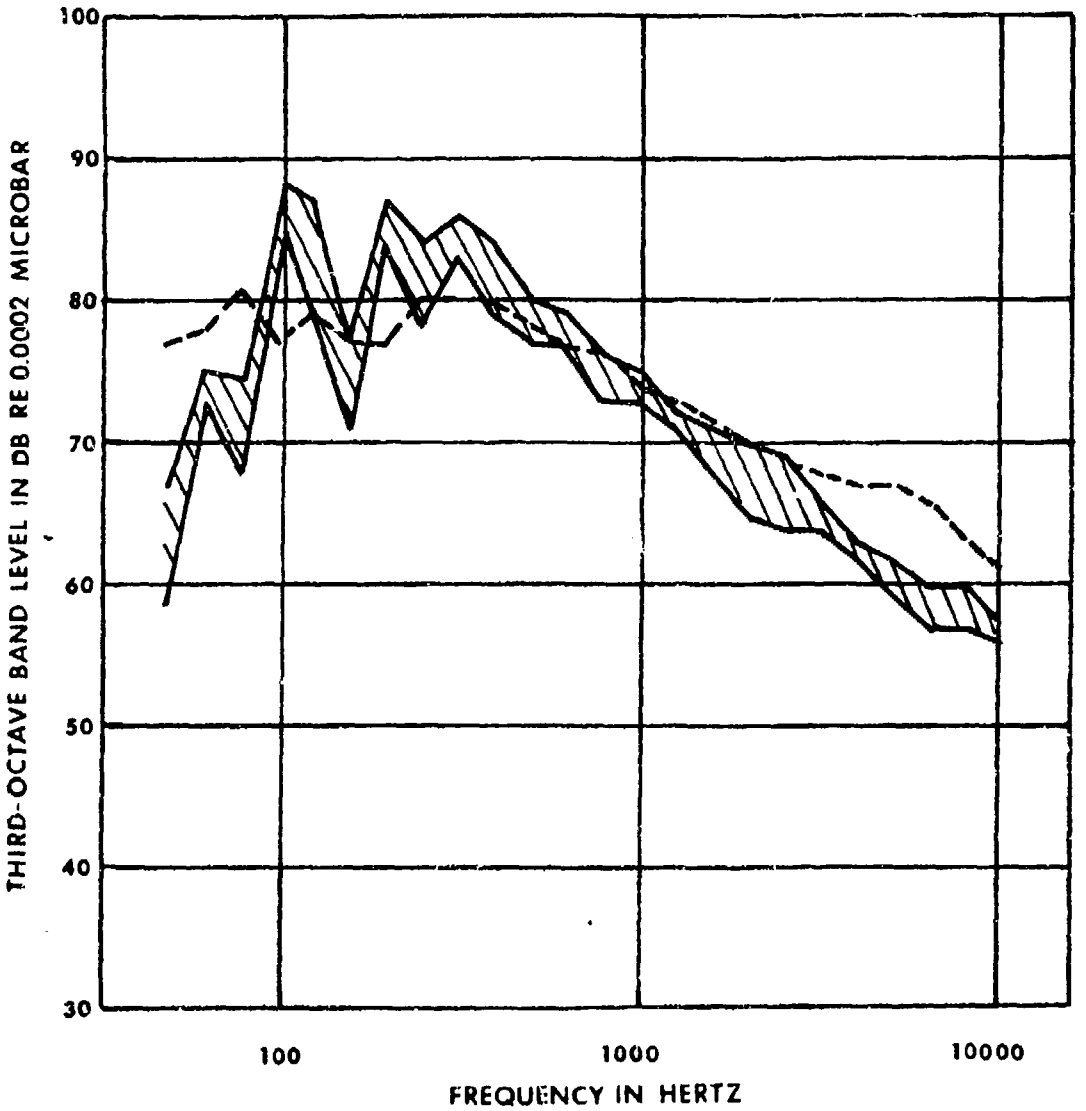

A. OH-6A (H-500) Fly-Over, 100 Ft Altitude, 120 Kts S.L. Flight

Figure 16. Comparison of Measured and Calculated Vehicle Noise

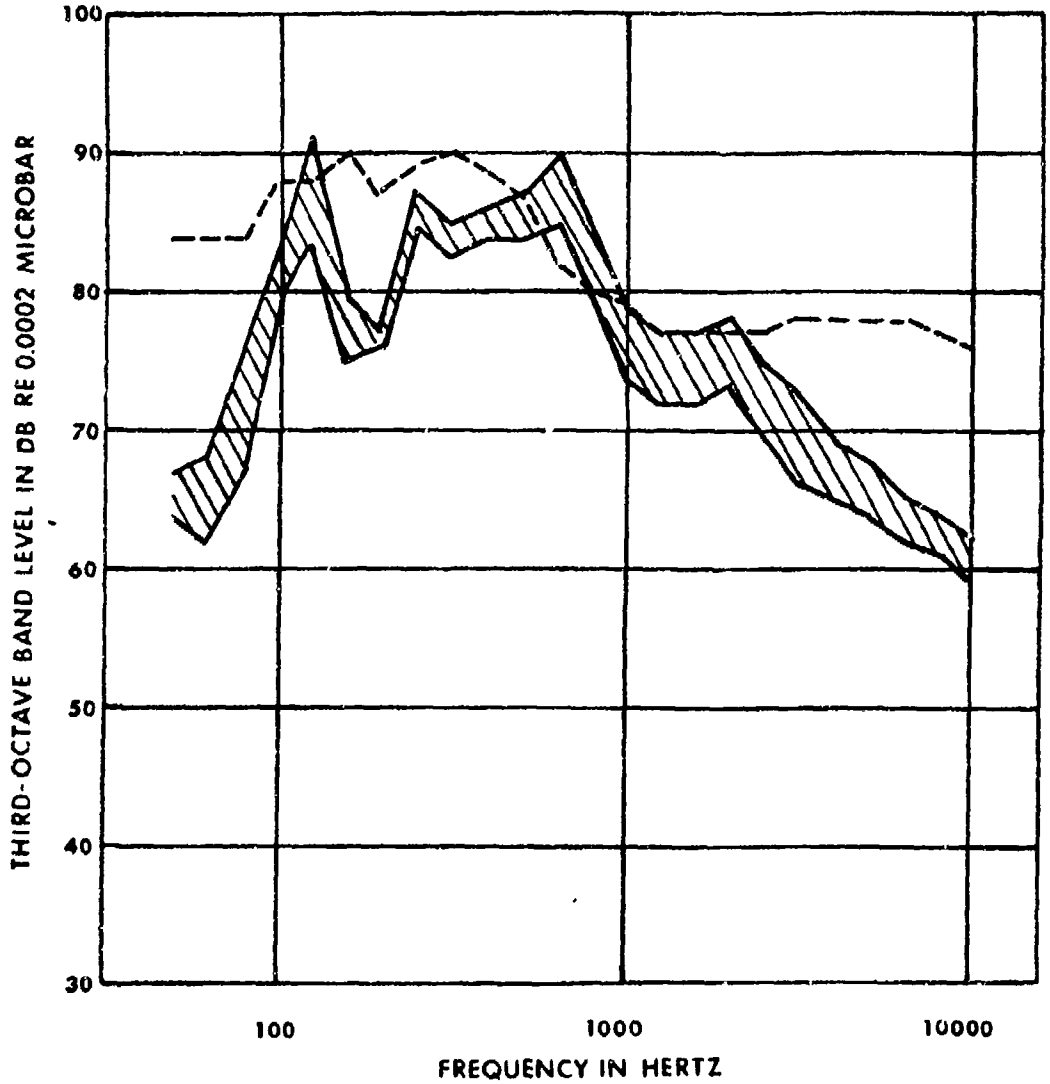

B. SH-3A (S-61) Fly-Over, 200 Ft Altitude, 120 Kts S.L. Flight

Figure 16. Comparison of Measured and Calculated Vehicle Noise - Concluded

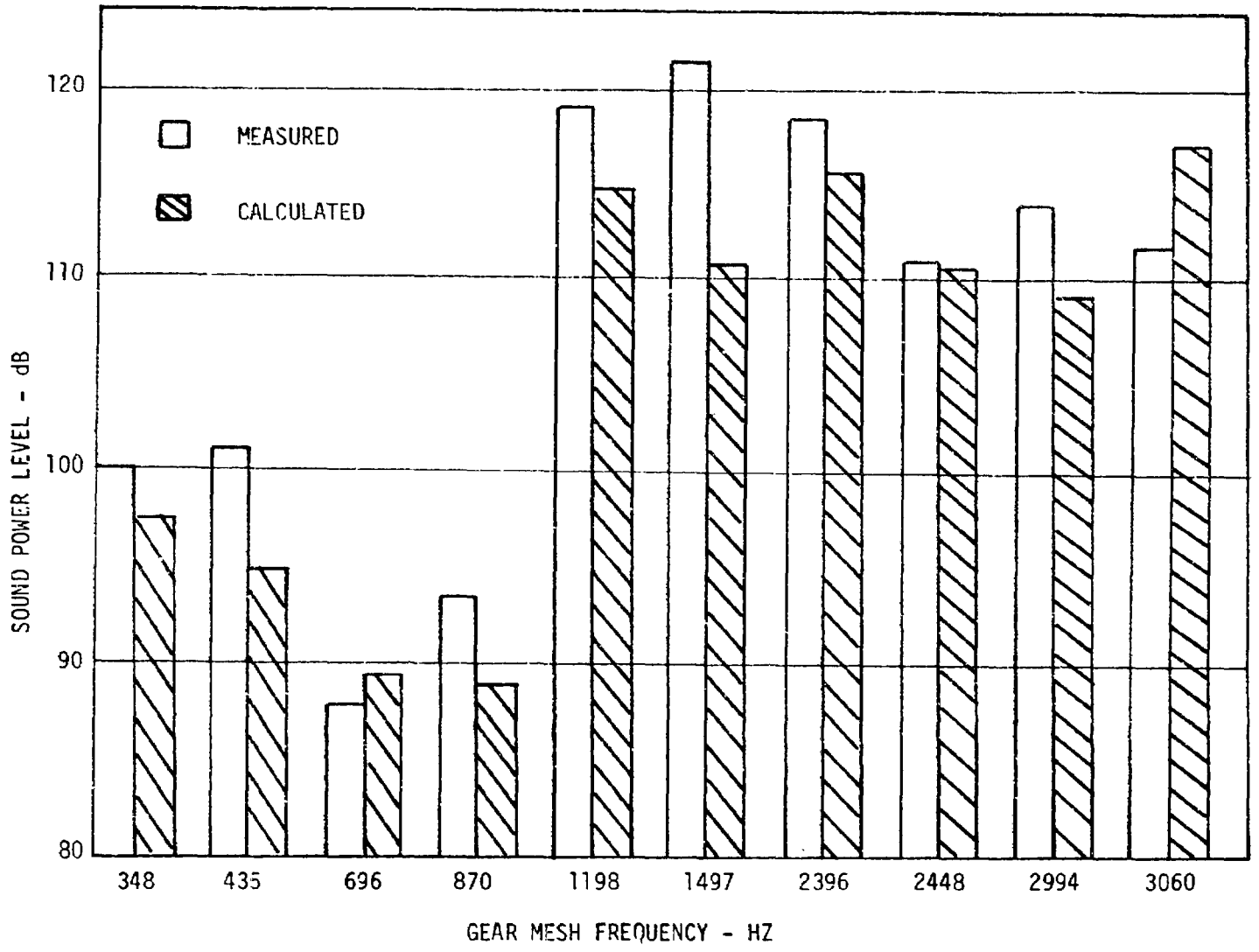

Figure 17. Comparison of Measured and Calculated SH-2D Transmission Noise, Using Detailed Transmission Noise Model

transmissions. This assumption is believed to be appropriate, since the SH-2D transmission is similar in design to most existing helicopter transmissions and its operating torque and rpm conditions are near median values for the vehicles considered in the present study.

The transmission noise calculation method developed for the present study is based on a simple parametric relationship between the physical variables of a given gear mesh and the sound power level of the discrete frequency component due to that mesh. The general form of this relationship is:

$$PWL_G = A \, Log_{10}(\tau) + B \, Log_{10}(f) + C + D \qquad (21)$$

where: PWL_G = sound power level - dB re 10^{-12} watts

A = a constant indicative of the relationship between torque and sound power level

τ = transmitted torque (in-lb)

B = a constant indicative of the relationship between gear clash frequency and sound power level

f = gear clash frequency - Hz

C = a constant indicative of the type of gear mesh

D = a constant indicative of the gear clash harmonic number

A parametric study was performed, using the available SH-2D transmission analytical model, considering three types of gear meshes, all of which were represented in the SH-2D model. Gear mesh types considered were: spur gear, spiral bevel gear and planetary system. Based on this study three equations, of the form of Equation (21), were derived for the three gear mesh types considered. These derived equations are:

$$PWL_{SG} = 20 \, Log \, (\tau) + 37.8 \, Log \, (f) - 91 + D_{SG}$$

$$PWL_{SBG} = 20 \, Log \, (\tau) + 37.8 \, Log \, (f) - 100 + D_{SBG}$$

$$PWL_{PS} = 12.8 \, Log \, (\tau) + 37.8 \, Log \, (f) - 59 + D_{PS} \qquad (22)$$

where: PWL_{SG} = sound power level of spur gear mesh

PWL_{SBG} = sound power level of spiral bevel gear mesh

PWL_{PS} = sound power level of planet system

The constants D_{SG}, D_{SBG}, and D_{PS} in Equation (22) are indicative of the relationship between sound power level and gear mesh harmonic number, which was found to be specific to a particular gear mesh type. Values of these constants were defined to be equal to zero for the gear clash fundamental frequency. Finite values were established for these constants for the second and third harmonics of gear clash frequency, and these are given in Table 8.

Equation (22) could not be used directly in the total helicopter vehicle noise calculation model for two reasons. First, the sound power levels calculated with Equation (22) are in terms of a "Spectrum Level" with a frequency bandwidth of one Hz, while the vehicle noise model deals in 1/3 octave bands. This problem was overcome by converting these "Spectrum Levels" to a 1/3 octave format using a digital 1/3 octave filter representation. The second, and more significant problem in using these equations, relates to the fact that, in general, helicopter transmissions are enclosed within the vehicle fuselage or pylon structure. Equation (22) refers to sound radiation in free space, and therefore, the levels calculated with these equations must be reduced to account for the sound attenuation characteristics of any enclosing vehicle structure.

The sound attenuation of a partial acoustic enclosure may be simply related to enclosure surface density open area ratio, and source frequency, if the structural material is assumed to act as a limp mass[37]. The transmittance (T) of such a structural material is given by:

$$T = \left[\frac{.1}{f^2 \cdot \rho^2}\right] \qquad (23)$$

where: T = transmittance, ratio of transmitted to incident sound

f = source frequency - Hz

ρ = surface density - lb/in^2

[37] Beranek, L. L., "The Transmission and Radiation of Acoustic Waves by Solid Structures", CH-13, Noise Reduction, L. L. Beranek, ed., McGraw-Hill, 1960.

TABLE 8. VALUES OF THE CONSTANTS D_{SG}, D_{SBG}, AND D_{PS} IN EQUATION (22)

Gear Clash Type	Harmonic No.	
	2	3
Spur Gear	-5	-22
Spiral Bevel Gear	+7	+6
Planet System	-10.5	-23

For a partial enclosure, the enclosure transmission loss or attenuation (in decibels), is a function of the transmittance of the solid portion of the enclosure, given by Equation (23), and the ratio of open area to total enclosure area. This transmission loss is given by:

$$T.L. = 10 \text{ Log}_{10} \left[\frac{1}{T(1 - A_R) + A_R}\right] \quad (24)$$

where: T.L. = enclosure transmission loss (dB)

A_R = ratio of open area to total enclosure area

Equation (24) is used in the transmission noise calculation model in conjunction with the transmission case radiated sound power level relationships of Equation (22).

CORRELATION OF TRANSMISSION NOISE CALCULATIONS

The transmission component of helicopter noise is not readily measurable external to the helicopter, and no external noise data were found to be available, suitable for correlating transmission noise calculations. However, since the method is equally well suited to calculating helicopter internal noise, which is normally dominated by the transmission component, it was decided to use available measured internal noise data for this purpose.

Measured internal noise levels of the Bell/Army UH-1 (Model 205 civil designation) are given in Reference 38. These measurements were made in terms of 1/3 octave bands, for three different vehicles. The data of Reference 37 are compared to a calculated UH-1 transmission noise spectrum in Figure 18. The degree of correlation indicated by this comparison is considered adequate for present program purposes.

[38] Laskin, I., F. K. Orcutt and E. E. Shipley, "Analysis of Noise Generated by UH-1 Helicopter Transmission", USAAVLABS TR 68-41, June 1968.

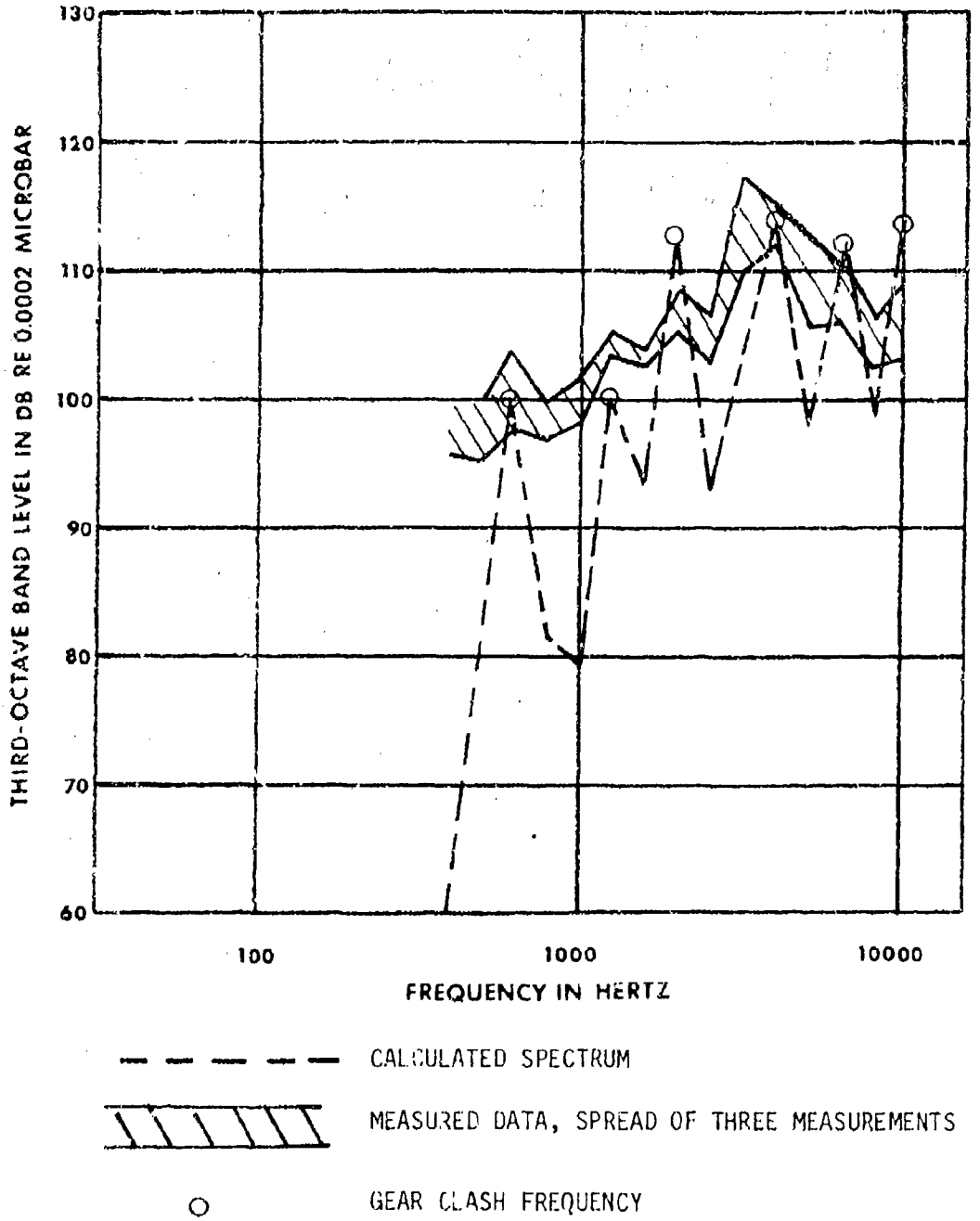

Figure 18. Comparison of Measured and Calculated UH-1 (B-205) Internal Noise, Using Simplified Transmission Noise Model

VEHICLE DESIGN AND PERFORMANCE

The noise calculation methods of the previous section provide the means for evaluating the potential for helicopter noise reduction. To apply these methods realistically, however, it is necessary to determine the nature and extent of changes in vehicle design and performance characteristics which must be made to incorporate noise reduction methodology. This information is also required to assess the economic cost of helicopter noise reduction. This section of the report discusses the analytical method which has been developed to obtain the required information.

Mission Performance Criteria

The intent of the overall study effort is to determine how much noise reduction can be achieved in future design civil helicopters using existing noise reduction technology, and what changes in total life cycle cost will result from the achievement of this noise reduction. Since the study concerns itself only with future design civil helicopters, it is necessary to make certain assumptions as to the nature of these vehicles and what their noise and cost characteristics would be if noise reduction was not considered in their design. The effects of noise reduction can then be determined relative to these baseline characteristics. In the present program it is assumed that future design civil helicopters will be required to perform similar missions to those presently being performed. Since vehicle design is principally a function of required mission performance, it is further assumed that future civil helicopters will be similar in design to existing vehicles. These assumptions lead directly to the use of existing civil helicopter characteristics as the baseline for determining changes due to the introduction of noise reduction methodology, and this approach has been taken in the present program.

The basic premise of the present effort is that noise reduction of future civil helicopters will be achieved in addition to, rather than at the expense of, required mission performance. Noise-reduced vehicles will fly as fast, as high, as far and with the same payload, although they may be heavier and more costly to own and operate. This concept of a constant mission performance requirement provides a realistic context within which the effects of helicopter noise reduction can be determined and assessed.

In specific terms, the following mission performance criteria have been established:

(1) Constant payload.

(2) Constant out-of-ground effect hover ceiling.

(3) Constant range (at the best cruise speed of the baseline vehicle).

(4) Adequate (equal or greater) stall margin.

In general terms, these criteria have been applied in the following manner. First, the direct effect of the introduction of a noise reduction method was determined in terms of a change in vehicle gross weight at the constant payload. This new gross weight was then used to establish a new installed power requirement, and the consequent changes in engine weight and rated fuel consumption rate which result from this change in installed power. Installed power, as well as engine weight and rated fuel consumption, were also changed to reflect any direct effects of noise reduction such as engine silencer losses. Weight and installed power changes were then iterated until a combination was arrived at which satisfied the baseline vehicle out-of-ground effect hover ceiling capability.

The above procedure resulted in a vehicle configuration which could operate at the same altitude with the same payload as the reference configuration. Forward flight performance was then considered in order to satisfy the established range and speed capability criteria. Given the new vehicle gross weight determined by hover performance requirements, rotor stall margin was calculated and compared to that of the baseline vehicle. If insufficient stall margin was indicated, changes in rotor design were effected, which increased stall margin to that of the baseline configuration. Any changes in weight which resulted from this rotor design change were calculated and accounted for, iteratively, through reconsideration of the hover performance requirement. Once stall margin and hover perforamnce were determined to be consistent with the established criteria, forward flight power required for the new vehicle configuration was calculated.

The forward flight power required was determined for flight at the best cruise speed* of the baseline vehicle. This power was used to determine the need for any change in fuel load required to maintain a maximum range equal to that of the baseline vehicle. If fuel load was changed, vehicle gross weight was adjusted accordingly and, again, compensated for through consideration of hover performance and stall margin criteria.

In the above manner, a new vehicle design was defined in terms of changes in vehicle:

* Best cruise speed is defined as the speed for maximum range.

(1) Gross weight.

(2) Airframe weight.

(3) Installed power.

(4) Engine weight.

(5) Fuel load.

These changes in vehicle design are in addition to and are the direct result of one or more changes in vehicle design associated with the introduction of some noise reduction methodology. All of these changes have the potential for affecting the net noise reduction which is achieved with a given noise reduction methodology and, therefore, all must be considered in the calculation of vehicle noise reduction. Similarly, all changes in vehicle design influence vehicle cost. The individual analytical relationships which have been used to determine the above changes in vehicle design are described in the following paragraphs.

Hover Performance

The installed engine power required for a given helicopter design is dictated by desired hover performance, as stated in terms of out-of-ground effect hover ceiling. While power is required for many aircraft systems, including the main and auxiliary rotors, electrical generators, hydraulic and fuel pumps, etc., the main rotor absorbs the largest fraction of total power required. Power requirements of the other systems are relatively small and, furthermore, their sum tends to be a constant fraction of total power required. Because of these factors, installed power requirements have been found[39] to be a function of main rotor characteristics only, specifically main rotor thrust required and main rotor disk loading. The introduction of noise reduction methodology is not expected to affect this functional relationship, except in the case where engine noise reduction methods may cause engine power losses which would necessitate increasing installed power. This effect is discussed in a subsequent section of this report.

[39] Metzger, R. F., et al, "Development of a Method for the Analysis of Improved Helicopter Design Crtieria", USAAMRDL TR 74-30, July 1974.

The relationship between main rotor thrust, disk loading and installed power is illustrated in Figure 19. If main rotor thrust required is assumed as equal to vehicle gross weight, the relationship expressed in Figure 19 reduces to:

$$HP_I = (.051)(GW)(DL/DR)^{.41} \tag{25}$$

where: HP_I = installed power (HP)

GW = vehicle gross weight (lb)

DL = main rotor disk load (= $GW/\pi R^2$, R = Rotor Radius) - (lb/ft^2)

DR = density ratio (ratio of air density at altitude to sea level air density)

Given the above relationship between rotor disk load, gross weight and rotor radius, Equation (25) may be further reduced to:

$$HP_I = .0318 \left(\frac{GW}{DR}\right)^{1.41} \cdot (1/R)^{.82} \tag{26}$$

Of interest in the present analysis is the change in installed power which occurs as a result of the introduction of noise reduction methodology. Equation (26) indicates that installed power will change only as a result of changes in vehicle gross weight, main rotor radius or density ratio. Established mission performance criteria, however, require that reduced noise vehicle configurations have hover ceiling capability equal to baseline vehicle configuations, and this requirement can only be met by keeping a constant, though unspecified, density ratio. This can be accomplished by normalizing Equation (26) with regard to baseline vehicle characteristics. The resulting normalized installed power required relationship is then given by:

$$HP_I' = HP_{I_o} (GW'/GW_o)^{1.41} (R'/R_o)^{.82} \tag{27}$$

where: HP_{I_o}, GW_o, R_o = installed power, gross weight and rotor radius of baseline vehicle

HP_I', GW', R' = installed power, gross weight and rotor radius of reduced noise vehicle

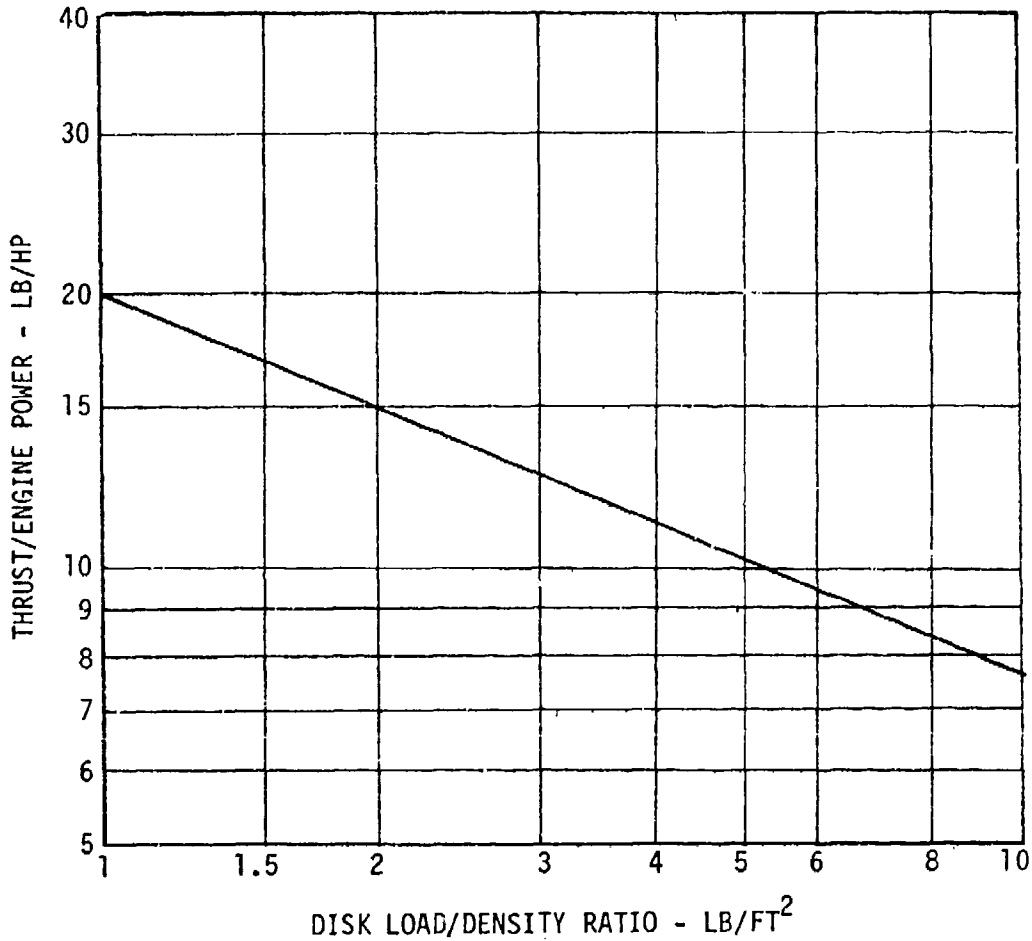

Figure 19. Hover Performance

Equation (27) has been used in the present analysis to determine the effect of introduction of noise reduction methodology on installed power.

Engine Weight and Rated Fuel Consumption

Given the installed power requirement of Equation (27), engine weight and rated fuel consumption rate can be determined. The relationship between installed power and engine weight is given by:

$$W_E = N_E \cdot 5.36 \cdot \left(\frac{HP_I}{N_E}\right)^{.568} \tag{28}$$

where: W_E = installed engine weight lbs

N_E = number of engines

This relationship, which was obtained from Reference 40, can be normalized in a manner similar to that of Equation (27), with:

$$W_E' = W_{E_o} \cdot \left(\frac{HP_I'}{HP_{I_o}}\right)^{.568} \tag{29}$$

where: W_{E_o}, HP_{I_o} = installed engine weight and horsepower for baseline vehicle

W_E', HP_I' = installed engine weight and horsepower for reduced noise vehicle

Installed power also determines the rated fuel consumption rate which, in specific terms, is the rate of fuel consumption per horsepower-hour, at rated horsepower. This engine characteristic is necessary to determine the rate of fuel consumption and, consequently, the fuel load required at the part power cruise flight condition. Rated fuel consumption rate is given by[39]:

$$SFC_R = N_E(1.136)\left(\frac{HP_I}{N_E}\right)^{-.105} \tag{30}$$

where: SFC_R = rated fuel consumption rate (lb-fuel/HP-hr)

[40] Bentele, M. and J. Laborde, "Evolution of Small Turboshaft Engines", SAE Paper 720820, October 1972.

[illegible]

[illegible]

where: [illegible]
[illegible] = [illegible]
power of baseline vehicle

[illegible] = related [illegible] data and [illegible]
power of replacement vehicle

Airframe weight

[illegible] aircraft [illegible] primarily by [illegible]
performance characteristics [illegible]. [illegible]
as a result of changes in their [illegible], in particular [illegible]
Table 10 the present analysis [illegible] airframe weight due to
changing vehicle [illegible] weight and motor [illegible]. As [illegible]
vehicle gross weight, such as the [illegible] of [illegible]
increasing rotor blade area, must be [illegible] with added [illegible]
structure, in order to [illegible]. Airframe
weight is particularly sensitive to rotor [illegible]
size, and consequently weight, [illegible] to [illegible]
rotor.

Airframe weight is defined as vehicle gross weight less useful load, fuel load and engine weight. Vehicle [illegible] airframe weight are:

1) Rotor group.

2) Tail group.

3) Body, fuselage group.

4 [illegible]

5) Flight [illegible]

6 [illegible]
group

7 Auxiliary power [illegible]

8 [illegible]
equipment, [illegible], etc.

Forward flight effects

Equations [illegible] have been used to determine the main rotor power required, which has been found to be readily related to total engine power required according to:

$$[illegible] \qquad [illegible]$$

where: $[illegible]$ = total engine power required in forward flight [illegible]

Main rotor thrust required in forward flight was found to be a function of vehicle gross weight, forward speed and effective flat plate drag area. The relationship developed for main rotor thrust is:

$$T_{MR} = \frac{[illegible]}{[illegible]} \qquad (35)$$

where: T_{MR} = main rotor thrust required in forward flight

The forward flight performance relationships expressed in absolute terms in Equations (32), (34) and (35) have been normalized for use in the present analysis. Baseline vehicle forward flight performance characteristics, calculated with the comprehensive helicopter analysis method discussed previously, were used to normalize these equations.

Generally, engine power required in forward flight, at best cruise speed, is substantially less than rated power, and the fuel consumption rate for this flight condition will be significantly less than the rate at full continuous rated engine power, which is usually [illegible]. The variation of specific fuel consumption rate with power demand for turboshaft engines is shown in Figure [illegible] which was obtained from reference [illegible]. In equation form, this relationship is expressed as:

$$[illegible] \qquad (36)$$

where: [illegible]

Assuming a constant ratio between engine and fuel consumption rates and forward flight power required, from Equations (31) and (34) respectively, the change in fuel flow rate due to the introduction of noise reduction devices may be determined with:

$$[illegible] \qquad [illegible]$$

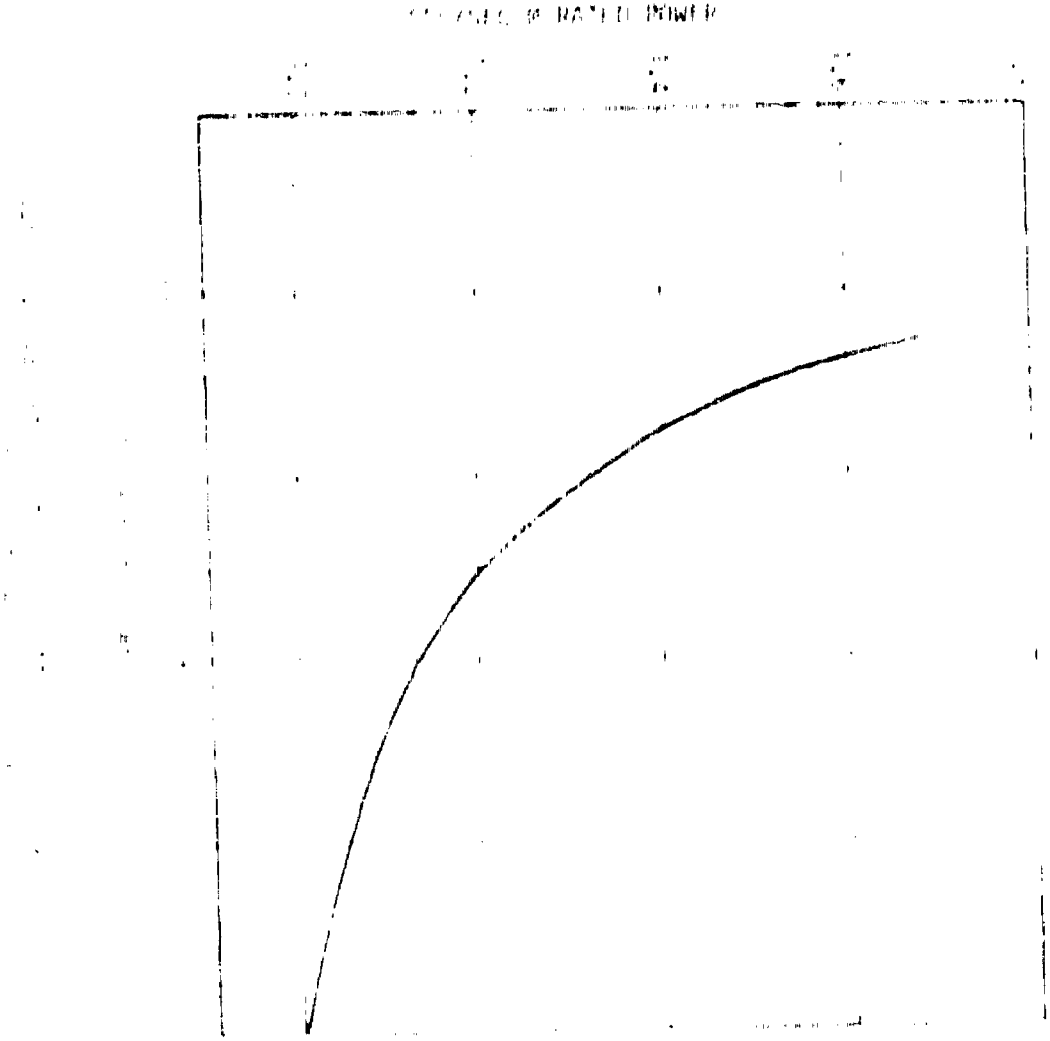

where [illegible]

[illegible]

[illegible]

Rotor Retreating Stall Margin

Rotor retreating stall margin can be defined as the difference in speed between any given speed and the speed at which the retreating rotor blade tip angle of attack first exceeds the blade section aerodynamic stall angle. At this speed rotor thrust and inertia begins to diverge and as speed is increased beyond this point, rotor power required will increase rapidly to the point where rotor power required exceeds the power available. Generally, vehicle climbing levels and ceiling will decrease, and vehicle handling characteristics will degrade, limiting maximum allowed power, and thus failure rather than power limitations, will usually limit forward speed capability. All of these factors are, however, directly related to the onset of rotor stall and, therefore, rotor stall margin has a very significant influence on helicopter rotor and vehicle design.

As stated in a previous section of this report, rotor performance criteria determine the main rotor size (diameter, solidity) required for a given vehicle gross weight and installed power. Given this basic rotor size, the preliminary analysis will generally determine the combination of total rotor blade area and rotor speed which must be used. The relationship between the airfoil section and rotor performance, characteristics and rotor size is discussed in the generalized stall limit boundary of figure 4 which was obtained from reference 4.[1] This curve is presented in terms of thrust coefficient, which is the ratio of forward speed to rotor tip speed, and the thrust coefficient to rotor solidity ratio, which is a measure

$$\frac{M_c}{\sigma}$$

where [illegible] rotor solidity ratio

M_c = [illegible] rotor tip speed Mach number

---

[1] Wells, [illegible], Performance, and Limitations, Presented at the 24th Annual National Forum of the American Helicopter Society, May [illegible].

STALLED REGION
UNSTALLED REGION

ρ = air density, $lb\text{-}sec^2/ft^4$

R = rotor radius, ft.

Ω = rotor speed, rad/sec

b = no. of rotor blades

c = blade chord, ft

Rotor advance ratio is given by:

$$\mu = \frac{V}{\Omega R} \qquad (39.$$

where: μ = rotor advance ratio

V = forward speed, ft/sec

The graphical expression of figure 21 may be stated in equation form as:

$$\mu_s = \frac{.1363 - C_T}{.333} \qquad (40.$$

where μ_s = advance ratio for the onset of stall

The stall speed V_s, in knots, at any given C_T and Ω is then equal to:

$$V_s = \frac{.1363 - C_T}{.333} \cdot \frac{\Omega}{1.689} \cdot$$

The stall margin M_s, again in knots, at any given airspeed V is given by:

$$M_s = \frac{.1363 - C_T}{.333} \cdot \frac{\Omega}{1.689} - V \qquad (4$$

within the present program. The [illegible] criterion was limited to the evaluation of main rotor noise reduction methodology. In this report, tip-path plane tilt angle was used as the criterion for determining how to trade off rotor speed reduction which could be obtained in conjunction with an equal rotor tip chord increase (see blade chord). Equation 1 was used directly, to relate tip speed reduction, and its use in this manner is described in a subsequent section of this report.

HELICOPTER COST ANALYSIS

All cost calculations have been made using a parametric cost model, consisting of the following basic cost elements:

- Initial investment cost
- Indirect operating cost
- Direct operating cost

These elements have been further divided into readily calculable cost components, each of which may be related to one or more of the basic vehicle design parameters.

Initial investment cost has been divided into airframe cost, engine cost, avionics cost, initial spares cost and added equipment cost. Figure 22 shows the relationship between airframe cost and airframe weight used in the cost model. Engine cost has been related to installed power and this trend is given in Figure 23. Figure 24 and Figure 25 relate initial spares cost and avionics equipment cost as a weight ratio to airframe and engine weight. The airframe, initial spares and avionics trends are based on historical helicopter cost data, References [illegible], 44, and 45 and include all design and development, as well as unit, costs. The engine cost trend is similarly based and was derived from data in Reference 4.

Indirect operating cost [illegible] in terms of dollars per year of aircraft operation, is related to the unit weight in Figure 26. This trend is based on 3% airframe yearly insurance cost of [illegible] aircraft flyaway cost, which combined the cost of airframe and engines.

[1] "Helicopter Operating Costs," Flight International, October 1971.

[2] "Sikorsky Direct Operating Cost," Sikorsky Aircraft, 1971.

[3] "Bell Model 204, 205, 206A, 206L and 212 Summary," Bell Helicopter Co., August 1971.

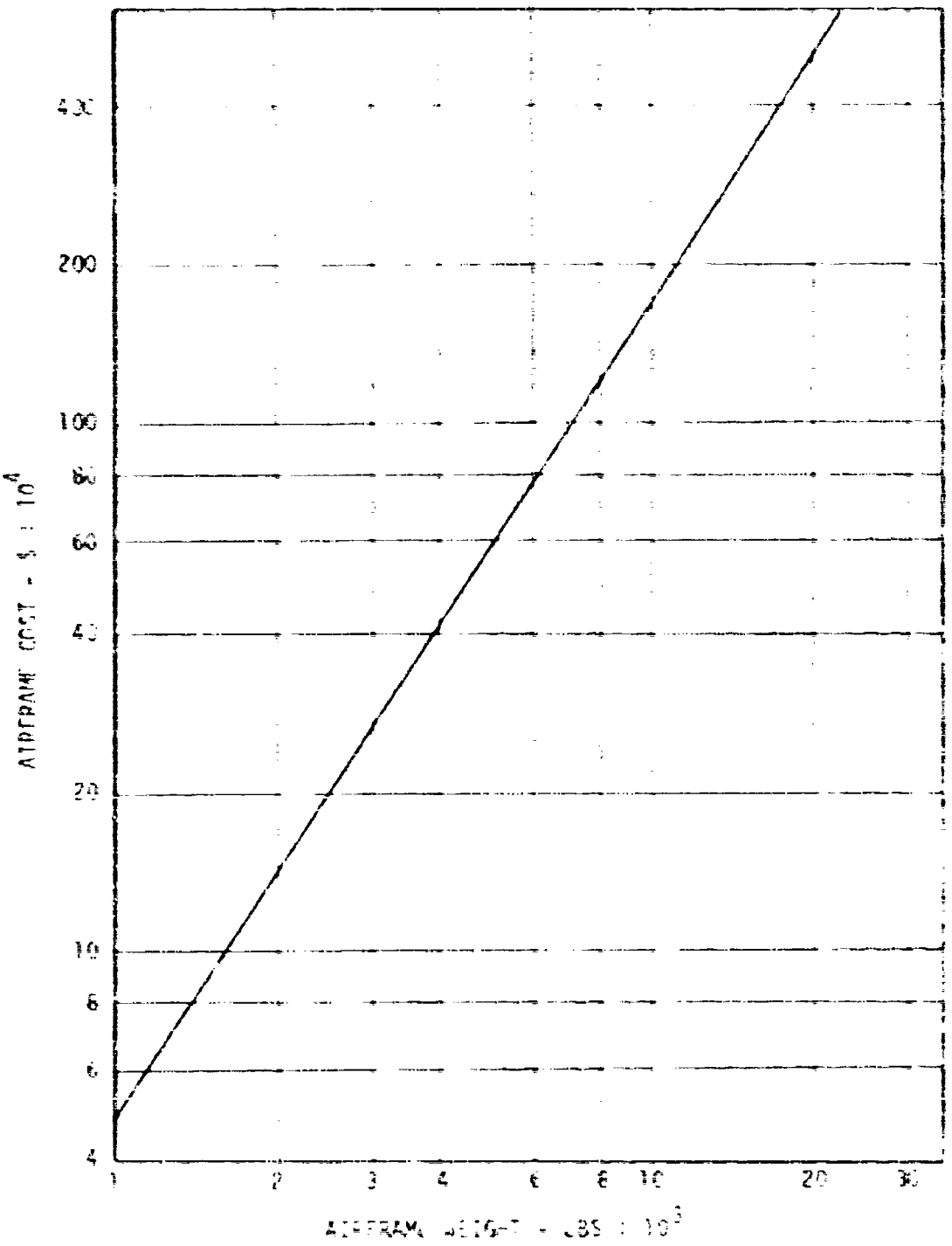

Figure 22. Helicopter Airframe Cost vs Airframe Weight

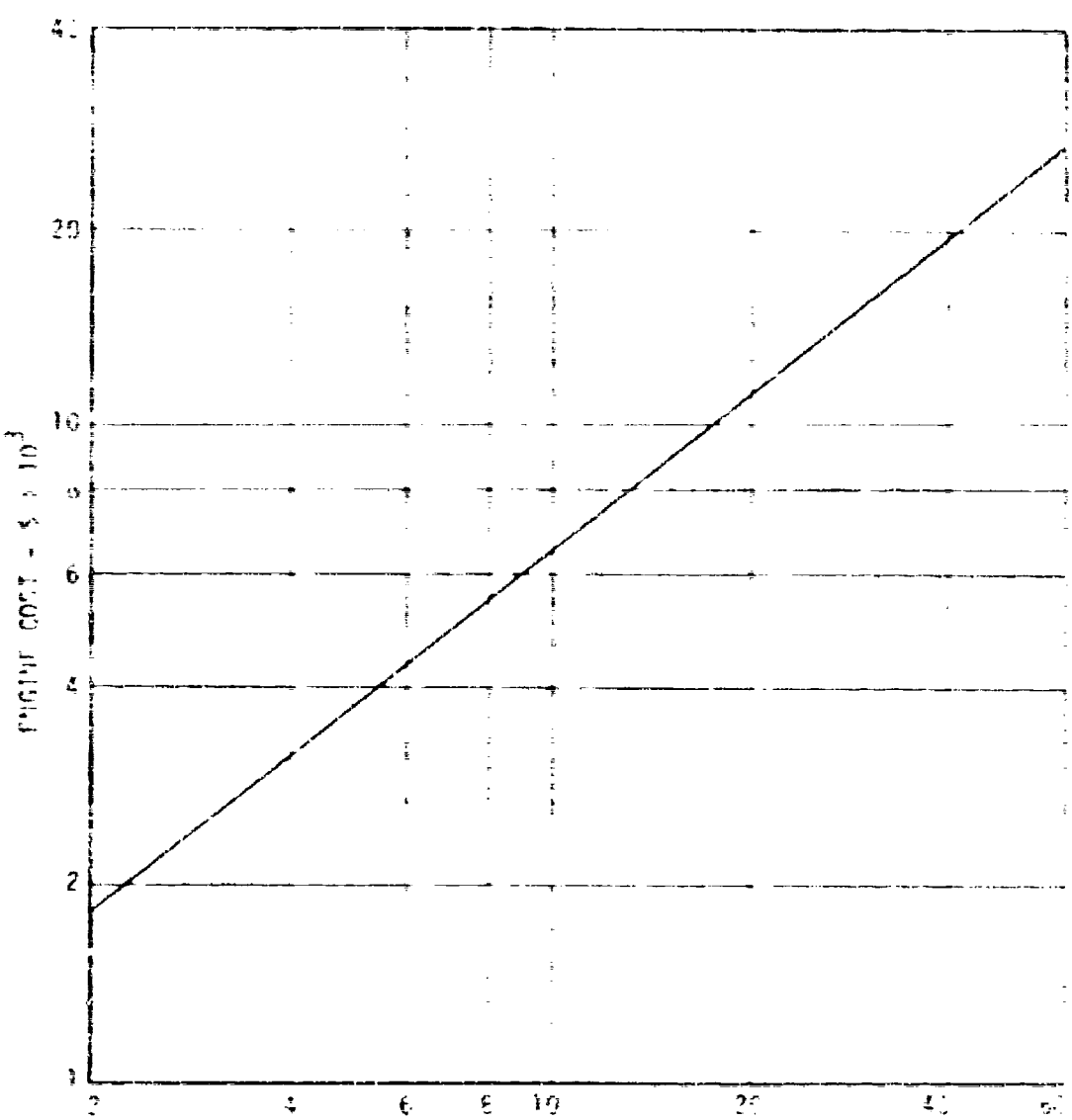

Figure 23. Helicopter Engine (Turboshaft) Cost vs Installed Power

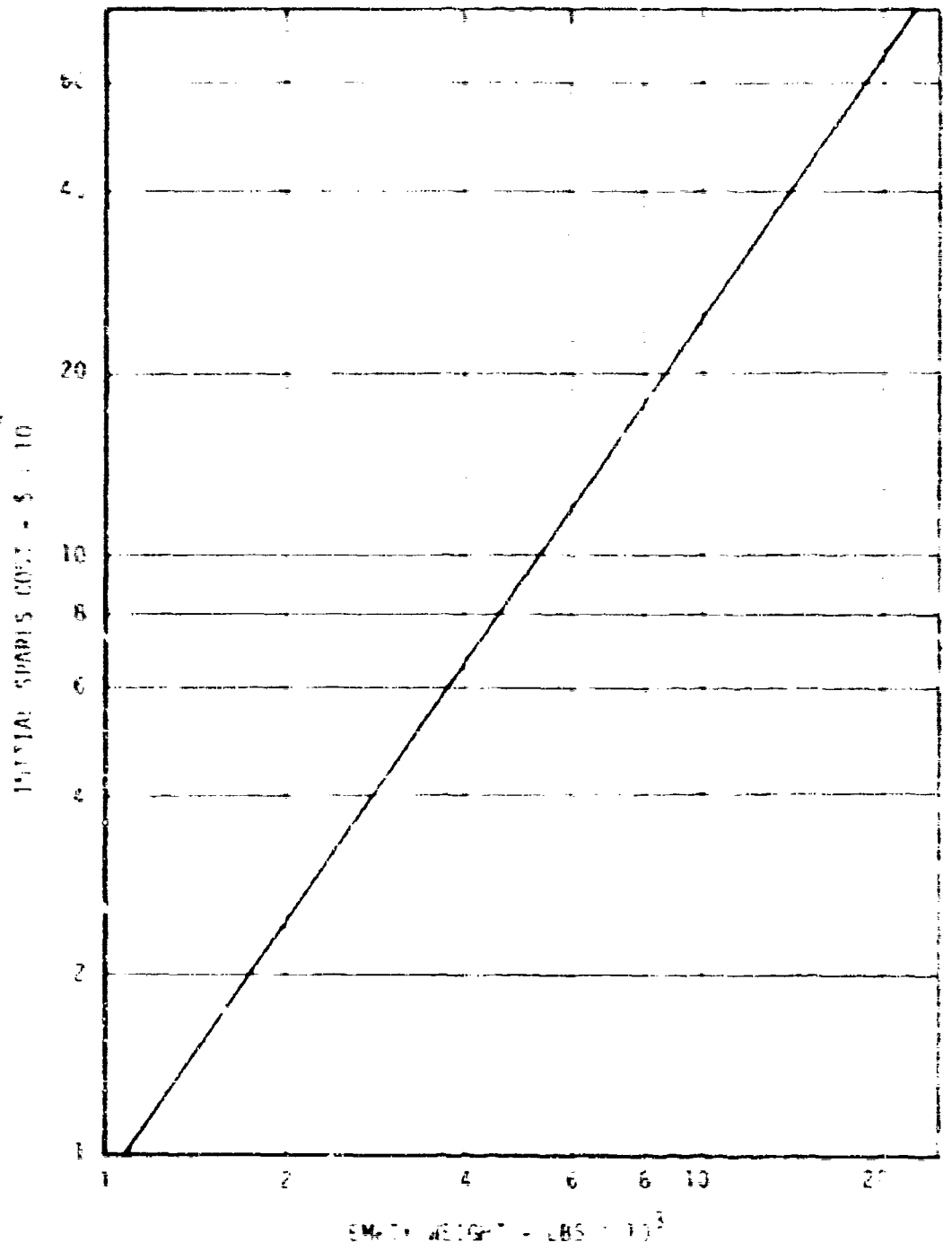

Figure 24. Helicopter Initial Spares Cost vs Empty Weight

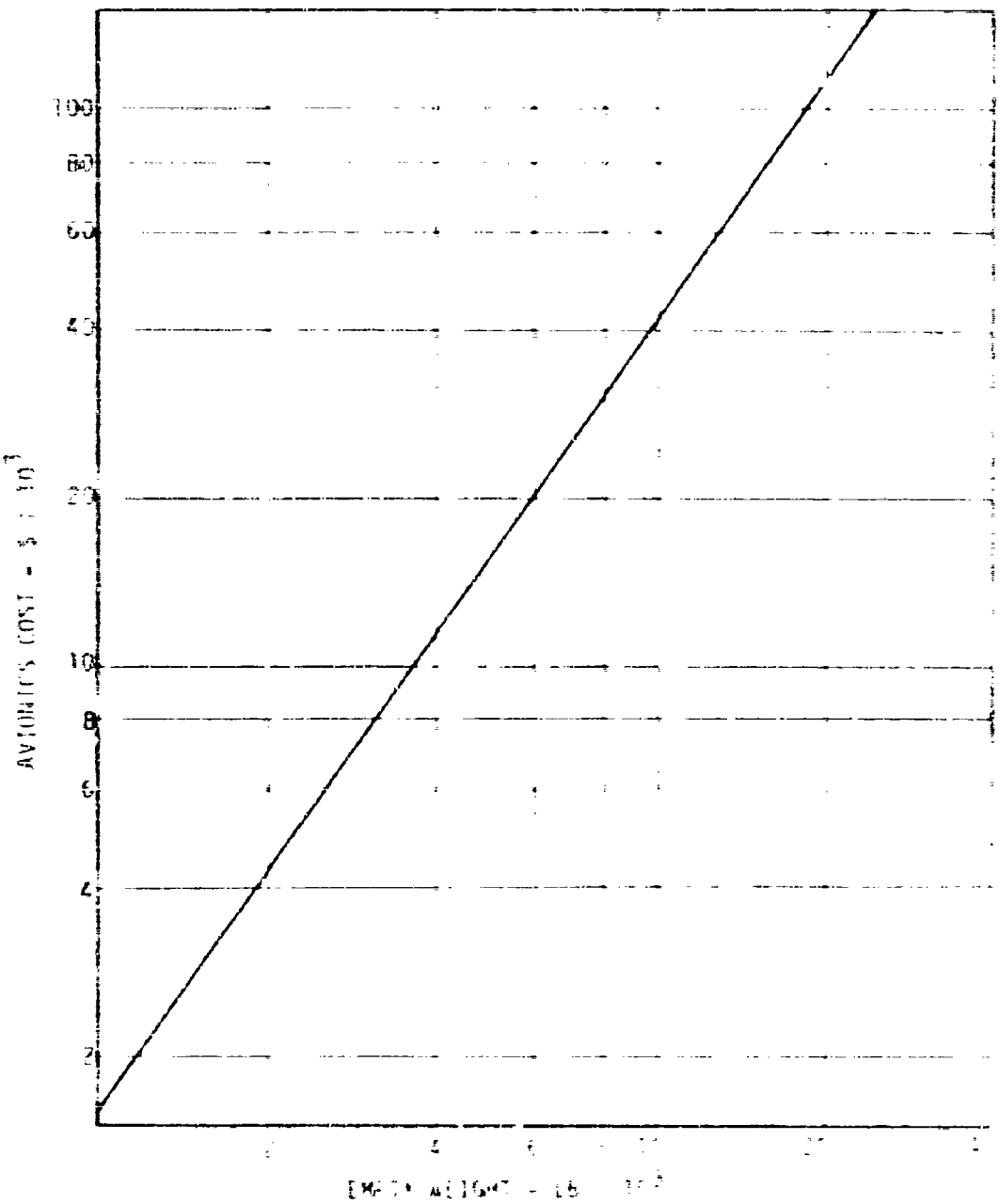
100
80
60
40
20
10
8
6
4
2

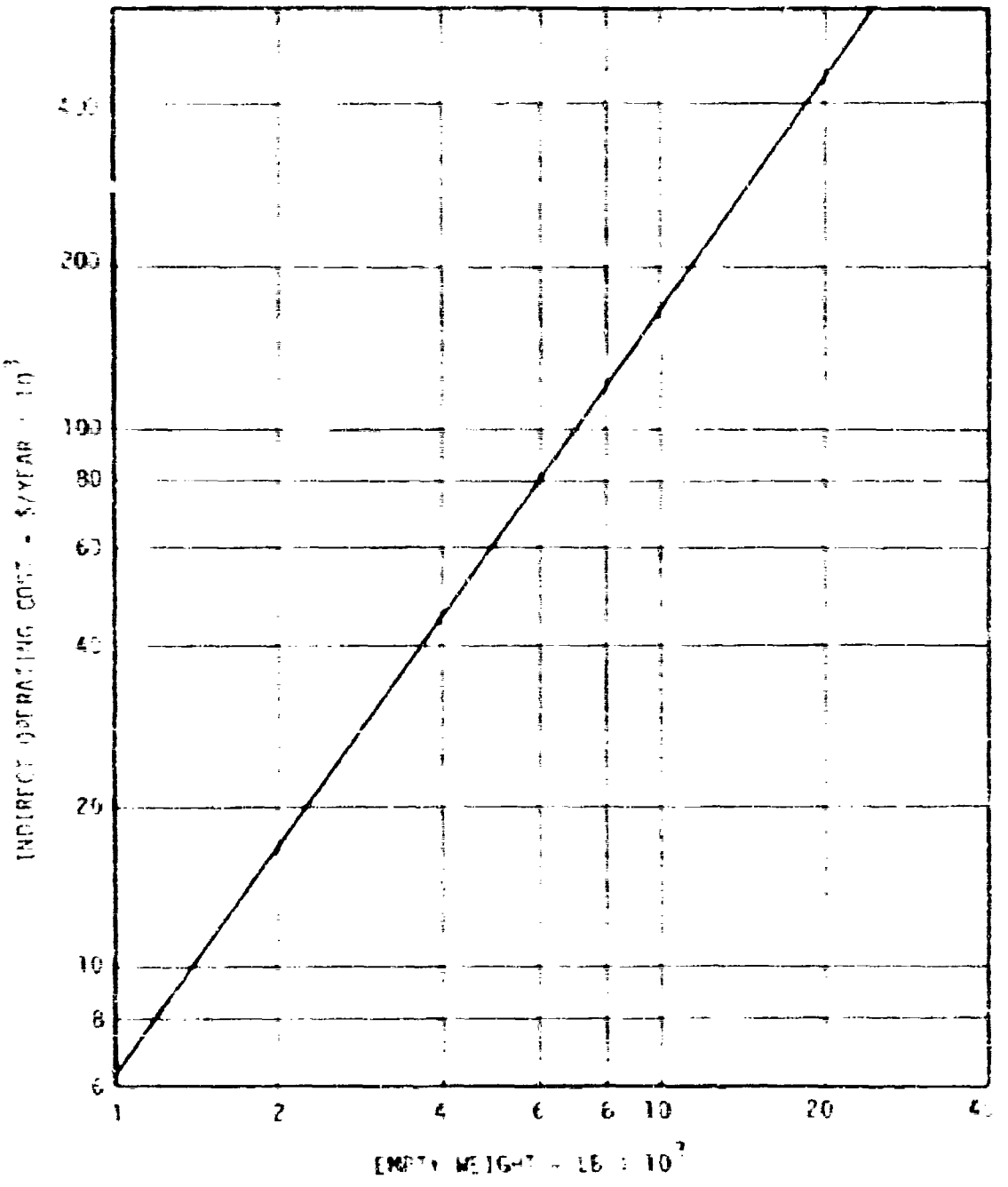

Figure 26. Helicopter Indirect Operating Cost Vs Empty Weight

Direct operating cost (DOC) includes costs of fuel and oil, maintenance and spares, and crew. Each of these cost components is expressed in terms of dollars per aircraft hour. Maintenance and spares cost is shown as a function of empty weight in figure 27. Cost of fuel and oil is shown in figure 28 as a function of installed engine power. The trend of crew cost with aircraft weight is given in figure 29. As for previous cost elements, DOC component costs are based on historical helicopter operating data.

In applying the preceding relationships, the following cost elements have been allowed to escalate, commensurate with changes in vehicle design:

- Investment cost
  - Airframe cost
  - Engine cost
  - Initial spares cost
- Indirect operating cost
- Direct operating cost
  - Fuel and oil cost
  - Maintenance and spares cost

Avionics equipment and crew costs were not permitted to vary.

Total life cycle cost (LCC), the cost to own and operate the vehicle over its useful life, is made up of contributions from each of the cost elements, and is a function of the annual utilization rate (N_A) in aircraft hours per year and useful life (L_U) in years. The functional relationship is:

$$LCC = C_I + DOC \times N_A \times L_U + IOC \times L_U \qquad (1)$$

where: LCC = life cycle cost - $

C_I = initial investment cost - $

DOC = direct operating cost - $/hr-yr

IOC = indirect operating cost - $/yr

N_A = annual utilization - hr/yr

L_U = useful life - yrs

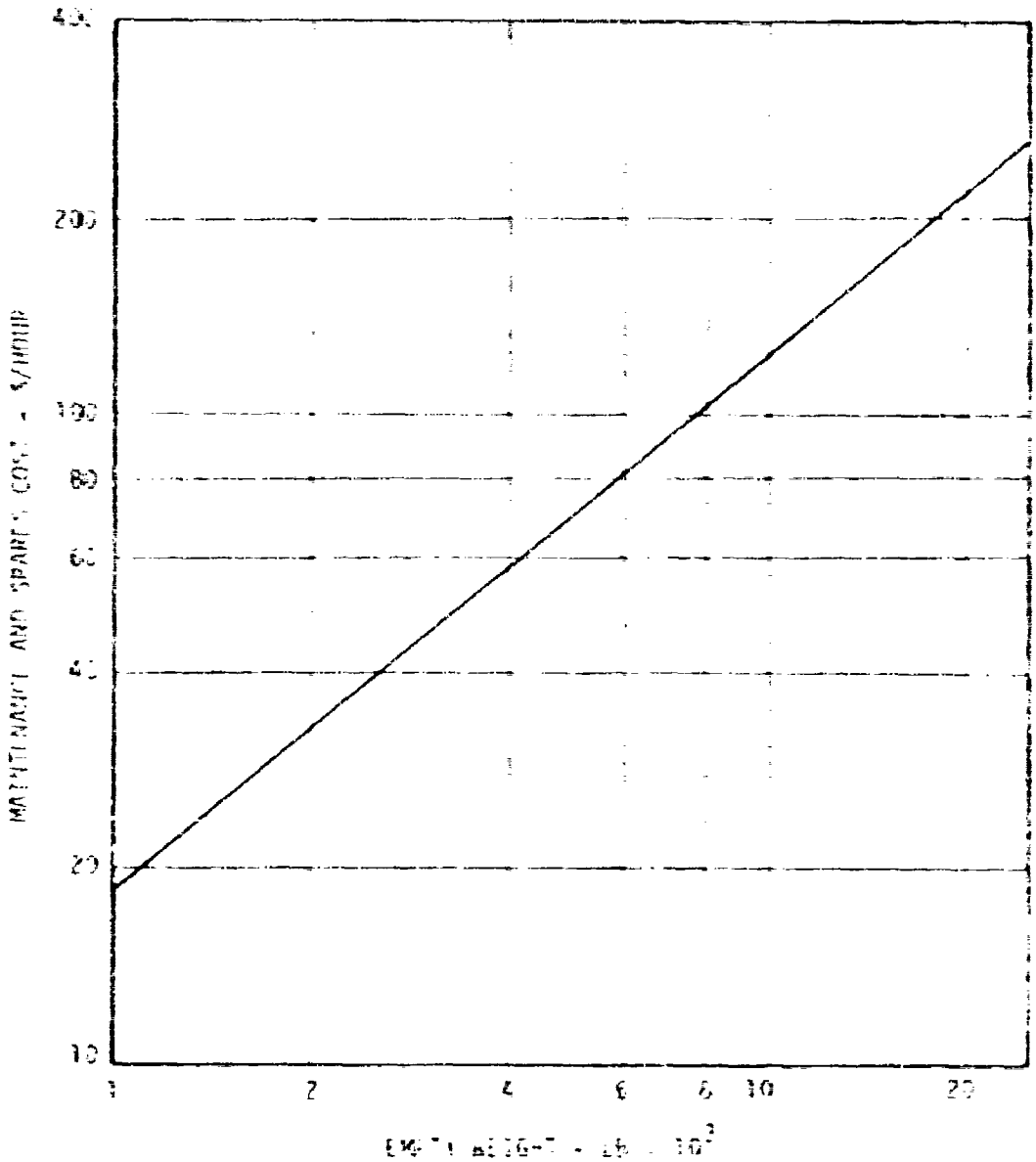

Figure 27. Helicopter Maintenance and Spares Cost as Empty Weight

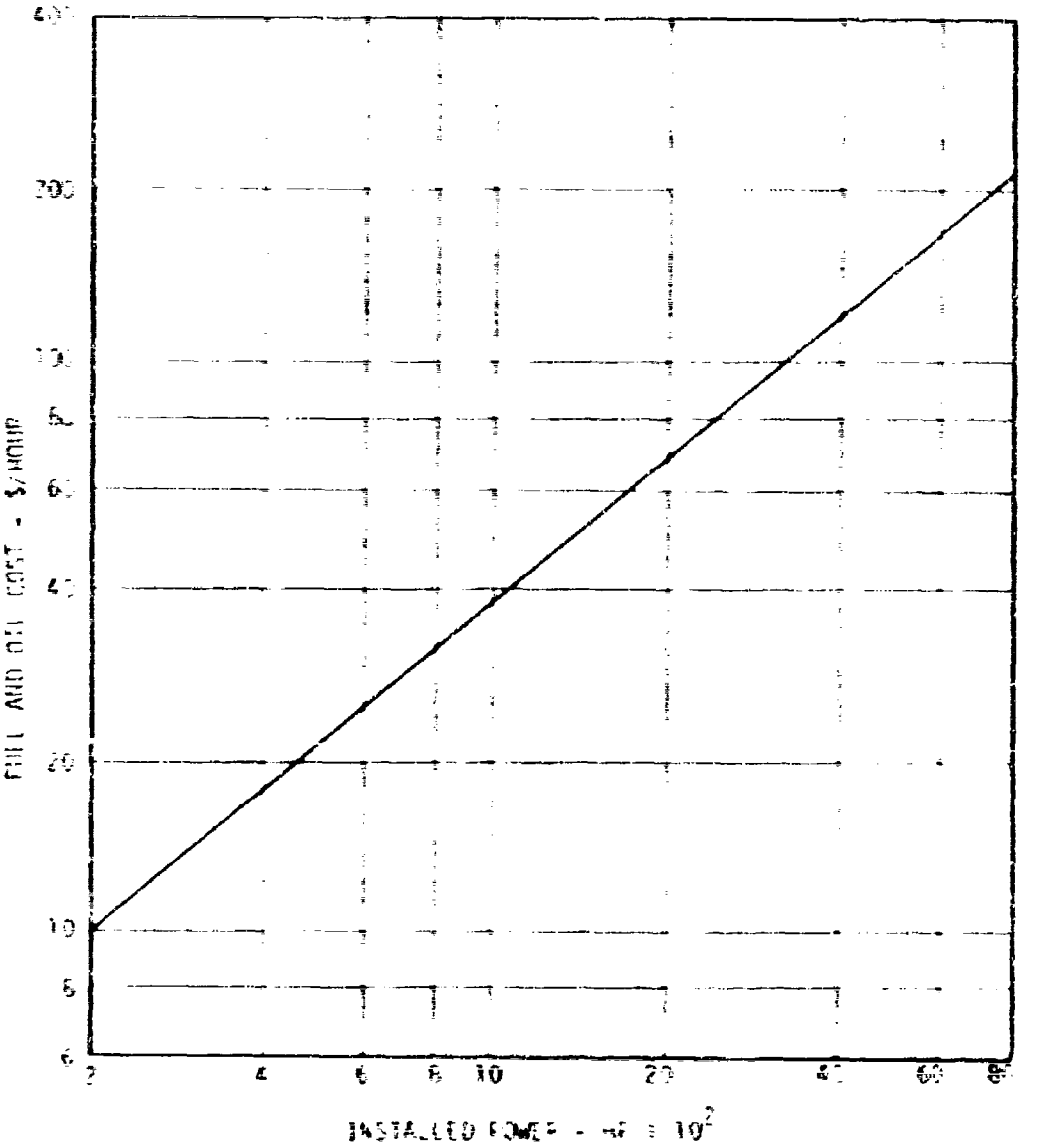

Figure 28. Helicopter Fuel and Oil Cost vs Installed Power

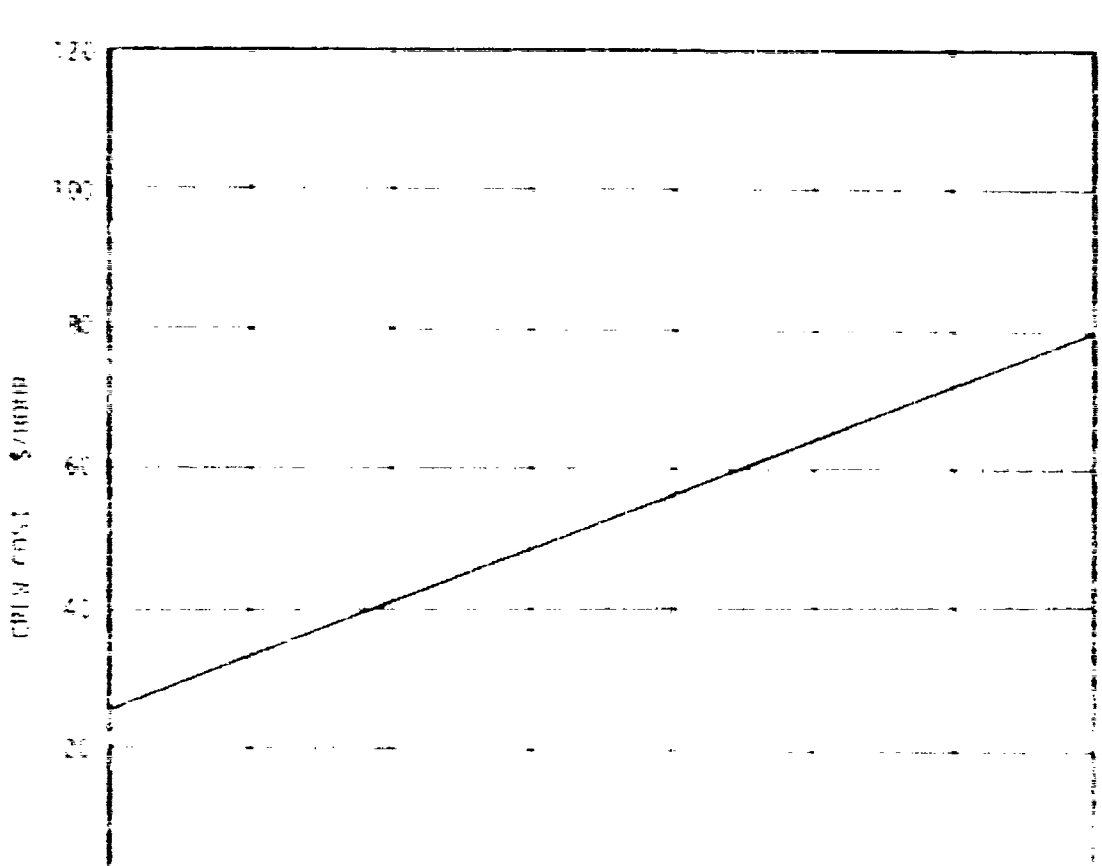

[illegible] NOISE CALCULATION

Baseline noise levels have been calculated for seven existing light helicopter models selected as being representative of the entire civil helicopter fleet. These calculations have been made for a steady level flight condition at the best cruise speed specific to each selected baseline vehicle, at an altitude of 500 feet. A simulated flight duration of 30 seconds was used, with vehicle and component noise spectra, in 1/3 octave bands, calculated at one second intervals over the entire flight duration. Noise levels were calculated for observer locations five feet above ground level directly below the vehicle flight path and 500 feet to either side of the flight path. Differing initial points were used for each vehicle evaluated. These initial points were selected, considering the best cruise speed of each vehicle, such that each vehicle would pass over the observer locations approximately halfway through the simulated flight. The geometrical layout for these noise calculations is illustrated in Figure 31.

VEHICLE TRIM CALCULATIONS

Prior to making the baseline vehicle noise calculations it was necessary to analytically trim the selected vehicles for their respective best cruise speed flight conditions. This was necessary in order to generate the rotor airload and vehicle performance data needed to make the noise calculations. The results of these trim calculations are summarized in Table 9.

VEHICLE NOISE LEVELS

Total vehicle noise levels, including the contributions from the rotor systems, engine(s) and transmission, were calculated for the vehicle trim conditions of Table 9, and observer locations of Figure 31. Calculations were made in terms of 1/3 octave band spectra at one second time intervals for a total flight duration of 30 seconds. These spectra were converted to effective perceived noise level (EPNL), maximum overall sound pressure level (OASPL) and A-weighted sound pressure level (dBA) units for each vehicle and observer location.

Table 10 summarizes the calculated baseline vehicle noise levels in terms of EPNL. Shown are the EPNL values calculated for each vehicle and observer location, and the corresponding range* at which the maximum tone corrected perceived noise level occurred. In all cases, vehicle EPNL was found to be equal to tone corrected perceived noise level, indicating that the duration correction was zero. [illegible] data are shown in Table 11 for the [illegible]. [illegible] data were available for the calculation of [illegible] noise, and [illegible] noise was assumed to contribute [illegible] to vehicle EPNL.

---

* Range is defined as the distance from the observer to the vehicle measured parallel to the vehicle flight path.

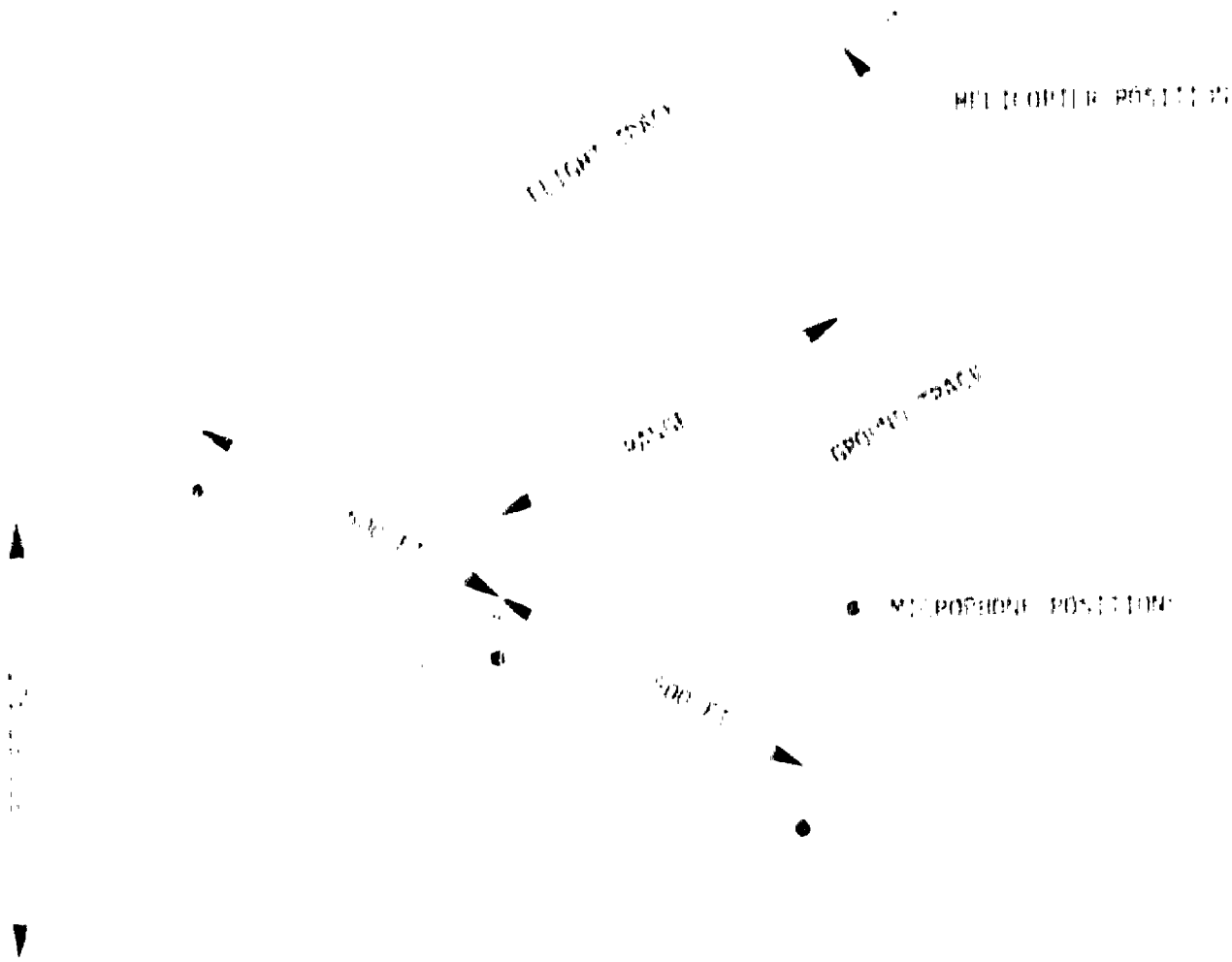

[illegible] [illegible] [illegible]

Vehicle	Main Rotor		Tail Rotor				Fuselage	
	Thrust (lb)	Power (hp)	Thrust (lb)	Power (hp)	Tip Speed (fps)	Airspeed (kts)	Angle of Attack (deg)	Net Lift (lb)
Bell Model 47	2951	181	151	3.1	2655	70	-6.67	-39.0
Bell Model 205	[illegible]	760	452	13.4	9500	110	-4.93	-431.7
Bell Model 206	3236	174	116	7.7	3000	112	-5.29	-203.3
Hughes 300	1974	130	111	4.2	1900	70	-6.33	-73.9
Hughes 500	2405	191	135	3.6	2417	110	-.699	-9.4
Sikorsky S-61	19600	1411	1759	20.1	1950	121	-5.19	-47.7
Sikorsky S-64	35431	1544	3172	121.7	3x400	80	-5.56	-27.8

* Positive Nose Up

[illegible] [illegible] [illegible]
[illegible] [illegible] [illegible] [illegible]
[illegible]

	Fly Over		Port Fly-By		Starboard Fly-By	
[illegible]	Range ft	[illegible]	Range ft	[illegible]	Range ft	[illegible]
[illegible]	[illegible]	[illegible]	[illegible]	[illegible]	[illegible]	[illegible]
[illegible]	[illegible]	[illegible]	[illegible]	[illegible]	[illegible]	[illegible]
[illegible]	[illegible]	[illegible]	[illegible]	[illegible]	[illegible]	[illegible]
[illegible]	[illegible]	[illegible]	[illegible]	[illegible]	[illegible]	[illegible]
[illegible]	[illegible]	[illegible]	[illegible]	[illegible]	[illegible]	[illegible]

The calculated vehicle [illegible] of Table I would correlate well with vehicle gross weight. Trends of [illegible] for each observer location are like in Figure 5. The slopes of these trends are similar, with a [illegible] for a change of vehicle gross weight. A [illegible] between the flyover and flyby [illegible] is attributed to the vehicle airspeed accounting for approximately [illegible], with the remainder [illegible] most probably due to the [illegible] directionality, [illegible] between the two [illegible] is also due to [illegible] directionality of the main rotor. Standard side [illegible] for all the vehicles evaluated, the left side observer of the standard side. [illegible] is [illegible] is also expected to be the source of most [illegible], which is discussed in a subsequent section of the report. The rotor noise was [illegible] insignificant contributor to vehicle noise for the flight condition and observer locations evaluated.

The data of Table I indicate that reflection [illegible] noise level [illegible] is a maximum at or near the point of minimum slant range, at least for the flight condition and observer orientations considered in the present study. Since vehicle noise is [illegible] a function of maximum [illegible], this means that it is only a function of the instantaneous vehicle noise location at or near the point of closest approach to the observer (minimum slant range), and is not influenced in any [illegible] by the directionality of vehicle noise sources (fore and aft of the flight path) in the plane of the main rotor shaft. This is of significance because it means that the vehicle [illegible] can be eliminated by determining from available or the per [illegible] noise location at only one point in time, and for the [illegible] of relative vehicle observer orientation. It should be pointed out, however, that this approximation may only be valid for the [illegible] flight condition and observer orientations used in the present study.

[illegible] noise [illegible] for the [illegible] of Table II are shown in Figures 3-5. The [illegible] corresponds to the data conditions of Table I. Comparisons are given for the left and standard side flyover observer locations only, since the [illegible] flyby locations are, in all cases, less than the standard side location.

* Slant range is the [illegible] between the vehicle and observer [illegible]. At the point of closest [illegible] the flyover observer vehicle slant range is 500 ft, while the flyby observer vehicle slant range is 500 ft.

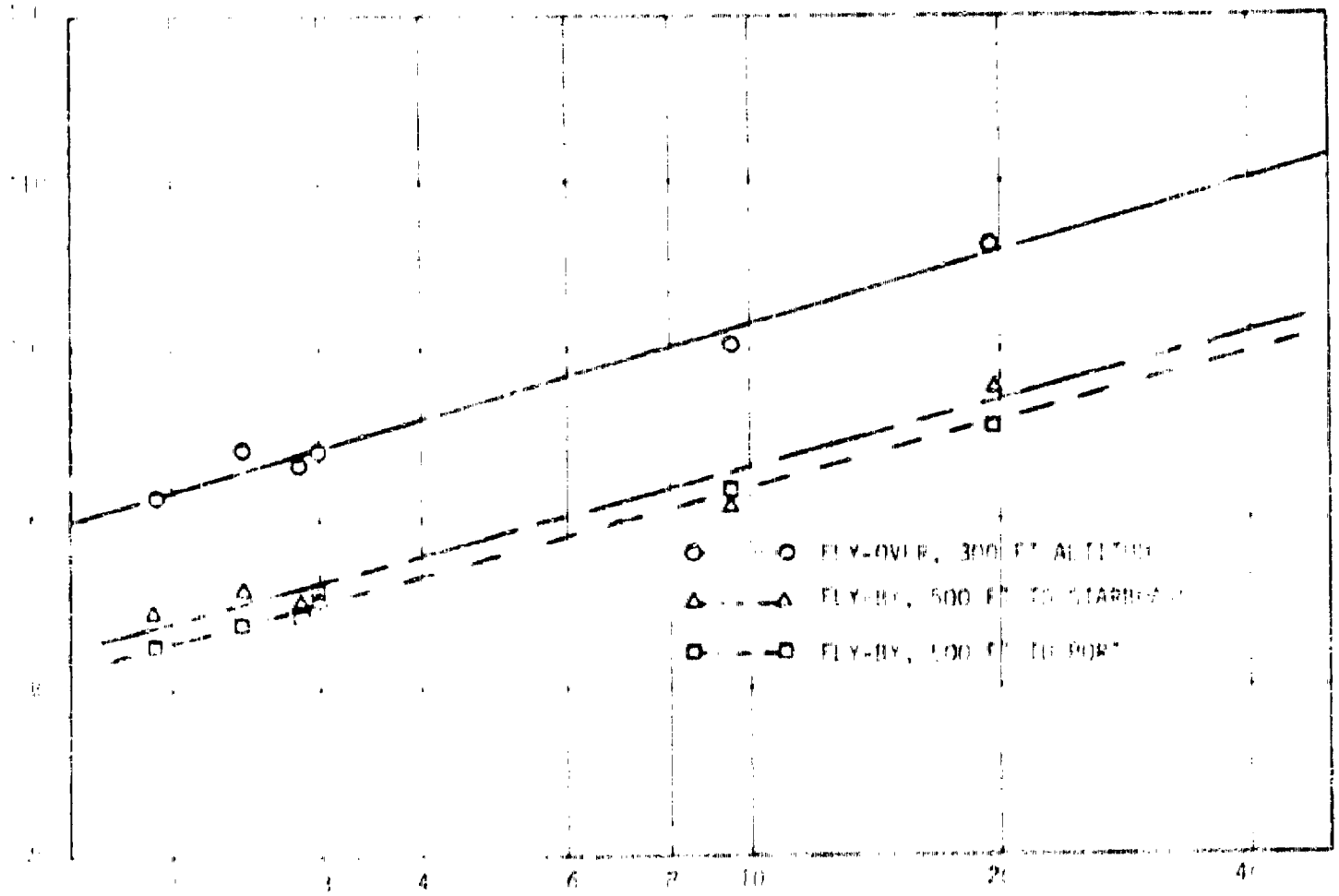
FLY-OVER, 300 FT ALTITUDE
FLY-BY, 500 FT
FLY-BY, 100 FT
GROSS WEIGHT - LBS

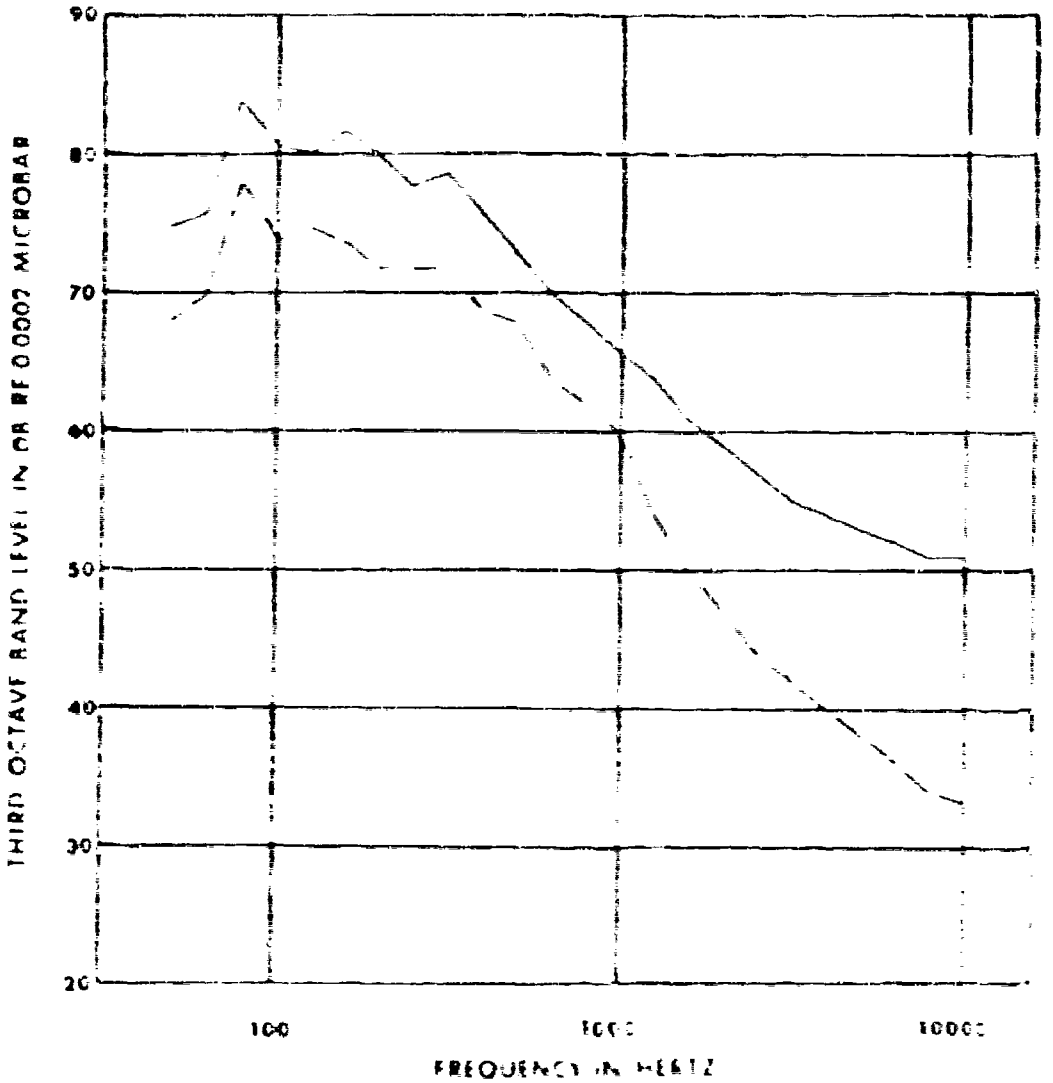

Figure [illegible]

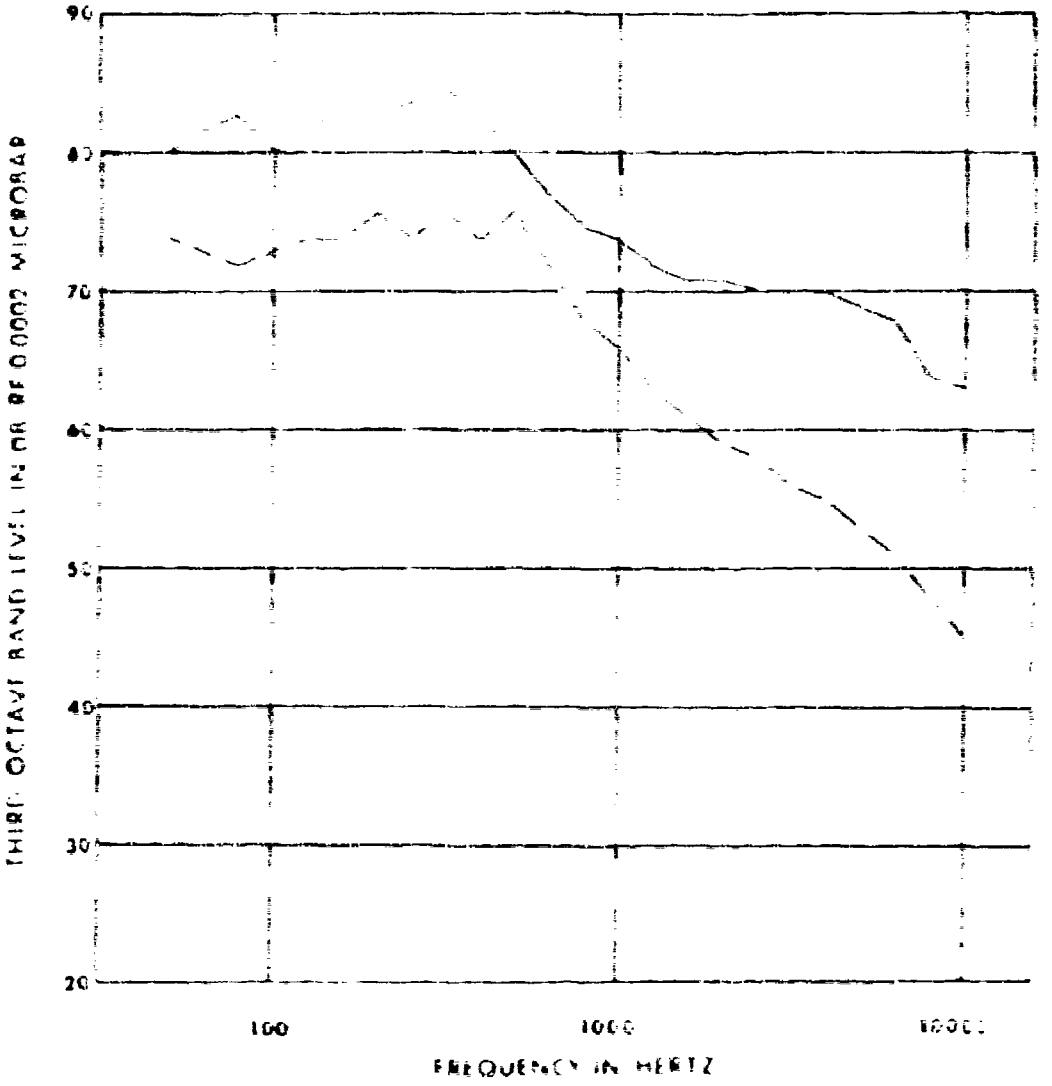
90
80
70
60
50
40
30
20
100
1000
10000
FREQUENCY IN HERTZ

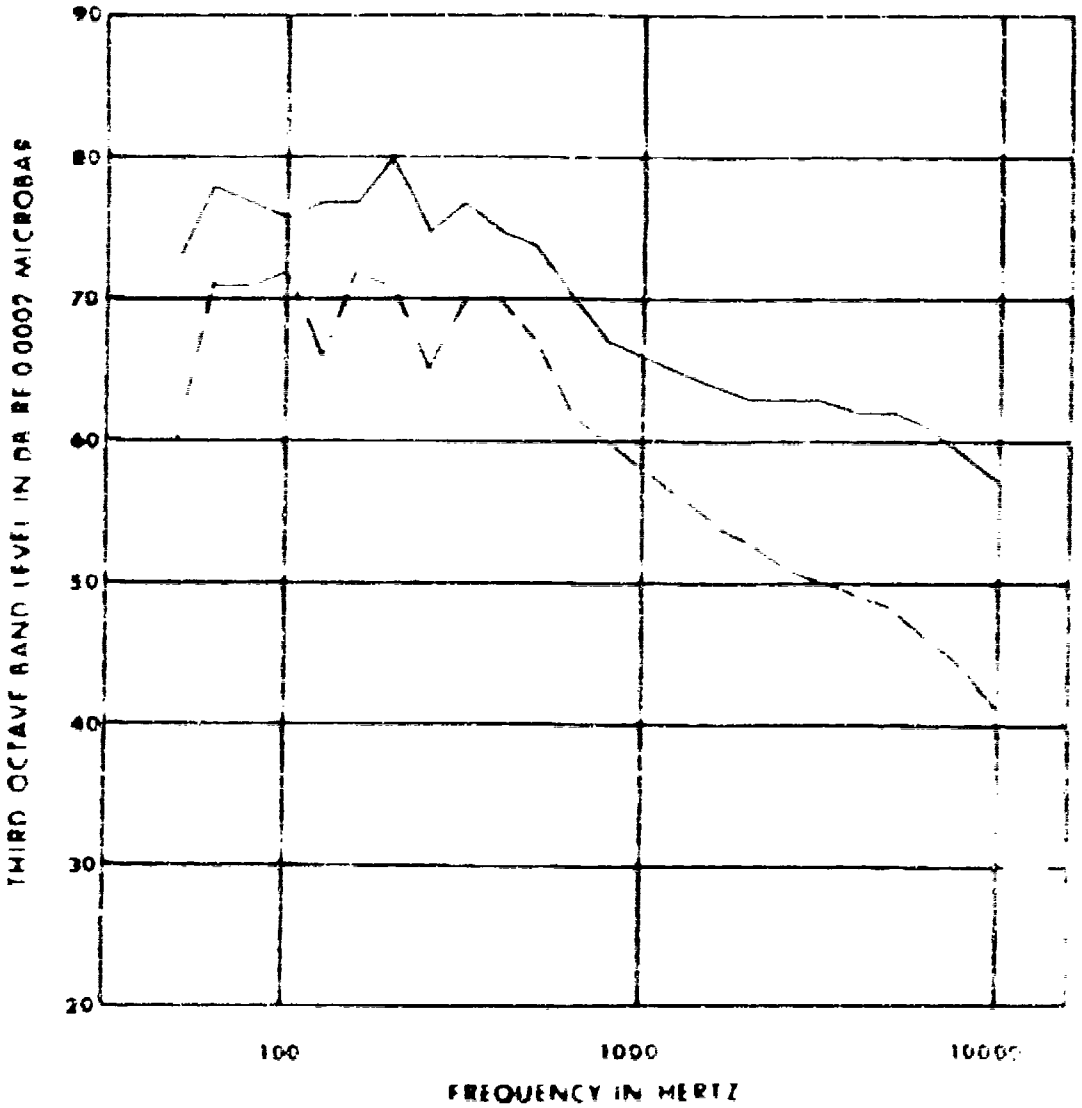

Figure 34. Calculated Baseline Noise Spectra for Bell Model 206, 112 kts S.L. Flight, 300 Ft Altitude, at Time of Maximum PNL

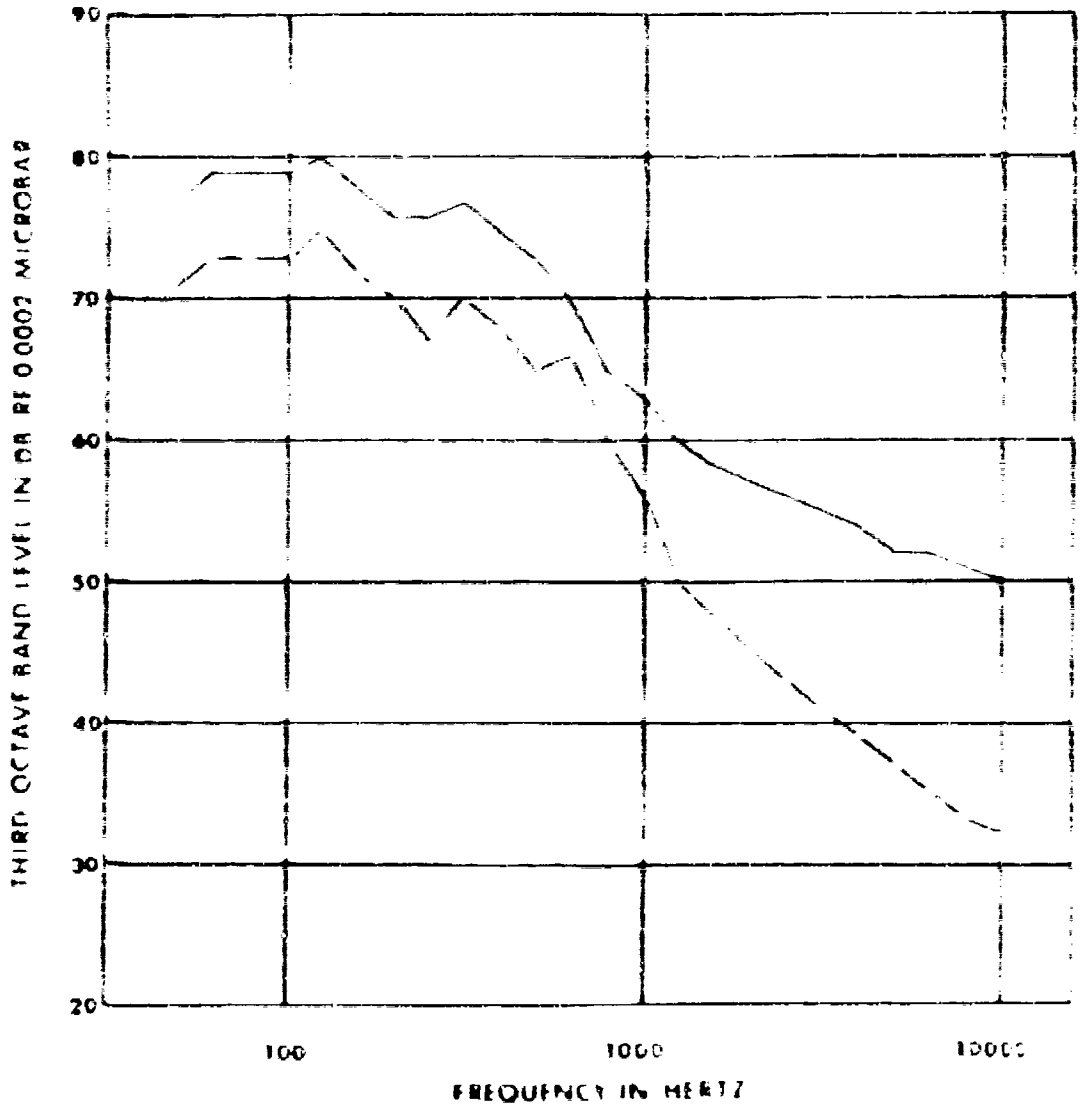

Figure 35. Calculated Baseline Noise Spectra for Hughes [illegible] at Time of Maximum [illegible]

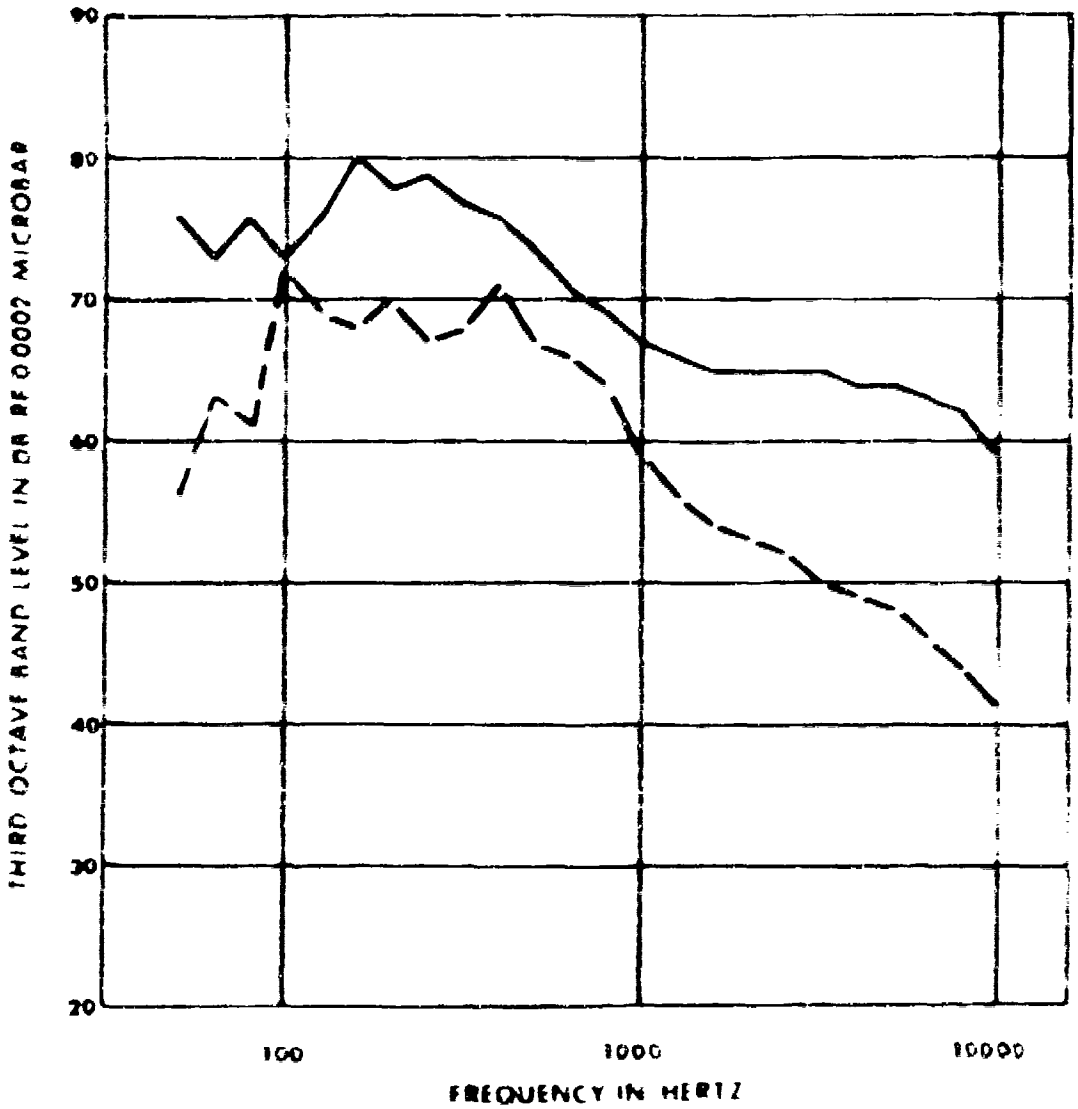

Figure 30. Calculated Baseline Noise Spectra for Engine Model 500, 110 kts S.L. Flight, 300 Ft Altitude, at Time of Maximum PNLT

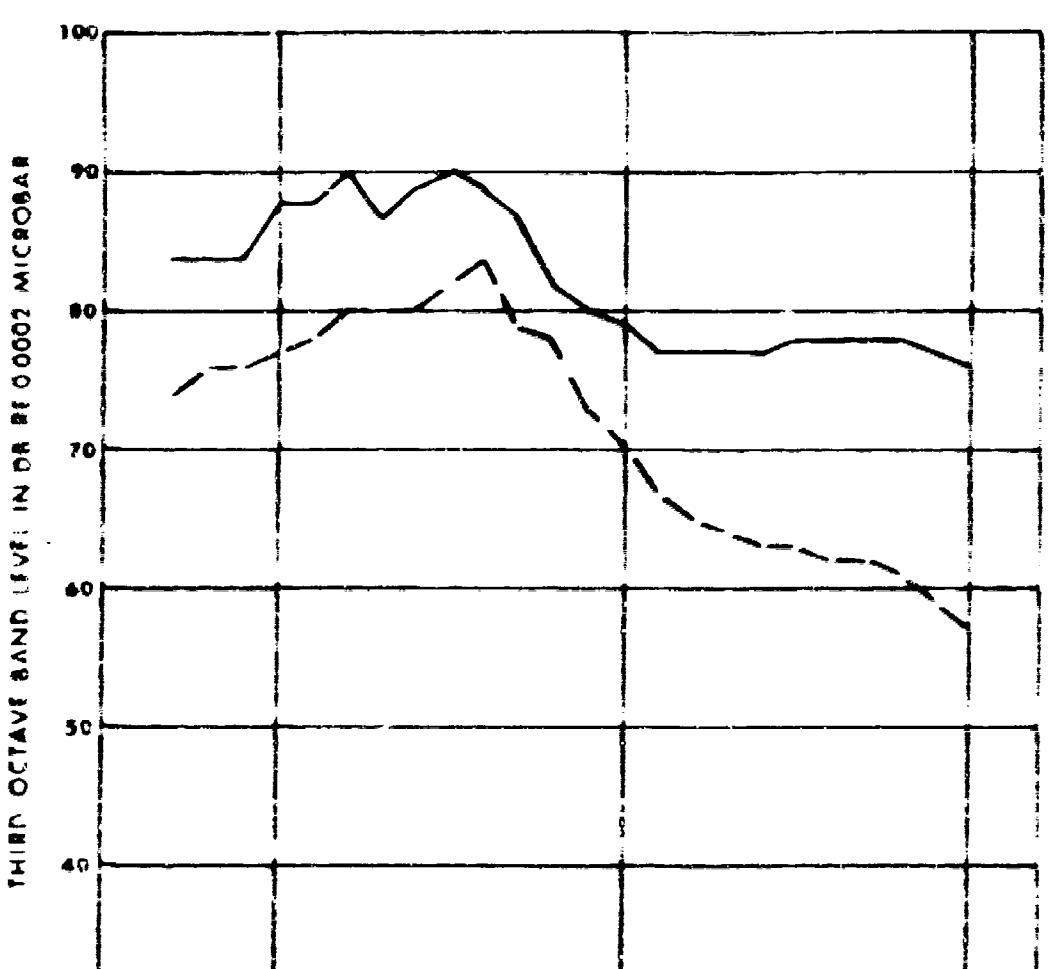
100
90
80
70
60
50
40
30
THIRD OCTAVE BAND LEVEL IN DB RE 0.0002 MICROBAR
100
1000
10000
FREQUENCY IN HERTZ

Figure 37. [illegible]

Calculated overall and A-weighted sound pressure levels for the baseline vehicles are shown in Tables 11 and 12. Overall sound pressure levels (OASPL) have been calculated from the available 1/3 octave band spectra and consequently only include vehicle noise within the frequency range covered by the 50 Hz to 10 kHz 1/3 octave bands. These data do not, therefore, include the low frequency components of main rotor noise which tend to dominate helicopter OASPL, and the levels shown should be interpreted accordingly.

COMPONENT NOISE SOURCE SIGNIFICANCE

In keeping with the overall program objectives, analyses were performed to determine the relative significance of the various baseline helicopter vehicle noise components. The results of these analyses were essential for establishing the appropriateness of the many available potential means of reducing helicopter noise, and for the selection of specific noise reduction methods for evaluation. These analyses consisted of comparisons of the various component noise source spectra, with each other, as well as with the total vehicle noise spectra. Based on these comparisons determinations were made as to which noise components contributed most to vehicle noise, and consequently, which component noise reductions would produce the most significant reduction in total vehicle noise.

The various helicopter component noise sources, including the main and tail rotors, engines and transmission, contribute to the total vehicle noise spectrum in a very complex way, which is highly dependent on both vehicle flight condition and observer orientation. The relative importance of these sources is also a function of the criteria which is used to evaluate the resulting vehicle noise spectrum. Within the present program, however, vehicle flight condition can be removed as a variable, since only one flight condition was been considered. Furthermore, since vehicle EPNL has been established as the primary evaluation criteria of interest, consideration of the influence of variation in evaluation criterion can similarly be removed. Consequently, since vehicle EPNL has been shown previously to be only a function of instantaneous peak PNL, component source significance can be established solely on the basis of comparison of individual source spectra at the instant of maximum PNL.

Evaluation of relative component source significance within the present program has been limited to three of the seven selected baseline vehicles. The vehicles considered were the Hughes 500, Bell 205 and Sikorsky S-61. Pertinent vehicle noise level spectra for these vehicles are shown in Figures 36, 37 and 37.

TABLE 11. BASELINE VEHICLE MAXIMUM UNIFORM SOUND PRESSURE LEVEL (DBASPL) AND RANGE FOR MAXIMUM DBASPL

Vehicle	Fly-Over		Fore Fly-by		Sideboard Fly-by	
	Range (ft)	DBASPL (dB)	Range (ft)	DBASPL (dB)	Range (ft)	DBASPL (dB)
Bell 47	400	91.5	400	83.4	400	83.5
Bell 205	374	91.4	375	87.1	436	84.1
Bell 206	35	97.6	35	91.4	224	80.1
Hughes 369	33	95.8	33	81.6	33	82.1
Hughes 500	126	97.5	126	79.3	450	82.1
Sikorsky S-61	97	96.7	97	90.2	97	91.2

TABLE [illegible]. BASELINE VEHICLE MINIMUM AVAILABLE SOUND PRESSURE LEVELS (dBA, A/C SYSTEM FOR MINIMUM dBA)

	Fly Over		Fore Fly-By		Starboard Fly-By	
Vehicle	Range (ft)	dBA (dB)	Range (ft)	dBA (dB)	Range (ft)	dBA (dB)
Bell 47	54	79.7	197	72.6	66	74.8
Bell 205	175	86.1	175	79.5	175	76.6
Bell 206	35	80.1	35	72.1	224	71.4
Hughes 300	13	76.[illegible]	13	69.3	147	72.1
Hughes 500	126	80.5	126	70.[illegible]	-52	73.5
Sikorsky S-61	9[illegible]	9[illegible].3	9[illegible]	61.6	9[illegible]	64.3

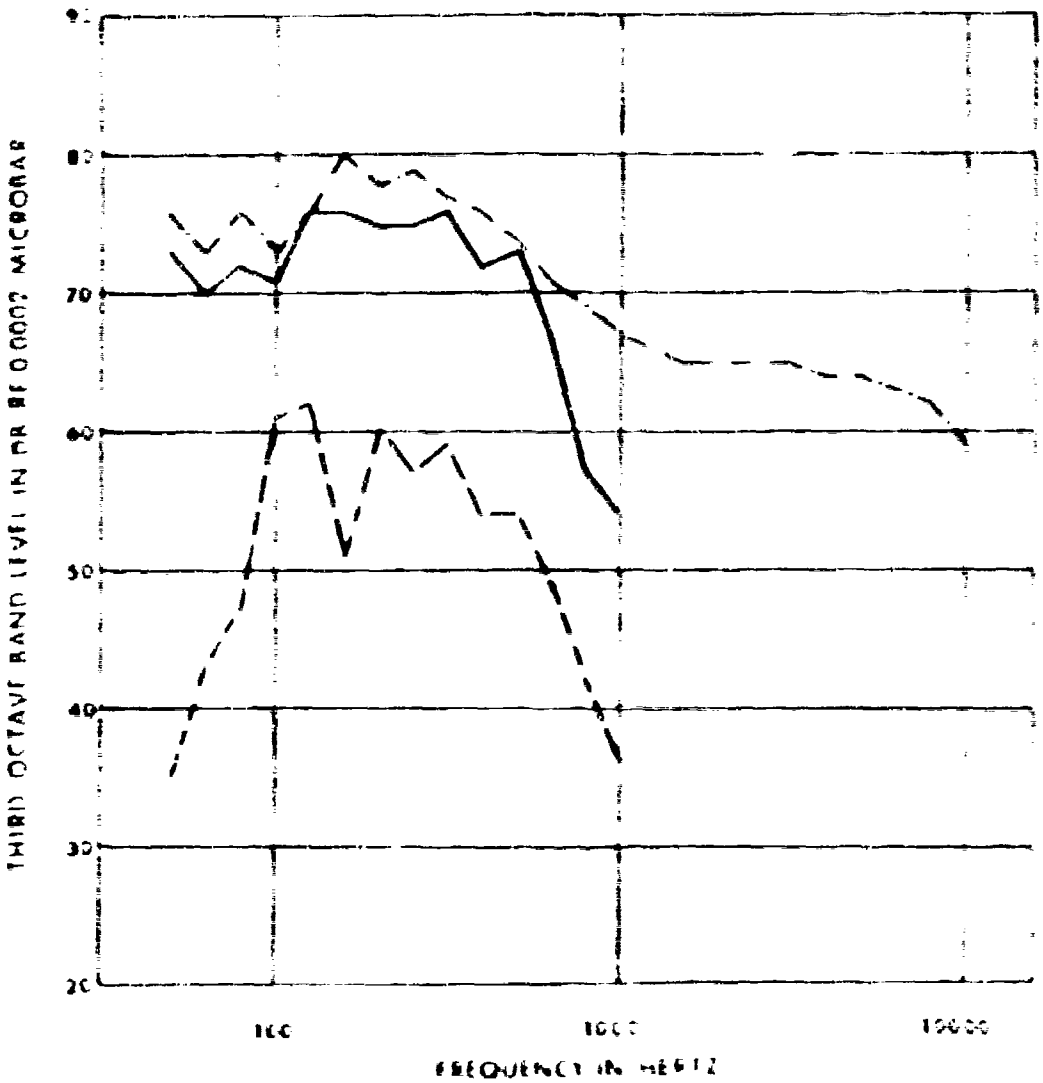
70
60
50
40
30
20
100
1000
10000
FREQUENCY IN HERTZ

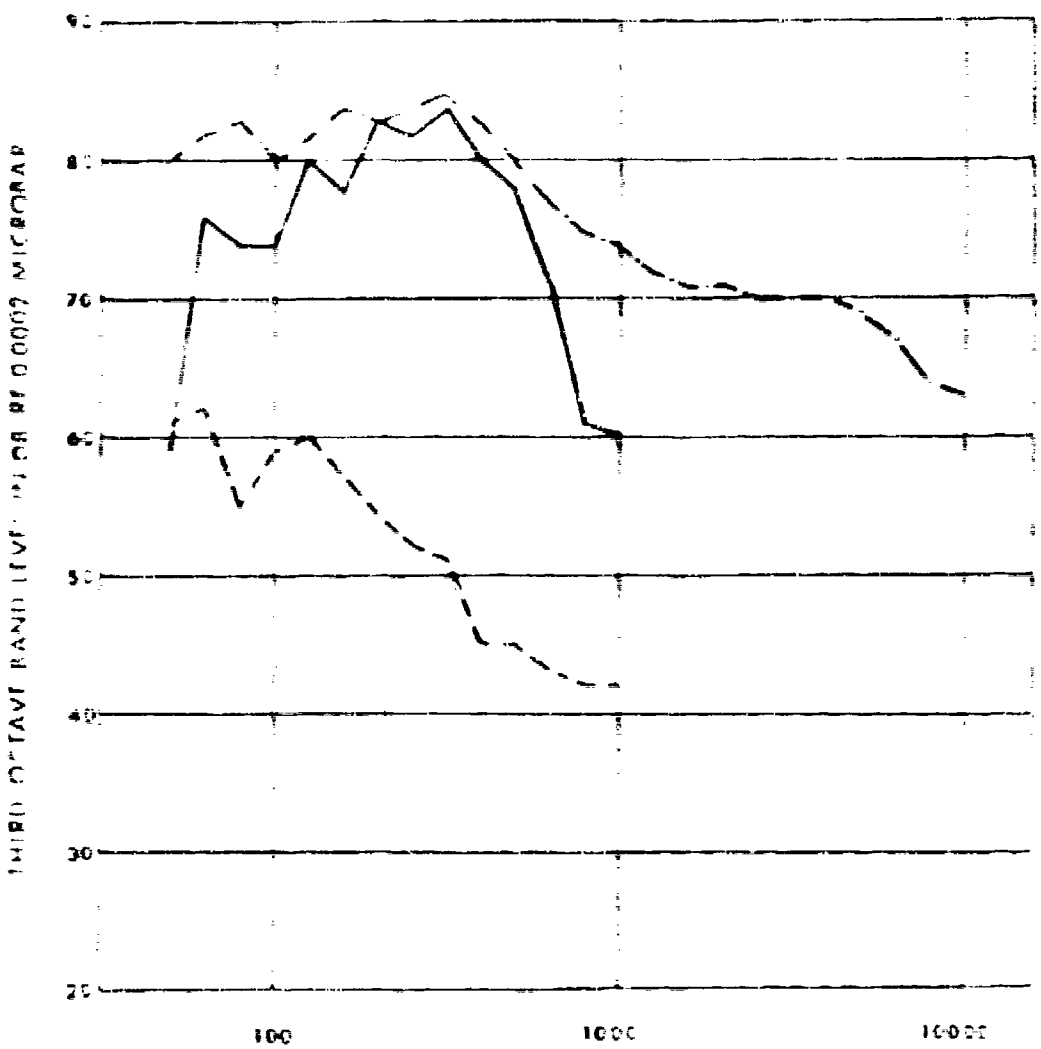
90
80
70
60
50
40
30
20
100
1000
10000
FREQUENCY IN HERTZ

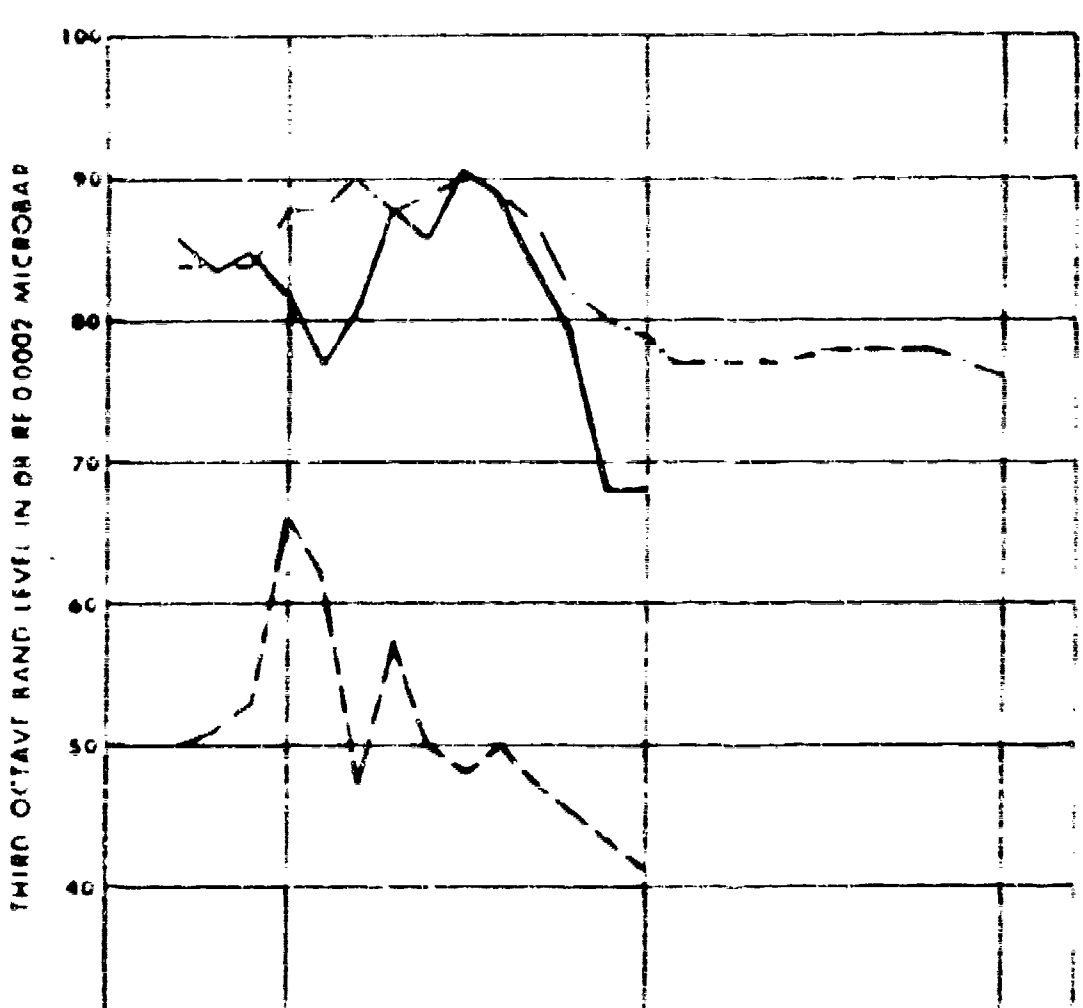
100
90
80
70
60
50
40
30
THIRD OCTAVE BAND LEVEL IN DB RE 0.0002 MICROBAR
100
1000
10000
FREQUENCY IN HERTZ

Figure 4. [illegible]

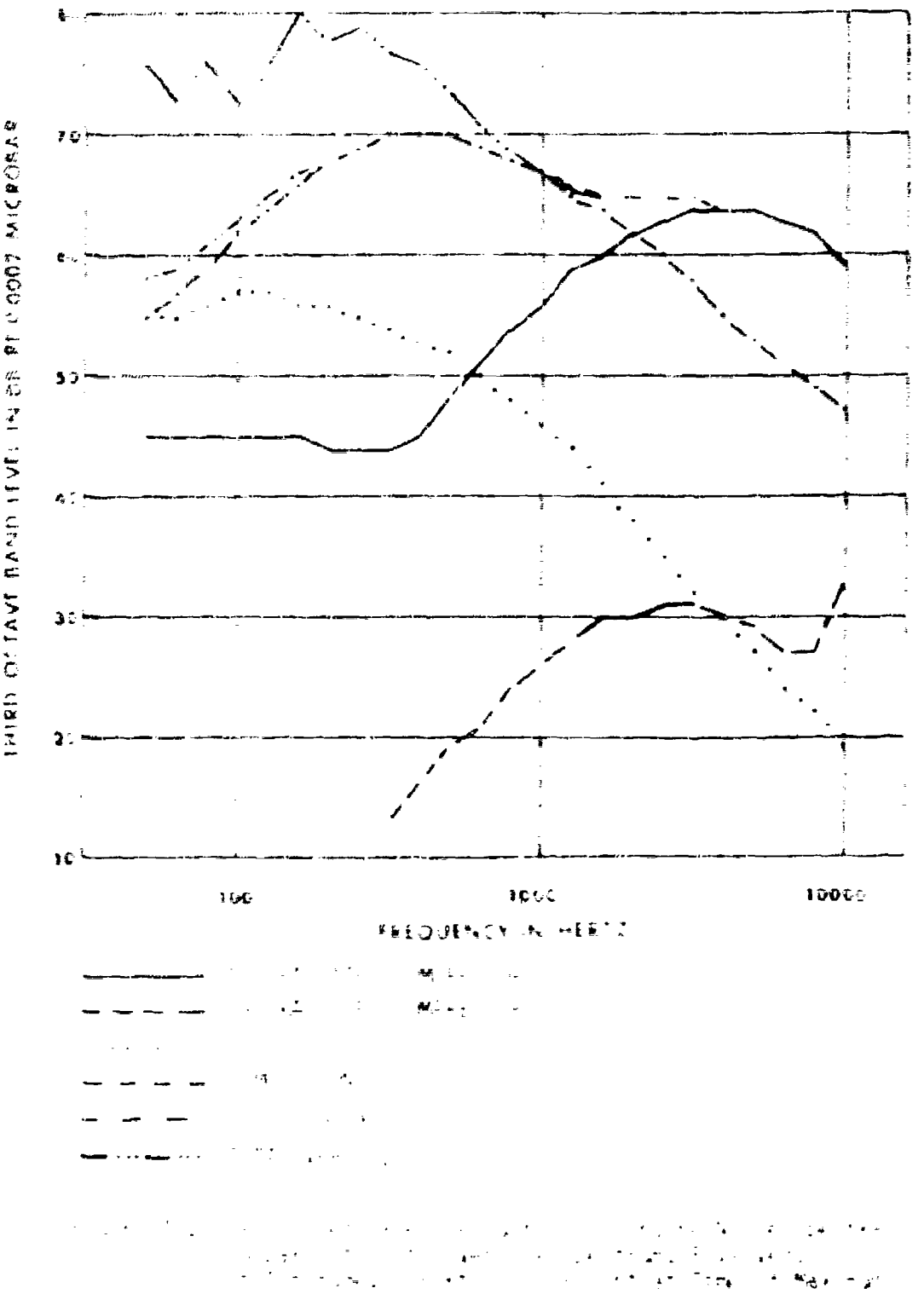

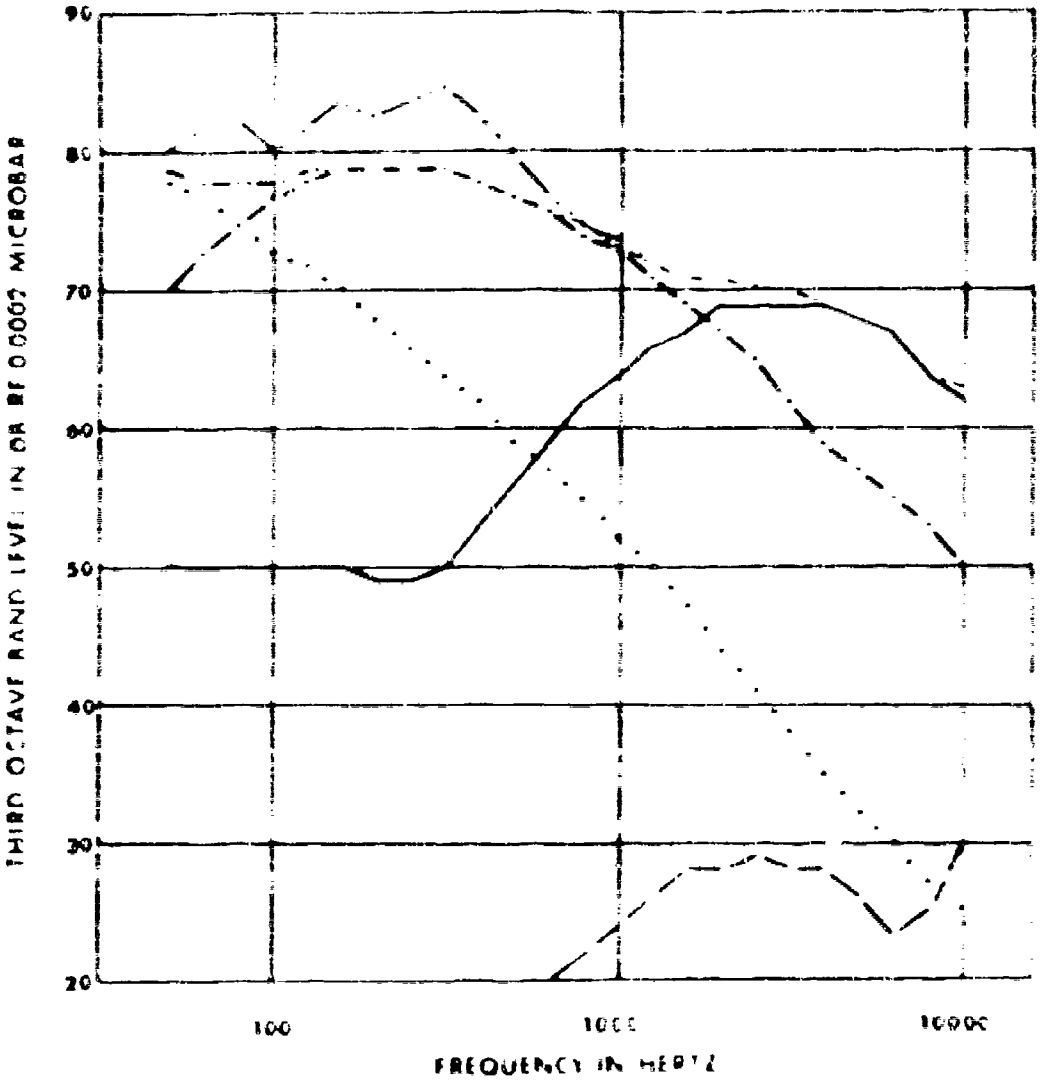
THIRD OCTAVE BAND LEVEL IN DB RE 0.0002 MICROBAR
90
80
70
60
50
40
30
20
100
1000
10000
FREQUENCY IN HERTZ

Figure 22. [illegible]

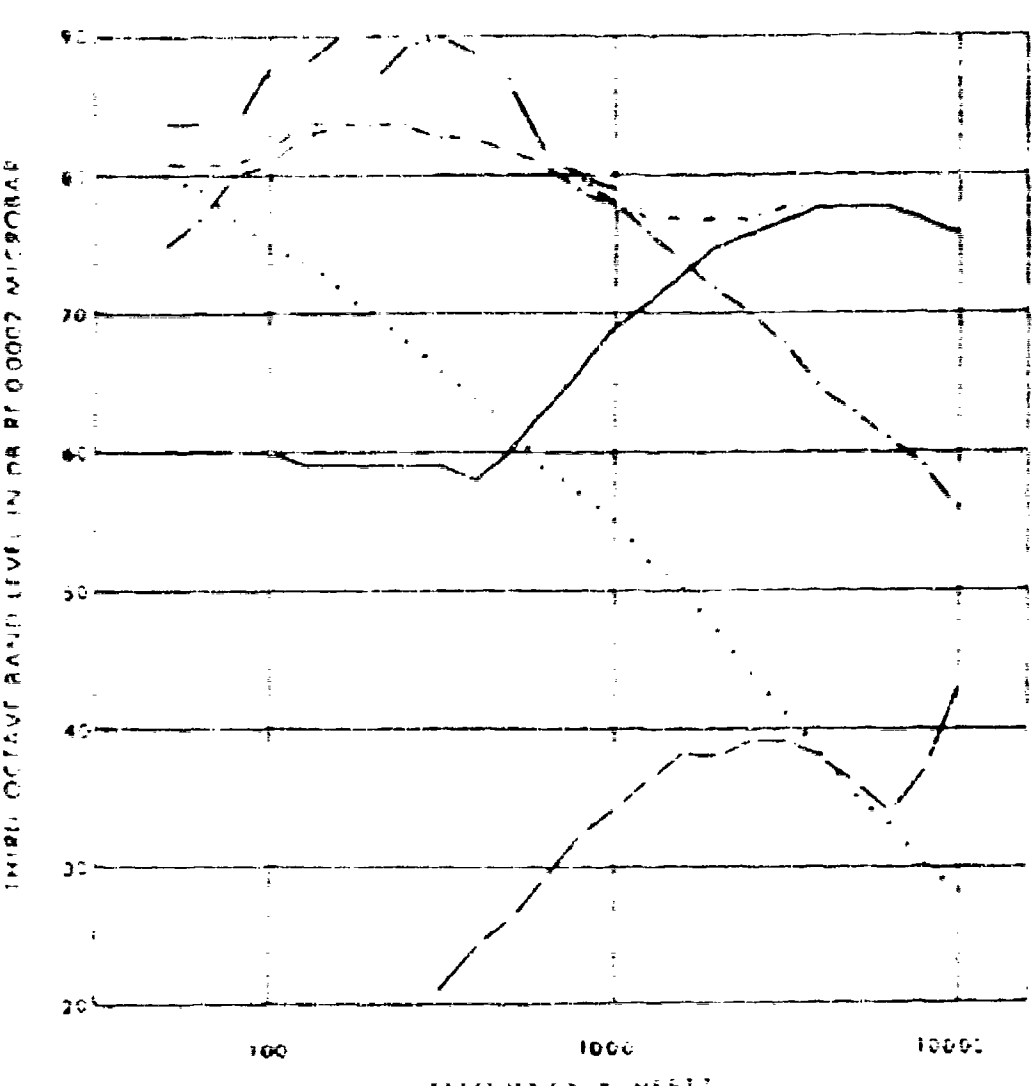
100
1000
10000

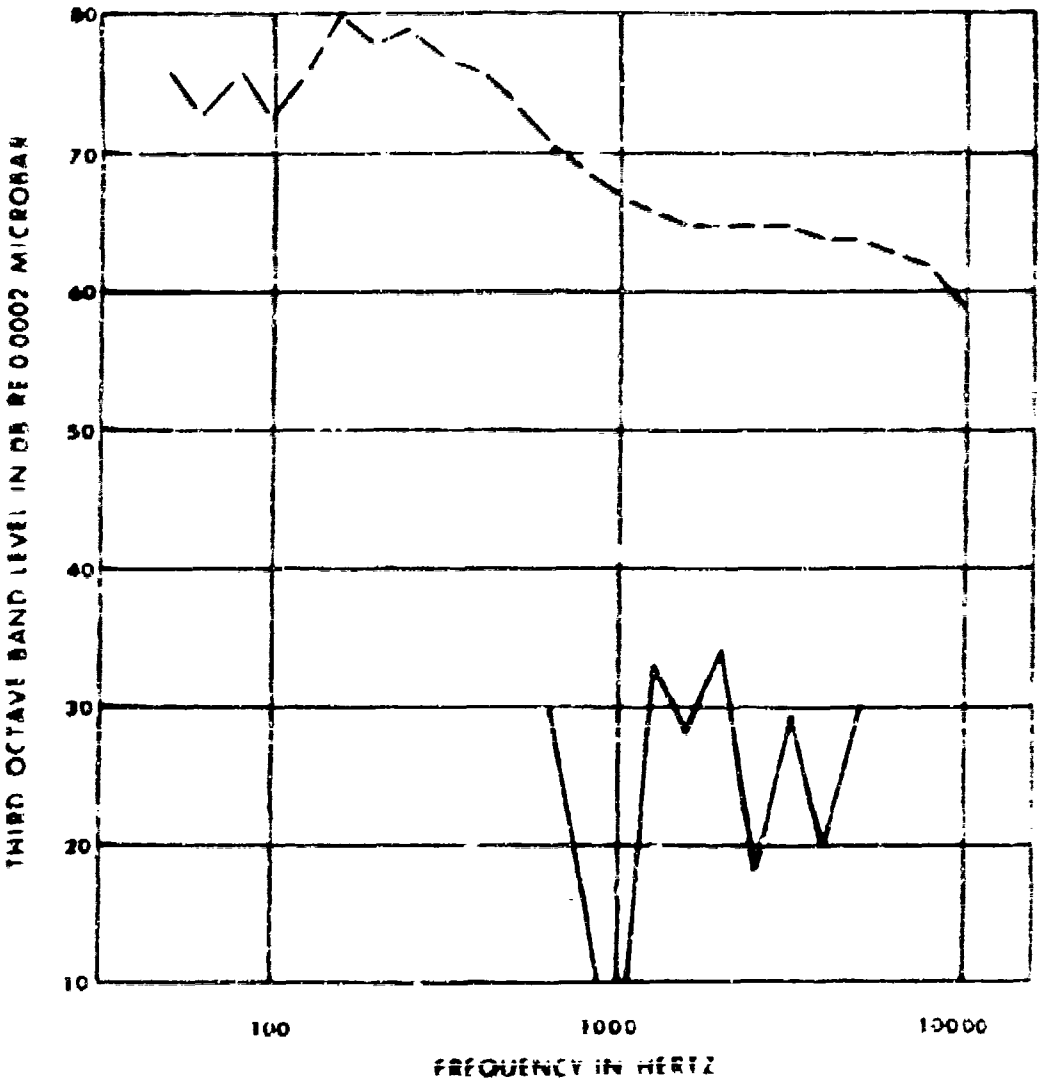

Figure 44. Calculated Baseline Hughes 500 Transmission Noise Spectrum, Compared to Total Vehicle Spectrum, Fly-Over, 300 Ft Altitude, 110 Kts S.L. Flight, at Time of Maximum PNL

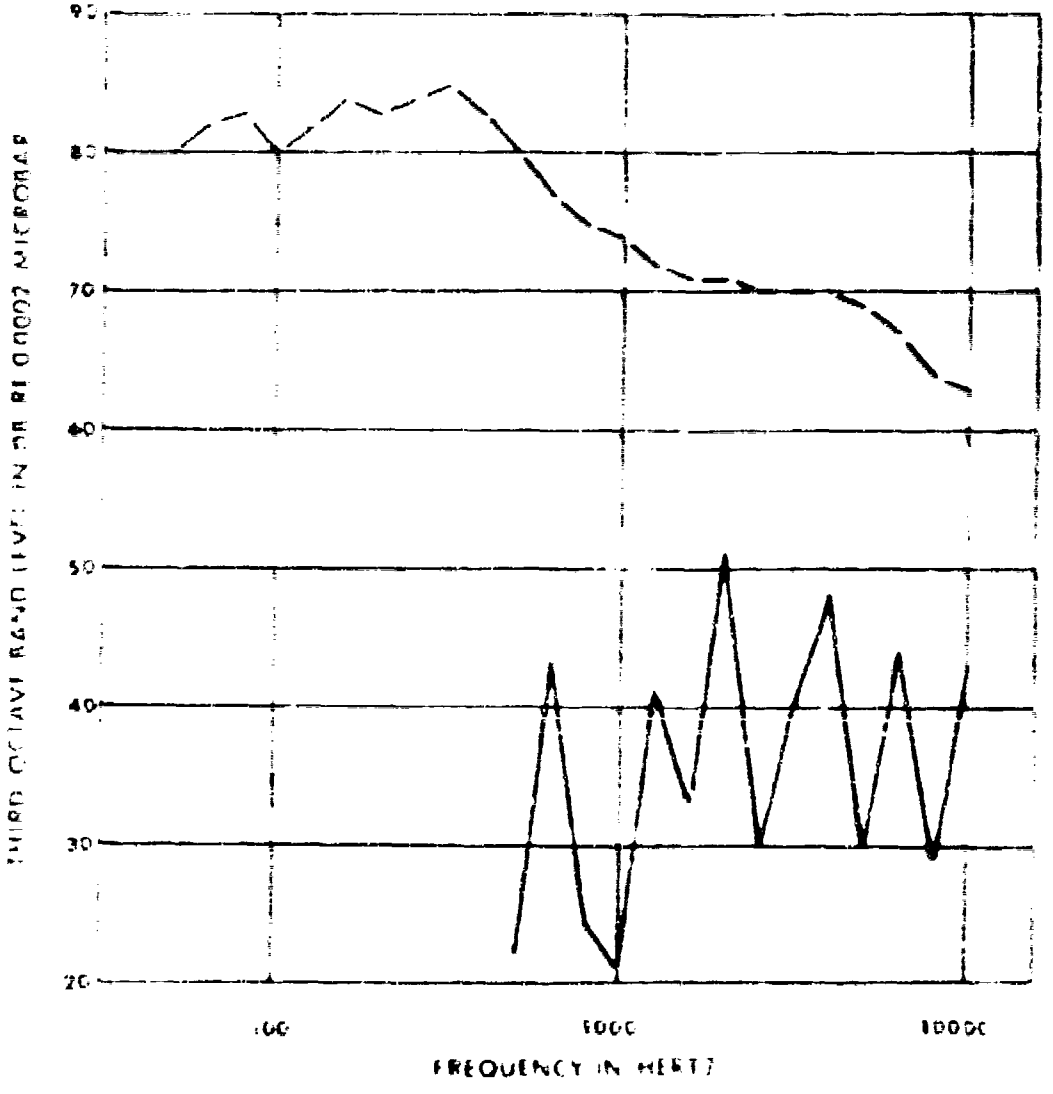

Figure 41. Calculated Baseline [illegible] Transmission Noise Spectrum Compared to "Total" Vehicle Spectrum, Flyover, 300 Ft Altitude, [illegible] Weight, at Time of Maximum [illegible]

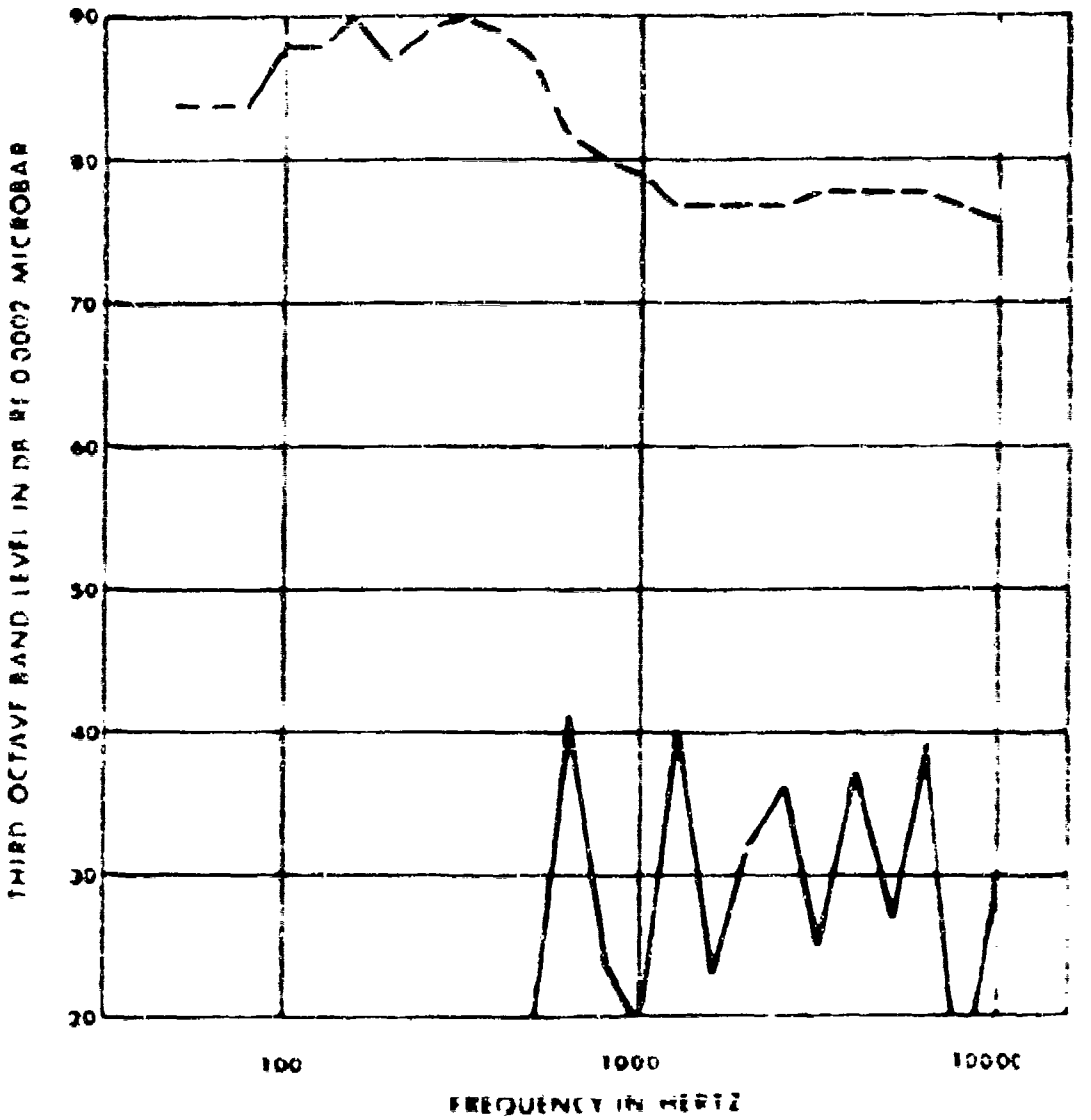

Figure 40. Calculated Baseline Silicone S-61 Transmission Noise Spectrum Compared to Total Vehicle Spectrum, Fly-Over, 300 Ft Altitude, 120 Kts S.L. Flight, at Time of Maximum PNL

[illegible] METHODOLOGY

[illegible] results in [illegible] of [illegible] methods.[illegible] many of these methods have been shown [illegible] to reduce the noise of [illegible] components, [illegible] the rotor system, engine [illegible] and transmission, only limited efforts have been made to determine their effectiveness within the context of the total helicopter vehicles. Studies which have attempted to obtain this type of information, for example those of References 46, 47, and [illegible], have generally been too research oriented. Vehicle noise reductions obtained in these studies while tending to verify theoretical projections, were obtained at the expense of [illegible] vehicle performance. Furthermore, these studies [illegible] the potentially offsetting effects of changes [illegible] vehicle design and performance which would be required to incorporate the tested noise reduction method in a practical design.

Although the results of these previous efforts cannot be directly applied to satisfy the objectives of the present program, they do provide the data base [illegible] to make reasonable judgments as to the relative merit of the [illegible] noise reduction methods. In this regard these study results are valuable [illegible], where appropriate, these results are [illegible] in the following discussion of helicopter component noise reduction methods.

ROTOR NOISE REDUCTION

[illegible] helicopter rotor noise is fundamentally aerodynamic in origin, reduction of this component of vehicle noise must rely on a thorough understanding of rotor aerodynamics. In very simplified terms, the [illegible] radiation from any elemental station within the rotor disk will [illegible] the aerodynamic loading at that station, the rate of change [illegible] with time and proportional to some power [illegible] of the [illegible] loading, the load rotates with the blade [illegible]

[illegible] W. A., Test and Evaluation of a Quiet Helicopter Configuration [illegible], USAAMRDL TR [illegible], January, 1972.

[illegible] Final Report - Quiet Helicopter Program, [illegible] Internal Report, [illegible], Sikorsky Aircraft Co., 1970.

[illegible] Program to Reduce the Noise Signature of the [illegible] Helicopter, [illegible] Internal Report [illegible], November [illegible]

respect to a fixed observer. Low aerodynamic loads, rapid rates of change in loading and low relative velocity tend to produce low rotor noise levels. Factors which reduce these characteristics tend to reduce rotor noise, and most, if not all, of the methods used to reduce rotor noise are reflections of these relationships.

Methods which have been proposed for reducing rotor noise include both gross changes in rotor system parameters and detail changes in blade geometry. Among the gross rotor parameter changes suggested are:

- Reduced rotor tip speed
- Increased number of rotor blades
- Increased rotor radius (at constant tip speed)
- Increased blade chord

Detail rotor geometry changes which have been postulated include:

- Use of special rotor tip shapes
- Use of special blade leading edge treatments
- Modified blade airfoil shape and distribution
- Modified blade twist rate

Each of the gross rotor parameter changes listed above were evaluated in one or more of the studies of References 4-6. However, because of the manner in which these changes were evaluated, it is difficult to determine the extent of noise reduction achieved with each individual parameter, although in all cases, some degree of noise reduction was attributed to changes in these parameters. As a consequence of this fact, and also because of the extensive analytical background indicating the significance of these parameters as determinants of rotor noise levels, it is concluded that they are suitable variable for evaluation in the present program.

With respect to the detail rotor geometry changes listed above, only the use of special rotor tip shapes has been subjected to extensive experimental evaluation, and this has led to conflicting results. While in some cases modification of the rotor blade tip shape appears to be beneficial, use of this same shape on a different vehicle will not guarantee the same benefit. Because of this lack of generality and, furthermore, because rotor tip shape modification is not readily amenable to analytical evaluation, this noise reduction method is not considered suitable for evaluation in the present effort. The remaining detail rotor changes are similarly not considered suitable for present program purposes. Because of the general lack of either analytical or experimental evaluation of these methods, they cannot be considered to be

-
-
-
-
-
-
-
-

ENGINE NOISE REDUCTION

Two types of engines are in current use on civil helicopters. Many of the older, light helicopters use reciprocating piston engines, and the engines of these vehicles do contribute substantially to the vehicle noise. Methods for reducing reciprocating engine noise do exist. For example, exhaust silencers are currently available and in use. Consequently, the effectiveness and cost of helicopter reciprocating engine noise reduction can be obtained by means other than the present study, and it was therefore decided to concentrate study efforts on the other helicopter power source, the turboshaft engine. This decision also reflects the conclusion that future design helicopters are more likely to use turboshaft engines.

Turboshaft engine noise reduction methods include:

- Intake duct treatment
- Exhaust duct treatment
- Compressor blade modification
- Exhaust redirection
- Burner combustion modification
- Engine core shielding

Of these methods, the internal engine modifications, specifically modifications of the compressor and combustor, have been subjected to little or no experimental evaluation and, therefore, cannot be considered to be within the state of the art. The remaining methods have been used extensively for noise reduction of ground based shaft turbines and, to some extent, have been evaluated through flight testing of helicopters.[1,2,3,4,5,6]

Discussions of the previous section indicate that exhaust radiated turbine noise components contribute most significantly to total helicopter noise. Both exhaust redirection and exhaust duct treatment are potentially beneficial means of reducing exhaust radiated turboshaft noise, however, of these, exhaust duct treatment is most amenable to evaluation. Exhaust redirection, while theoretically cost effective, cannot be evaluated in a straightforward manner because of the unknown potential for interaction between the redirected exhaust flow and the rotor system[6], which may increase rotor noise, and also because of the equally unknown potential for harmful exhaust recirculation. Consequently, efforts in the present program have concentrated on the evaluation of exhaust duct treatment.

[illegible]

[illegible]

SILENCER DESIGN

[illegible]

[illegible]

[illegible]

[illegible]

* [illegible]

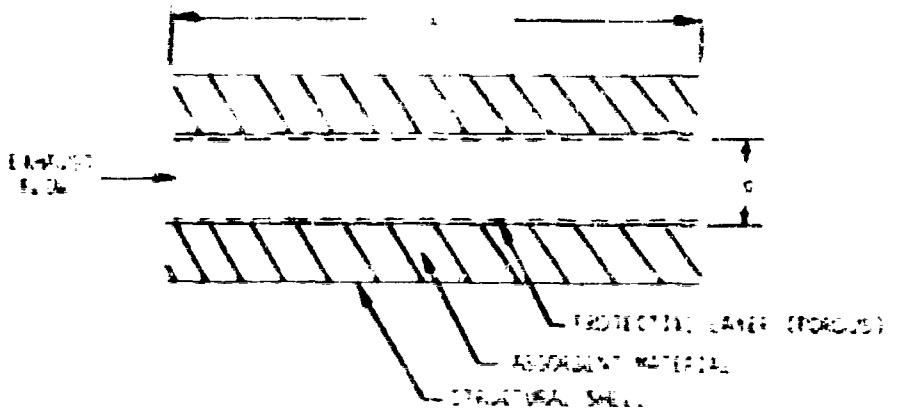

A. Generalized Design

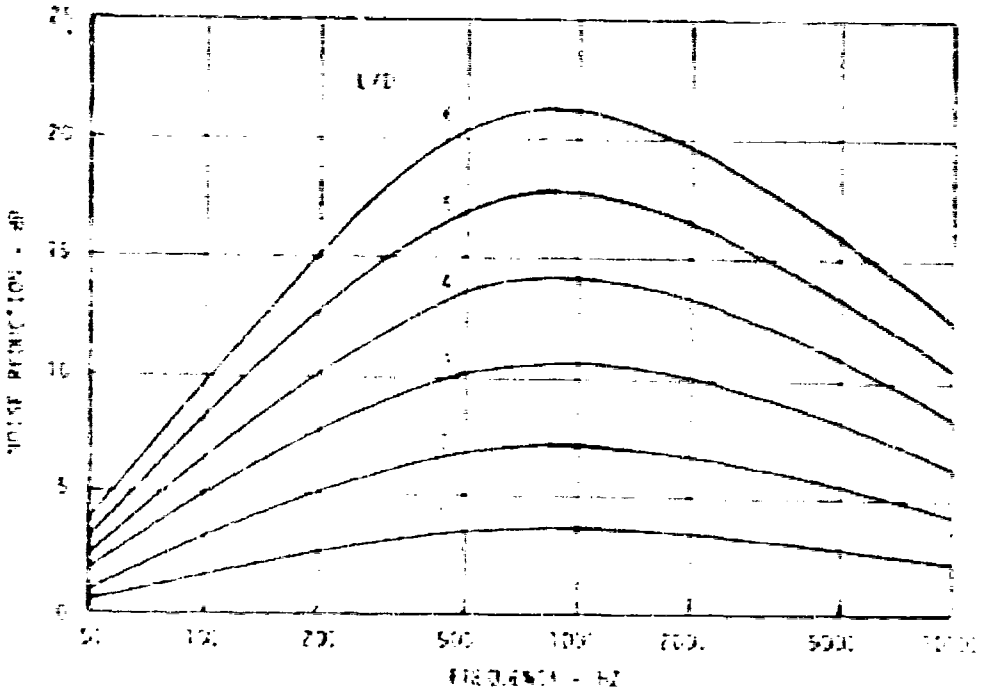

B. Acoustic Performance

Figure 51. Exhaust Silencer Design and Performance

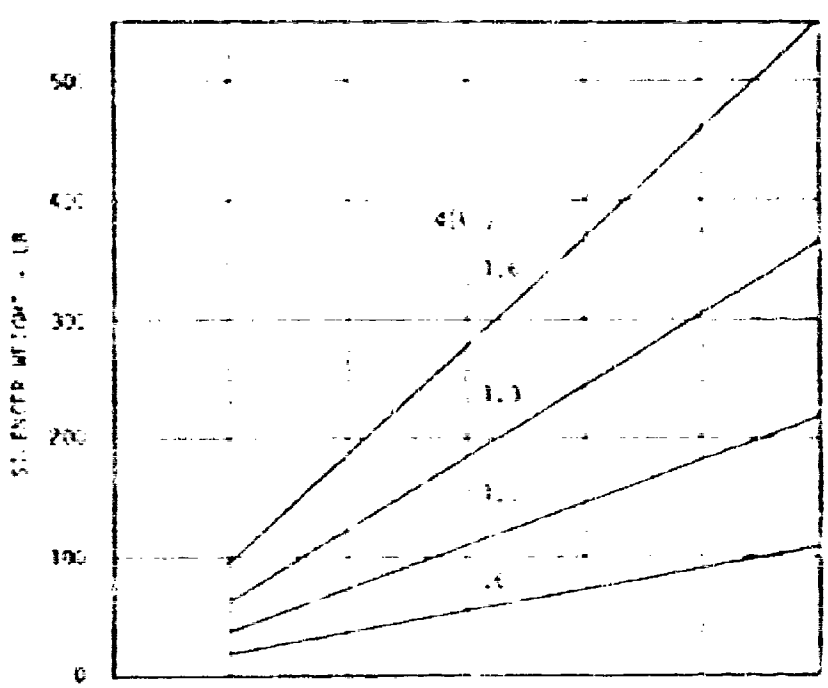

c. Sediment weight

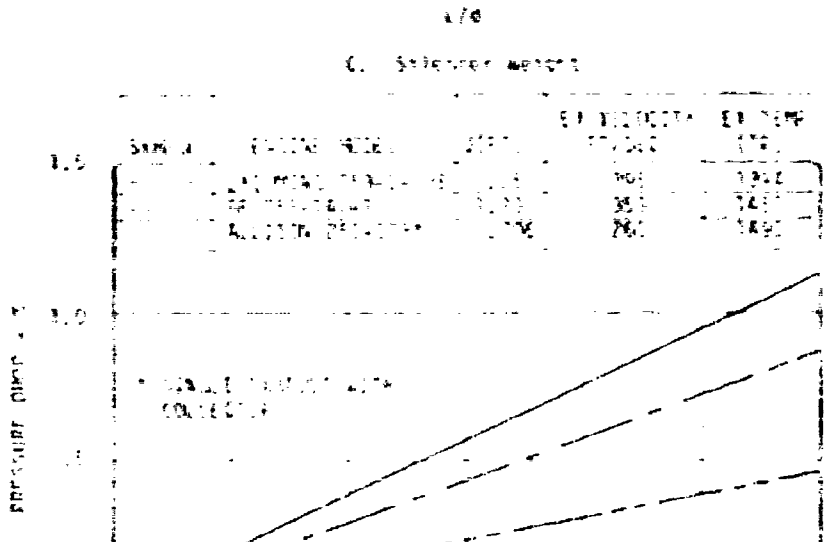

d. [illegible]

Figure 27. (Concluded)

For the present study, a dual silencer noise reduction frequency of 1000 Hz has been selected, since this noise component contributes most strongly to effective perceived noise level (EPNL). Based on this selection, noise reduction curves for various duct length-to-diameter ratios have been calculated, and are shown in Figure 47b. These curves have been derived from available silencer manufacturers' data[4]. These data have also been used to derive the silencer weight trends which are shown in Figure 47c. These trends include 20 weight reduction over manufacturer-supplied data which it is assumed can be achieved in silencers suitable for flight.

Silencer pressure loss data, given in Reference 4, have been used to generate the installed pressure loss curves shown in Figure 47d. These curves relate silencer induced exhaust pressure loss as a function of silencer length to diameter ratio for each of three turbine engines considered in the present study. Engine cycle data pertinent to the generation of these curves are tabulated in Figure 47e.

The engine noise reductions of Figure 47b have been applied to baseline engine noise levels for three of the study vehicles (Sikorsky S-61, Bell 205 and Hughes 500), and the resulting changes in vehicle noise characteristics have been calculated. Silencer characteristics, in terms of silencer weight, length, pressure loss, engine power loss and specific fuel consumption increase, are summarized in Tables 13, 14, and 15, along with the calculated vehicle noise levels associated with each silencer configuration studied. In preparing these tables, the relationship between silencer duct length-to-diameter ratio and pressure loss expressed in Figure 47d have been used, in conjunction with typical engine specification data [5,6], to calculate silencer induced horsepower losses (hp), and increases in specific fuel consumption (SFC). Review of engine specification data indicates that, in general, horsepower loss, in percent, is equal to the percentage change in pressure loss, while specific fuel consumption increases by half this value.

---

[4] Industrial Acoustics Co., Bulletin 4.130(1.0, POWER-FLO TUBULAR SILENCERS.

[5] MODEL SPECIFICATION (T53 ENGINE, AIRCRAFT, TURBOSHAFT GENERAL ELECTRIC CO. T58-GE-8B and -8F ENGINES, July, 1966.

[6] MODEL SPECIFICATION T53-L-11, T53-L-11A AND T53-L-11B SHAFT TURBINE ENGINES, Specification No. 104-28, January 1966.

TABLE 11. SILENCER CHARACTERISTICS AND EFFECTS OF SILENCING ON VEHICLE NOISE
S[illegible] 25XX S-61

Silencer Characteristics					Calculate Vehicle Noise Levels								
					Fly-Over			Fly-By to Starboard			Fly-By to Port		
Wt (lb)	Length (in)	( )	( )	( )	$OASPL_{max}$	dBA_{max}	EPNL	$OASPL_{max}$	dBA_{max}	EPNL	$OASPL_{max}$	dBA_{max}	EPNL
122	1.3	.14	.14	.07	97.1	91.6	104.9	89.5	83.4	96.5	89.1	83.1	96.1
243	2.6	.29	.29	.14	97.4	89.9	104.1	89.1	82.9	95.6	88.5	82.4	95.4
365	3.9	.41	.43	.22	97.1	89.1	103.2	88.9	82.6	94.9	88.2	82.1	95.0
486	5.2	.58	.58	.29	96.9	88.9	102.6	88.8	82.5	94.6	88.0	82.0	94.8
608	6.5	.72	.72	.36	96.8	88.7	101.8	88.7	82.4	94.5	88.0	82.1	94.7
730	7.8	.87	.87	.43	96.7	88.6	101.7	88.7	82.4	94.5	87.9	82.1	94.9

[a] Two Silencers

TABLE 13. SILENCER CHARACTERISTICS AND EFFECTS OF SILENCING ON VEHICLE NOISE - BELL 205

Silencer Characteristics					Calculated Vehicle Noise Level										
					Fly-Over			Fly-By to Starboard			Fly-By to Port				
$\dot{W}$ (lb)	Length (ft)	ΔP ( )	ΔHP (%)	ΔSHP (%)	$OASPL_{max}$	dBA_{max}	EPNL	$OASPL_{max}$	dBA_{max}	EPNL	$OASPL_{max}$	dBA_{max}	EPNL		
55	1.25	.19	.19	.09	92.5	84.8	98.5	86.6	77.1	90.5	86.7	78.5	90.4		
110	2.5	.38	.38	.19	91.9	83.8	97.3	86.5	76.6	89.5	86.1	77.9	90.5		
163	3.75	.56	.56	.28	91.5	83.4	96.6	86.4	76.3	88.7	85.9	77.6	90.2		
218	5.0	.75	.75	.38	91.3	83.2	96.0	86.4	76.1	88.1	85.7	77.5	90.1		
272	6.25	.94	.94	.47	91.1	83.1	96.0	86.4	76.0	87.9	85.6	77.4	90.1		
327	7.5	1.13	1.13	.56	91.0	83.0	96.2	86.4	76.0	88.1	85.6	77.3	90.1		

TABLE 14. SILENCER CHARACTERISTICS AND EFFECTS OF SILENCING ON VEHICLE NOISE - HUGHES 500

Silencer Characteristics					Calculated Vehicle Noise Levels								
					Fly-Over			Fly-By to Starboard			Fly-By to Port		
Wt (lb)	Length (ft)	ΔP (")	THP (")	SPEC (")	OASPL$_{max}$	dBA$_{max}$	EPNL	OASPL$_{max}$	dBA$_{max}$	EPNL	OASPL$_{max}$	dBA$_{max}$	EPNL
21	.70[illegible]	.08	.08	.04	87.1	79.1	92.8	80.0	73.1	86.8	79.0	[illegible]	92.6
41	1.41[illegible]	.15	.15	.08	86.9	78.1	91.7	79.9	71.0	86.6	78.9	[illegible]	91.7
61	2.1[illegible]	.23	.23	.11	86.8	77.6	91.0	79.8	72.9	83.6	78.7	[illegible]	91.0
80	2.82	.30	.31	.15	86.8	77.4	90.2	79.8	72.8	83.0	78.6	[illegible]	90.5
101	3.53	.38	.39	.19	86.7	77.2	89.6	79.8	72.8	83.5	78.6	[illegible]	90.5
120	4.23	.45	.45	.23	86.7	77.2	89.3	79.8	72.8	83.6	78.6	[illegible]	90.5

The average of tip-over and tip-by vehicle EPNL reductions achieved with engine silencing is shown in figure 48, as a function of silencer weight, for each study vehicle. To provide a meaningful comparison, silencer weight is expressed as a percentage of vehicle gross weight. On this basis, achieved noise reductions are roughly comparable, for comparable weight penalties, for the three vehicles.

The additions to vehicle gross weight and reductions in engine performance indicated in tables VIII-IX and figure 48 do not reflect the total impact of engine silencing, and these changes alone do not represent an adequate basis for estimating changes in vehicle cost due to silencer use. To provide this basis, the changes in vehicle design necessary to accommodate these direct penalties must be determined.

IMPACT ON VEHICLE DESIGN

The direct penalties associated with engine silencing can be accommodated by reducing vehicle performance capability, changing vehicle design to maintain constant performance capability or by some combination of these. At one extreme, these penalties can be assessed in terms of their effect on vehicle performance only; with silencer weight decreasing payload and/or fuel load and engine losses decreasing hover capability, forward flight speed capability and range. With this approach, vehicle gross weight and consequently airframe weight, are kept constant along with installed power, and vehicle design is affected only the need to provide structural attachment points for the silencing system. This approach, however, violates the basic premise upon which new vehicle design is predicated. Since new helicopter vehicles are designed to perform specific missions, having definite performance requirements, and not to some arbitrarily established gross weight limitation. The most appropriate approach, then, is to consider the impact of engine silencing in the context of maintaining basic mission capability, allowing vehicle gross weight, airframe weight, fuel load and installed power to vary, but keeping payload, range and hover ceiling capability constant. As discussed in a previous section, this approach has been followed in the present study.

Basic mission capability has been defined in terms of both a hover and a forward flight performance requirement. With regard to hover performance, vehicle configurations with engine silencing are required to have hover ceiling capability equal to their respective baseline, unsilenced vehicle, with equal payload. Silenced configurations are also required to have forward flight speed and range capabilities equal to those of the baseline vehicle, again with equal payload. Within these performance restraints, the impact of engine silencing can be uniquely determined in terms of necessary growth in vehicle gross weight, airframe weight, engine weight, fuel load and installed power, using the previously described helicopter design and performance model.

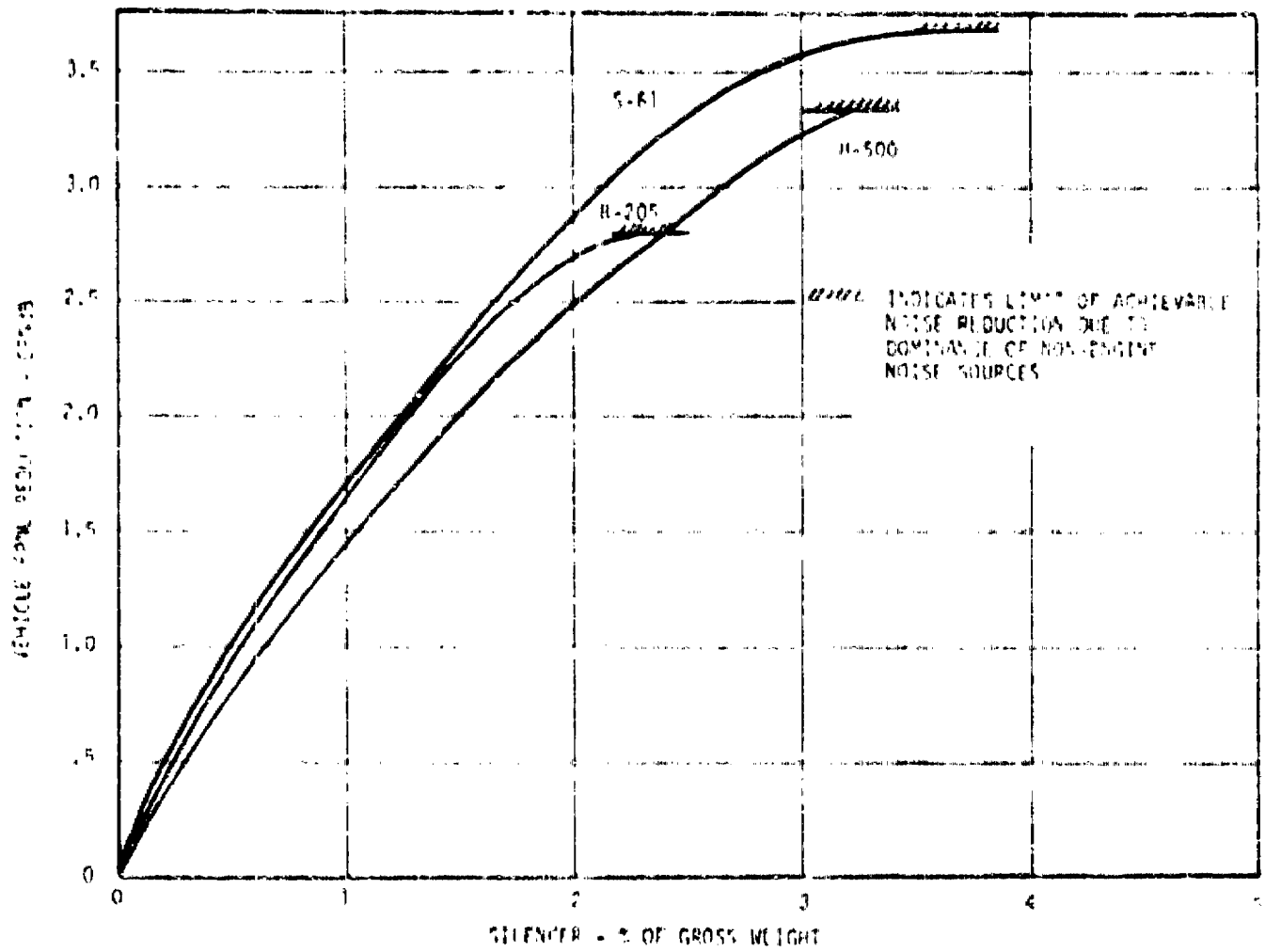

Figure 48. Silencer Performance Vs Weight

Incorporation of an engine silencer increases vehicle gross weight by an amount equal to the silencer weight (ΔW). Vehicle airframe weight must also increase, to carry the added silencer weight. This change in airframe weight further increases gross weight, requiring additional engine power and, consequently, increased engine weight. These three weight changes increase the fuel load required to maintain constant range capability. Additions to fuel load and engine weight further increase airframe weight, gross weight and power required. The ultimate gross weight, airframe weight, engine power and weight and fuel load can be calculated through an iterative solution of the individual weight and power relationships involved in the analytical method.

In considering the effects of engine silencing, two of the relationships of the analytical method must be changed to account for direct silencer induced losses. First, excess installed power is required because of silencer power losses, which are given in percentage terms in Tables 13-15. This effect modifies the installed power relationship of Equation (27), resulting in a new relationship given by:

$$HP_E' = HP_{E_0}\left(G_W'/G_{W_0}\right)^{1.41}\left(R'/R_0\right)^{.82}\left(1 + \frac{\Delta P}{100}\right) \qquad (44$$

where: ΔP = percentage silencer induced engine power loss - (%)

Engine silencing also causes an increase in specific fuel consumption, which in turn changes fuel load requirements. Percentage changes in fuel consumption for the study silencer configurations are given in Tables 13-15. This effect modifies the basic fuel load relationship of Equation (37) according to:

$$F' = F_0\left(\frac{SFC_C'}{SFC_{C_0}}\right)\left(\frac{HP_E'}{HP_{E_0}}\right)\left(1 + \frac{\Delta SFC}{100}\right) \qquad (45$$

where: ΔSFC = percentage silencer induced change in specific fuel consumption

The preceding installed power and fuel load relationships have been included in the design and performance method and used to determine the total impact of engine silencing on the three study vehicles. Input data and baseline characteristics pertinent to this evaluation are summarized in Tables 16 and 17. Percentage changes in airframe weight, engine weight, engine installed power, fuel load and gross weight, relative to baseline values, have been calculated for each level of silencing indicated in Tables 13, 14 and 15. These calculated changes are presented in Figure 69.

TABLE 16. AIRCRAFT PARAMETER VALUES USED AS INPUT TO HELICOPTER DESIGN AND PERFORMANCE MODEL

Input Parameter	Vehicle		
	S-61	B-205	H-500
Gross Weight (lb)	19500	9500	2550
Engine Weight (lb)	682	328	140
Fuel Load (lb)	2665	1430	400
Installed Power (HP)	3000	1400	317
Number of Engines	2	1	1
Normal Capacity (Crew + Pass.)	26	15	5
Rotor: Radius (ft)	30.5	24	13.16
Chord (ft)	1.52	1.75	.56
No. of Blades	5	2	4
RPM	203	324	470
Aft Fuselage Type	8	15	10
Pylon Type	45	14	25
Landing Gear Type	.0247	.0157	.0157
Engine Installation Type	.96	1.16	1.19
No. of Auxiliary L.S.	1	0	0

TABLE IV. CALCULATED BASELINE AIRFRAME WEIGHT COMPONENTS

Component	Vehicle		
	S-61	S-205	S-300
Rotor Group	2129	736	212
Tail Group	201	145	16
Fuselage Group	1940	841	241
Landing Gear	441	111	32
Flight Controls	494	390	96
Propulsion Group (less Engine)	696	440	233
Drive System	1697	663	170
Auxiliary Power Group	69	0	0
Fixed weight	2247	1435	713
Airframe Weight	8636	5101	1329

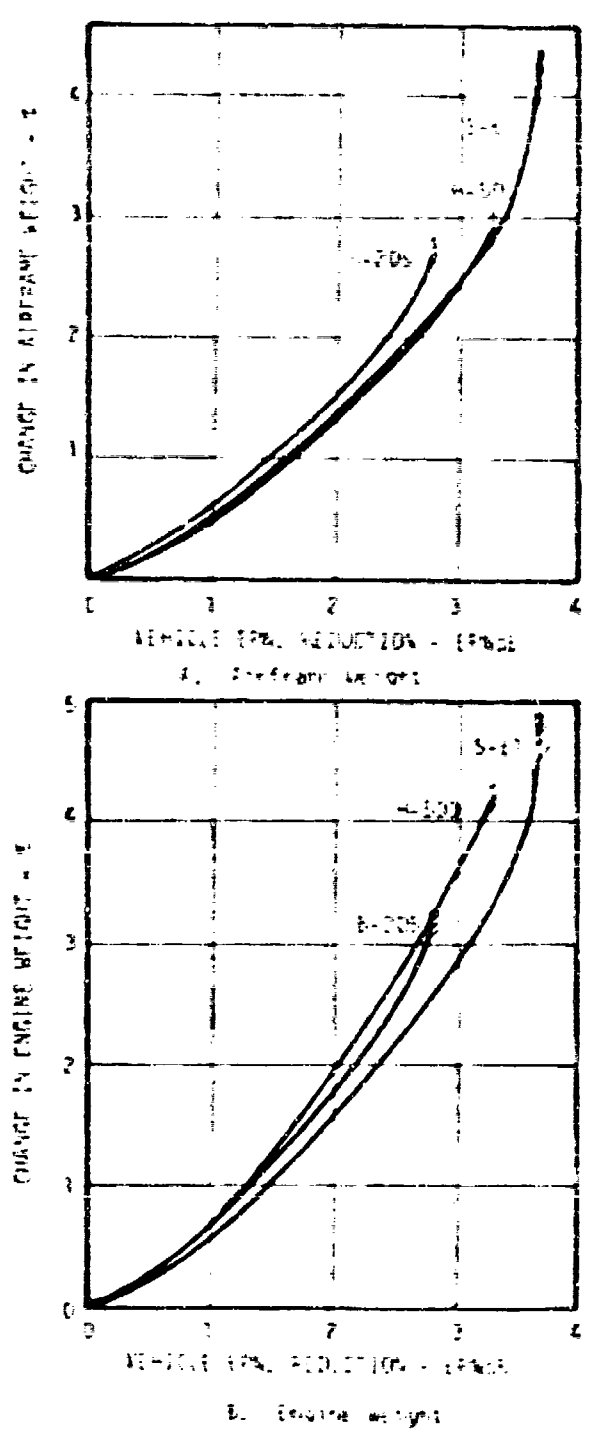

Figure 69. Effect of Silencer Use on Vehicle Design Characteristics

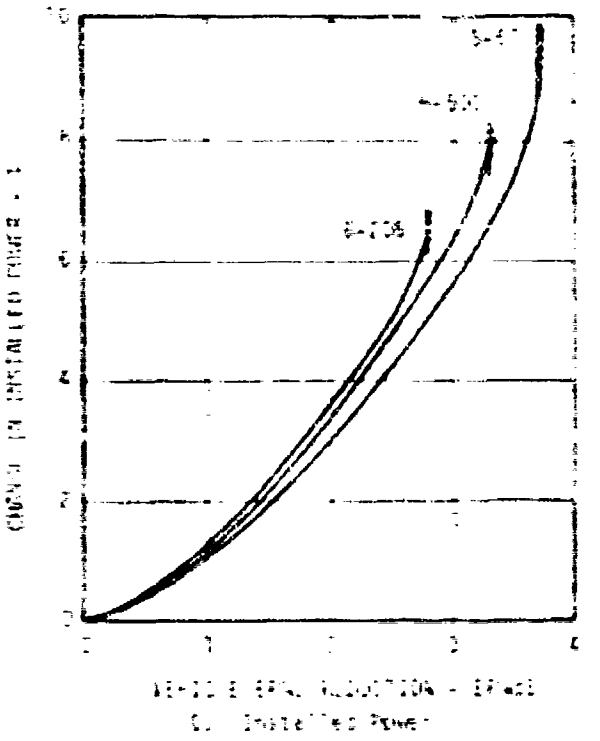

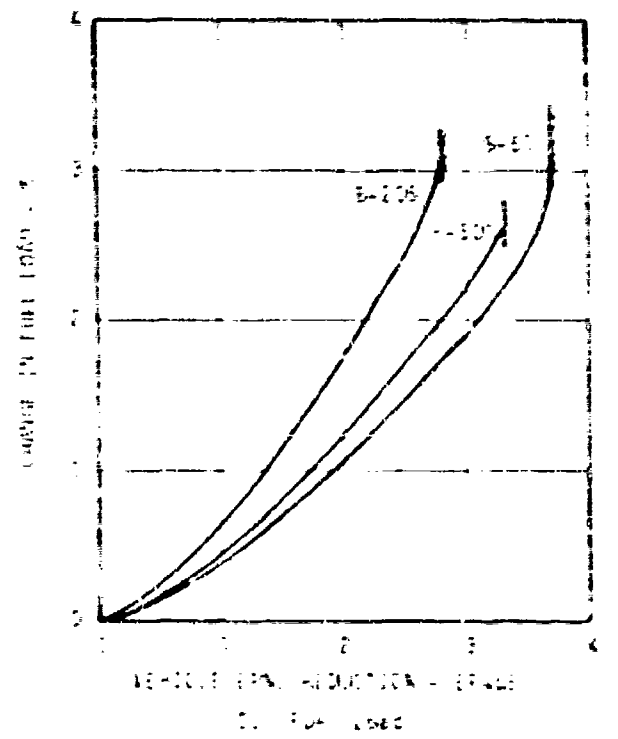

Figure 4b. (Continued).

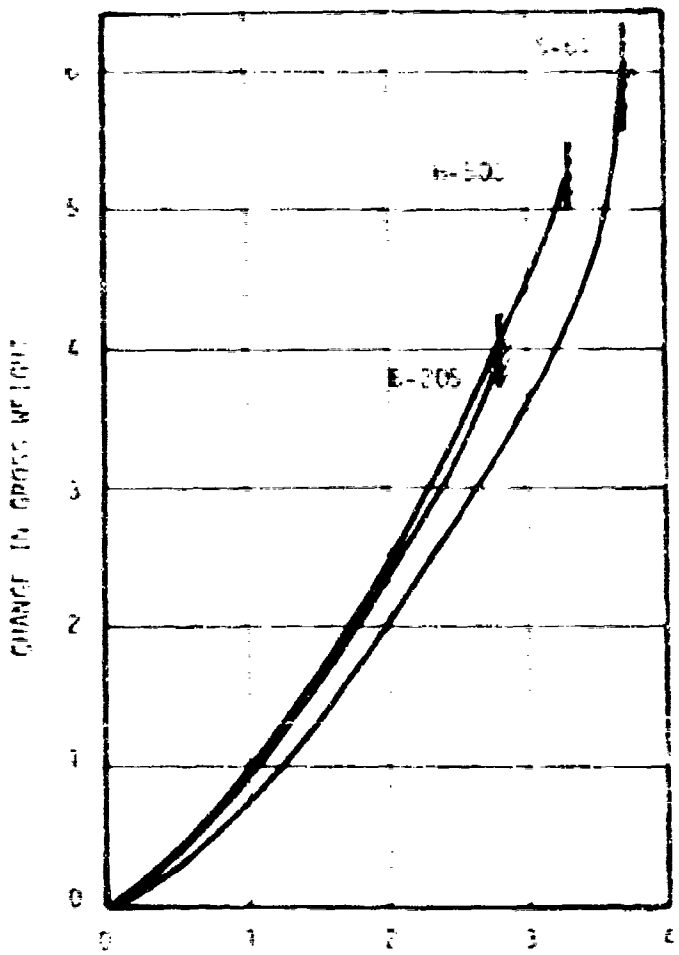

VEHICLE EPAL REDUCTION - EPASS

Figure 49 (Concluded)

The changes in vehicle design characteristics shown in Figure 49 are, in most cases, similar for the three study vehicles. For example, the change in airframe weight due to a vehicle noise reduction of 2.5 EPNdB ranges from 1.9% to 2.1%, a 10% less of a spread for these noise reduction. The change in engine weight, again for a 2.5 EPNdB reduction, ranges from 2.2% to 2.7%. Installed power change to achieve this level of noise reduction shows a spread of from 4.3 to 5.2%. Changes in gross weight range from 2.5 to 3.4%. The effect of this level of noise reduction on fuel load does, however, show some significant disparity between the S-61 and H-500 vehicles, and the B-205 vehicle. Changes in fuel load for the S-61 and H-500 range from 1.5 to 1.7%, while a 2.5% change is shown for the B-205, all at a constant vehicle noise reduction of 2.5 EPNdB.

The magnitude of vehicle design changes required to achieve vehicle noise reduction through engine silencing indicated in Figure 49 may be more readily appreciated by considering, in absolute terms, the changes in gross weight which result from a given level of noise reduction. For a 2.5 EPNdB reduction, the gross weight of the S-61 vehicle increases from a baseline of 19500 lb to 20046 lb for an increase of 546 lb. B-205 vehicle gross weight increases from 9500 lb to 9834 lb, a change of 334 lb. The H-500 vehicle gross weight goes from 2550 lb to 2637 lb, or 87 lb increase. These weight changes are in themselves significant, and they translate directly into changes in vehicle cost.

IMPACT OF ENGINE SILENCING ON VEHICLE COST

The changes in vehicle design, shown in Figure 49, have been interpreted in terms of changes in vehicle costs. Cost changes have been calculated in terms of percentage changes in the basic cost elements of initial investment cost, indirect operating cost and direct operating cost, as well as total life cycle cost, for a range of utilization rates and assumed useful life. These calculations have been made using the parametric helicopter cost model discussed previously. Cost of the silencer itself, which is considered as added equipment, is related to silencer weight in Figure 50.

Baseline costs for the three study vehicles have been calculated in 1972 dollars, and are given in Tables 19-20. These calculations have been made for an assumed useful life range of ten to twenty years, and for annual utilization rates of 500 to 1500 hours per year.

Changes in investment cost, DOC and IOC resulting from engine exhaust silencing have also been calculated and these are given in Figure 51. These changes in cost are given in terms of percentage change relative to the baseline costs of Tables 19-20. Changes in cost shown in Figure 51 are related to the average vehicle EPNL reductions obtained by engine exhaust silencing. Changes in total life cycle cost, expressed in a similar manner, are shown in Figure 52. All of the data shown in Figure 51 relate to a useful life of 15 years, since the analyses indicate that changes in useful life over the range studied do not substantially impact changes in life cycle cost.

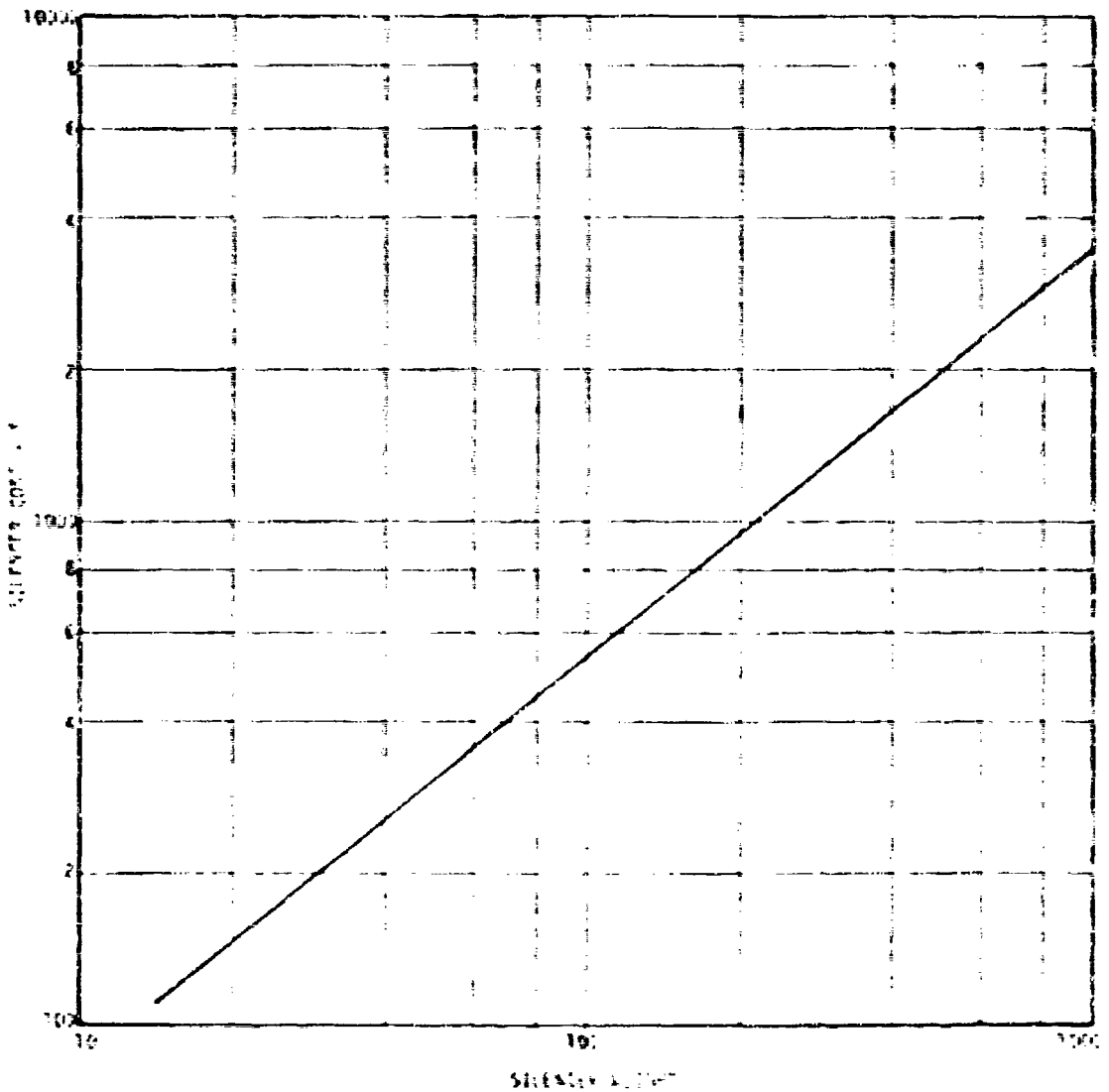

Figure 56. Silencer Cost vs Weight

TABLE 16. BASELINE COSTS OF SIKORSKY S-61

Initial Investment Cost: $1779291.

Indirect Operating Cost: $147086./Year

Direct Operating Cost: $272.75/hr

Annual Use (Hrs/Year	Life Cycle Cost for Life of: ($)		
	10 Years	15 Years	20 Years
300	4066852.	5210671.	6354491.
500	4611317.	6027439.	7443561.
1000	5972620.	8069323.	10166026.
1500	7333923.	10111216.	12888584.

TABLE 19. BASELINE COSTS OF BELL 205

Initial Investment Cost: $699130.

Indirect Operating Cost: $57955./Year

Direct Operating Cost: $157.02/hr

Annual Use (Hrs/Year	Life Cycle Cost for Life of: ($) 10 Years	15 Years	20 Years
300	1599716.	2095018.	2590321.
500	1913751.	2566071.	3218392.
1000	2698842.	3743704.	4788565.
1500	3483928.	4921337.	6358745.

Table II. Basic Costs of Model 500

Initial Investment Cost: $12140.

Indirect Operating Cost: $[illegible]/Year

Direct Operating Cost: $7[illegible]/Year

Annual Use (Hrs/Year)	Life Cycle Cost for Life of: 15 Years	25 Years	35 Years
300	440053.	606342.	770644.
500	561354.	824136.	1056657.
1000	953421.	1364936.	1779386.
1400	1317641.	1918305.	2499313.

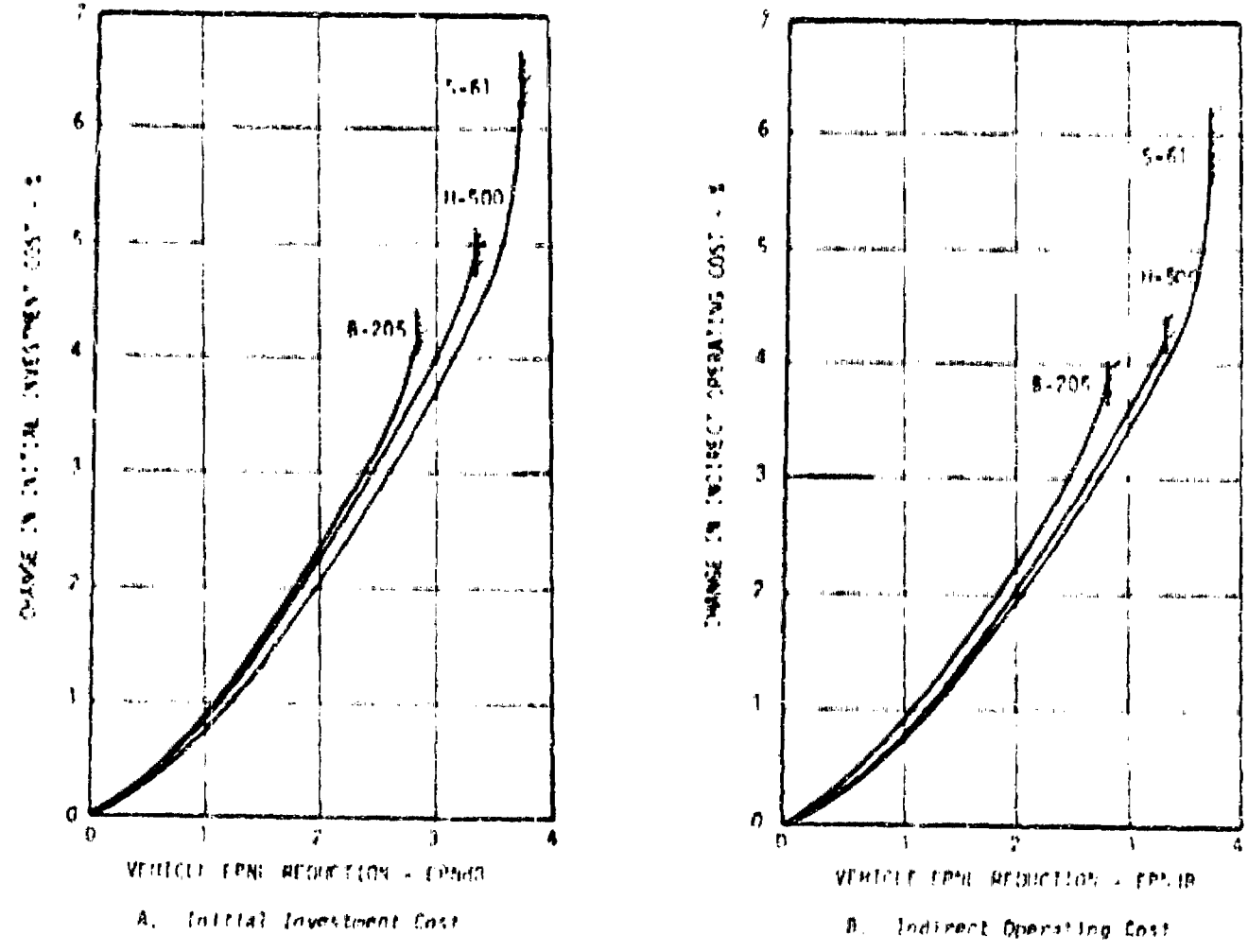

A. Initial Investment Cost

B. Indirect Operating Cost

Figure 51. Changes in Cost Elements Due to Engine Silencing

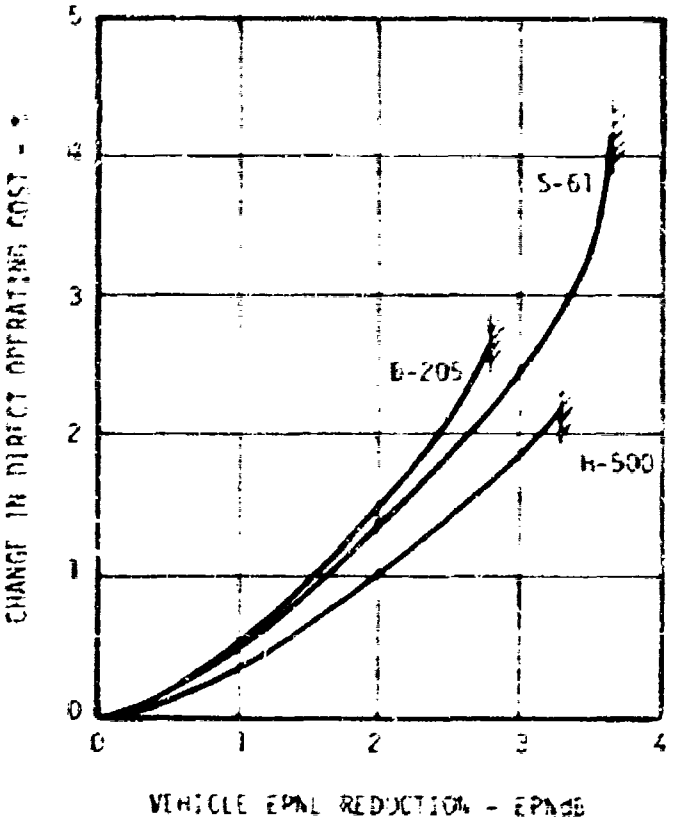

C. Direct Operating Cost

Figure 51 (Concluded)

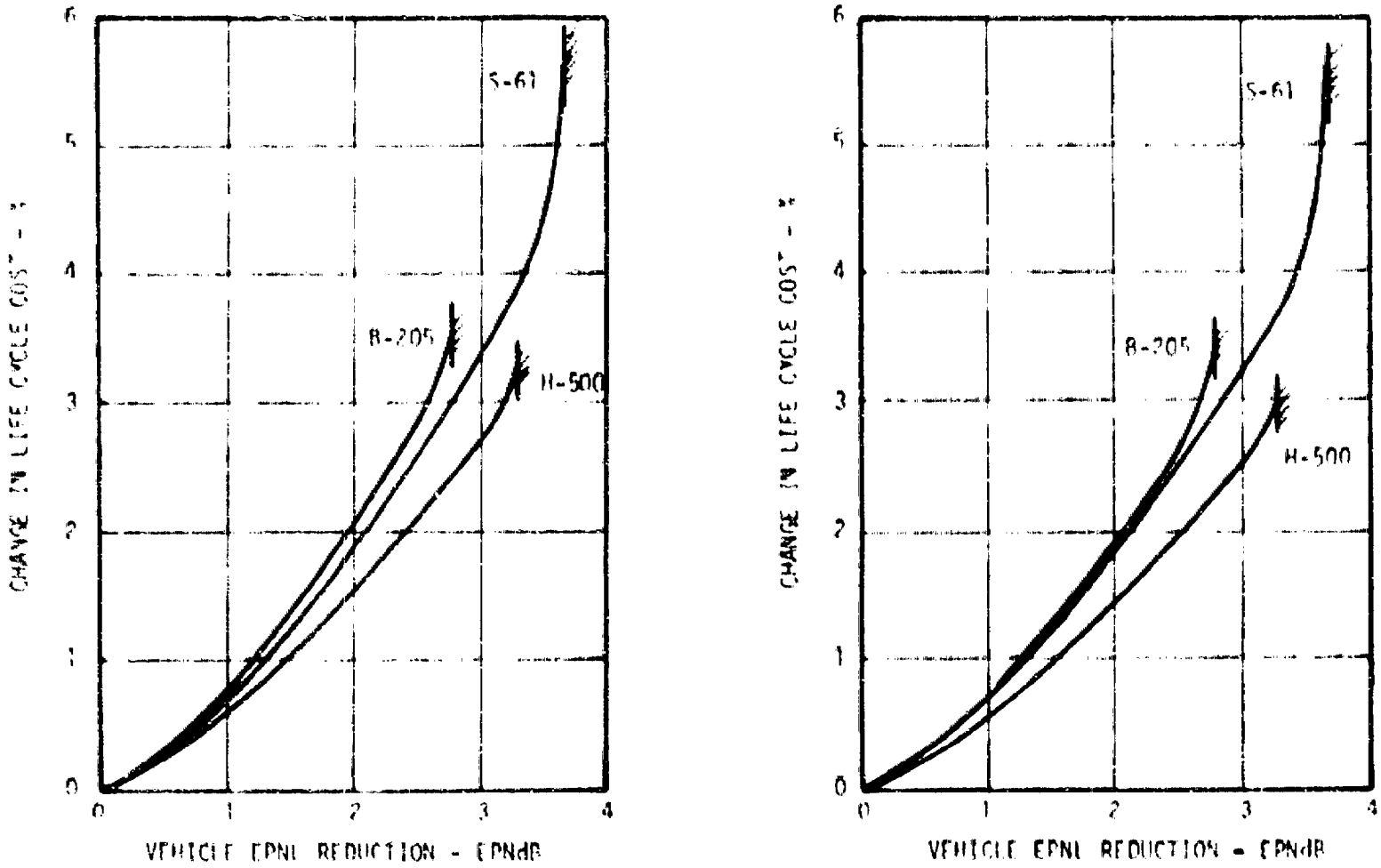

A. 300 A/C Hours/Year

B. 500 A/C Hours/Year

Figure 52. Change in Life Cycle Cost Due to Engine Silencing for a Useful Life of 15 Years

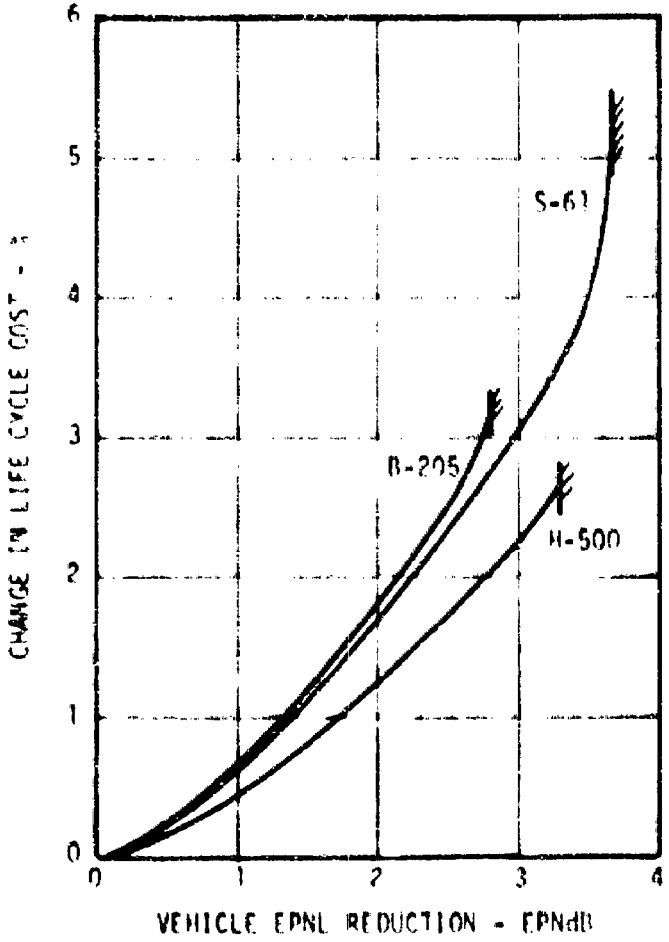

C. 1000 A/C Hours-Year

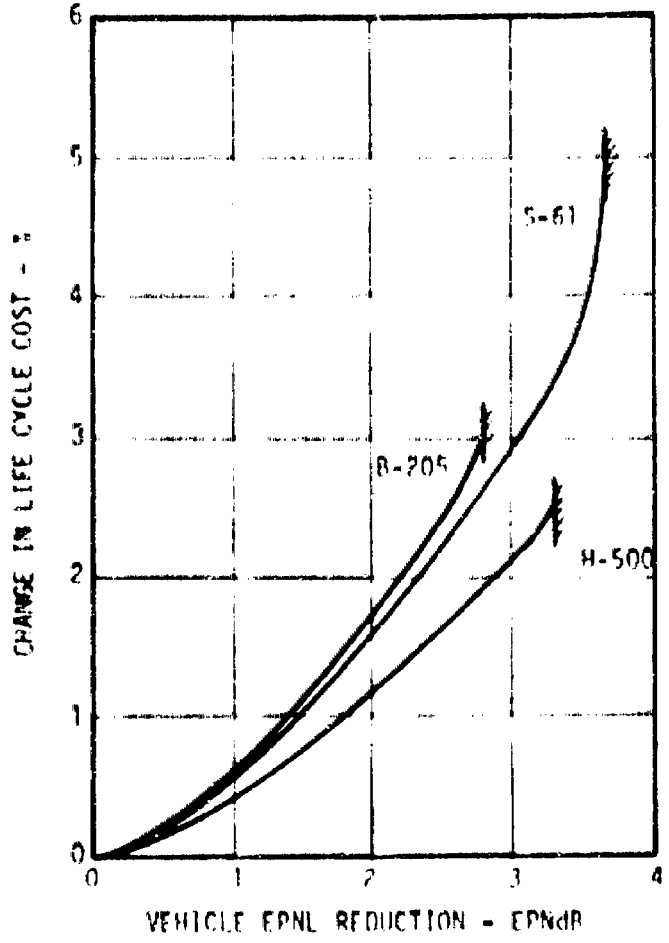

D. 1500 A/C Hours-Year

Figure 52 (Concluded)

The sensitivity of life cycle cost change to annual usage rate and useful life is indicated in Figure 55. The curves shown relate LCC change to useful life, at constant use rate, and to use rate, at a constant useful life, for a fixed degree of noise reduction. Sensitivity of LCC change to these two operating parameters is similar, although the sensitivity to annual use rate is somewhat more pronounced. Neither parameter influences the percentage change in life cycle cost to a significant degree over the ranges shown.

As for the vehicle design changes discussed previously, the magnitude of cost increase resulting from engine silencing is best illustrated by considering this change in absolute terms. Considering an S-61 vehicle, for example, a 3 EPNdB noise reduction obtained through engine silencing would raise initial investment cost from $1.779 million per aircraft to $1.846 million per aircraft, an increase of $67,000. Indirect costs, on a yearly basis, would rise by over $5000 per year, from $147,000/year to $152,000/year. Direct operating cost, initially at $272 per hour would go up to $281. per hour, an increase of over $8 per hour. Taken together, and assuming a useful life of 15 years with a usage rate of 1500 hours/year, total cost to own and operate this aircraft would increase by $233,000, from a baseline of $10.111 million to $10.404 million. This represents an annual cost increase of nearly $20,000.

EFFECTS OF CHANGES IN BASELINE COSTS

The changes in elemental costs and total life cycle costs presented in the previous section are felt to be a realistic estimate of the impact of engine silencing. These changes do, however, reflect only present technology and economic conditions and, in addition, include errors inherent in any parametric study, where general trends are derived from available data. The possibility of errors in the baseline vehicle costs, presented in Tables 18-20, is of particular significance, since definition of accurate baseline costs is essential to accurate prediction of changes in life cycle costs. Further, while these data may be a good approximation under present technological and economic conditions, changes in these conditions could very well invalidate the predicted cost changes. For these reasons, an analysis of the relative impact of changes in baseline vehicle initial investment cost, indirect operating cost, and direct operating cost on total life cycle cost has been performed. This analysis provides both an indication of the sensitivity of change in life cycle cost to errors in calculated baseline cost, and a means for revising life cycle cost change predictions to reflect changes in base vehicle costs due to changes in technology and economic conditions.

The percentage changes in elemental vehicle costs due to engine silencing, presented in Figure 51, reflect physical changes in vehicle design only, and will not be influenced by changes in baseline vehicle costs. Life cycle cost changes given in Figure 52 do, however, reflect baseline vehicle costs to the extent that changes in baseline costs change the

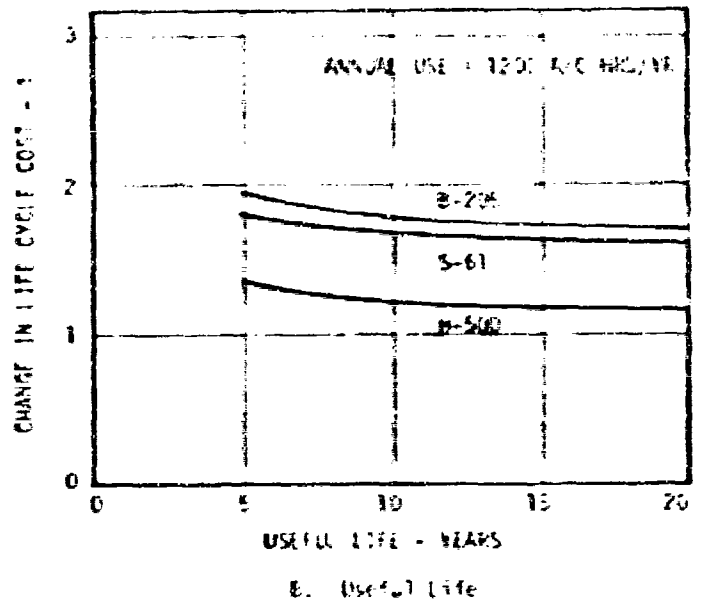

B. Useful Life

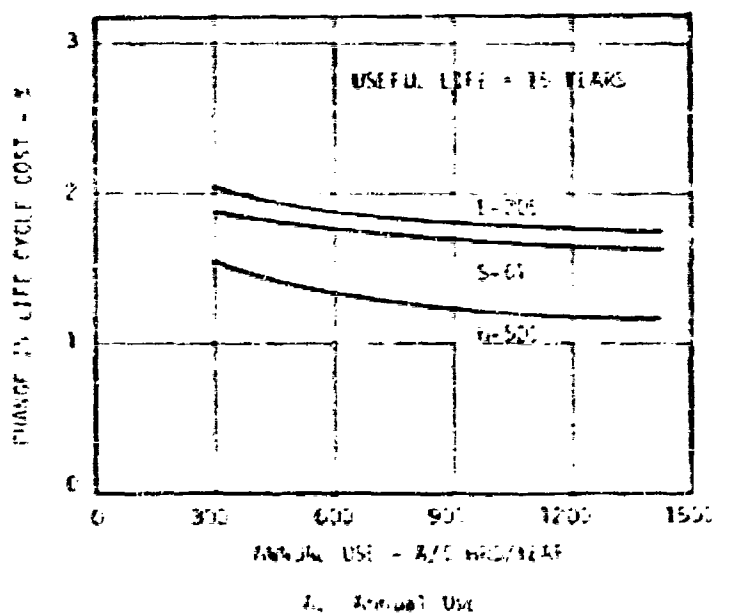

A. Annual Use

Figure 53. Change in Life Cycle Cost as a Function of Useful Life and Annual Use for a 2 EPNdB Noise Reduction

ratios between investment, indirect and direct operating costs. Change in life cycle cost is related to the baseline cost elements by:

$$\Delta LCC = \frac{\Delta I \cdot I_0 + \Delta IOC \cdot (IOC_0 \cdot N) + \Delta DOC (DOC_0 \cdot N \cdot R)}{I_0 + (IOC_0 \cdot N) + (DOC_0 \cdot N \cdot R)} \qquad (46)$$

where: ΔLCC = change in life cycle cost due to silencing ($)

$\Delta I, \Delta IOC, \Delta DOC$ = changes in investment, indirect and direct operating cost due to silencing ($)

I_0, IOC_0, DOC_0 = baseline vehicle investment, indirect and direct operating costs ($), ($/YEAR)($/HR)

N = useful life years

R = usage rate - hrs

Sensitivities of life cycle cost change to baseline elemental costs are reflected in the partial derivatives of Equation (46) with:

$$\frac{\partial LCC}{\partial I_0} = \frac{[(\Delta I - \Delta IOC)(IOC_0 \cdot N) + (\Delta I - \Delta DOC)(DOC_0 \cdot N \cdot R)]\frac{I_0}{100}}{[I_0 + IOC_0 \cdot N + DOC_0 \cdot N \cdot R]^2}$$

$$\frac{\partial LCC}{\partial IOC_0} = \frac{[(\Delta IOC - \Delta I)I_0 + (\Delta IOC - \Delta DOC)DOC_0 \cdot N \cdot R)]\frac{N \cdot IOC_0}{100}}{[I_0 + IOC_0 \cdot N + DOC_0 \cdot N \cdot R]^2}$$

$$\frac{\partial LCC}{\partial DOC_0} = \frac{[(\Delta DOC - \Delta I)I_0 + (\Delta DOC - \Delta IOC)IOC_0 \cdot N]\frac{N \cdot R \cdot DOC_0}{100}}{[I_0 + (IOC_0 \cdot N) + (DOC_0 \cdot N \cdot R)]^2} \qquad (47)$$

where: $\frac{\Delta LCC}{\Delta DOC}_0$ = absolute variation in the change in LCC due to a percentage change in baseline DOC

$\frac{\Delta LCC}{\Delta I}_0$ = absolute variation in the change in LCC due to a percentage change in baseline investment cost

$\frac{\Delta LCC}{\Delta IOC}_0$ = absolute variation in the change in LCC due to a percentage change in baseline IOC

Equation (47) calculates the number of percentage points, in absolute terms, the predicted changes in life cycle cost will vary, for a given percentage variation in any one of the three baseline cost elements. These equations have been used to calculate sensitivities to varying baseline costs, and the results of these calculations are given in Table 21.

The data of Table 21 indicate that predicted changes in life cycle cost will increase with increasing baseline investment cost and IOC, and will decrease with increasing baseline DOC. The H-50 vehicle is, in general, most sensitive to baseline cost changes and will be used to illustrate the magnitude of the sensitivities indicated in Table 21.

The change in LCC predicted for the H-500 is influenced by a change in investment cost most strongly at a useful life of 5 years and a utilization rate of 300 hrs/year. If, under these operating conditions, the baseline investment costs were to vary by +10%, a .0318% change in life cycle cost would result, increasing the predicted change in LCC from 2.46% to 2.49%. Considering the influence of baseline IOC, in this case for a useful life of 20 years and a use rate of 300 hrs/year, a +10% variation in baseline IOC would result in a .0196% increase in predicted life cycle cost change, which would go from 2.11% to 2.13%. A similar +10% change in baseline DOC, again for a 20 year life and a 300 hr/year use rate, would decrease the predicted change in LCC by -.0365 , from 2.11% to 2.07%. As demonstrated, variation in predicted life cycle cost change is relatively insensitive to changes in baseline elemental costs, with large variations required to produce significant changes. However, large changes in elemental costs could very well occur either due to technology change or changes in prevailing economic conditions, and under these circumstances, either Equation (46) or Equation (47) or the data of Table 21 can be used to adjust predicted life cycle cost changes, given in Figure 52.

TABLE 71. SENSITIVITY OF PREDICTED CHANGES IN LIFE CYCLE COST TO BASELINE ELEMENTAL COSTS

A. Sensitivity to % Change in Investment Cost

Useful Life (Years)	Numerical Change in Percentage LCC Change					
	S-61		B-205		H-500	
	300 Hr/Yr	1500 Hr/Yr	300 Hr/Yr	1500 Hr/Yr	300 Hr/Yr	1500 Hr/Yr
5	.00125	.00198	.00171	.00214	.00316	.00229
20	.00105	.0010	.00124	.0009	.00172	.00075

B. Sensitivity to % Change in DOC

Useful Life (Years)	Numerical Change in Percentage LCC Change					
	S-61		B-205		H-500	
	300 Hr/Yr	1500 Hr/Yr	300 Hr/Yr	1500 Hr/Yr	300 Hr/Yr	1500 Hr/Yr
5	-.00006	.0008	.00019	.00062	.00066	.00072
20	.00068	.0011	.0012	.00114	.00196	.00100

C. Sensitivity to % Change in DOC

Useful Life (Years)	Numerical Change in Percentage LCC Change					
	S-61		B-205		H-500	
	300 Hr/Yr	1500 Hr/Yr	300 Hr/Yr	1500 Hr/Yr	300 Hr/Yr	1500 Hr/Yr
5	-.00161	-.00243	-.00189	-.00276	-.00383	-.00301
20	-.00173	-.00210	-.00244	-.00202	-.00368	-.00175

MAIN ROTOR NOISE REDUCTION

Evaluation of the significance of the various helicopter noise components indicates that the main rotor contributes substantially to the total vehicle noise signature. Consequently, analyses have been performed to determine the extent of vehicle noise reduction obtainable through the application of rotor noise reduction technology. Rotor noise reduction methods considered in these analyses consist of changes in gross rotor design parameters only, including increased rotor radius, blade chord and blade number and reduced rotor speed. The effects of these changes have been evaluated in terms of the net vehicle noise reduction obtainable, considering potentially offsetting induced changes in vehicle design and performance. These induced design and performance changes have also been interpreted in terms of changes in vehicle cost, and these cost changes are compared to anticipated vehicle noise reductions. The study vehicles used for the preceding engine noise reduction study, the Hughes 500, Bell 206 and Sikorsky S-61, have also been used in the performance of the main rotor noise reduction study.

STUDY APPROACH

The previously described helicopter design and performance analysis method has been used to determine the nature and extent of vehicle design changes induced by changes in the various rotor design parameters. The changes in vehicle design considered are those changes necessary to maintain established mission performance capabilities, defined in terms of payload, hover ceiling, forward flight range and speed and rotor stall margin. In addition, the established rotor stall margin restraint has been used to determine the extent of rotor speed reduction obtainable, in conjunction with changes in rotor radius, blade chord or blade number.

The rotor geometry changes considered in the present analyses all tend to increase rotor stall margin. The trends of stall margin with increasing blade chord and blade number are identical, when considered in terms of equal percentage change in total blade area. Stall margin also increases with increasing rotor radius, but the trend of stall margin with rotor radius is different from that associated with blade chord and blade number. Rotor speed reduction, on the other hand, tends to reduce stall margin.

The preceding trends are predicated on the stall margin relationship of Equation (42), which can be applied given a knowledge of the trends of rotor thrust required with these same rotor parameters. These variables affect rotor thrust required only to the extent that rotor parameter changes influence vehicle gross weight. The design and performance analysis method calculates rotor thrust required, on this basis, and uses this information to determine the effects of these variables on stall margin.

As stated previously, stall margin has been used to determine allowable rotor speed reduction. Since stall margin decreases with reduced rotor speed, rotor speed cannot be reduced independently to reduce noise, since this would violate the established performance requirement for equal or greater stall margin of reduced noise vehicle configurations. Based on this consideration, rotor speed reduction has not been treated as an independent rotor noise reduction technique, and rotor speed reduction has been evaluated only in conjunction with offsetting rotor geometry changes. The approach taken in the present study is, therefore, two-fold. First, the effects of rotor geometry changes are determined, as independent variables, in the context of increasing stall margin relative to baseline vehicle stall margin. These same changes are then evaluated in conjunction with rotor speed reductions, with the amount of rotor speed reduction predicated on stall margin equal to that of the baseline vehicle.

The following changes in rotor geometry have been considered with the preceding approach:

(1) Increased rotor radius, in 5% increments, to a maximum 25% radius increase.

(2) Increase in blade chord, in 10% increments, up to a 50% chord increase.

(3) Increased number of blades, in increments of one blade up to twice the number of blades on the baseline rotor.

These changes have been considered independently, at constant rotor speed, and also with rotor speed reductions consistent with stall margin requirements.

EFFECTS ON VEHICLE DESIGN

The parameters of the main rotor strongly influence total helicopter vehicle design, and changes in rotor parameters cause significant changes in vehicle design and performance characteristics. Changes in vehicle design and performance due to rotor parameter variations have been calculated in terms of:

- Gross weight
- Airframe weight
- Engine weight
- Installed power
- Forward flight thrust required
- Stall margin

These data are presented in Tables 22-24, for the three study vehicles. Also shown in Tables 22-24 are maximum rotor speeds, corresponding to stall margin equal to the baseline stall margin, associated with each rotor geometry change evaluated.

Trends of vehicle gross weight and installed power with increasing rotor blade area are shown in Figure 54. The data shown relate to the S-61 study vehicle (Table 22) only, but similar trends are evident, in Tables 23 and 24, for the B-205 and H-53 study vehicles. In Figure 54A, gross weight is seen to increase with rotor radius, blade chord and blade number, with identical trends shown for chord and blade number. Rotor radius increases gross weight most quickly and the trend indicated is nonlinear, with increasing scope. This is due to the fact that rotor radius growth necessitates an increased fuselage size, in addition to increased structural weight due to load requirements. The maximum 25% increase in S-61 rotor radius results in a 6.6% increase in vehicle gross weight.

The trend of gross weight with either chord or blade number is linear, and less steep than the trend with rotor radius. In this case, airframe weight only increases due to the added rotor system weight, and the added structural weight needed to support the heavier rotor. Only a 4.1% gross weight increase is indicated for a 25% blade area change, whether due to chord or blade number increase. Doubling the chord or number of blades causes a 16.4% increase in gross weight.

The trends of installed power with chord/blade number, and rotor radius are given in Figure 54B. Installed power is shown to increase linearly with both chord and blade number, but to decrease nonlinearly with rotor radius increases, in this case with decreasing (absolute) slope. A 9.1% installed power reduction is indicated for the maximum 25% rotor radius increase. Installed power increases 6.3% for a 25% increase in blade area, whether due to blade chord or blade number. Doubling chord or number of blades increases installed power by 24%.

The data of Figure 54 show only an insignificant difference in the effects of rotor geometry changes evaluated alone and evaluated in conjunction with rotor speed reduction. The magnitude of rotor speed reduction considered in these data is, however, relatively small, as indicated in Figure 55. This figure relates rotor tip speed to change in blade area, and the curves shown represent lines of constant stall margin. As shown, only a 3.1% reduction in rotor tip speed can be accommodated by a 25% radius increase. A 3.7% reduction in rotor speed is indicated for a similar 25% blade area increase, accomplished by increasing chord or blade number. A 12% tip speed reduction can be obtained by doubling either blade chord or blade number.

TABLE 22. EFFECTS OF CHANGES IN ROTOR PARAMETERS ON S-61 VEHICLE DESIGN AND PERFORMANCE

Parameter Varied	Gross Weight (lb)	Airframe Weight (lb)	Engine Weight (lb)	Installed Power (HP)	Forward Flight Thrust (lb)	Stall Margin (kts)	Tip Speed (ft/sec)
Baseline	19500	8536	682	3000	19102	32.3	649
+1 Blade	20122	9100	699	3132	19707	43	↑
+2 Blades	20769	9682	717	3277	20335	51	
+3 Blades	21425	10273	735	3426	20974	58	
+4 Blades	22089	10871	754	3576	21621	63	
+5 Blades	22768	11482	772	3732	22281	67	
+10% Chord	19609	8816	690	3065	19403	36	No Tip Speed Reduction
+20% Chord	20122	9099	699	3132	19707	42	
+30% Chord	20447	9392	708	3206	20023	47	
+40% Chord	20769	9682	717	3277	20335	51	
+50% Chord	21090	9973	726	3348	20649	54	
+5 Radius	19692	8680	671	2917	19289	33	
+10% Radius	19923	8848	663	2854	19514	36	
+15% Radius	20179	9028	655	2799	19762	38	
+20% Radius	20464	9223	650	2755	20039	40	
+25% Radius	20786	9442	645	2725	20355	42	↓

TABLE 22 (Concluded)

Parameter Varied	Gross Weight (lb)	Airframe Weight (lb)	Engine Weight (lb)	Installed Power (HP)	Forward Flight Thrust (lb)	Stall Margin (kts)	Tip Speed (ft/sec)
+1 Blade -2.9% ΔR	20124	9102	699	3136	19711	33	630
+2 Blades -6.0% ΔR	20757	9671	717	3277	20325	33	610
+3 Blades -8.3% ΔR	21390	10241	734	3420	20941	33	595
+4 Blades -10.3% ΔR	22025	10813	752	3566	21556	32	582
+5 Blades -12.0% ΔR	22662	11386	770	3712	22175	32	571
+10% Chord -1.2% ΔR	19813	8819	691	3068	19406	32	647
+20% Chord -2.9% ΔR	20126	9102	699	3136	19711	33	630
+30% Chord -4.4 ΔR	20443	9388	708	3207	20020	33	620
+40% Chord -6.0% ΔR	20758	9671	717	3277	20325	32	610
+50% Chord -7.2% ΔR	21072	9956	726	3348	20631	32	602
+5% Radius -0% ΔR	19698	8685	672	2921	19295	33	649
+10% Radius -1.0% ΔR	19930	8854	663	2857	19529	33	642
+15% Radius -1.8% ΔR	20191	9039	656	2805	19774	33	637
+20% Radius -2.4% ΔR	20487	9243	651	2765	20062	33	633
+25% Radius -3.1 ΔR	20810	9461	647	2733	20378	33	629

TABLE 23. EFFECTS OF CHANGES IN ROTOR PARAMETERS ON H-500 VEHICLE DESIGN AND PERFORMANCE

Parameter Varied	Gross Weight (lb)	Airframe Weight (lb)	Engine Weight (lb)	Installed Power (HP)	Forward Flight Thrust (lb)	Stall Margin (kts)	Tip Speed (ft/sec)
Baseline	2590	1322	140	317	2406	31	646
+1 Blade	2627	1393	143	330	2477	47	▲
+2 Blades	2706	1464	147	345	2550	57	
+3 Blades	2784	1536	150	359	2624	66	
+4 Blades	2864	1608	154	374	2699	70	
+10% Chord	2581	1350	141.4	322.6	2434	36.2	
+20% Chord	2612	1378	142.8	328	2463	41.4	
+30% Chord	2643	1407	144.2	334	2492	46.6	
+40% Chord	2674	1435	145.6	339	2521	52	
+50% Chord	2706	1464	147	345	2551	57	
+5% Radius	2576	1332	138	309	2439	35	
+10% Radius	2609	1343	136	302	2461	38	
+15% Radius	2650	1362	135	298	2498	40	
+20% Radius	2698	1381	134	295	2543	42	
+25% Radius	2753	1408	134	293	2595	43	▼

Max Tip Speed Reduction

TABLE 23 (CONCLUDED)

Parameter Varied	Gross Weight (lb)	Airframe Weight (lb)	Engine Weight (lb)	Installed Power (HP)	Forward Flight Thrust (lb)	Stall Margin (kts)	Tip Speed (ft/sec)
+1 Blade - 5 % DR	2626	1392	143	330	2476	31	616
+2 Blades -8.5% DR	2702	1461	147	344	2598	31	593
+3 Blades -11.2% DR	2778	1530	150	358	2618	31	575
+4 Blades -13.4% DR	2855	1599	153	372	2690	31	561
+10% Chord -1.7% DR	2581	1350	141.4	323	2434	31	637
+20% Chord -3.4% DR	2612	1378	142.8	328	2463	31	626
+30% Chord -5.1% DR	2643	1407	144.2	334	2493	31	615
+40% Chord -6.8% DR	2674	1435	145.6	339	2521	31	604
+50% Chord -8.5% DR	2702	1461	147	344	2548	31	593
+5% Radius -1.1% DR	2576	1332	138	309	2429	31	641
+10% Radius -2.0% DR	2609	1345	136	302	2469	31	635
+15% Radius -3.1% DR	2651	1363	135	298	2499	30	628
+20% Radius -3.2% DR	2700	1383	134	295	2545	32	627
+25% Radius -3.7% DR	2757	1406	134	294	2598	32	624

TABLE 24. EFFECTS OF CHANGES IN ROTOR PARAMETERS ON B-205 VEHICLE DESIGN AND PERFORMANCE

Parameter Varied	Gross Weight (lb)	Airframe Weight (lb)	Engine Weight (lb)	Installed Power (HP)	Forward Flight Thrust (lb)	Stall Margin (kts)	Tip Speed (ft/sec)
Baseline	9500	4101	328	1400	10191	74	814
+10% Chord	9605	4197	331	1420	10211	84	↑
+20% Chord	9716	4298	334	1444	10329	92	
+30% Chord	9825	4396	337	1466	10443	98	
+40% Chord	9938	4498	340	1491	10562	104	
+50% Chord	10048	4598	343	1515	10678	109	
+5% Radius	9591	4158	323	1361	10197	78	
+10% Radius	9705	4228	319	1332	10317	83	
+15% Radius	9838	4308	316	1308	10457	86	
+20% Radius	9990	4398	313	1290	10617	89	— No Reduction in Tip Speed
+25% Radius	10165	4499	311	1278	10801	99	↓
+10% Chord -2.2% DR	9591	4184	330	1418	10197	75	796
+20% Chord -4.2% DR	9680	4266	332	1436	10291	75	780
+30% Chord -6.0% DR	9777	4353	336	1458	10393	75	765
+40% Chord -7.6% DR	9872	4438	338	1477	10493	74	752
+50% Chord -8.9% DR	9966	4524	341	1498	10592	74	741
+5% Radius -.8 DR	9586	4154	323	1361	10191	75	807

TABLE 24 (CONCLUDED)

Parameter Varied	Gross Weight (lb)	Airframe Weight (lb)	Engine Weight (lb)	Installed Power (HP)	Forward Flight Thrust (lb)	Stall Margin (kts)	Tip Speed (ft/sec)
+10% Radius -1.6% DR	9693	4217	318	1329	10304	76	801
+15% Radius -2.4% DR	9820	4292	315	1305	10438	76	794
+20% Radius -3.3% DR	9968	4376	313	1287	10594	75	787
+25% Radius -3.9% DR	10138	4473	311	1274	10773	75	782

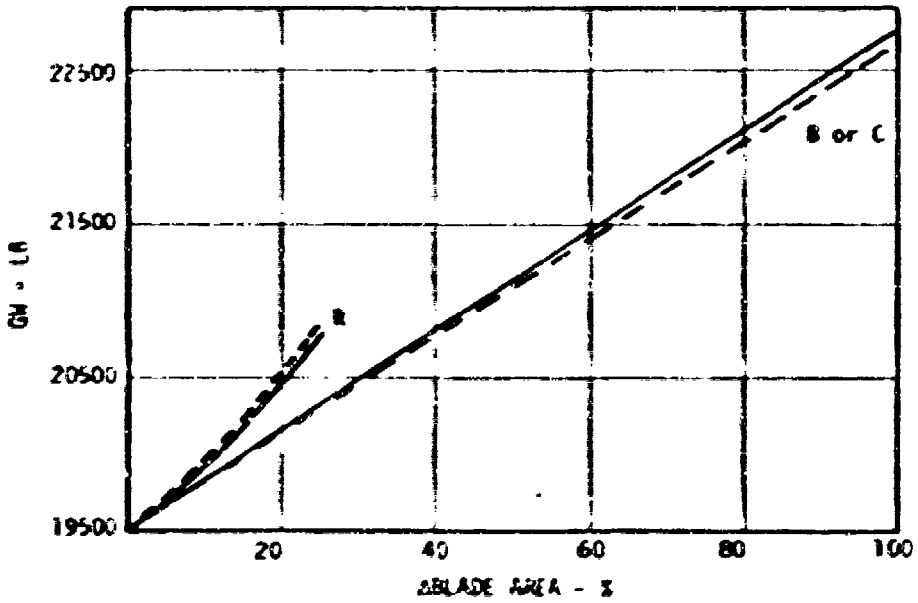

A. Gross Weight Vs Blade Area

——— AT CONSTANT ROTOR SPEED

– – – – WITH REDUCED ROTOR SPEED

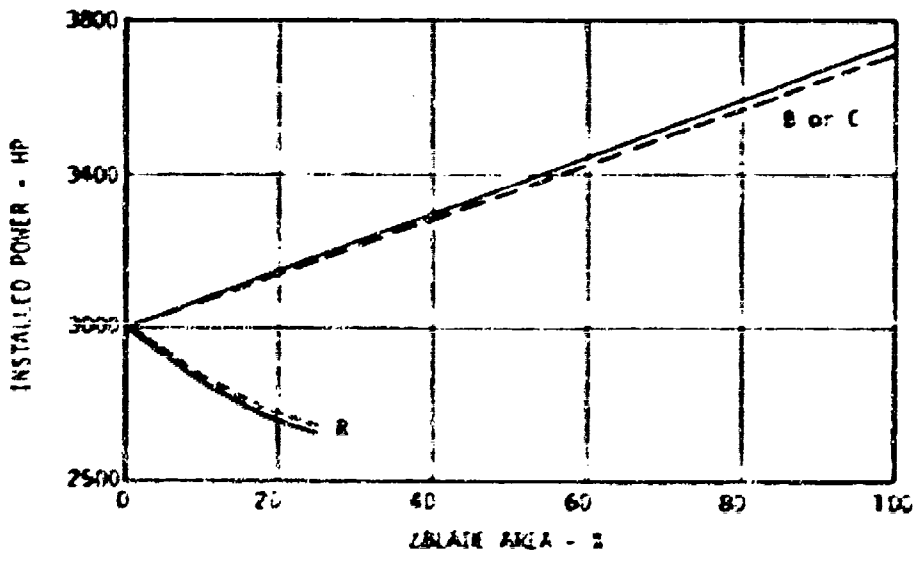

B. Installed Power Vs Blade Area

Figure 54. Effect of Main Rotor Blade Area Change on S-61 Gross Weight and Installed Power

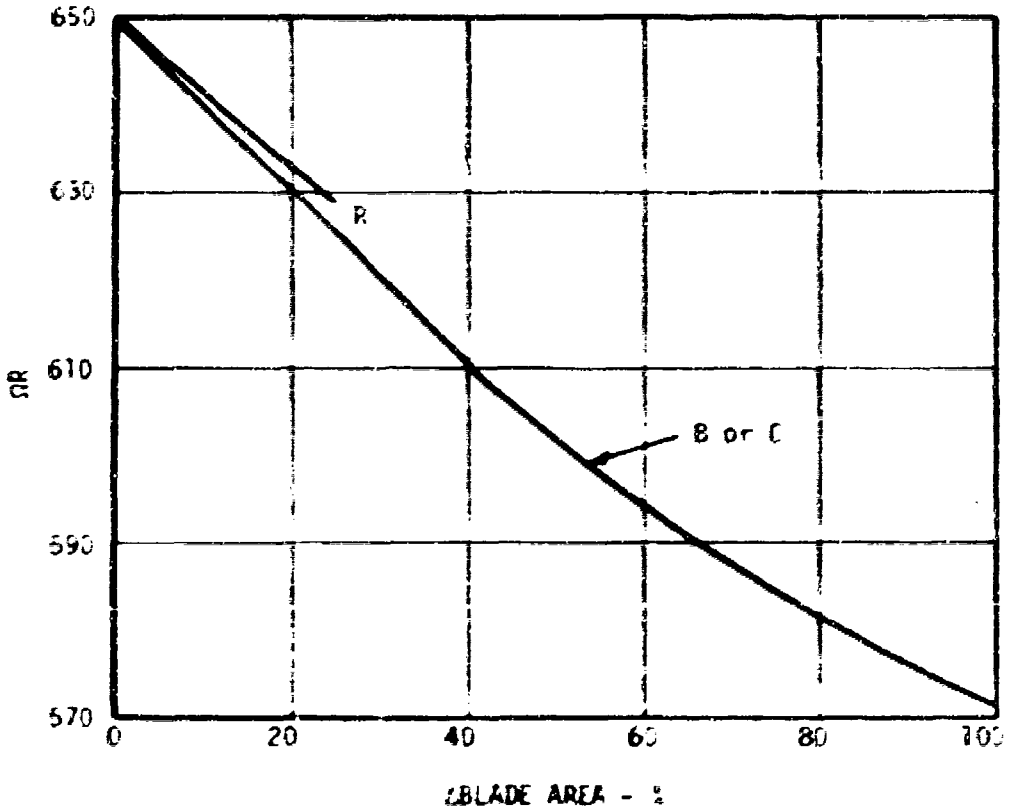

Figure 55. S-61 Main Rotor Speed Reduction Vs Blade Area Increase

The magnitude of vehicle gross weight increase associated with the various rotor system changes strongly indicates that noise reductions anticipated to result from the rotor system changes would tend to be offset by increases in noise due to rotor thrust increase. Based on this indication, it was decided to use a simplified rotor noise calculation method to determine the approximate magnitude of achievable net rotor noise reductions, and based on the results of these calculations, decide whether to proceed with the more involved rotor and total vehicle noise calculations. This approach was arrived at as a result of economic considerations and was based on the premise that unless significant rotor noise reductions were shown through the simple analysis, no worthwhile reductions would be calculated for the total vehicle using the detailed analysis.

APPROXIMATE ROTOR NOISE CALCULATION METHOD

The simplified rotor noise calculation method chosen for use was obtained from Reference 52. This equation relates the magnitude of the high frequency random component of rotor noise to rotor speed, thrust and blade area. The change in rotor sound pressure level due to these combined variables is given by:

$$\Delta SPL = 20 \text{ Log}_{10} \left(\frac{\Omega R}{\Omega R_o}\right) + 20 \text{ Log } (T/T_o) - 10 \text{ Log } \left(\frac{AB}{AB_o}\right) \qquad (48)$$

where: ΔSPL = change in sound pressure level between baseline and modified rotor (dB)

$\Omega R, T, AB$ = tip speed, rotor thrust and total rotor blade area of modified rotor

$\Omega R_o, T_o, AB_o$ = tip speed, rotor thrust and total rotor blade area of baseline rotor

Equation (48) has been used to estimate the maximum possible rotor system noise reduction obtainable with the various rotor system parameter changes considered. The results of these calculations are summarized in Tables 25-27, for the three study vehicles. Also given in Tables 25-27 are the rotor system parameters, blade area, rotor tip speed and thrust required used to make these calculations.

---

[52] King, R. J. and R. G. Schlegel, "Prediction Methods and Trends for Helicopter Rotor Noise", CAL/AVLABS Symposium, June 1969.

TABLE 26. APPROXIMATE MAXIMUM ROTOR SYSTEM NOISE REDUCTION - S-61

Parameter Varied	Blade Area (ft)	Tip Speed (ft/sec)	Thrust Required (lb)	dB
Baseline	231.8	649	19108	-
+25% Rotor Rad	289	649	20355	-.4
+50% Chord	347.7	649	20649	-1.06
+5 Blades	463.6	649	22281	-1.67
+25% Rotor Radius - 3% DR	289	629.3	20376	-.68
+50% Chord -7.2% DR	347.7	602	20631	-1.74
+5 Blades -11.9% DR	463.6	571.2	22179	-2.82

TABLE 26. APPROXIMATE MAXIMUM ROTOR SYSTEM NOISE REDUCTION - h-500

Parameter Varied	Blade Area (ft²)	Tip Speed (ft/sec)	Thrust Required (lb)	dB
Baseline	29.5	647.7	2405	-
+25% Radius	36.8	642.7	2595	.3
+50% Chord	44.2	647.7	2550	-1.25
-4 Blades	59	647.7	2699	-2.00
+25% Radius +3.6% ΔR	36.8	624.4	2598	-.6
+50% Chord +8.59 ΔR	44.2	592.8	2548	-2.0
+4 Blades +13 ΔR	59	560.9	2690	-3.3

TABLE 27. APPROXIMATE MAXIMUM ROTOR SYSTEM NOISE REDUCTION, B-205

Parameter Varied	Blade Area (ft)	Tip Speed (ft/sec)	Thrust Required (lb)	dB
Baseline	89	814	10101	-
+25% Radius	105	814	10801	-.4
+50% Chord	126	814	10878	-1.3
+25% Radius -3.9% DR	105	782	10773	-.8
+50% Chord -8.9% DR	126	741	10592	-2.2

The rotor system noise reductions indicated in Tables 25-27 are, in themselves, small and their significance is further reduced if consideration is given to their probable impact on total vehicle noise. Based on the discussion of helicopter component noise source significance, presented in a previous section of this report, the main rotor and engine contribute approximately equally, and their contributions effectively determine the total vehicle noise signature. On this basis, a rotor system noise reduction of 3.3 dB, which is the maximum shown in Tables 25-27, will result in approximately a 1.6 dB reduction in total vehicle noise.

The noise reductions of Tables 25-27, although approximate, are a good indication that only a small reduction in helicopter noise can be achieved by modifying the main rotor in the manner studied. These data are not, however, sufficient to dismiss further consideration of these methods, since even the small reductions may be of benefit, provided that they can be achieved at reasonable cost. To ascertain the costs associated with the application of these methods, the design and performance data of Tables 22-24 have been used, with the established helicopter cost model, to calculate induced changes in vehicle life cycle, and elemental costs.

COST ANALYSIS

Calculated changes in helicopter cost associated with the various rotor system noise reduction methods are summarized in Tables 28-30. Cost data shown reflect the rotor/vehicle configurations with the greatest potential noise reduction, as indicated in Tables 25-27. Life cycle cost changes shown are for an assumed useful life of 15 years, with annual use rates of 300 and 1500 hours per year.

Comparison of the cost data of Tables 28-30 with the approximate rotor noise reduction data of Tables 25-27 reveals that the cost of reducing helicopter rotor noise levels is very high. Considering the S-61 study vehicle, for example, increasing rotor size by 25%, raises life cycle cost by over 5.7%, for a 1500 hour per year use rate, and the cost differential is greater for lower annual use rates. In absolute terms, the 25% greater rotor radius increases life cycle cost by almost $.6 million dollars, or more than $38,000/year. This rotor design change reduces rotor noise by less than .5dB which, in all probability, would produce no measurable change in total vehicle noise.

The most beneficial rotor design change, doubling the number of blades and reducing rotor speed by approximately 12%, raises life cycle cost by almost 30%. This translates into a $3.03 million dollar life cycle cost increase, or in yearly terms, over $200,000 added annual cost. In terms of total vehicle noise, as discussed previously, the 2.8 dB rotor noise reduction associated with this design change, would probably only result in a 1.6 dB reduction in vehicle noise.

TABLE 28. VEHICLE COST CHANGES FOR MAXIMUM NOISE REDUCTION ROTOR CONFIGURATIONS - S-61

Parameter Varied	ΔInvestment Cost ($)	ΔIOC-%	ΔDOC-%	ΔLCC - % (15 Yr Life) 300 Hr/Yr	ΔLCC - % (15 Yr Life) 1500 Hr/Yr
+25" Radius	13.66	13.65	.58	10.58	5.73
+50% Chord	25.0	23.66	9.0	20.44	14.86
+5 Blades	51.83	49.82	18.15	93.06	30.99
+25% Radius -3% DR	14.02	13.98	.73	10.88	5.96
+50% Chord -7.2% DR	24.04	23.30	8.61	20.15	14.65
+5 Blades -11.9% DR	50.05	48.12	17.61	41.6	29.98

TABLE 29. VEHICLE COST CHANGES FOR MAXIMUM NOISE REDUCTION ROTOR CONFIGURATIONS - H-500

Parameter Varied	ΔInvestment Cost (%)	ΔIOC-%	ΔDOC-%	ΔLCC - % (15 Yr Life 300 Hr/Yr	1500 Hr/Yr
+25% Radius	5.73	7.36	.19	3.21	1.15
+50% Chord	19.16	14.78	4.44	9.13	5.94
+4 Blades	29.2	30.35	8.91	18.66	12.02
+25% Radius -3.6% ΩR	6.0	7.66	.31	3.40	1.29
+50% Chord -8.5% ΩR	13.89	14.47	4.33	8.94	5.80
+4 Blades -13% ΩR	28.11	29.3	8.61	18.01	11.61

TABLE 30. VEHICLE COST CHANGES FOR MAXIMUM NOISE REDUCTION ROTOR CONFIGURATIONS - S-205

Parameter Varied	Investment Cost (%)	DOC-%	IOC-%	DOC - % (15 Yr Life) 300 Hr/Yr	1500 Hr/Yr
+25% Radius	11.54	12.43	.48	8.14	3.74
+50% Chord	16.77	16.81	5.98	13.14	9.03
+25% Radius -3.9% DR	10.7	11.57	.21	7.49	3.31
+50% Chord -6.9% DR	14.23	14.26	5.10	11.16	7.68

Because of the high cost to benefit ratios determined for the selected rotor noise reduction methods, it was concluded that these methods are not practical means for reducing helicopter noise, and that further analyses of these methods was not warranted. Consequently, these methods were not evaluated with the more involved noise calculation techniques originally intended for use. However, a small number of rotor noise reduction design changes were subjected to further evaluation in order to verify the appropriateness of the approximate noise calculation method. In all cases studied, the involved noise calculation technique indicated noise reductions similar in magnitude to those obtained with the approximate method.

CONCLUSIONS

Analysis of noise calculations made for existing civil helicopters indicate that the main rotor and engine(s) contribute most to vehicle noise, at least in terms of effective perceived noise level, although this conclusion is limited to the particular flight conditions, attitudes and observer locations studied. Furthermore, the main rotor and engine(s) contribute approximately equally to total vehicle noise, and their combined contribution dominates the remaining vehicle noise sources, the tail rotor and transmission. Consequently, it is concluded that helicopter noise can be reduced by reducing main rotor and engine noise only, although both sources must be dealt with to produce substantial vehicle noise reduction.

Evaluation of helicopter engine noise, specifically shaft turbine engine noise, indicates the exhaust radiated noise components to be the dominant contributors to the total engine spectrum. These components, consisting of aft radiated compressor noise, combustion noise and, to a lesser extent, jet noise may be effectively reduced through the use of exhaust duct treatment. Analytical evaluation indicates that an approximate 3 EPNdB reduction in helicopter vehicle noise may be achieved through application of this approach. This reduction requires a treated duct weighing from 2-3% of baseline vehicle gross weight.

The use of exhaust duct treatment directly adds to vehicle gross weight, reduces engine power available, and increases specific fuel consumption. These direct changes induce changes in airframe weight, engine installed power and weight and fuel load. To achieve the above 3 EPNdB reduction, airframe weight must grow by approximately 3-4%, installed engine weight and power must increase by 3-4% and 7-8%, respectively, and fuel load must grow by 2.5-3%. These combined changes add approximately 4-5% to vehicle gross weight.

The direct and induced changes in vehicle design associated with exhaust duct treatment tend to increase helicopter life cycle cost. Calculated changes in life cycle cost, again for an approximate 3 EPNdB vehicle noise reduction, range from 2.5-4%, with a generally smaller increase in cost for higher annual usage rates.

An evaluation of existing methods for reducing helicopter main rotor noise was performed. The specific methods considered were:

- Increasing rotor radius
- Increasing blade chord
- Increasing blade number
- Decreasing rotor speed

These methods were evaluated analytically, using an approximate rotor noise calculation technique, and considering rotor parametric changes within the context of maintaining established mission performance.

The main rotor noise reduction methods chosen for evaluation did not result in substantial reductions in rotor noise. This was due to the fact that application of these methods induced large changes in vehicle design and performance. These induced changes resulted in large vehicle gross weight increases, which tended to offset much of the anticipated rotor noise reductions. These same induced vehicle design and performance changes did, however, cause large increases in vehicle life cycle costs.

APPENDIX I

HELICOPTER PARAMETRIC WEIGHT ANALYSIS

INTRODUCTION

This Appendix presents the parametric weight analysis used to calculate helicopter component weights, using limited data such as are available in a typical pre-design situation. Three categories of data are used in the component weight equations:

1. Input Data, generally the result of analysis of helicopter performance specifications. An example is Rotor Radius.

2. Intermediate Data, where actual values may be used if known from design definition. If an actual value is not available, an intermediate data value can be calculated using input data and the equations given herein. An example is Tail Rotor Radius. If not known from design definition, the tail rotor radius (in feet) is estimated, using input data only, by .087 (Rotor Radius)$^{1.22}$.

3. Calculated Weight Data, where the weight calculated by a weight equation is used in a subsequent weight equation. An example is Blade Weight, which is subsequently used to calculate Hub Weight.

In the parametric analysis which follows, each item is listed in the order in which it appears on the standard AN Weight Statement per Mil-Std-451, Part I. Each item is listed with an equation and a definition of all terms used in that equation. The terms may use any of the three data categories. The rationale used to find a component weight for the warm cycle system is shown after the equation definitions, as applicable. Each equation page is followed by a graph showing the equation and the data used in its derivation. This parametric analysis is a guide, to be used with care, and improved with use.

INPUT DATA FOR PARAMETRIC WEIGHT ANALYSIS

Symbol	Data
MOW	Maximum Operating Weight - Lbs
NMR	Number of Main Rotor Blades
NR	Number of Main Rotors
NULT	Ultimate Load Factor
RM	Main Rotor Radius - Feet
S	Main Rotor Solidity
SDG	Weight of Engine Speed-Decreaser Gearbox - Lbs

TAF = Type of Aft Fuselage - Values/Configuration

8 - Full fuselage depth at splice of main fuselage to aft fuselage.
Example: SH3A

9 - Tailboom configured for rear ramp.
Example: CH53

10 - Tailboom without rear ramp.
Example: UH19

13 - Full fuselage depth at splice of main fuselage to aft fuselage and with a tail wheel full aft.
Example: HH2D

15 - Tailcone upswept from fuselage splice.
Example: UH1D

INPUT DATA FOR PARAMETRIC WEIGHT ANALYSIS

Symbol	Data
AG	Number of Auxiliary Landing Gears
CAP	Gallons of Fuel - Gals
CB	Blade Chord - Feet
EN	Number of Engines
HP1	Rotor Horsepower - Hp
HP2	Installed Horsepower - Hp

KLG = Landing Gear Geometry - Values/Configuration

- .0157 - Skid Gear
- .0247 - Sponson Mounted
- .0280 - Quadricycle
- .0329 - Tricycle - Fuselage Mounted
- .0405 - Crane - Straddle Type

KNAC = Nacelle Arrangement - Values/Configuration

- .96 - Twin engines mounted to transmission forward or aft of main rotor
- 1.19 - Single engine mounted to fuselage forward or aft of main rotor
- 1.23 - Twin engines with combining gearbox.
- 2.26 - Twin engines outboard of main fuselage.

Add factors for more than two engines.

INPUT DATA FOR PARAMETRIC WEIGHT ANALYSIS

Symbol		Data
TPY	=	Type of Pylon Configuration - Values/Configuration (depends on type of aft fuselage)
	14 -	Tailcone upswept from fuselage splice. Example: UH1D
	25 -	Tailboom without rear ramp. Example: UH19
	45 -	Tailboom configured for rear ramp. Example: CH53
	46 -	Full fuselage depth at splice of main fuselage to aft fuselage. Example: SH3A
	62 -	Full fuselage depth at splice of main fuselage to aft fuselage and with a tail wheel full aft. Example: HH2D
VM		Main Rotor Tip Speed - FPS
WENG		Total Weight of Engines - Lbs

BLADE WEIGHT (WBL)

$$WBL = .151 \times 10^{4} \left(\frac{\left(\frac{NGW \times NULT}{100} \right)}{AR \times VM^{.331} \times DMRN^{.65} \times NOF^{.41}} \right)$$

where:

NGW = Normal Gross Weight = $2.145 \times MOW^{.893}$

MOW = Maximum Operating Weight - Lbs - Input Parameter

NULT = Ultimate Load Factor - Input Parameter

AR = Blade Aspect Ratio = R^2/AB

R = Rotor Diameter - Feet - Input Parameter

AB = Total Blade Area - Sq.Ft. = RM x CB x NMR

RM = Main Rotor Radius - Feet - Input Parameter

CB = Main Rotor Blade Chord - Feet - Input Parameter

NMR = Number of Main Rotor Blades - Input Parameter

VM = Main Rotor Tip Speed - fps - Input Parameter

DMNR = Disc Loading x Number of Rotors

DM = Disc Loading - Lbs/Sq.Ft. = $MOW/\pi RM^2$

NOF = Effective Number of Rotor Blades = $14.259 \times S^{.409}$

S = Main Rotor Solidity - Input Parameter

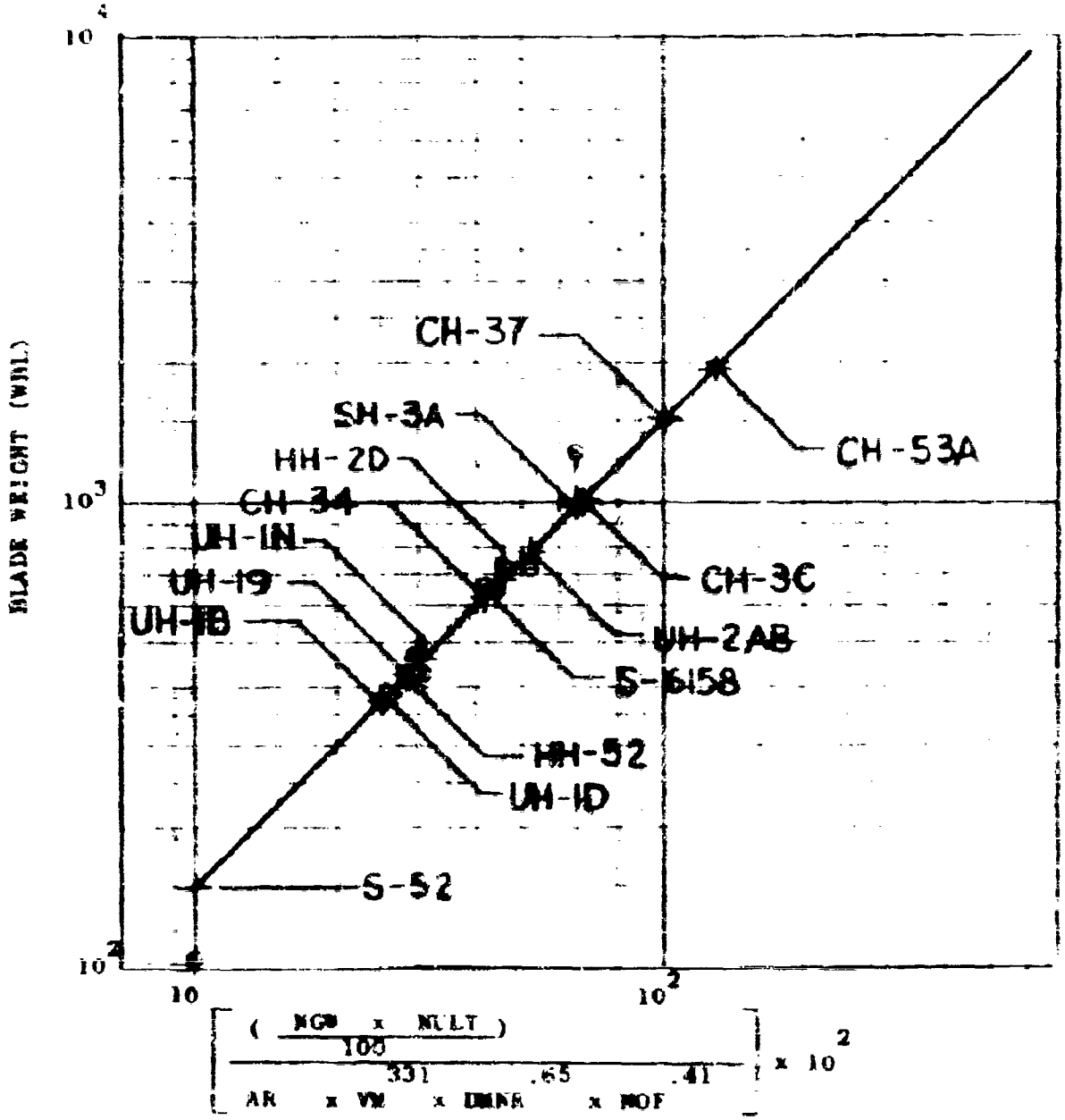

Figure I-1. Blade Weight

HUB WEIGHT (WHUB)

$$WHUB = .0104\left[\frac{WBL \times .5RM \times RPM^2 \times 10^{-6}\right)^{1.127} \times QMP^{.405} \times NOF^{.058}}{IY^{.059}}\right]$$

where:

WBL = Blade Weight - Lbs - See Blade Weight Equation

RM = Main Rotor Radius - Feet - Input Parameter

RPM = Main Rotor rpm = 9.549 x VM/RM

VM = Main Rotor Tip Speed - fps - Input Parameter

QMP = Main Rotor Torque - Ft-Lbs = 5250 x HP1/RPM

HP1 = Main Rotor Horsepower - Input Parameter

NOF = Effective Number of Rotor Blades = $14.259 \times S^{.409}$

S = Main Rotor Solidity - Input Parameter

IY = Aircraft Pitch Inertia - Slug-Ft^2 - If Known, otherwise use $.6296 \times 10^{-2} \times MOW^{1.635}$

MOW = Maximum Operating Weight - Lbs - Input Parameter

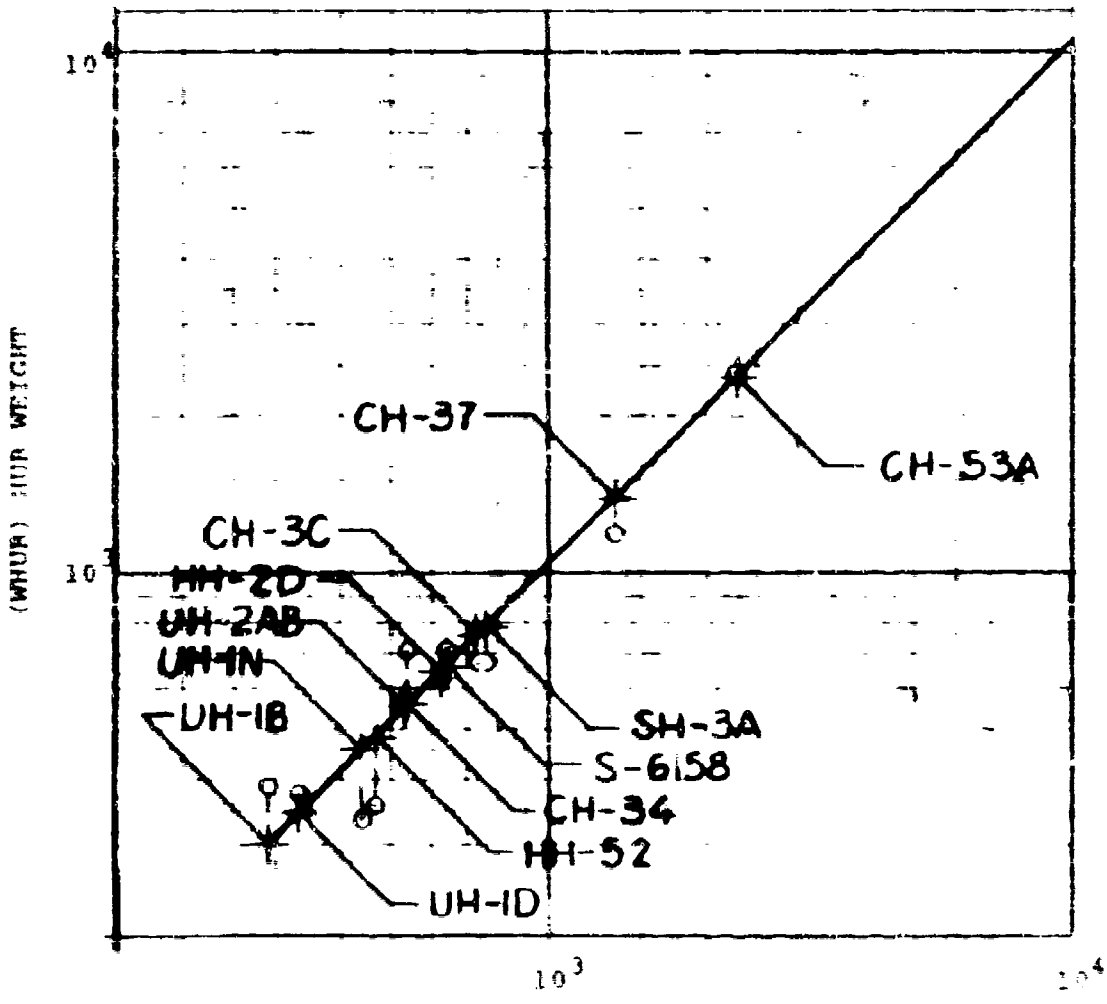

$$\left[\frac{(\%BL \times .5RM \times RPM^2 \times 10^{-6})^{1.127} \times QMR^{.405} \times MOF^{.056}}{IY^{.059}}\right] \times 10^{-2}$$

Figure 3-1. Hub Weight

BLADE FOLDING (FLD)

Power folding weight: A limited number of statistical samples exist forming almost a single point when plotted. The correlation outside this specific grouping is unpredictable. For this reason, a penalty was derived based on a current model in the higher gross range.

$$FLD = .12(WBL + WHUB)$$

TAIL ROTOR WEIGHT (WTR)

$$WTR = K \times 10^{-6} (RT \times C \times N \times VM^2)^{1.29}$$

where:

RT = Tail Rotor Radius - Feet - If Known, otherwise use $.087 \times RM^{1.22}$

RM = Main Rotor Radius - Feet - Input Parameter

C = Tail Rotor Blade Chord - Feet - If Known, otherwise use $.092 \times RM^{.661}$

N = Number of Tail Rotor Blades - If Known, otherwise use $1.062 \times RT^{.773} = .1608\ RM^{.943}$

VM = Main Rotor Tip Speed - fps - Input Parameter

K = .183 (Constant - Conventional Geared)

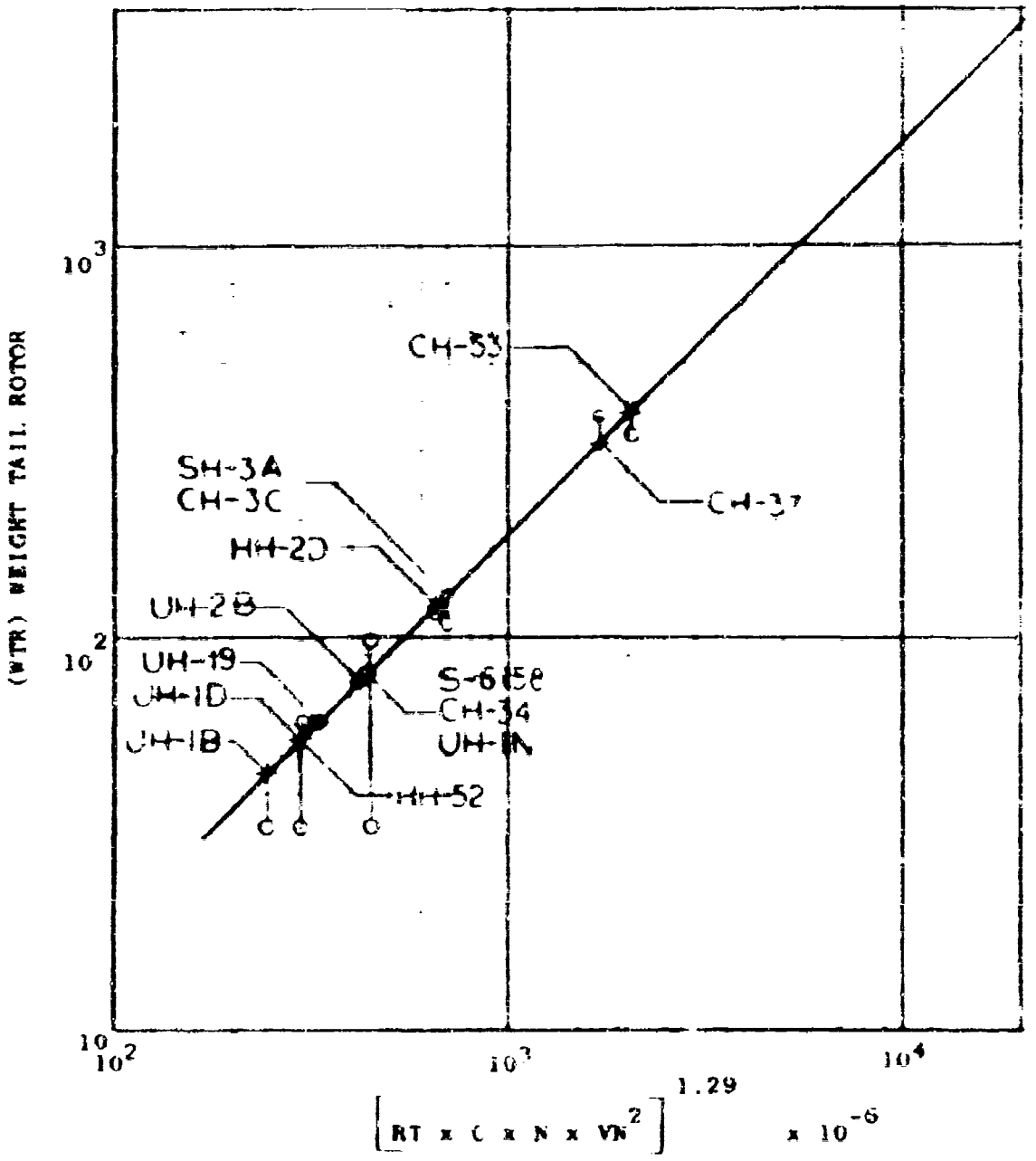

Figure [illegible] Tail Rotor Weight

HORIZONTAL STABILIZER (WHS)

$$WHS = .0049(ATF^{.5} \times LTF^{1.78} \times (DM \times 10)^{.2} \times TAF^{.28})$$

where:

ATF = Horizontal Tail Area - Sq.Ft. - If Known, otherwise use $1.433 \times DM^{1.53}$

DM = Disc Loading = $MOW/\pi RM^2$

MOW = Maximum Operating Weight - Lbs - Input Parameter

RM = Main Rotor Radius - Feet - Input Parameter

LTF = Distance From ℄ Main Rotor to the Leading Edge of the Horizontal Stabilizer - Feet
If Known, otherwise use $.96 \times RM^{1.62}$

TAF = Type of Aft Fuselage - Values/Configuration

8 - Full fuselage depth at splice of main fuselage to aft fuselage.
Example: SH3A

9 - Tailboom configured for rear ramp.
Example: CH53

10 - Tailboom without rear ramp.
Example: UH19

13 - Full fuselage depth at splice of main fuselage to aft fuselage and with a tail wheel full aft.
Example: HH2D

15 - Tailcone upswept from fuselage splice.
Example: UH1D

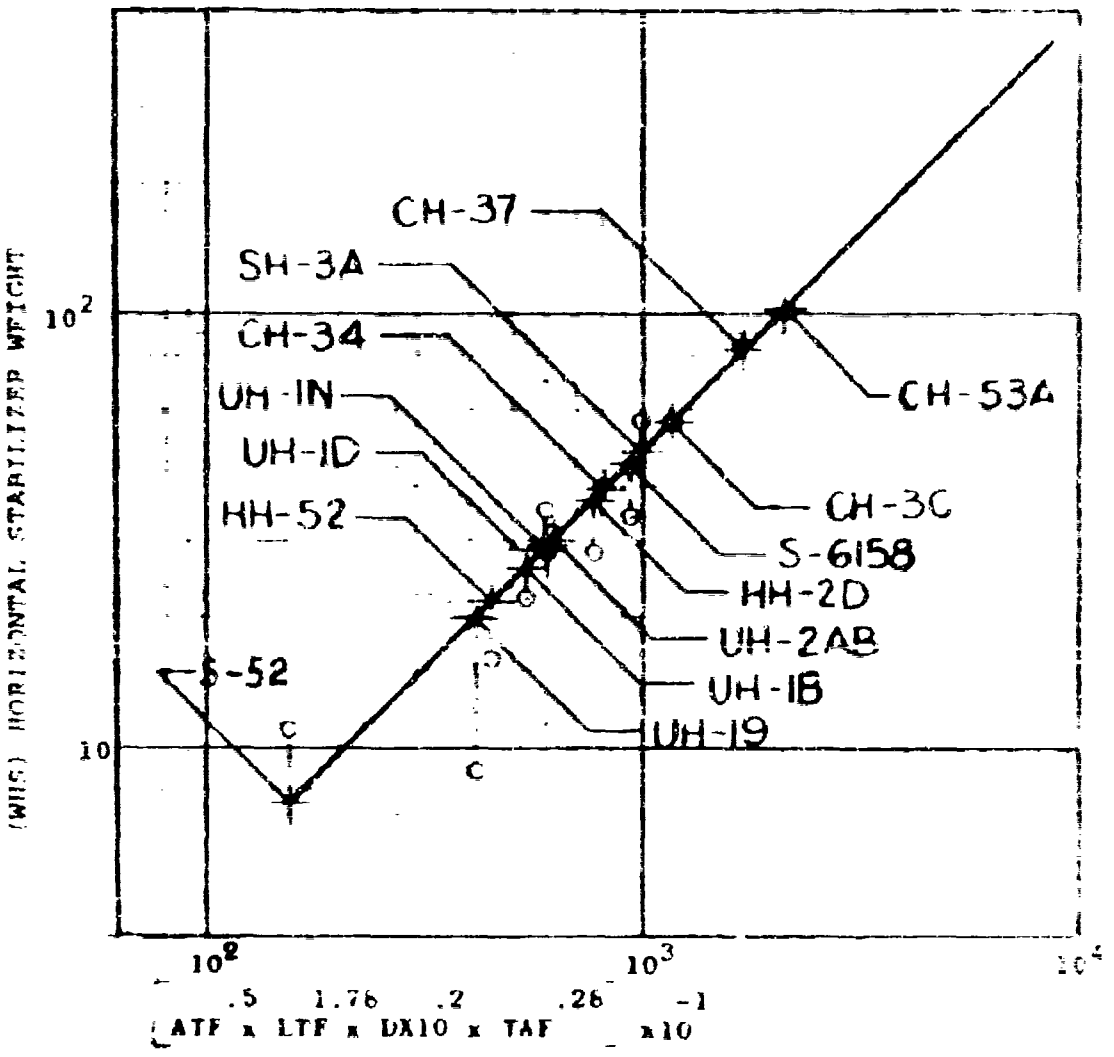

Figure 1-4. Horizontal Stabilizer Weight

FUSELAGE WEIGHT (FUS)

$$FUS = K \times \left[\frac{(LU(W+H))^{.93} \times CM^{.05} \times NGW \times QMH^{1.15}}{(MOW \times WTRD)^{.23} \times TTR^{.62} \times IX^{.36}}\right]$$

where:

LU = Usable Fuselage Length - Feet, If Known, otherwise use $.225 \times RM^{1.474}$

RM = Main Rotor Radius - Feet - Input Parameter

W = Maximum Fuselage Width - Feet - If Known, otherwise use $2.53 \times IX^{.115}$

IX = Aircraft Roll Inertia - Slug-Ft^2 - If Known, otherwise use $.221 \times 10^{-3} \times MOW^{1.807}$

MOW = Maximum Operating Weight - Lbs - Input Parameter

H = Maximum Fuselage Height - Feet - If Known, otherwise use $.406(LDIA \times SINL)^{1.226}$

LDIA x SINL =

LDIA = Distance from ℄ Tail Rotor to Cockpit Control Grouping - Feet

SINL = Sine of Angle at Intersection Between LDIA and Aircraft Waterline

If LDIA x SINL is not known, use $.981 \times RM^{.743}$

CM = Major Structural Cutouts, Use the Sum of the Weighted Values Per Configuration

Cutouts - Values/Configuration - Use 3.0 as Minimum

Nose Enclosure (side x side)	1.00
Nose Enclosure (tandem)	.50
Pilot's Door	.75
Co-Pilot's Door	.75
Rescue Door	1.00
Cargo Door	1.00
Nose Doors - Avionics	.25
Nose Doors - Engine	.75
Rear Loading Doors	1.50
Windows	.25 each
Through Floor Entrance	1.00

Use Weighted Values - If Known, otherwise use

$CM = 1.36 \times MOW^{.172}$

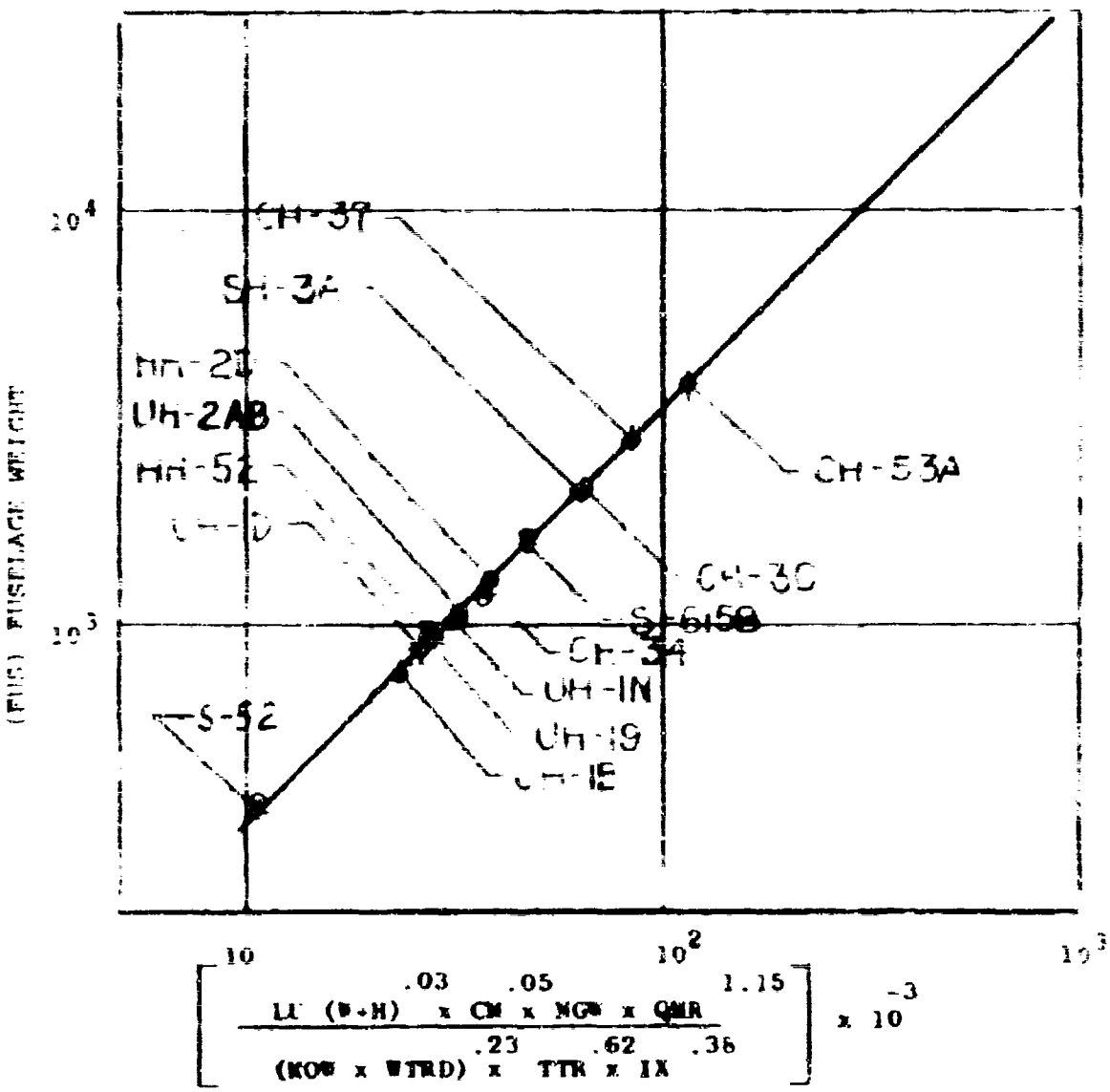

Figure 7-5. Fuselage Weight

FUSELAGE WEIGHT (FUS) (Continued)

NGW = Normal Gross Weight = $2.145 \times MGW^{.893}$

QMR = Main Rotor Torque - Ft-Lbs = 5250 x HP1/RPM

HP1 = Main Rotor Horsepower - Input Parameter

RPM = Main Rotor RPM = 9.549 x VM/RM

VM = Main Rotor Tip Speed - fps - Input Parameter

WTRD = Main Wheel Tread - Feet - If Known, otherwise use $.41 \times W^{1.75}$

TTR = Tail Rotor Thrust - Lbs = HP2/RPM x RM

HP2 = Installed Horsepower - Input Parameter

F_C = .0328 (Constant - Conventional Geared)

AFT FUSELAGE (AFUS)

$$AFUS = .183\left[\frac{LTRP^{.95} \times TAF^{.13} \times FUS^{.64}}{\left(\frac{QMP}{TTP \times LTB}\right)^{.45}}\right]$$

where:

LTRP = Length of the Tail Rotor Pylon - Feet - If Known, otherwise use $1.67 \times RT^{.334}$

RT = Tail Rotor Radius - Feet - If Known, otherwise use $.087 \times RM^{1.22}$

RM = Main Rotor Radius - Feet - Input Parameter

TAF = Type of Aft Fuselage - Values/Configuration See Horizontal Stabilizer (WHS) weight equation

FUS = Fuselage Weight - See Fuselage Weight Equation

QMP = Main Rotor Torque - Ft-Lbs = 5250 x HP1/RPM

HP1 = Main Rotor Horsepower - Input Parameter

RPM = Main Rotor RPM = 9.549 x VM/RM

VM = Main Rotor Tip Speed - fps - Input Parameter

TTP = Tail Rotor Thrust - Lbs = 13392.66 x HP2/RPM x RM

HP2 = Installed Horsepower - Input Parameter

LTB = Length of Tailboom - Feet - If Known, otherwise use $36.07 \times \frac{\lambda}{RM^{.273}}$

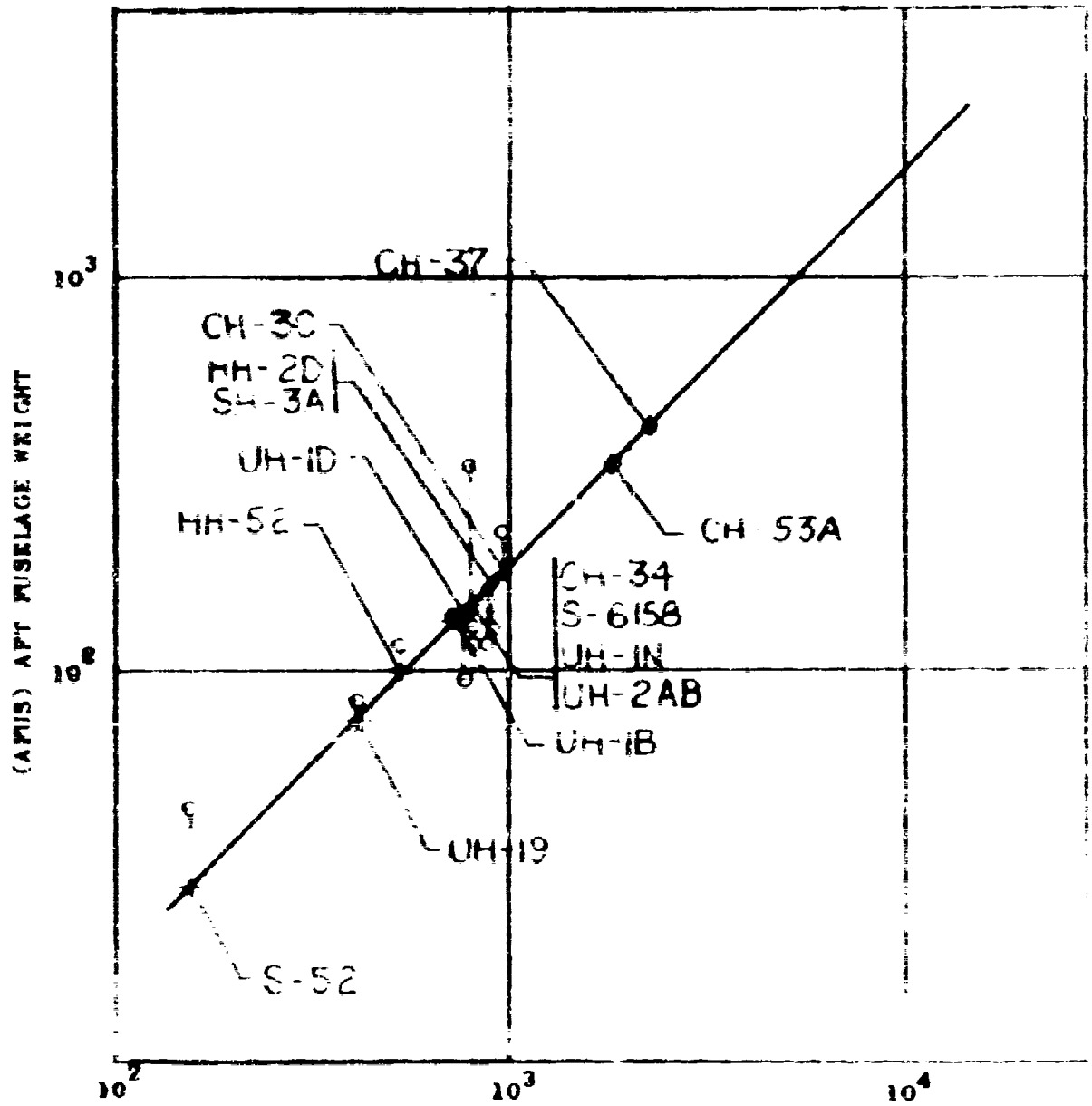

Figure I-6. Aft Fuselage Weight

PYLON WEIGHT (WPY)

$$WPY = .063 \times [PA^{.76} \times TTP^{.42} \times TPY^{.24}]$$

where:

PA = Pylon Profile Area - Sq.Ft - If Known, Otherwise use $.38 (.5\ RT \times LTRP)^{.48} \times TPY^{.74}$

RT = Tail Rotor Radius - Feet - If Known, otherwise use $.067 \times RM^{1.22}$

RM = Main Rotor Radius - Feet - Input Parameter

LTRP = Length of Tail Rotor Pylon - Feet - If Known, otherwise use $1.67 \times RT^{.334}$

TPY = Type of Pylon Configuration - Values/Configuration (depends on type of aft fuselage)

- 14 - Tailcone upswept from fuselage splice. Example: UH1D
- 25 - Tailboom without rear ramp. Example: UH19
- 45 - Tailboom configured for rear ramp. Example: CH53
- 46 - Full fuselage depth at splice of main fuselage to aft fuselage. Example: SH3A
- 62 - Full fuselage depth at splice of main fuselage to aft fuselage and with a tail wheel full aft. Example: HH2D

TTP = Tail Rotor Thrust - Lbs = 13392.66 x HP2/RPM x RM

HP2 = Installed Horsepower - Input Parameter

RPM = Main Rotor RPM = 9.549 x VM/RM

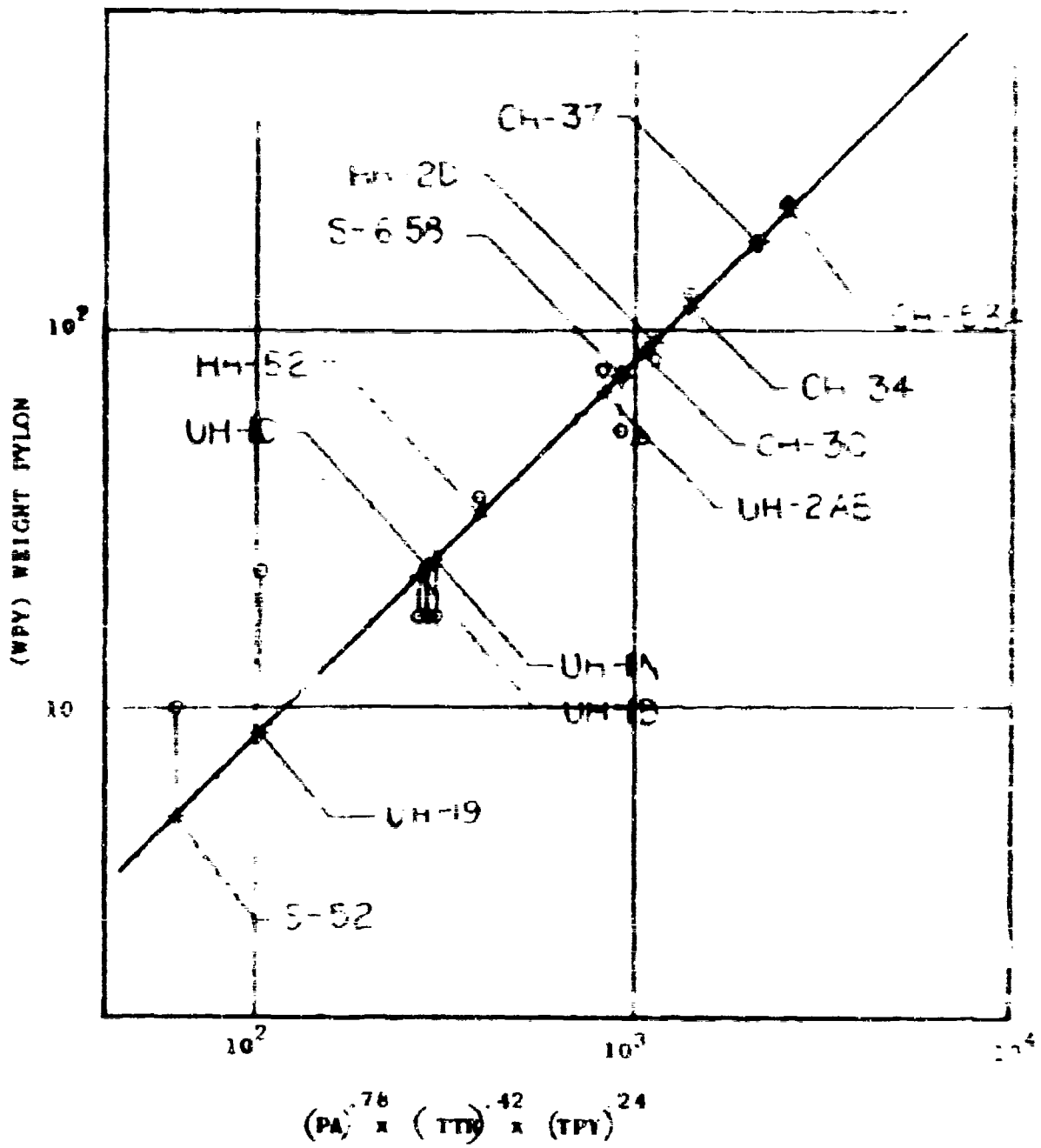

Figure [illegible], Pylon Weight

LANDING GEAR WEIGHT (WLGI)

$$WLGI = .1904 \times \frac{KLG \times MOW^{.67} \times (AG+2)^{.61} \times WTRL^{1.45}}{IX^{.46}}$$

Where:

KLG = Landing Gear Geometry = Values/Configuration

.0157 - Skid Gear

.0247 - Sponson Mounted

.0260 - Quadricycle

.0329 - Tricycle - Fuselage Mounted

.0495 - Crane - Straddle Type

MOW = Maximum Operating Weight - Lbs - Input Parameter

AG = Number of Auxiliary Gear - Input Parameter

WTRL = Main Wheel Tread - Feet - If Known, otherwise use $.41 \times W^{1.75}$

W = Maximum Fuselage Width - Feet - If Known, otherwise use $2.53 \times IX^{.115}$

IX = Aircraft Roll Inertia - Slug-Ft^2 - If Known, otherwise use $.221 \times 10^{-3} \times MOW^{1.807}$

WEIGHT PROVISION FOR RETRACTING LANDING GEAR

11% of WLGI

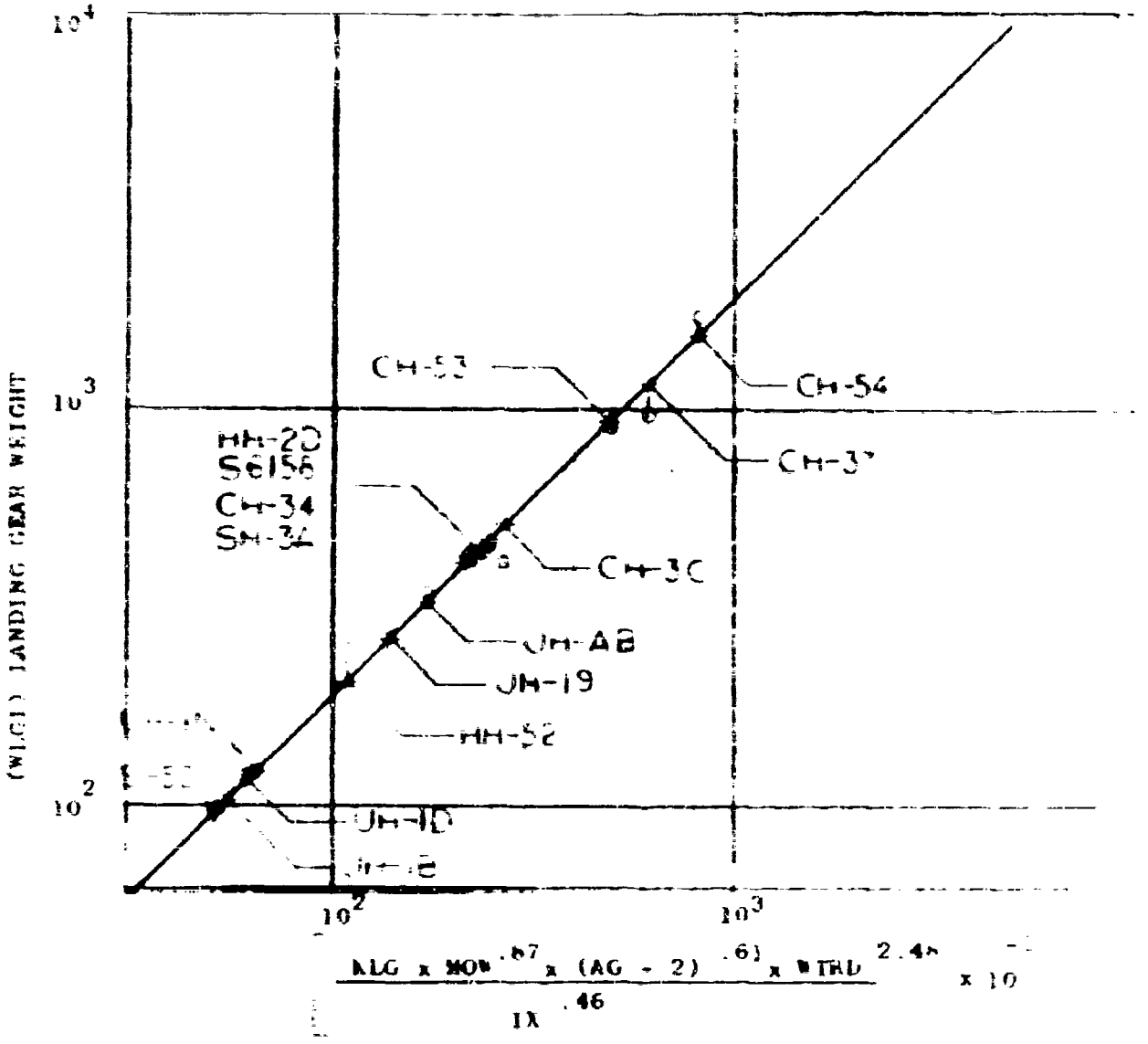

Figure [illegible], Landing Gear Weight

FLIGHT CONTROL WEIGHT (FC)

$$FC = .536 \times 10^{-6} \left[\frac{NWG^{1.07} \times NOF^{.30} \times VM^{1.696} \times NP^{.45}}{LDIA^{.69}} \right]$$

where:

NWG = Normal Gross Weight = $2.145 \times MOW^{.893}$

MOW = Maximum Operating Weight - Lbs - Input Parameter

NOF = Effective Number of Rotor Blades = $14.259 \times S^{.409}$

S = Solidity - Input Parameter

VM = Main Rotor Tip Speed - fps - Input Parameter

NP = Number of Main Rotors - Input Parameter

LDIA = Distance From ℄ Tail Rotor to Cockpit Control Groupings - Feet - If Known, otherwise use $1.717 \times RM^{1.005}$

RM = Main Rotor Radius - Feet - Input Parameter

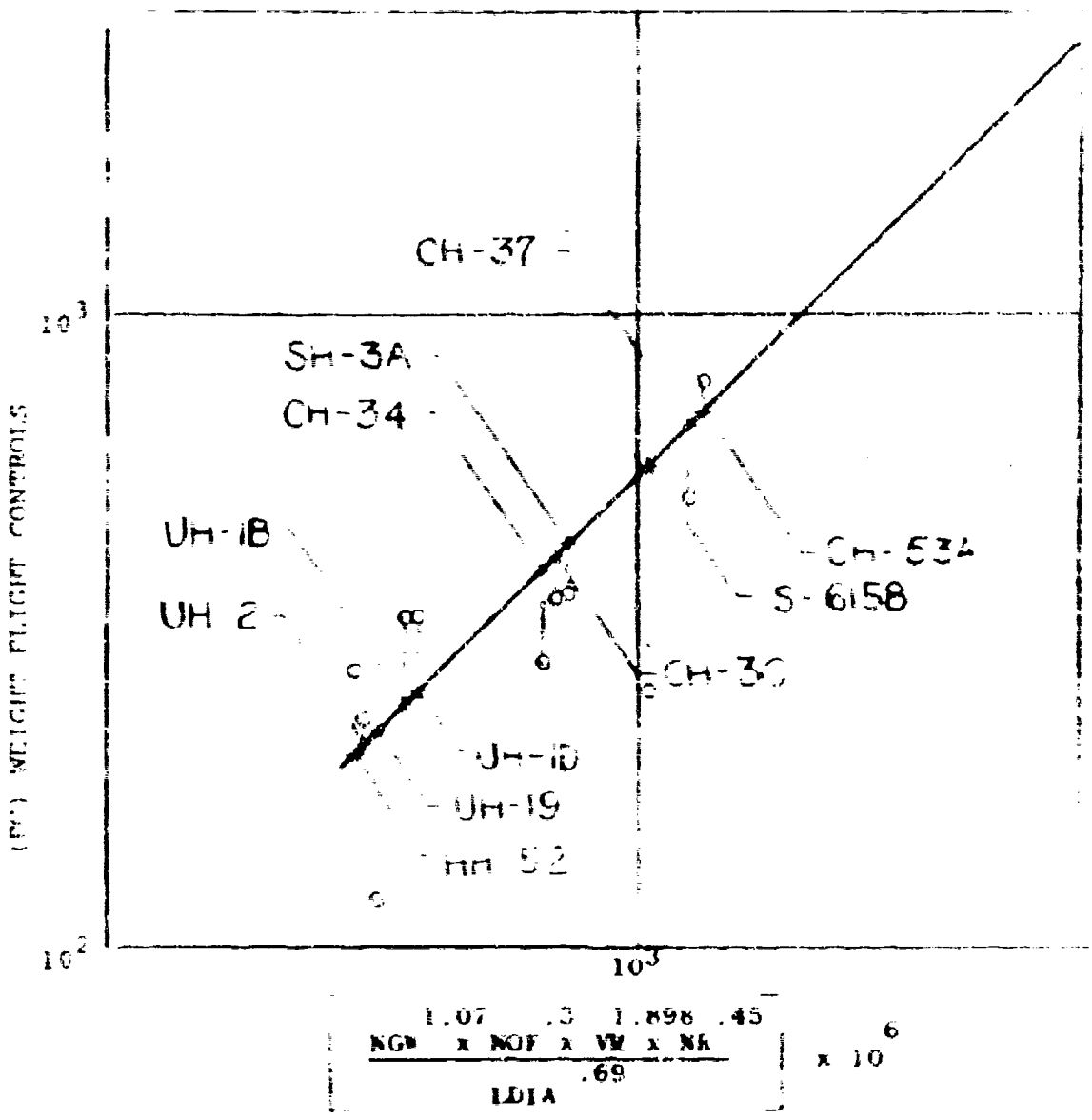

$$\left[\frac{NG^{1.07} \times NOF^{.3} \times VK^{1.898} \times NR^{.45}}{LDIA^{.69}}\right] \times 10^{6}$$

Figure [illegible]. Flight Controls Weight

ENGINE SECTION WEIGHT (WES) (Weight of Engine Nacelle and Engine Mounts)

$$WES = .068 \times \left[\frac{KNAC \times (FUS+WAF+WPY)^{.25} \times (WENG/ENF)^{1.06} \times VN^{.61}}{HP2^{.55}}\right]$$

where:

KNAC = Nacelle Arrangement = Values/Configuration

- .96 - Twin engines mounted to transmission forward or aft of main rotor.
- 1.19 - Single engine mounted to fuselage forward or aft of main rotor.
- 1.23 - Twin engines with combining gearbox.
- 2.26 - Twin engines outboard of main fuselage.

Add factors for more than two engines.

FUS = Fuselage Weight - See Weight Equation

WAF = Aft Fuselage Weight - See Weight Equation

WPY = Pylon Weight - See Weight Equation

WENG = Total Engine Weight - Input Parameter

ENF = Effective Number of Engines = $.279 \times HP2^{.235}$

VN = Nacelle Volume - Cu.Ft. - If Known, otherwise use $26.5 \times HP2^{.257} \times ENF^{.370}$

HP2 = Installed Horsepower - Input Parameter

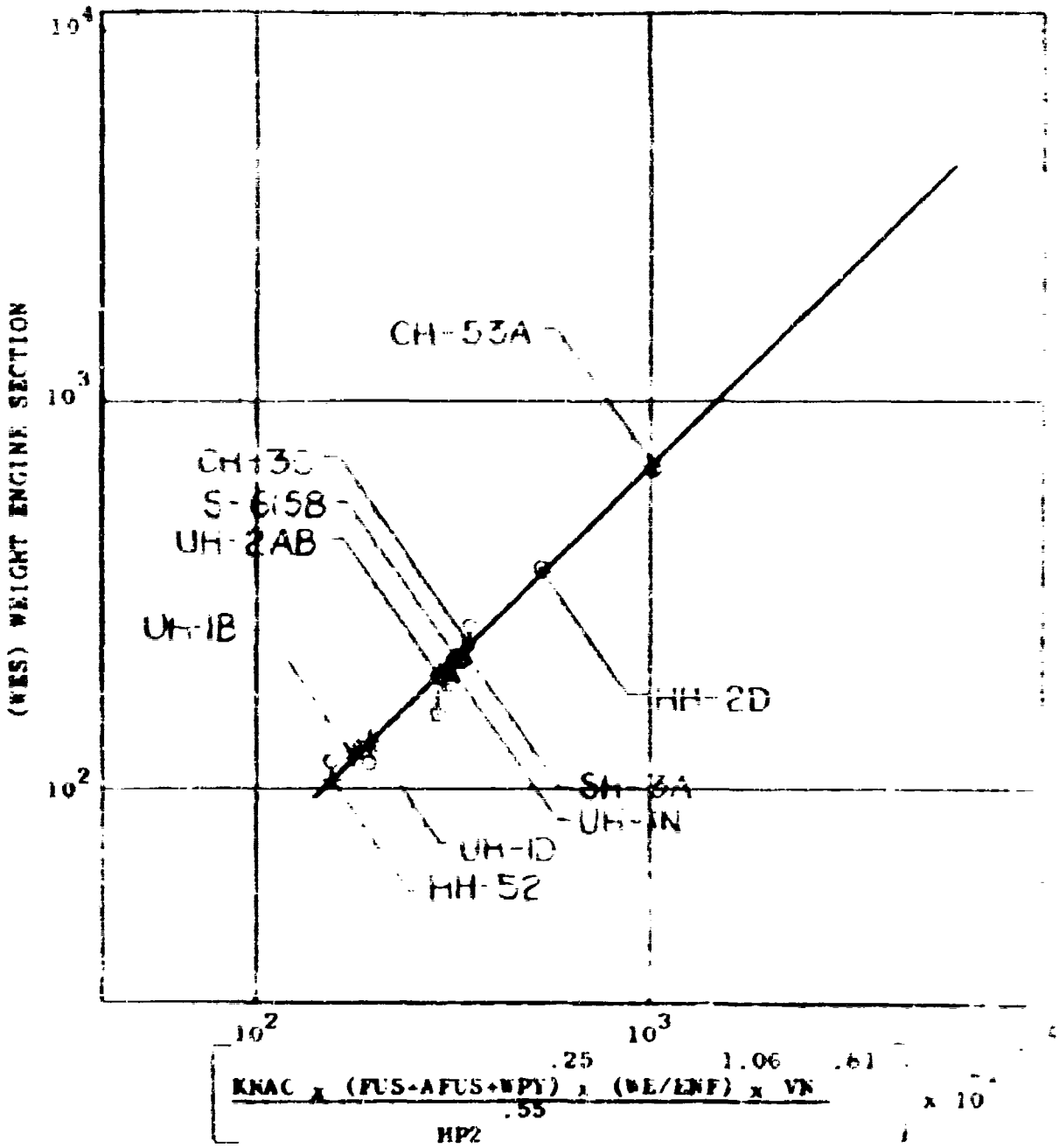

Figure 3-10. Engine Section Weight

PROPULSION GROUP - LESS ENGINE AND FUEL SYSTEM (WPTS)

$$WPTS = .434 \times 10^{-3} \times \left[\frac{DMNP^{1.62} \times NOF^{1.69} \times 1.23RM^{3.67}}{QMR1^{.66} \times RR^{.14}}\right]$$

Where:

DMNP = Disc Loading x Number of Main Rotors

DM = Disc Loading = $MOW/\pi RM^2$

MOW = Maximum Operating Weight - Lbs - Input Parameter

RM = Main Rotor Radius - Feet - Input Parameter

NR = Number of Main Rotors - Input Parameter

NOF = Effective Number of Rotor Blades = $24.259 \times S^{.409}$

S = Solidity - Input Parameter

QMR1 = Main Rotor Torque/100 = 52.50 x HP1/RPM

HP1 = Main Rotor Horsepower - Input Parameter

RPM = Main Rotor RPM = 9.549 x VM/RM

VM = Main Rotor Tip Speed - fps - Input Parameter

RR = Main Transmission Reduction Ratio - If Known, otherwise use $.2157 \times 10^3 \frac{1}{RPM^{.174}}$

NOTE: The Propulsion Group is derived by using individual equations for each item. WPTS value is furnished for information and is used as an intermediate parameter in deriving lubricating system and engine driveshaft weight.

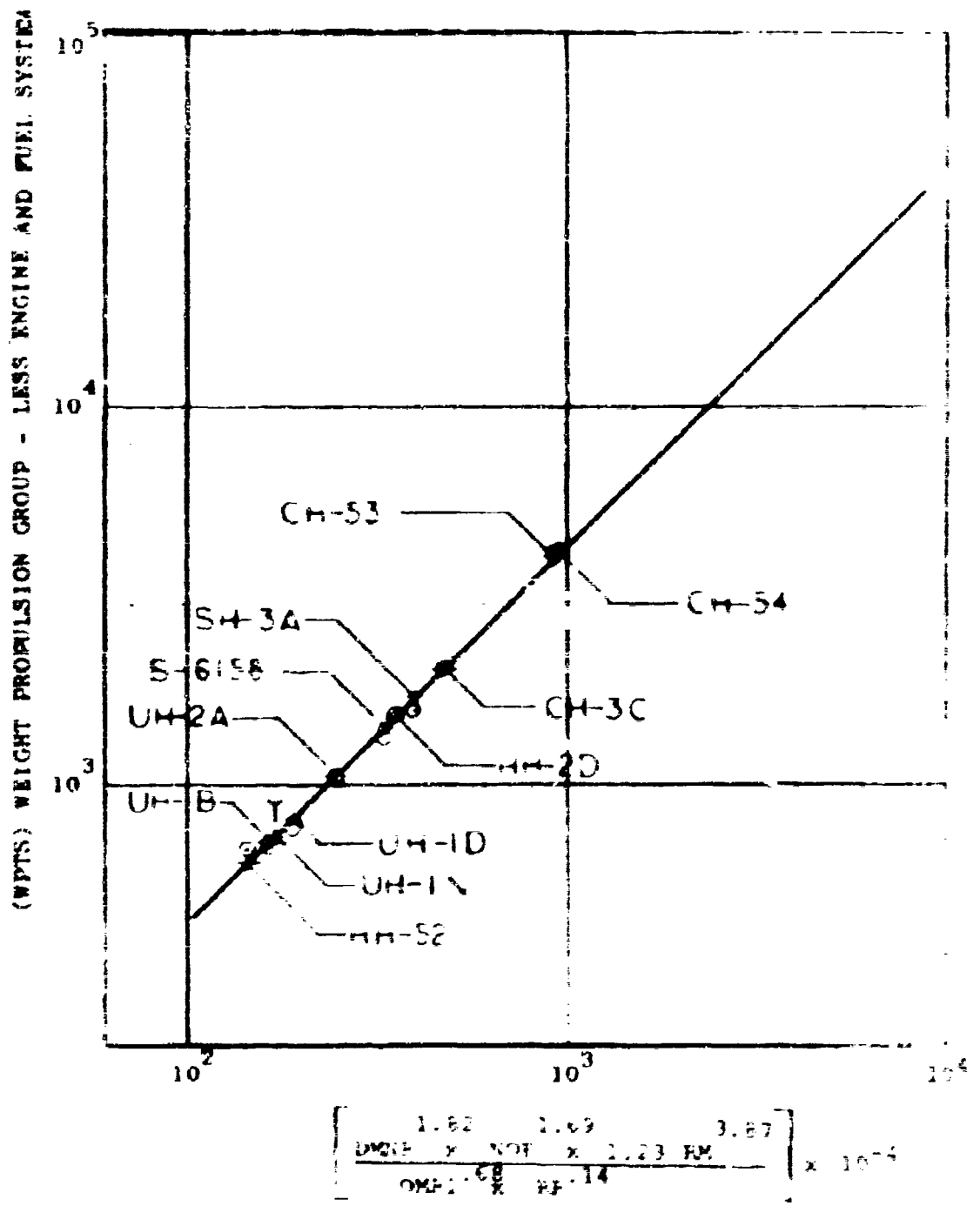

Figure 3-11. Propulsion Group Weight Less Engine and Fuel System Weight

ENGINE ACCESSORY WEIGHT (WEAC) (Engine Inlet and Exhaust Ductwork)

$$WEAC = .016\left[\frac{EN^{.06} \times WENG^{1.93}}{HP2^{.59}}\right]$$

EN = Number of Engines - Input Parameter

WENG = Total Engine Weight - Lbs - Input Parameter

HP2 = Installed Horsepower - Input Parameter

Distribution:

Induction System	53% WEAC
Exhaust System	47% WEAC

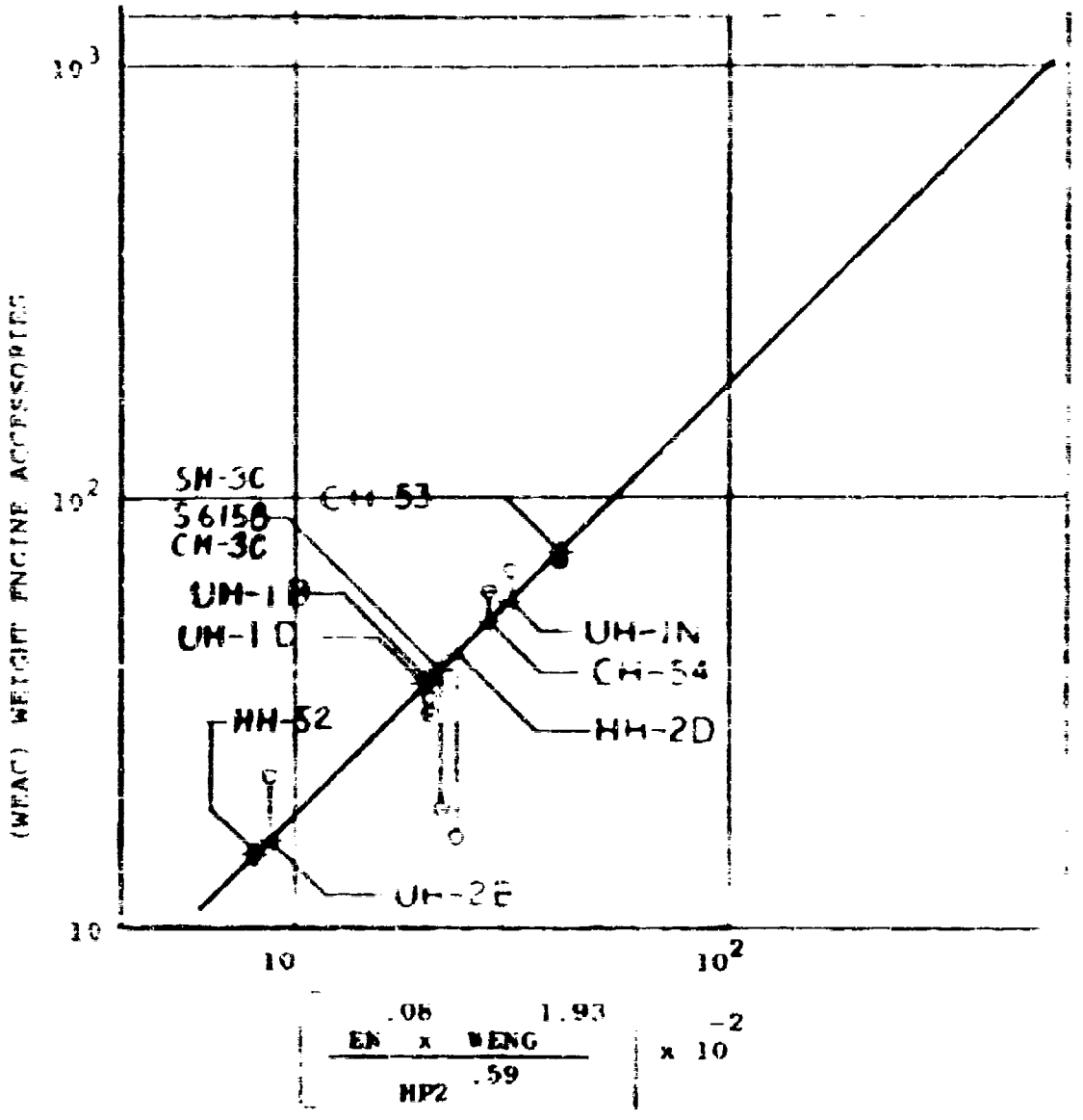

Figure 7-12. Engine Accessories Weight

LUBRICATING SYSTEM (WLS)

$$WLS = K \times \left\{ \frac{RR^{.5} \times (WTS)^{1.95} \times (CAP)^{.44}}{HP^{1.15}} \right\}$$

where:

RR = Main Transmission Reduction Ratio, If Known, otherwise use $.2157 \times 10^{3} \frac{1}{RPM^{1.174}}$

RPM = Main Rotor RPM

WTS = Weight of Propulsion Group Less Engine and Fuel System, See Weight Equation

WTS = .45 WPTS

CAP = Capacity of Fuel System - Gallons - Input Parameter

HP = Installed Horsepower - Input Parameter

K = .0021 for Engine and Transmission System

The distribution between engine and transmission lubrication system was taken as follows:

1. Engine Lub

$K_E = .00126$

2. Transmission Lub

$K_T = .00084$

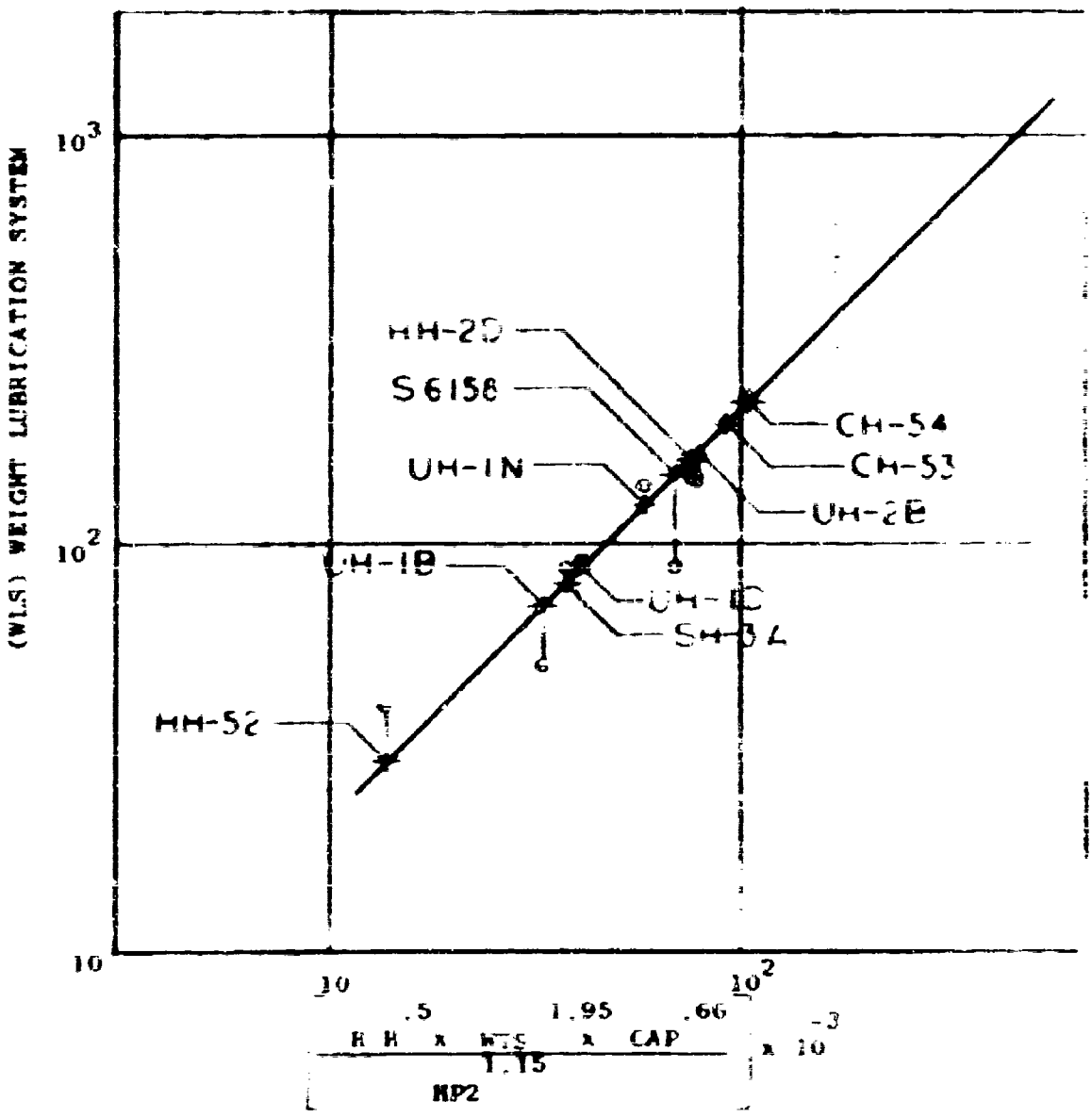

Figure 1-17. Lubrication System Weight

COOLING SYSTEM WEIGHT

WCS = .25 x WLS

WLS = Weight of Lubricating System

The distribution between basic engine and transmission cooling was taken as follows:

1. Engine Cooling = .15 x WLS
2. Transmission Cooling = .10 x WLS

Note: Graph omitted.

FUEL SYSTEM (WFS)

$WFS = 3.6 \times CAP^{.71}$

CAP = Capacity of Fuel System - Gallons - Input Parameter

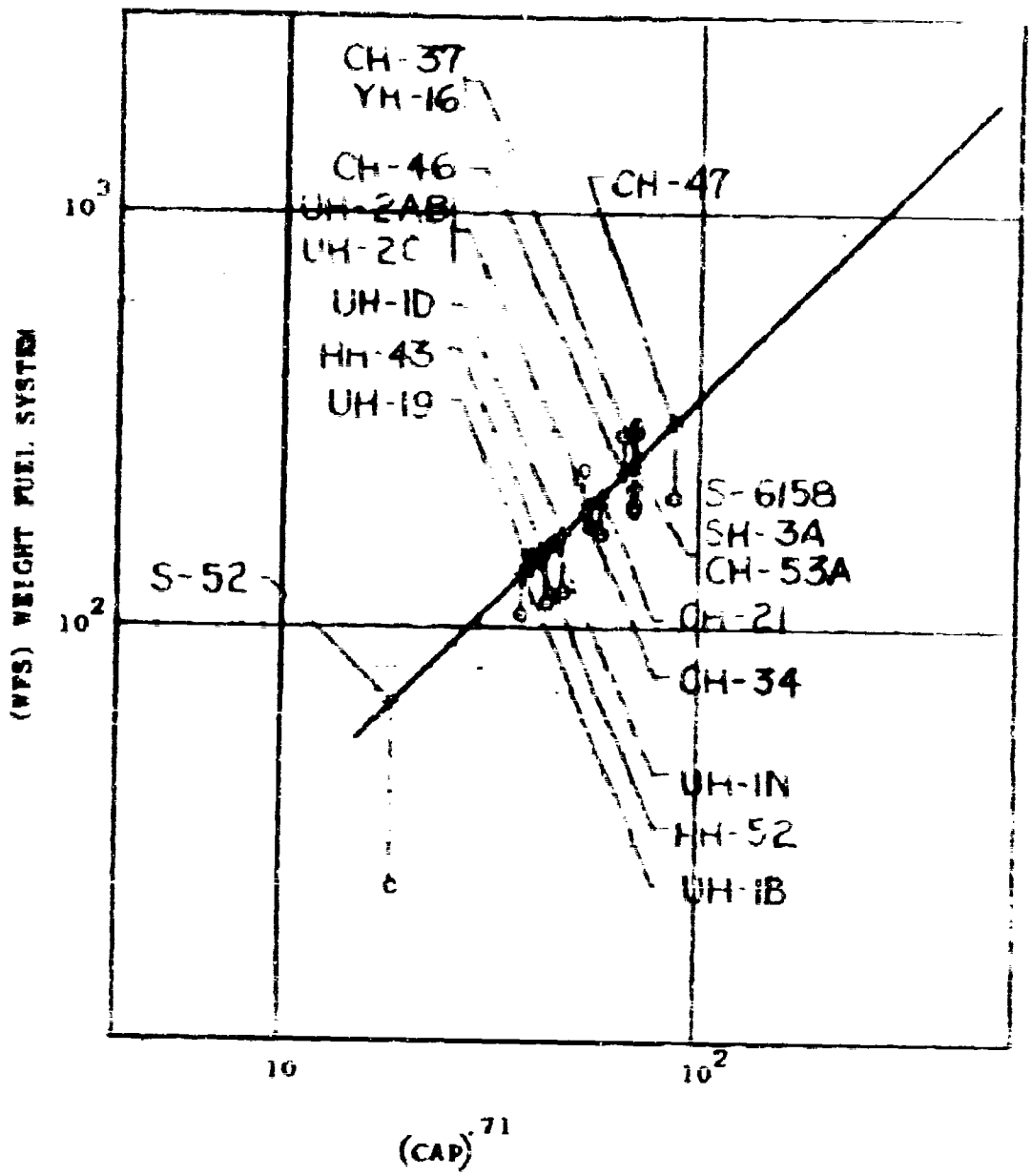

Figure I-14. Fuel System Weight

ENGINE CONTROLS (WEC)

$$WEC = 3.75 \times ENP^{1.63} \times .3RM^{.61}$$

where:

ENP = Effective Number of Engines = $.279 \times HP2^{.235}$

HP2 = Installed Horsepower - Input Parameter

RM = Main Rotor Radius - Feet - Input Parameter

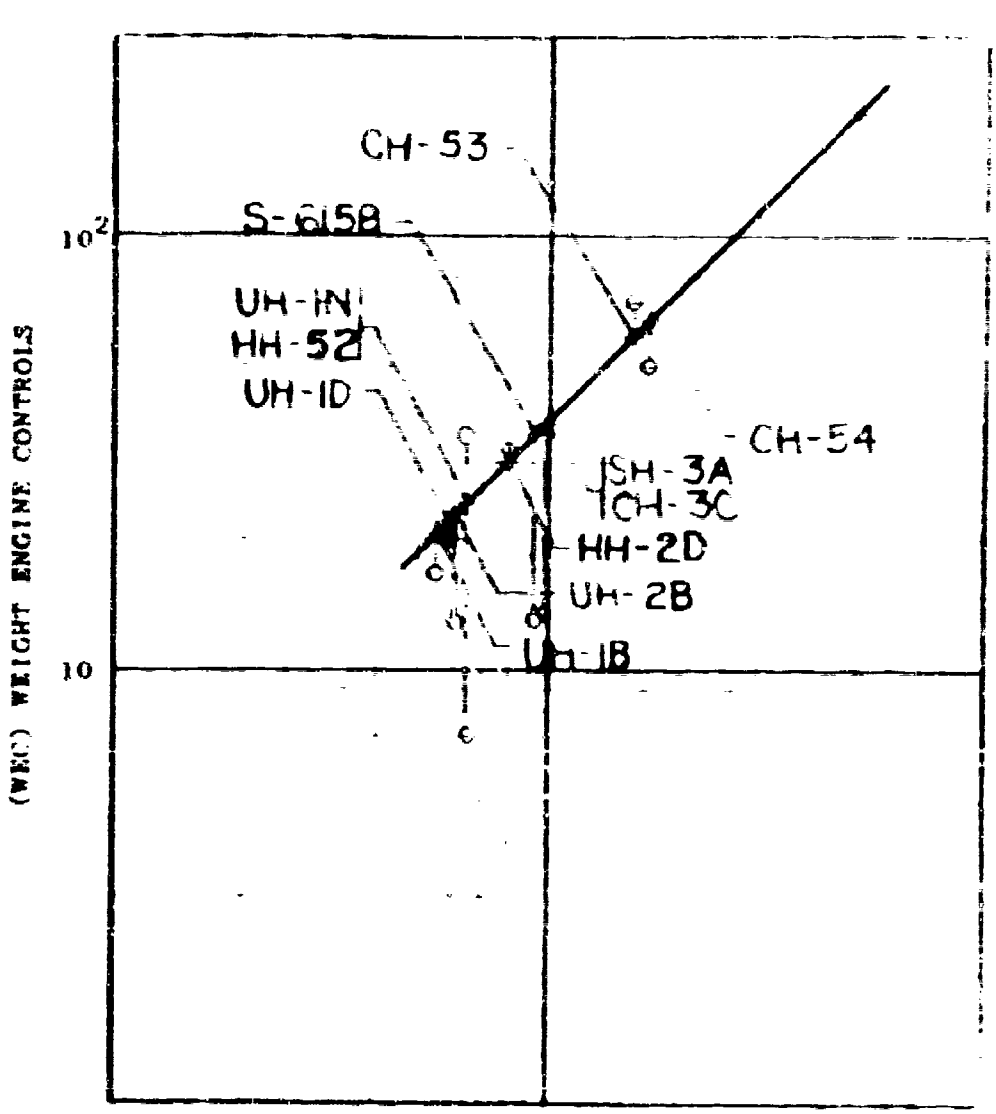

Figure I-13. Engine Controls Weight

STARTING SYSTEM (WSS)

$$WSS = 3.16 \times \left(\frac{SHP}{HP2}\right)^{1.1} \times \left(\frac{WENG}{ENF}\right)^{1.37}$$

where:

SHP = Total Starting Horsepower = $.0245 \times HP2^{.637}$

HP2 = Installed Horsepower - Input Parameter

WENG = Total Engine Weight - Lbs - Input Parameter

ENF = $.279 \times HP2^{.235}$

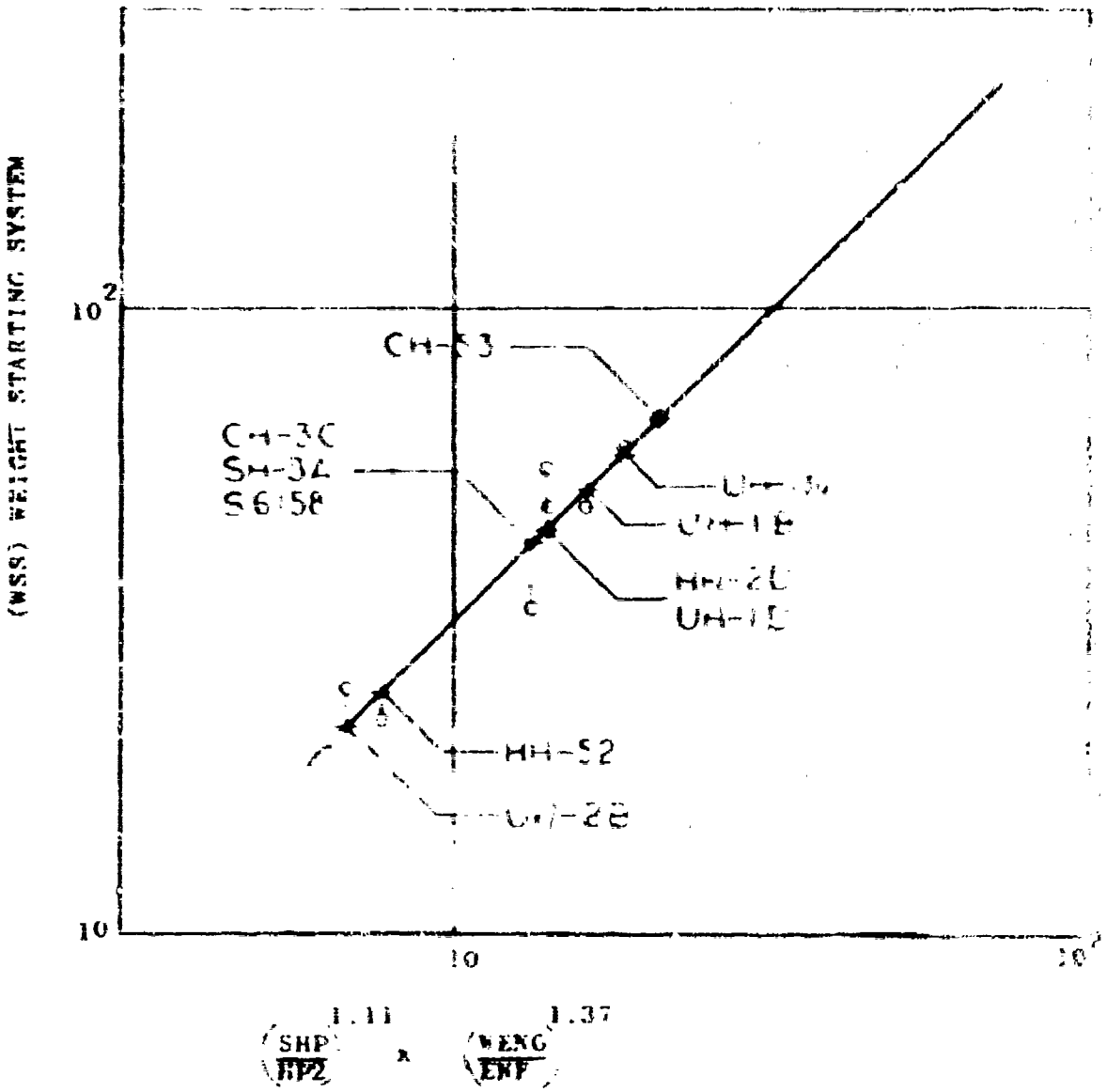

Figure 3-14. Starting System Weight

MAIN TRANSMISSION (WXS1), including Rotor Shaft Weight

$WXS1 = 0.2815 \times [QMR5^{.75}]$

QMR5 = Installed Power Converted to Torque in Ft-Lbs at Rotor RPM = 5250 x HP2/RPM

HP2 = Installed Horsepower - Input Parameter

RPM = Main Rotor RPM = 9.549 x VM/RM

VM = Main Rotor Tip Speed - fps - Input Parameter

RM = Main Rotor Radius - Feet - Input Parameter

Rotor Shaft Weight = 18% WXS1

ACCESSORY DRIVE PROVISION (ACPV)

$ACPV = .01278 \times QMR^{.766}$

QMR = Main Rotor Torque - Ft-Lbs = 5250 x HP1/RPM

HP1 = Main Rotor Horsepower - Input Parameter

RPM = Main Rotor RPM = 9.549 x VM/RM

VM = Main Rotor Tip Speed - fps - Input Parameter

RM = Main Rotor Radius - Feet - Input Parameter

Note: Graph Omitted

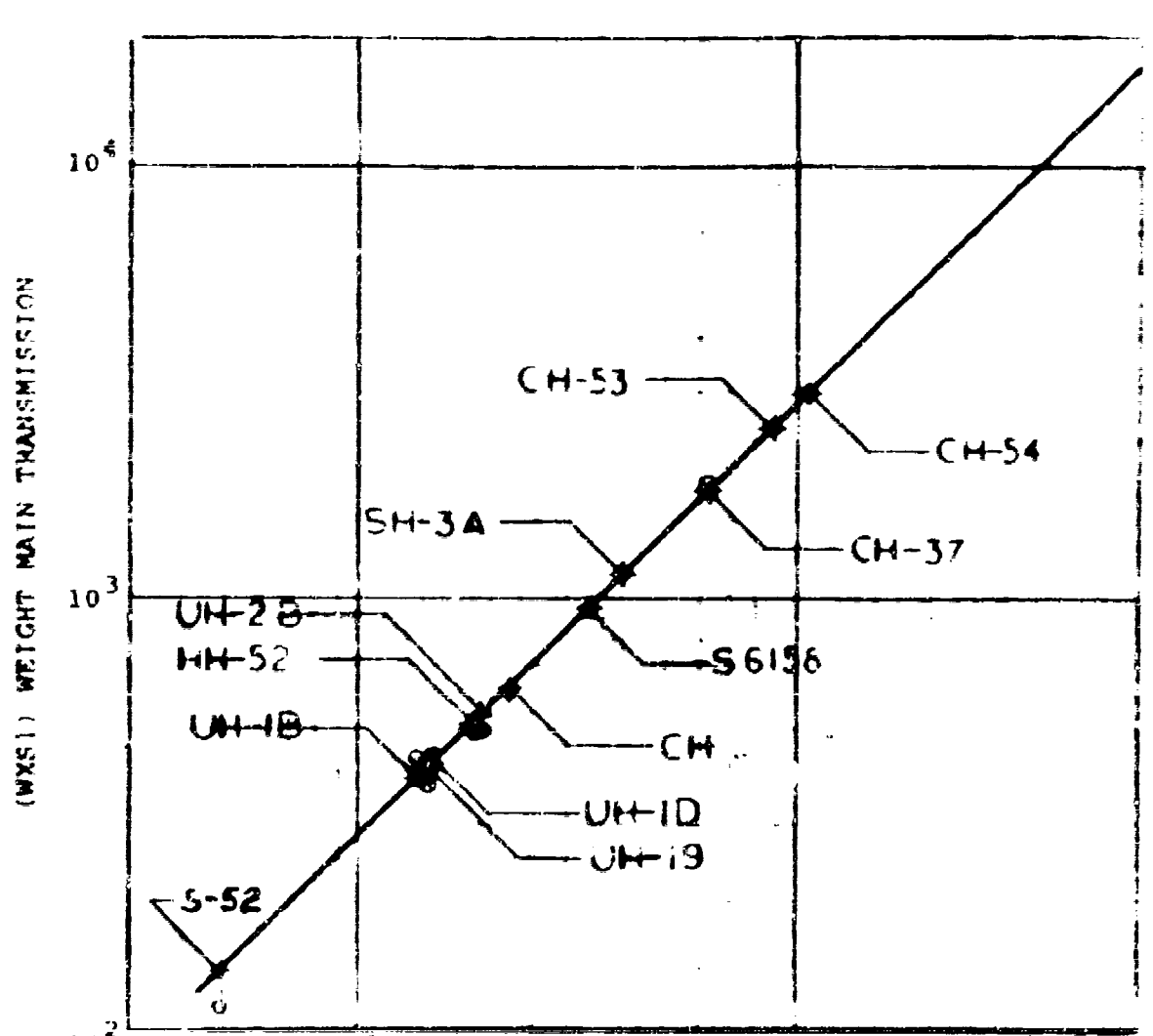

Figure 1-17. Main Transmission Weight

INTERMEDIATE TAIL ROTOR GEARBOX (WITR)

$$WITR = K \times QMR2^{.625}$$

QMR2 = .07 x QMR

QMR = Main Rotor Torque - Ft-Lbs = 5250 x HP1/RPM

HP1 = Main Rotor Horsepower - Input Parameter

RPM = Main Rotor RPM = 9.549 x VM/RM

VM = Main Rotor Tip Speed - fps - Input Parameter

RM = Main Rotor Radius - Feet - Input Parameter

K = .2298 Constant - Statistical Baseline

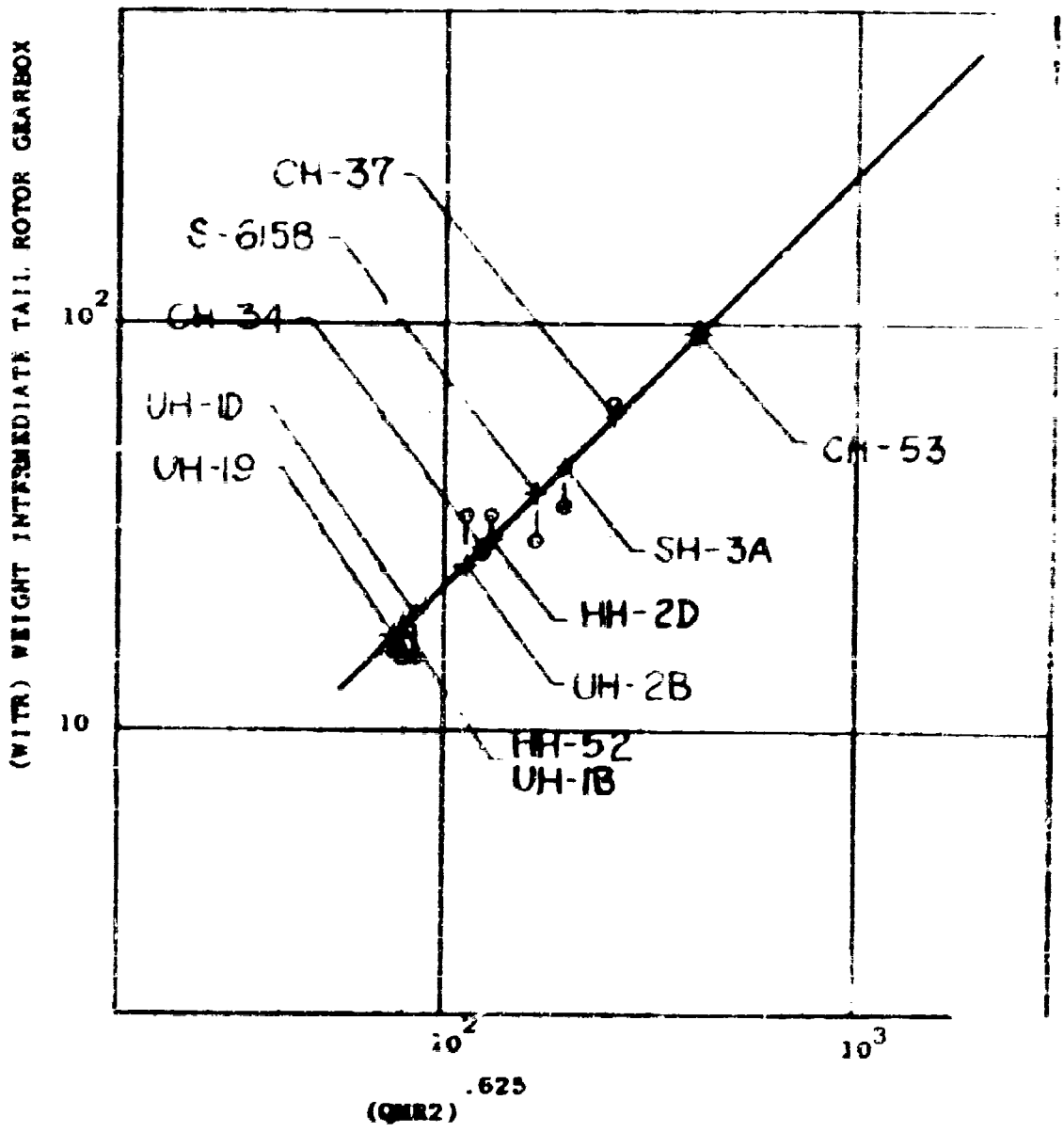

Figure 1-18. Intermediate Tail Rotor Gearbox Weight

TAIL ROTOR GEARBOX (WTRE)

$$WTRE = K \times (QMR3)^{.66}$$

QMR3 = .15 x QMR

QMR = Main Rotor Torque - Ft-Lbs = 5250 x HP1/RPM

HP1 = Main Rotor Horsepower - Input Parameter

RPM = Main Rotor RPM = 9.549 x VM/RM

VM = Main Rotor Tip Speed - fps - Input Parameter

RM = Main Rotor Radius - Feet - Input Parameter

K = .2279 Constant - Statistical Baseline

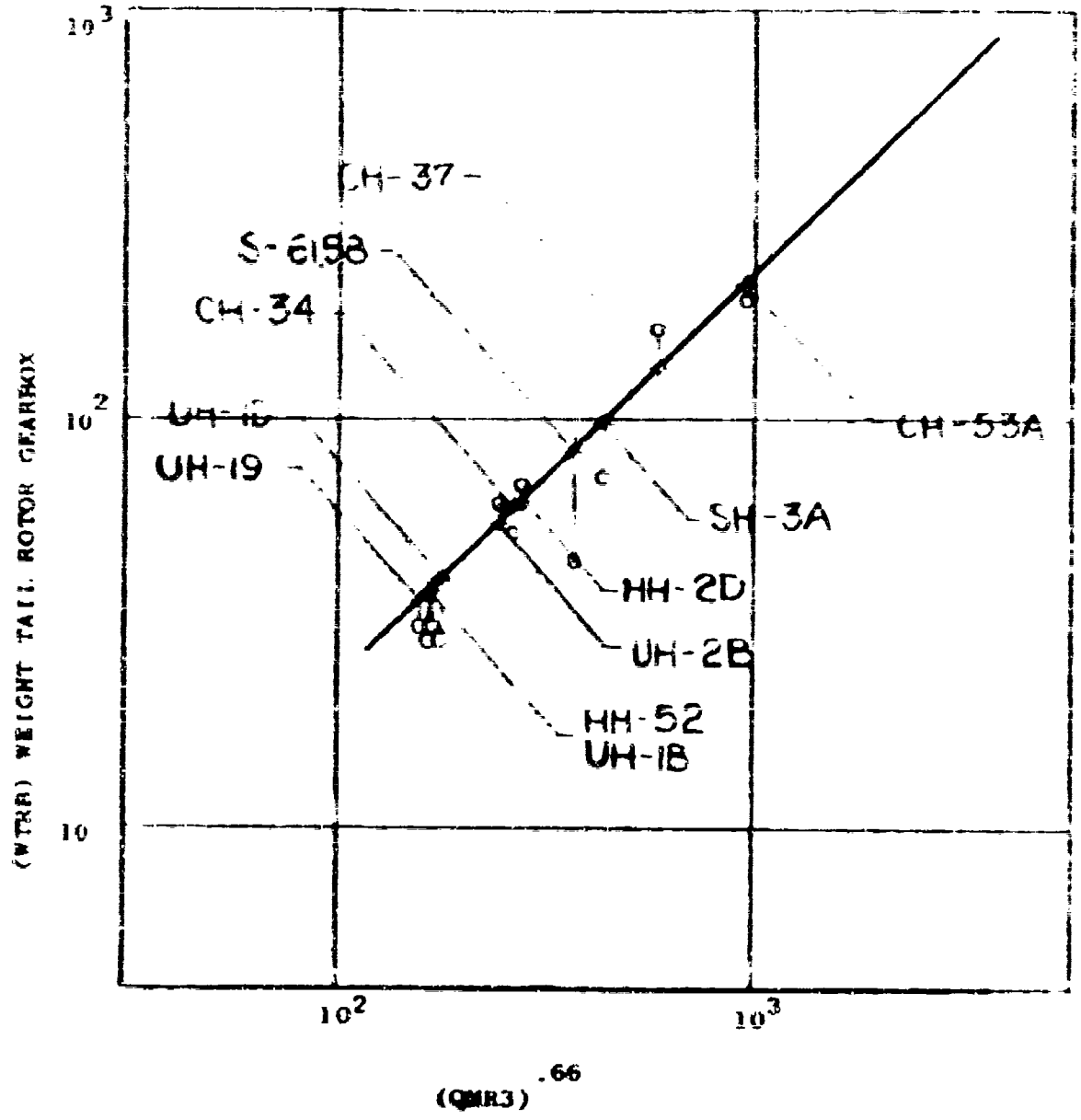

Figure 1-19. Tail Rotor Gearbox Weight

TAIL ROTOR DRIVE SHAFTING (WTRS)

$$WTRS = F \times 10^{-2} (QMR3^{.31} \times (1.23 \ RM)^{1.64})$$

QMR3 = .15 x QMP

QMP = Main Rotor Torque - Ft-lbs = 5250 x HP1/RPM

HP1 = Main Rotor Horsepower - Input Parameter

RPM = Main Rotor RPM = 9.549 x VM/RM

VM = Main Rotor Tip Speed - fps - Input Parameter

RM = Main Rotor Radius - Feet - Input Parameter

F = .658 Constant - Statistical Baseline

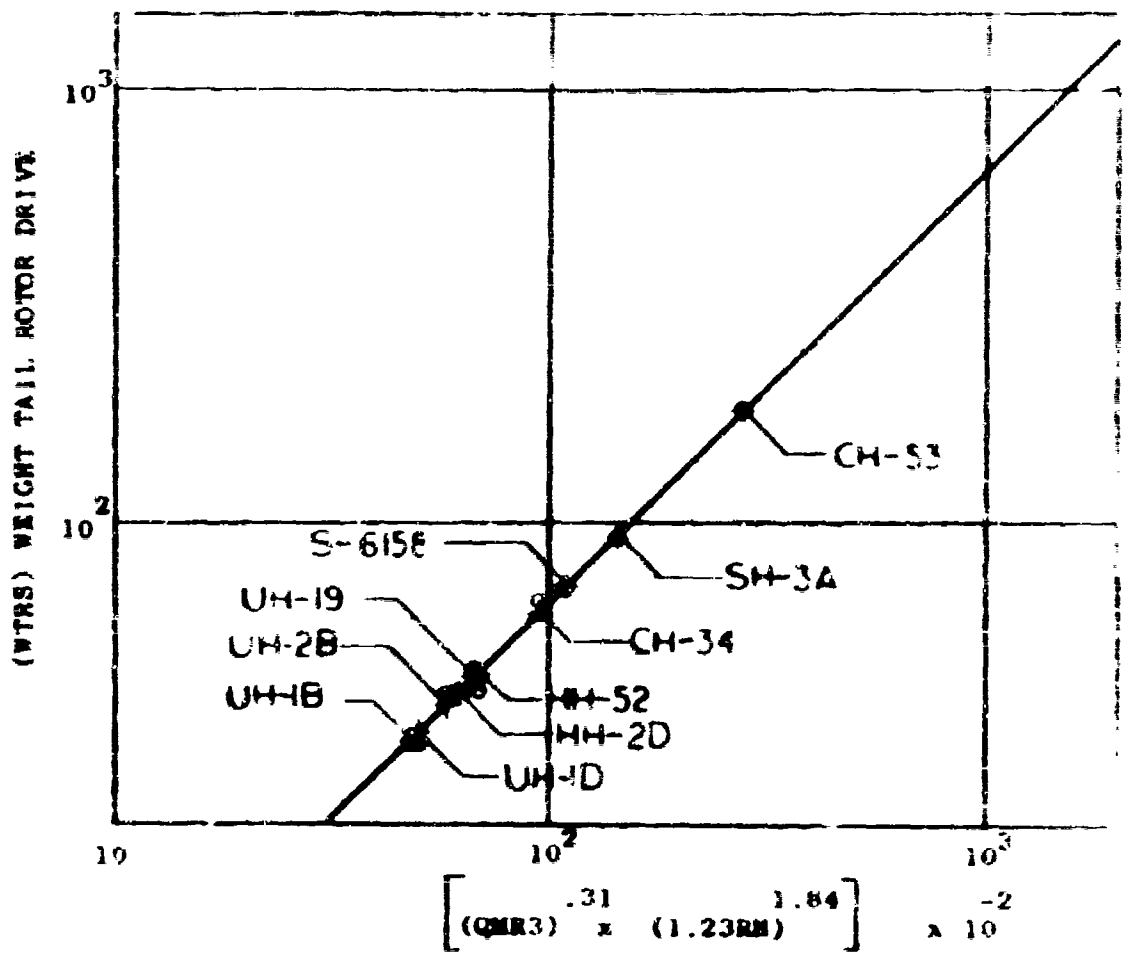

Figure 2-19. Tail Rotor Drive Weight

ENGINE DRIVE SHAFT (WEDS)

$$WEDS = 6.02 \left[\frac{WTS^{1.14}}{WENG^{.23}} \times \frac{EN^{1.4}}{HP1^{.67}} \right]$$

WTS = .45 WPTS

WPTS = Weight of Propulsion Group - Less Engine and Fuel System Weight - See Weight Equation

EN = Number of Engines - Input Parameter

WENG = Total Engine Weight - Input Parameter

HP1 = Main Rotor Horsepower - Input Parameter

ROTOR SHAFT

Rotor Shaft weight is included in the Main Transmission Weight in the WXSI equations. Rotor Shaft weight is taken as 10% of WXSI. Refer to Helicopter Main Transmission Section of this report for Rotor Shaft Weight calculation based on torsion or bending.

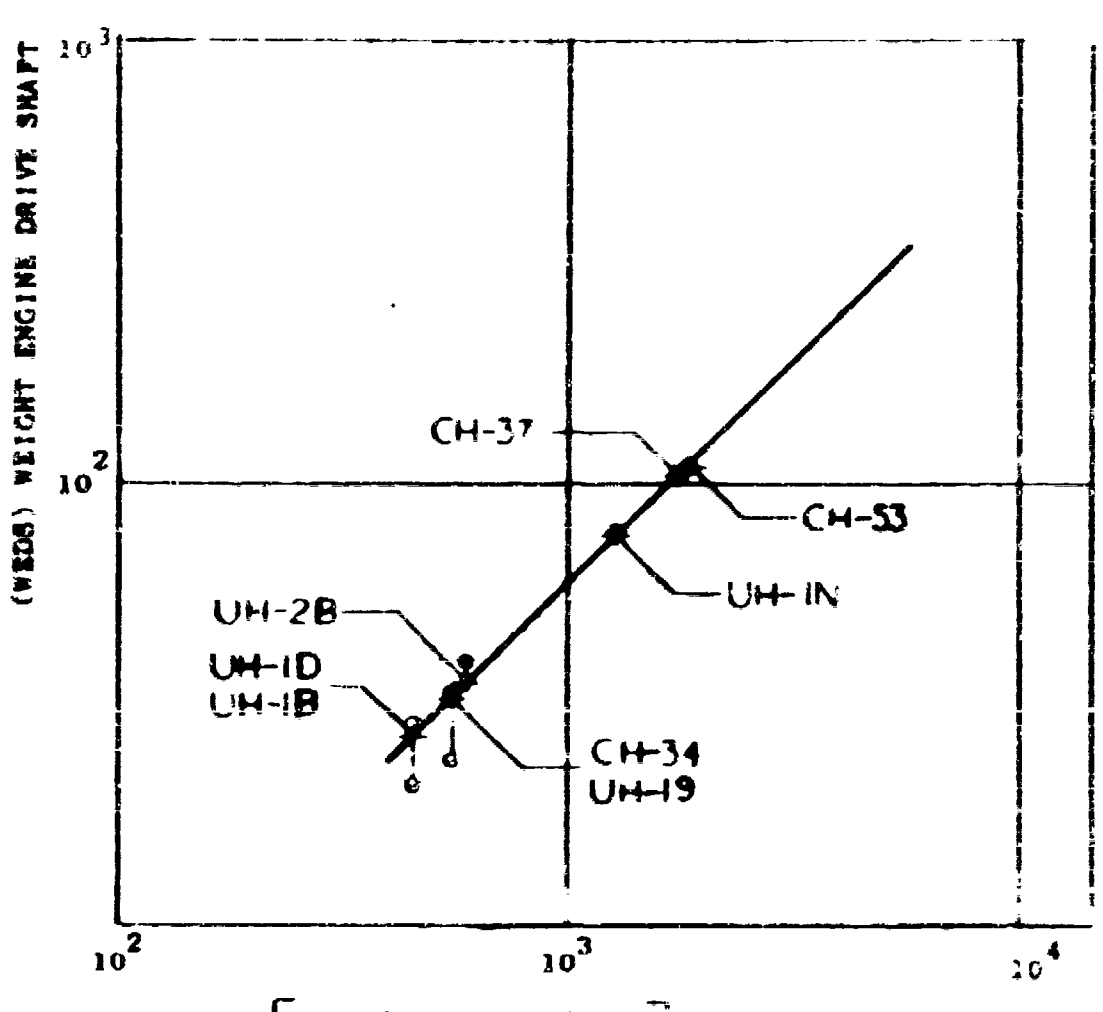

$$\left[\frac{WTS^{1.14} \times HP^{1.4}}{WRMG^{.22} \times RPI^{.67}}\right] \times 10^2$$

Figure I-21. Engine Driveshaft Weight

ROTOR BRAKE (WRB)

$$WRB = .219 \times [QMR^{.44} \times DPM^{.10}]$$

QMR = Main Rotor Torque - Ft-Lbs = 5250 x HP1/RPM

HP1 = Main Rotor Horsepower - Input Parameter

RPM = Main Rotor RPM = 9.549 x VM/RM

VM = Main Rotor Tip Speed - fps - Input Parameter

RM = Main Rotor Radius - Feet - Input Parameter

DPM = Main Rotor Polar Inertia - Slug-Ft^2 - If Known, otherwise use = $\frac{WBL \times RM^2}{9273.6}$

WBL = Main Rotor Blade Weight - Lbs - See Blade Weight Equation

AUXILIARY POWER PLANT GROUP (APU)

$$APU = 46.92 \times ACPV^{.0998}$$

ACPV = Transmission Accessory Provisions = .01276 x QMR$^{.764}$

QMR = Main Rotor Torque - Ft-Lbs = 5250 x HP1/RPM

HP1 = Main Rotor Horsepower - Input Parameter

RPM = Main Rotor RPM = 9.549 x VM/RM

VM = Main Rotor Tip Speed - fps - Input Parameter

RM = Main Rotor Radius - Feet - Input Parameter

Note: Graph Omitted

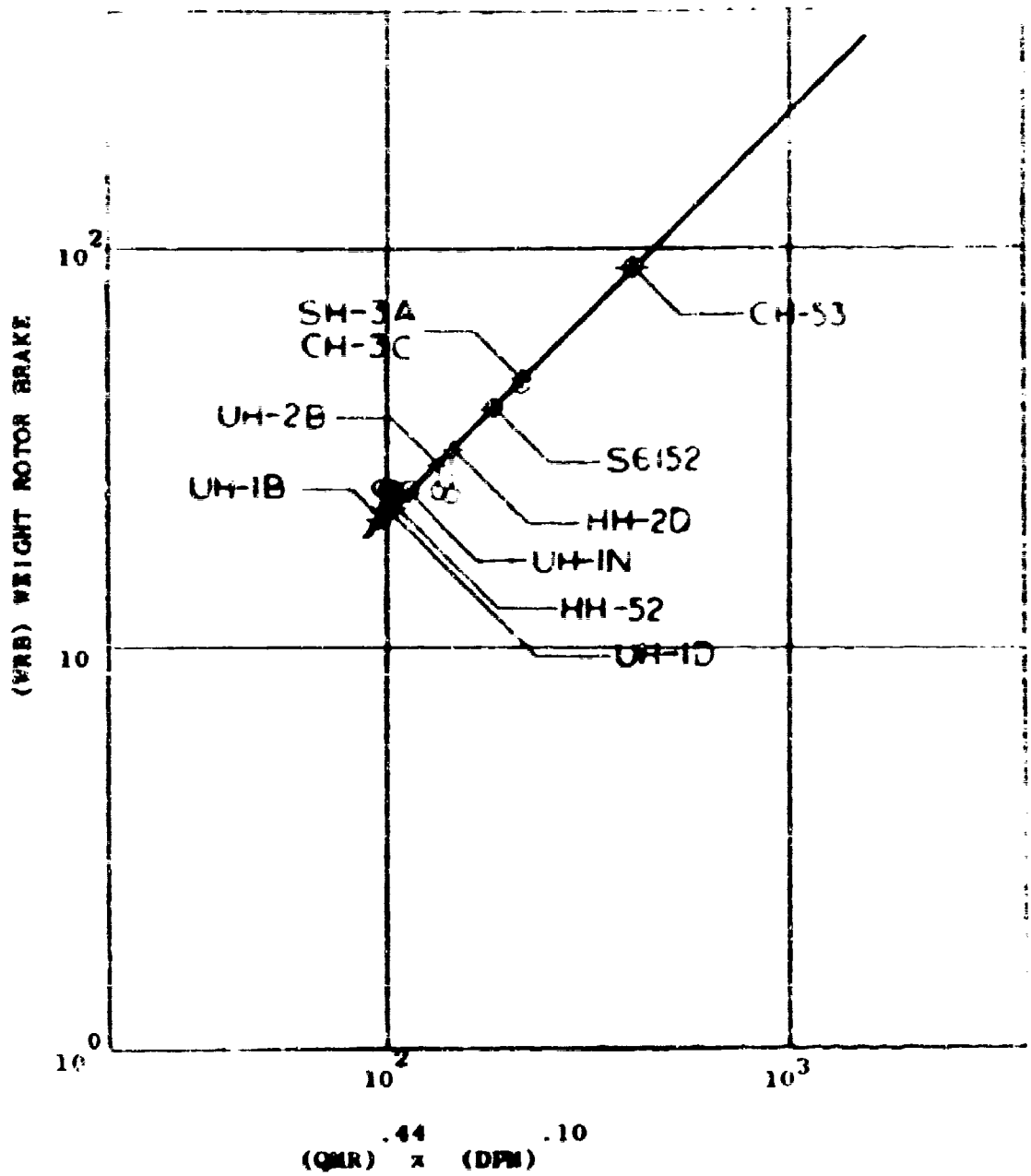

Figure I-22. Rotor Brake Weight

FIXED WEIGHT (WFIX)

$$WFIX = .176 \times 10^{5} \left(\frac{(C+P)^{.32} \times (LU(W+H))^{.14} \times CM^{.04} \times RM^{2.6}}{MOW^{.62}} \right)$$

C+P = Crew + Passengers - If Known - Otherwise use $.035 \times MOW^{.65}$

MOW = Maximum Operating Weight - Lbs - Input Parameter

LU = Usable Fuselage Length - Feet - If Known, otherwise use $.295 \times RM^{1.474}$

RM = Main Rotor Radius - Feet - Input Parameter

W = Maximum Fuselage Width - Feet - If Known, otherwise use $2.53 \times IX^{.115}$

IX = Aircraft Roll Inertia - Slug-Ft^2 - If Known, otherwise use $.221 \times 10^{-3} \times MOW^{1.867}$

H = Maximum Fuselage Height - Feet - If Known, otherwise use $.406(LDIA \times SIN\ell)^{1.226}$

LDIA x SINℓ =

LDIA = Distance From ℄ Tail Rotor to Cockpit Control Grouping - Feet

SINℓ = Sine of Angle at Intersection Between LDIA and Aircraft Water Line

If LDIA SINℓ is not known, use $.961 \times RM^{.743}$

CM = Major Structural Cutouts, If Known, Otherwise use $1.3t \times MOW^{.172}$ (See Fuselage Weight Equation for Weighted Values of Cutouts)

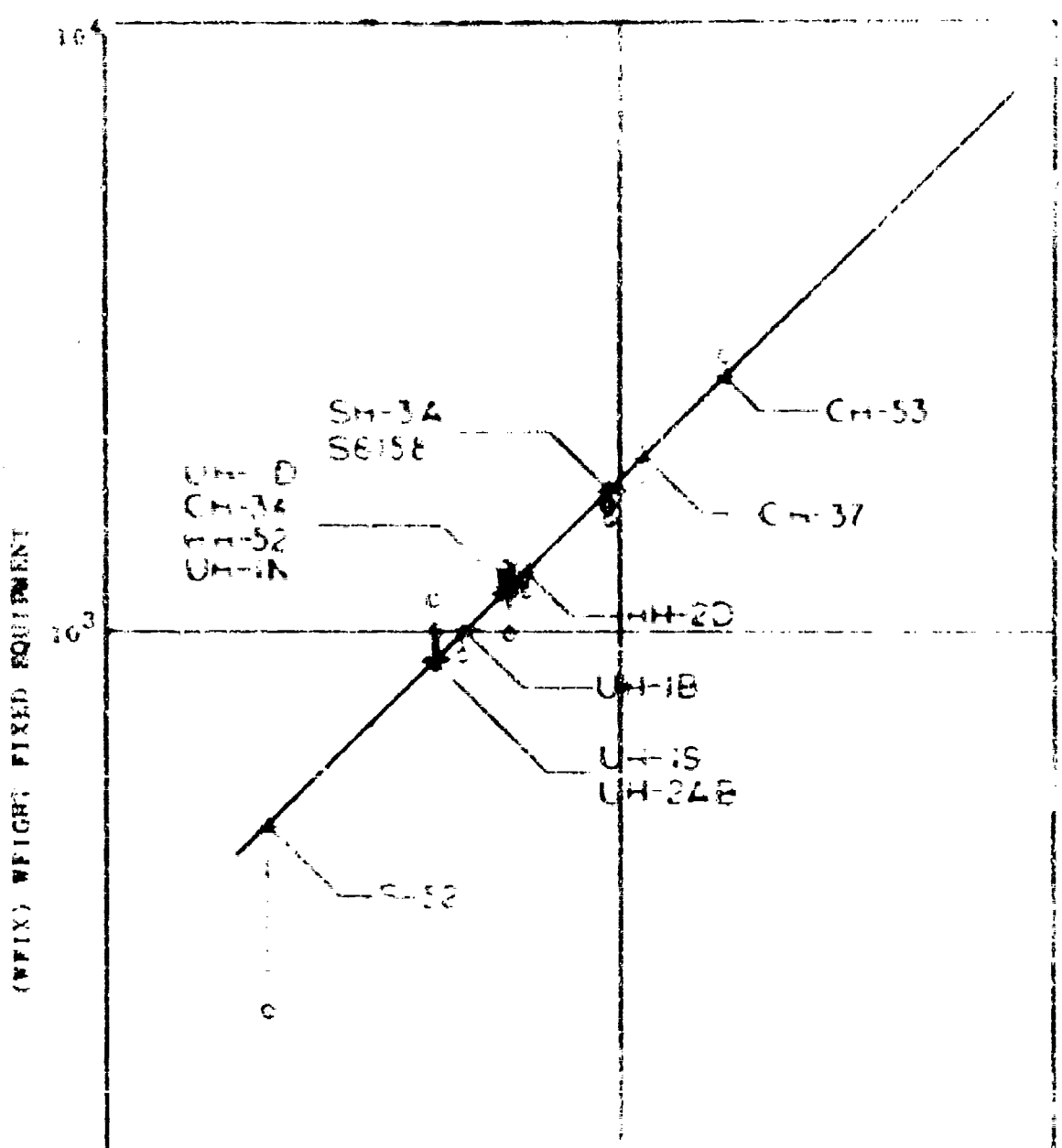

Figure 3-23. Fixed Weight

FIXED WEIGHT (WFIX) (Continued)

ENF = Effective Number of Engines = $.279 \times HP2^{.235}$

HP2 = Installed Horsepower - Input Parameter

NGW = Normal Gross Weight - Lbs = $2.145 \times MOW^{.893}$

Accountability:

Instruments	Furnishings & Equipment
Hydraulic	Air Conditioning
Electrical	Cargo Handling Gear
Electronics	

MISCELLANEOUS USEFUL LOAD (MUL)

MUL = $37.2 \times MOW^{.305}$

MOW = Maximum Operating Weight - Lbs - Input Parameter

Accountability:

Oil	Pyrotechnics
Trapped Liquids	Pararafts & Seat Pans
Flight Crew	Canteens

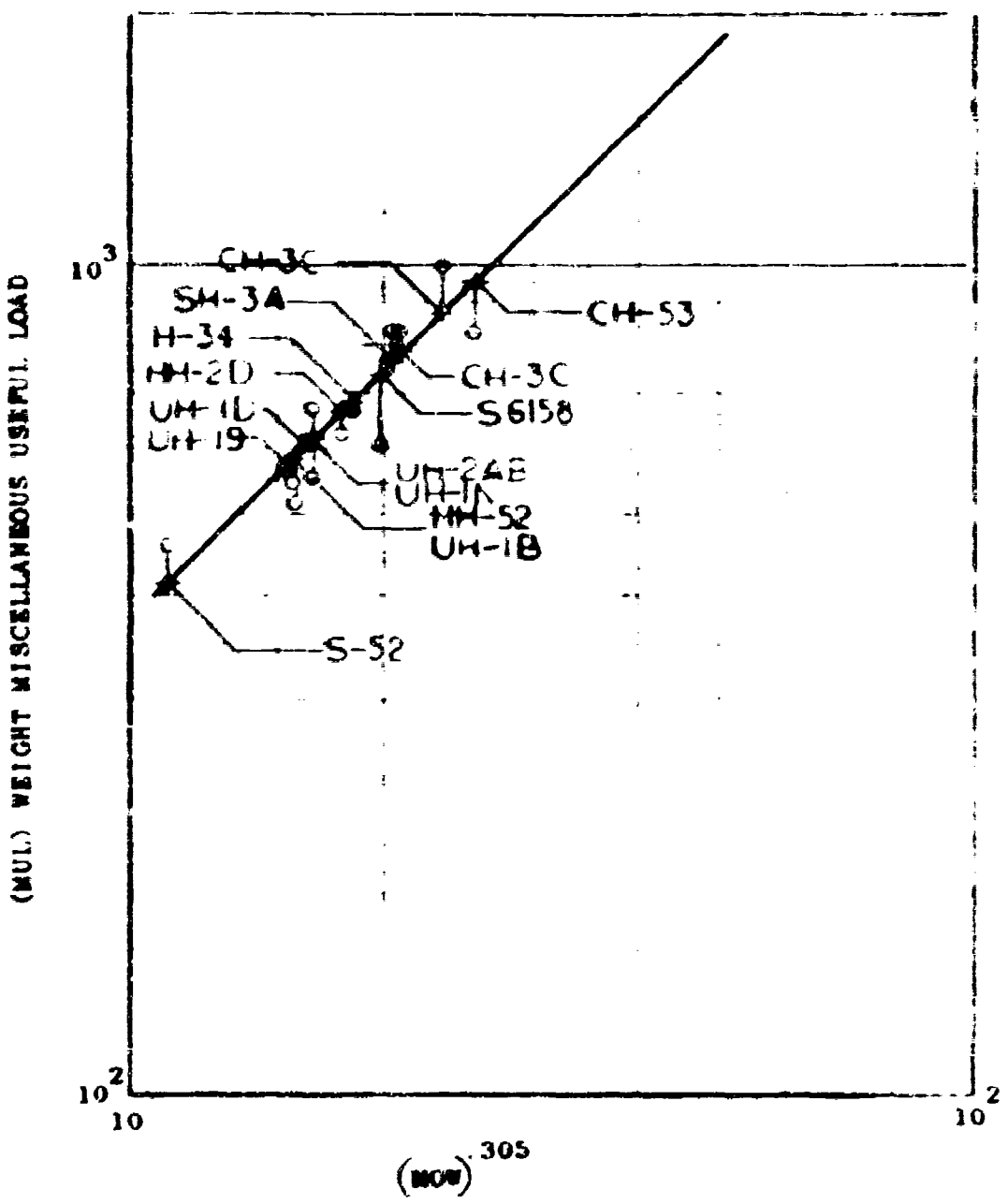

Figure 1-24. Miscellaneous Useful Load Weight

FIXED WEIGHT (WFIX) (Continued)

ENF = Effective Number of Engines = $.279 \times HP2^{.235}$

HP2 = Installed Horsepower - Input Parameter

NGW = Normal Gross Weight - Lbs = $2.145 \times MOW^{.893}$

Accountability:

Instruments	Furnishings & Equipment
Hydraulic	Air Conditioning
Electrical	Cargo Handling Gear
Electronics	

MISCELLANEOUS USEFUL LOAD (MUL)

MUL = $37.2 \times MOW^{.305}$

MOW = Maximum Operating Weight - Lbs - Input Parameter

Accountability:

Oil	Pyrotechnics
Trapped Liquids	Pararafts & Seat Pans
Flight Crew	Canteens

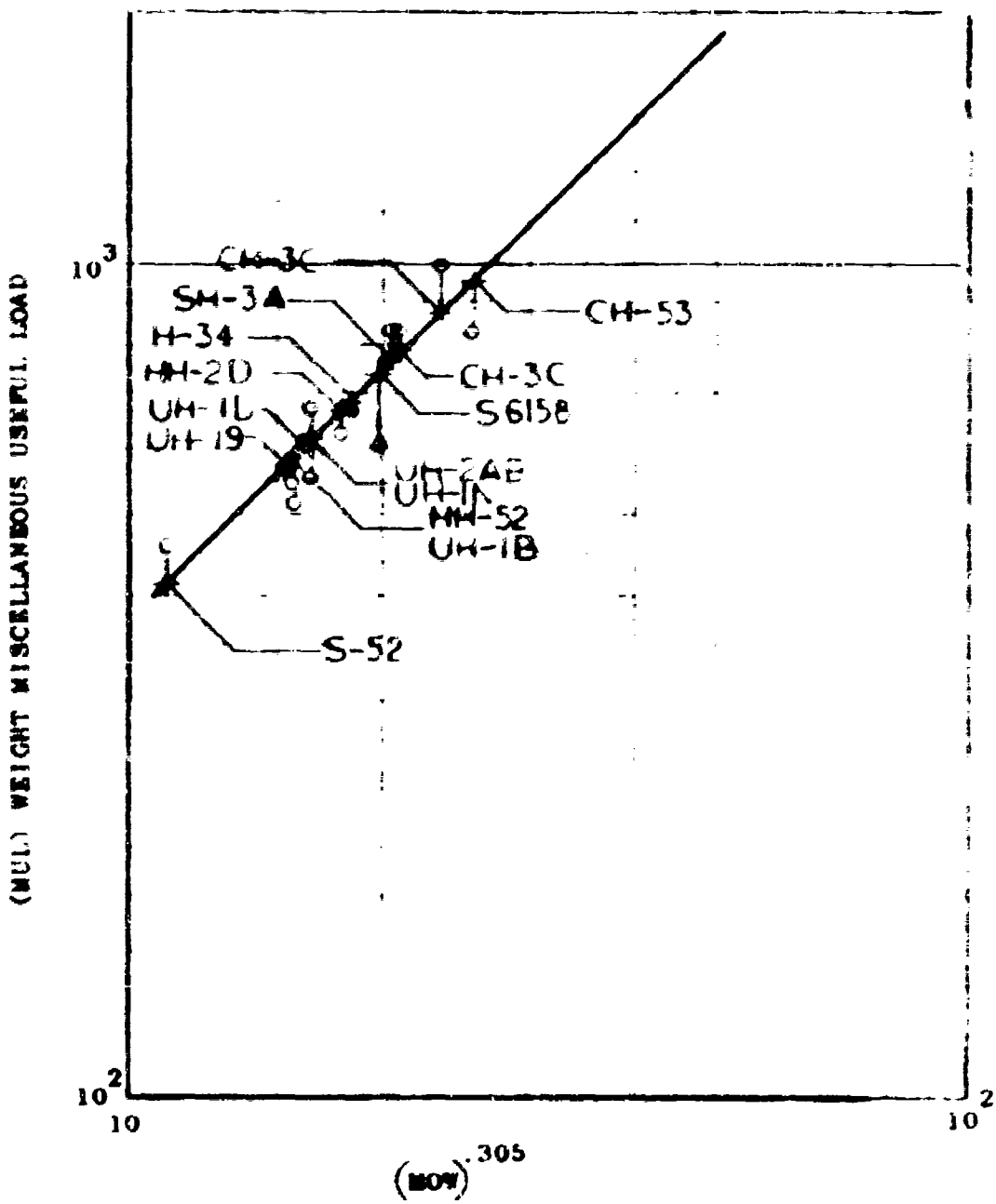

Figure I-24. Miscellaneous Useful Load Weight

REFERENCES

1. Magliozzi, B., et al, "A Comprehensive Review of Helicopter Noise Literature", DOT/FAA Report No. FAA-RD-75-79, June 1975.

2. Sperry, W. C., "Aircraft Noise Evaluation", DOT/FAA Report No. FAA-NC-68-34, September 1968.

3. "Directory of Helicopter Operators in the United States, Canada and Puerto Rico", Aerospace Industries Association of America, Inc., November 1975.

4. "Model Inventory Summary, July 1975", Helicopter Association of America, July 1975.

5. "Aviation Week and Space Technology - Aerospace Forecast and Inventory", Vol. 104, No. 11, March 15, 1976.

6. "The World's Current Helicopters - 1976", Interavia, January 1976, pp 66-71.

7. "1969 Encyclopedia of Vertical Lift Craft", Vertical World, Volume 3, No. 11, November 1968.

8. "Business Helicopters 75", Flight International, 30 October 1975.

9. "Janes All the World's Aircraft".

10. "Helicopters Meet New Challenges", Aviation Week and Space Technology, Volume 103, No. 13, September 29, 1975.

11. Cayce, B. V., "Census of U. S. Civil Aircraft - Calendar Year 1974", Federal Aviation Administration, DOT, December 31, 1974.

12. "General Optimism Among American Manufacturers", Interavia, January 1976, pp 39-43.

13. "European Helicopter Manufacturers - Pushing New Products and New Technologies", Interavia, January 1976, pp 27-31.

14. "The 1976 Helicopter Association of America Meeting", Interavia, March 1976, pp 206-210.

15. Johnson, W. R. and M. M. Katz, "Investigation of the Vortex Noise Produced by a Helicopter Rotor", USAAMRDL TR 72-2, February 1972.

16. Berner, A. and N. Giansante, "CHIANTI - Computer Programs for Parametric Variations in Dynamic Substructure Analysis", Kaman Aerospace Corporation, 47th Sound and Vibration Symposium, 19-21 October 1976.

17. Berman, A., "System Identification of a Complex Structure", Rand Aerospace Corporation, AIAA Paper 75-809, May, 1975.

18. Bowes, M. A., "Helicopter Transmission Vibration and Noise Reduction Program", USAAMRDL TR (To be published), 1977, Contract No. DAAJ02-74-C-0039.

19. Johnson, W. R., "Development of a Technique for Realistic Prediction and Electronic Synthesis of Helicopter Rotor Noise", USAAMRDL TR 73-6, March 1973.

20. Johnson, W. R., "Development of an Improved Design Tool for Predicting and Simulating Helicopter Rotor Noise", USAAMRDL TR 74-37, June 1974.

21. Henderson, H. R., F. J. Pegg and D. A. Hilton, "Results of the Noise Measurement Program on a Standard and Modified OH-6A Helicopter", NASA TN D-7216, September 1973.

22. Pegg, R. J., H. R. Henderson and D. A. Hilton, "Results of the Flight Noise Measurement Program Using a Standard and Modified SH-3A Helicopter", NASA TN D-7330, December 1973.

23. Sissom, A. and A. D. Crim, "A Method for Studying the Transient Blade-Flapping Behavior of Lifting Rotors at Extreme Operating Conditions", NACA TN 3366, January, 1955.

24. Lemnios, A. Z. and A. Gransalle, "The Dynamic Behavior of Rotor Into Vehicle Configurations. Volume I - Equation of Motion", NASA CR-73397, February, 1969.

25. Smith, M. J. T. and M. E. House, "Internally Generated Noise from Gas Turbine Engines: Measurement and Prediction", Journal of Engineering for Power, Trans. of ASME (April 1967), pp. 177-195.

26. Grande, E., D. Brown, J. Sutherland and R. Jeanice, "Small Turbine Engine Noise Prediction, Volume II, Noise Prediction Methods", Tech. Report AFAPL-TR-73-79, Volume II, December 1973.

27. Goldstein, M. E., "Aeroacoustics", NASA SP-346, November 1974.

28. Hoff, R. G., D. J. Clere and R. G. Dorsch, "Interim Prediction Method for Low Frequency Core Engine Noise", NASA TMX-71627, November 1974.

29. Metzinger, R. E. and J. J. Ewerling, "Review of Theory and Methods for Combustion Noise Prediction", AIAA Paper 75-56, 2nd Aeroacoustics Conference, Hampton, VA, March 1975.

REFERENCES (Continued)

30. Anonymous, "Jet Noise Prediction", SAE ARP 876, October 1965.

31. Heidmann, "Interim Prediction Method for Fan and Compressor Source Noise", NASA TMX-71763, December 1974.

32. Unger, E. E., "A Guide for Predicting the Aural Detectability of Aircraft", AFFDL-TR-71-22, July 1971.

33. Ungar, E. E. and F. R. Kern, "Exhaust, Casing, and Intake Noise of Continental IO-520D Aircraft Engine", BBN Report No. 2502A, June 1973.

34. Priede, T., "Diesel Engine Noise Conference", SAE Report SP-367, August 1975.

35. Bolt Beranek and Newman, Handbook for Shipboard Airborne Noise Control, USCG-NSES Report.

36. Parrott, T. L., "An Improved Method for Design of Expansion-Chamber Mufflers With Application to an Operational Helicopter", NASA TN D-7305, October 1973.

37. Beranek, L. L., "The Transmission and Radiation of Acoustic Waves by Solid Structures", Ch-13, Noise Reduction, L. L. Beranek, ed., McGraw-Hill, 1960.

38. Lasher, L., F. W. Orcutt and E. E. Shipley, "Analysis of Noise Generated by UH-1 Helicopter Transmission", USAAVLABS TR 68-41, June 1968.

39. Metzger, F. F., et al, "Development of a Method for the Analysis of Improved Helicopter Design Criteria", USAAMRDL TR 74-30, July 1974.

40. Bertele, M. and J. Laborde, "Evolution of Small Turboshaft Engines", SAE Paper 720920, October 1972.

41. Bossler, R. B., "Power Transfer Systems for Future Navy Helicopters", Naval Air Systems Command, Report No. R-1032, November 1972.

42. Wells, C. D. and T. L. Wood, "Maneuverability-Theory and Application", Presented at the 28th Annual National Forum of the American Helicopter Society, May 1972.

43. HELICOPTER OPERATING COSTS, Flight International, October 1976.

44. S-65-A2 DIRECT OPERATING COST, Sikorsky Aircraft, 1971.

45. BELL MODEL 204B PERFORMANCE AND COST SUMMARY, Bell Helicopter Co. August 1964.

46. Bowes, W. A., "Test and Evaluation of a Quiet Helicopter Configuration Hh-43B", USAAMRDL TR 71-31, January 1972.

47. Schlegel, R. G., "HuSh Final Report - Quiet Helicopter Program", Sikorsky Internal Report, SER-611476, Sikorsky Aircraft Co., 1970.

48. Mullusy, W. C., "Program to Reduce the Noise Signature of the OH-6A Helicopter", Hughes Tool Co. Internal Report ATL-AD 70-26, November 1969.

49. Industrial Acoustics Co., Bulletin 4.0301.0, POWER-FLOW TUBULAR SILENCERS.

50. MODEL SPECIFICATION T312 ENGINE, AIRCRAFT, TURBOSHAFT GENERAL ELECTRIC CO. T58-GE-8B and -8F ENGINES, July 1965.

51. MODEL SPECIFICATION T53-L-11, T53-L-11A and T53-L-11B SHAFT TURBINE ENGINES, Specification No. 104-28, January 1966.

52. King, R. J. and R. G. Schlegel, "Prediction Methods and Trends for Helicopter Rotor Noise", CAL/AVLABS Symposium, June 1969.